# MEASURED AND THEORETICAL RESPONSE OF PERPETUAL PAVEMENT STRUCTURES

by

MIGUEL M. PORTILLO

Presented to the Faculty of the Graduate School of

The University of Texas at Arlington in Partial Fulfillment

of the Requirements

for the Degree of

MASTER OF SCIENCE IN CIVIL ENGINEERING

THE UNIVERSITY OF TEXAS AT ARLINGTON

December 2008

ACKNOWLEDGEMENTS

First of all, I would like to acknowledge my advisor, tutor, and friend, Dr. Stefan Romanoschi, with my deepest appreciation for always providing life and academic guidance throughout this journey. None of this work would have been possible without his guidance. I appreciate his support and demands, which made me push myself to the limits and explore my capabilities.

I would like to express my gratitude to my committee members: Dr. Anand J. Puppala and Dr. Laureano R. Hoyos for their time, advice, and assistance in the preparation of this document.

My deepest gratitude to my mother, Teresa Yaluk, and to my father, Ing. Miguel O. Portillo K., for all your effort, love, and support from the beginning of this very important chapter of my life. Thank you for always being there for me, for your words, and your advices. Thank you for making me what I am. Without you, none of this would have been possible. Thank you to my brothers, Carlos Miguel and Rodrigo, for their support, love, and for reminding me that there is nothing more important in life than our family. My gratitude to my extensive list of aunts, uncles, and cousins for all your love and support.

Most important of all, I express my infinite gratitude and love to my wife Victoria, and our daughter Paula Maria. I cannot find enough words to tell you thank you for all your love, patience, and support. Thank you for joining me in this journey from the beginning, and for all the things you either gave up, or put aside. I love you both and you are my most precious treasure.

Special thanks to Paul Lewis and Cristian Dumitru. Thank you for your friendship and all your help, time, and hard work throughout the development of this work.

Last but not least, thank you to all my friends, Charly, Fede, Gonza, Vero, Nando, Alfre, Lelu, Pedro y Marian, Edgar y Adri, Martin y Monse, Marcos y Lore, Tito, and the list goes on. Thank you for your sincere friendship, for all the great memories, and for all your help. I am grateful to you all forever.

November 20, 2008

# ABSTRACT

## MEASURED AND THEORETICAL RESPONSE OF PERPETUAL PAVEMENT STRUCTURES

Miguel M. Portillo, M.S.

The University of Texas at Arlington, 2008

Supervising Professor: Stefan A. Romanoschi

The objectives of this research are to analyze field measured pavement response data recorded at the Kansas Perpetual Pavement experiment and to compare these measured values with theoretical response values obtained from linear elastic and visco-elastic models. All this is done to validate a perpetual pavement design implemented in Kansas on the US-75 project.

The Kansas Perpetual Pavement experiment includes the construction of four pavement sections on the US-75 highway designed according to the perpetual pavement concept. The sections were instrumented with strain gauges and pressures cells to measure strains and stress at the bottom of the base layer and at the top of the sub-base layer.

Pavement response measurements under known truck loads were carried out in seven occasions between July 2005 and October 2007 with a loaded truck. Measured values obtained showed that longitudinal and transverse strain values were almost always below the average endurance limit of 70 microstrains, which suggests that the perpetual pavement designs are valid. The measurements also showed that temperature and vehicle speed have large effects on the response of asphalt pavements. It was also observed that transverse strains were always larger than longitudinal strains.

The linear elastic software EVERSTRESS and the finite element software ABAQUS were used to theoretically predict the pavement responses using linear elastic and visco-elastic models respectively. Results from the linear elastic analyses were similar to the measured pavement response values, except for vertical pressures. On the other hand, results from the visco-elastic finite element model (FEM) were much smaller than the measured values. The FEM was run as an elastic model and the results were similar to the ones from EVERSTRESS, suggesting that there may have been a problem with the visco-elastic modeling of the asphalt concrete material. It is believed that the prony series parameters values are too large, thus, the material properties are very stiff, yielding to strain levels that are very small compared to the measured pavement response values.

TABLE OF CONTENTS

LIST OF FIGURES

LIST OF TABLES

Table Page

# CHAPTER 1

# INTRODUCTION

## 1.1 Introduction

The US has the most extensive highway network in the world consisting of approximately 3.9 million miles of paved and unpaved roads (Dumitru, 2006). The traffic volume on these roads is also the highest in the world: around 4.7 trillion passenger-miles and around 3.7 trillion ton-miles are recorded each year (“Transportation,” 2008). In the US, 11% of the gross domestic product (GDP), of around $950 billions, and 19% of the total spending of an average household are accounted by transportation costs (“Transportation,” 2008). More than $110 billions are spent yearly to build, rehabilitate, and maintain the nation’s pavements.

Despite this, seven percent of the interstate network is still in poor condition (Mahoney et al., 2000). Poor condition pavements can lead to an increase in user costs, travel delays, braking, fuel consumption, vehicle maintenance and repairs, and probability of crashes. If the pavement’s life is extended even by a small percentage by the implementation of newer and better technologies for design, construction, maintenance, and rehabilitation, a significant amount of money could be saved not only by the government, but also by the users.

A proper pavement design is the key to a long lasting pavement structure. The design process typically begins by the selection and design of the materials to be used. It is followed by the calculation of layer thicknesses depending on loading and environmental conditions. Finally, the pavement configuration and drainage system are designed, and the construction requirements are written. All these components must be considered for a low maintenance, long lasting, and well performing pavement structure (Romanoschi, 1999).

The major flexible pavement distresses are rutting, fatigue cracking, thermal cracking, and reflective cracking. Some other distresses such as potholes, bleeding, raveling, are recorded, but much less frequently. These distresses could be attributed to inadequate design procedures, inaccurate material characterization, variability in material quality, bad construction practices, and increase in traffic volumes and traffic loads (Palacios, 2007). From all these distresses, bottom-up cracks are the most difficult to identify and remediate. These cracks typically initiate at the bottom of the asphalt layers due to high tensile strains and stresses.

Huddleston, et al. (2001) presented the concept of “Perpetual Pavements” as a response to the necessity of extending pavement’s life. The concept is used to prevent the initiation of bottom-up cracks by implementing thick and stiff pavement layers composed of an impermeable, rut and wear resistant top structural layer placed on a rut resistant and durable intermediate layer. They must be placed on a fatigue resistant and durable base layer, which allows the material to undergo numerous stretch-release cycles without cracking (TRC 503, 2001). These pavements need only repairs of the surface layers since the lower asphalt layers do not crack.

The “perpetual pavement” concepts relies on the fact that asphalt mixes resist to one billion loading cycles if the tensile strain applied to the mix is below a certain value, called endurance limit. The evidence for the endurance limit has been recorded in several fatigue studies on the asphalt mixes (Thompson et al., 2006). The most typical values for the endurance limit ranges between 60 and 100 microstrains.

To verify the “perpetual pavement” concept, Kansas Department of Transportation (KDOT) built four experimental pavement sections in Sabetha, KS in 2005. The sections have asphalt layer thicknesses typical for Kansas pavements that do not exhibit bottom-up cracking. The four sections have been instrumented with strain gages to measure the tensile strain at the bottom of the asphalt layers to compare the strain values with the endurance limit.

However, in order to perform the comparison and validate the “perpetual pavement” design used, it is necessary to compare the field measured strains with the strain values predicted by theoretical models for asphalt pavements. The most common theoretical models for computing the response of flexible pavement structures are linear-elastic and visco-elastic models.

This thesis describes the research efforts conducted to validate the measured strains with the theoretical strains computed by linear-elastic and visco-elastic models. It presents the Kansas perpetual pavement experiment, the recorded response data, the material characterization data and the linear-elastic and visco-elastic modeling. The documents concludes with the major findings and recommendations from this research

## 1.2 Objectives

The objectives of this work are:

1. to assemble the information related to the design and construction of the instrumentation for measuring the response of the Kansas Perpetual Pavements;
2. to assemble the information related to the  the response measurement procedure and results and the laboratory tests conducted for material characterization.
3. to compare the measured pavement responses with theoretical responses predicted by linear elastic and visco-elastic models

# CHAPTER 2

# BACKGROUND

This chapter provides background information on the concepts of perpetual pavements, response measurements, and linear elastic and visco-elastic modeling of pavements.

## 2.1 Perpetual Pavement Concept

### *2.1.1 Overview*

Traffic volumes and loads on pavements of the transportation infrastructure have been increasing ever since the automobile was invented. These trends, along with people's desire of a longer lasting transportation infrastructure, have brought about the necessity of extending asphalt pavement's life from 20 years to 50 years or more. The asphalt paving industry responded to this need by introducing the concept of perpetual pavements, which has been gaining momentum nationally and internationally (Romanoschi et al., 2008). The perpetual pavement concept was introduced by Huddleston, et al. (2001) in an Asphalt Pavement Alliance publication called "Perpetual Pavements" (Thompson et al., 2006). The perpetual pavements concept has also been referred using other terms such as long-lasting, long-life, and extended life pavements. The main idea is to construct asphalt pavements with an impermeable, rut and wear resistant top structural layer placed on a rut resistant and durable intermediate layer and a fatigue resistant and durable base layer, as shown in Figure 2-1 (Romanoschi et al., 2008).

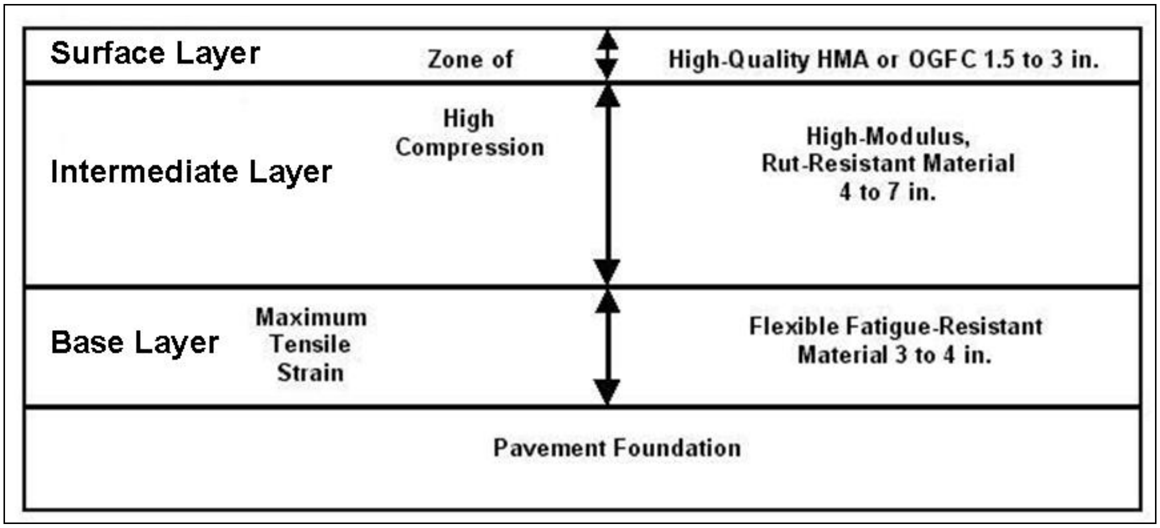


Figure 2-1: Perpetual Pavement Design Concept (TRC 503, 2001)

The perpetual pavement concept is used to prevent the initiation of bottom-up cracks on the pavements by minimizing tensile strains and stresses at the bottom of the asphalt layer, which is achieved by using thick and stiff pavement layers. Also, the risk of crack formation is reduced by the fatigue resistant base layers, which allow the material to undergo numerous stretch-release cycles without cracking (TRC 503, 2001).

The concept, however, does not eliminate the risk of formation of fatigue cracks. These types of cracks are usually called “top-down” cracks and tend to develop in the surface layer and propagate horizontally in the top lift. The advantage in this case is that these cracks can be seen and actions can be taken to eliminate them by the application of asphalt overlays or inlays (Romanoschi et al., 2008).

The perpetual pavement concept provides a pavement structure that can show distresses confined at the top of the pavement and needs periodic surface renewal actions only. This eliminates the need of any major structural rehabilitation or reconstruction, thus leading to significant monetary savings as well as a decrease in the construction or rehabilitation time (Romanoschi et al., 2008).

There are two main approaches that are recommended for the implementation of the perpetual pavement concept. In the first approach, the construction of a bottom lift for the base layer is recommended. The lift should have a softer binder grade and/or higher binder content to allow the mix to stretch without breaking at strain levels that will produce cracks in conventional mixes, thus increasing the mix's fatigue life. In the second approach, the increase of the total thickness and stiffness of asphalt layers is recommended, in order to reduce strains at the bottom of the asphalt layer to levels so small that the fatigue life of the material will be virtually infinite (TRC 503, 2001).

Laboratory fatigue testing of asphalt concrete materials have proven that if the asphalt concrete material is subjected to a small enough strain level, called the limiting strain, it will take billions of load repetitions to reach failure. The limiting strain is also called the fatigue endurance limit (FEL), term that is used for the fatigue of metals. The FEL is the flexural strain level below which damage is not cumulative, thus resulting theoretically in no fatigue failure in the HMA (Thompson et al, 2006). Extremely long laboratory tests at low strain levels are required to develop strain versus load repetitions curves, in order to obtain FEL values. Figure 2-2 shows a typical strain versus load repetition curve for HMA. As it is shown in the figure, there is a point in the curve where the curve starts to deviate from the linear relationship between flexural strain and load repetitions, and the curve becomes flat. This flatness of the curve suggests that strains below the flat line would yield a very long fatigue life of the HMA (Thompson et al, 2006). Researchers have reported that fatigue endurance limit of asphalt concrete ranges between 60 to 100 microstrains, depending on the mix.

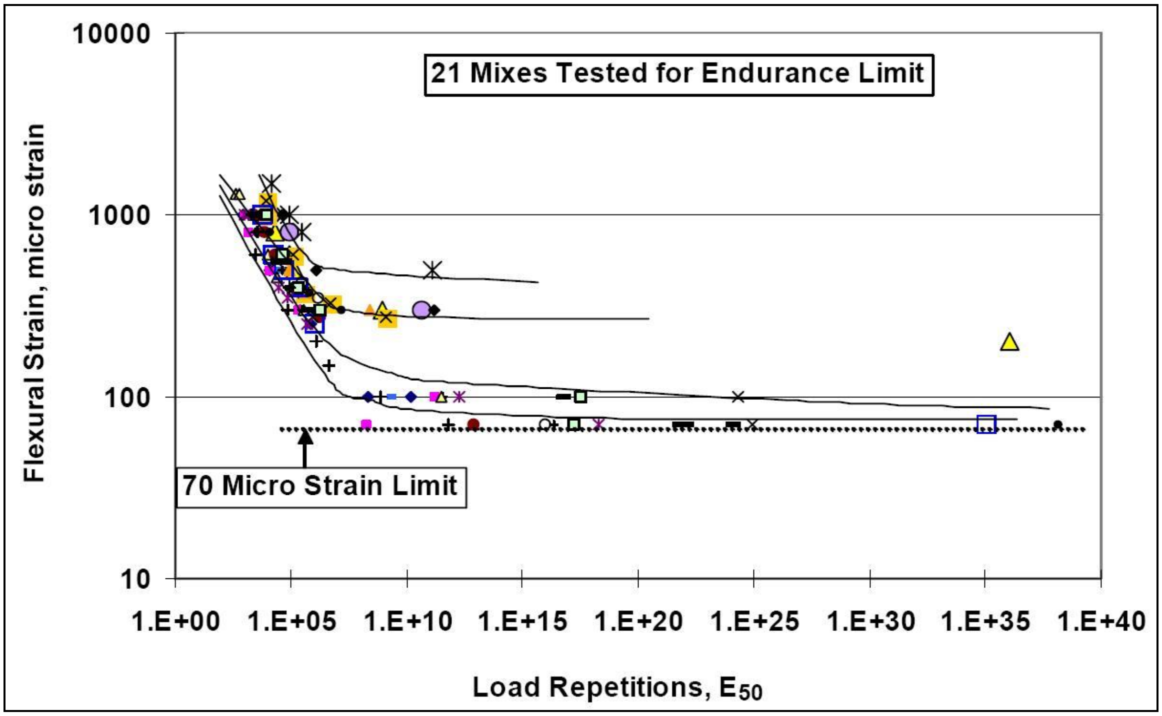


Figure 2-2: Strain vs Load Repetition Curve (Thompson et al, 2006)

## 2.2 Pavement Instrumentation and Response Measurements

### *2.2.1 Overview*

Throughout the past three decades, researchers have attempted to improve pavement analysis and design by comparing stresses and strains measured at critical locations in the pavement structure with the strains at the same locations calculated by theoretical pavement response models (Nassar, 2001).

As technology advances, scientists have more and more tools to improve their work. Pavement instrumentation has become an extremely important tool in the process of monitoring in-situ pavement material performance and measuring pavement response under different environmental and loading conditions. It encompasses the identification of critical locations in the pavement, the selection of sensors, the calibration of the sensors, the identification of possible errors, the installation, and the data collection (Yin, 2007).

The five most important pavement response variables that are measured in the field include the strains, stresses, deflections, moisture, and temperature. With these parameters, researchers are able to assess the major differences in the behavior of asphalt pavements between theory and measured field conditions. There are great benefits resulting from the implementation of these tools, from which a lot of information can be learned. However, the process itself is complex, and there is a lot of variability associated with the installation procedures, sensor-pavement interactions, data acquisition, and interpretations. Moreover, the improper assessment of the sensor performance may lead to unreliable results (Nassar, 2001).

Once all of these problems are addressed and the tools are implemented and working as expected, the data obtained from the instruments are used to fulfill two main objectives. The first objective is, as mentioned above, to validate pavement response models or design approaches by comparing field measured parameters with calculated parameters. The second objective encompasses the monitoring of trends in measured parameters to identify the proper theory to analyze these parameters. For example, the monitoring of moisture contents at different locations in the pavement may give an idea on how water moves within the pavement (Nassar, 2001).

The following subsections discuss the pavement instrumentation available today to monitor pavement response variables such as horizontal and vertical strains at the interface of different materials, vertical pressures at base, sub-base and sub-grade layers, deflections of the surface of the pavement, absolute and/or relative displacements, deformations of the pavement layers, temperatures in pavement at multiple depths, and soil moisture.

### *2.2.2 Strain Gauges*

A strain gauge is a device used to measure strain in objects. It consists of a long metallic foil pattern or semiconductor attached on a matrix support that is referred to as the carrier. The principle of the strain gauge is the dependence of a material's conductance not only on the material's conductivity, but also on the geometry of the object. For instance, when a material is stretched within its elasticity limits, the material will become longer and skinnier, and the material's electrical resistance will increase. Similarly, when a conductor is compressed within its elasticity limits, the conductor will become shorter and broader, which decreases its electrical resistance. The wire is arranged in a zig-zag pattern of parallel lines as shown in Figure 2-3 to maximize the sensitivity of the strain gauge and to reduce the influence of shear and Poisson's strains. Any suitable adhesive is used to attach the strain gauges to the objects so that the strains are transmitted to it. Nowadays there are various types of strain gauges commercially available, having different nominal resistance values which ranges from 30 to 3,000 Ω; the most common values are 120, 350, and 1,000 Ω (Dumitru, 2006).

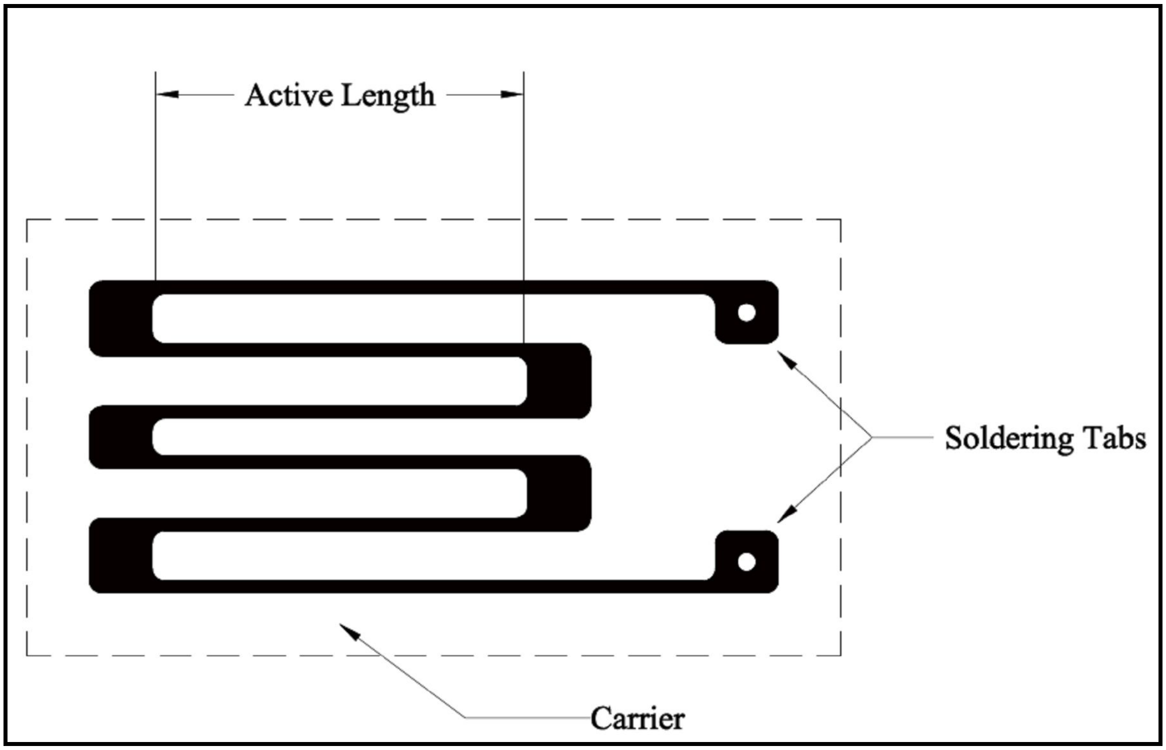


Figure 2-3: Strain Gauge (Dumitru, 2006)

In order to obtain reliable strain gauges measurements, the installation of the strain gauges must be carried out correctly. There are a number of factors that can cause problems. Some of these factors are lack of bonding between the strain gauge and the object or the use of a bonding agent that is too stiff. Moisture and temperature variation in pavements can also disturb the linearity of the relationship between strain and resistivity.

Various types of strain gauges are available in the market according to the application that they are going to be used for. For example, strain gauges used in Portland cement concrete are plastic coated against moisture and have a special texture to improve the bond to the concrete. In the case of strain gauges used in asphalt, the H-bar type strain gauge shown in Figure 2-4, is the most commonly used (Dumitru, 2006).

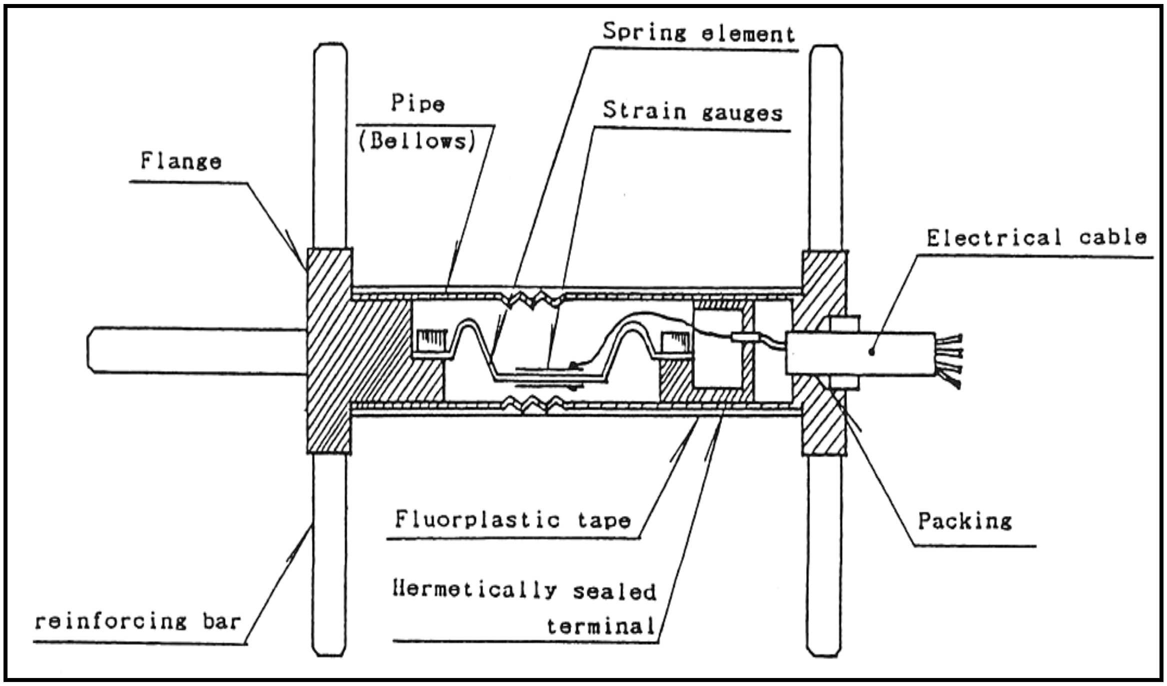


Figure 2-4: H-Bar Type Strain Gauge (Dumitru, 2006)

**F**our types of strain signal have been reported in the literature as representing the horizontal strain recorded at the bottom of the asphalt layers. These typical signals are: compressive peak value, tensile peak value, tensile peak value with compressive strain preceding the tensile strain, and tensile peak value with compressive strain before and after the tensile peak (Nassar, 2001). Examples of these responses are shown in Figure 2-5. Notice that these responses are for a single axle passing on top of the pavement, not for a load vehicle.

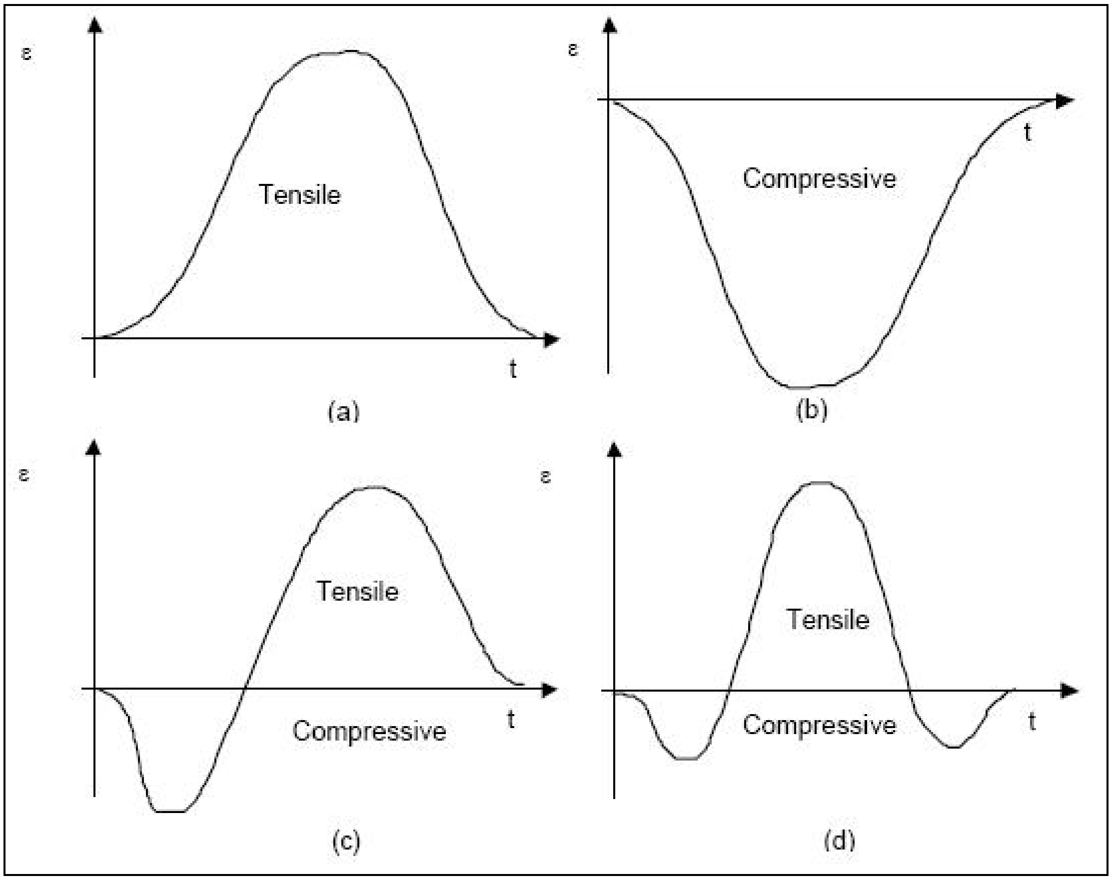


Figure 2-5: Typical Strain Gauge Responses (Nassar, 2001)

*2.2.3 Linear Variable Differential Transducer (LVDT)*

The LVDTs are instruments used for measuring displacement, deformations and deflections when used in pavements. An LVDT consists of a passive transformer (coil) with one primary and two secondary windings, and a moving core. When the primary winding is excited by an audio frequency range voltage, an imbalance is developed between the primary and the secondary windings, and this imbalance is proportional to the displacement of the core (Dumitru, 2006).

The most common LVDTs used for measuring the deformation of pavement layers are the spring deflection LVDT (Figure 2-6) and the multiple-depths LVDT (Figure 2-7). The deflections are measured at different depths by inserting LVDTs into housing units, which are bonded to the base or surface layers. The LVDT cores are bonded to a base plate located at the bottom of the test section. The LVDTs measure the relative displacement between the housing and the cores (Dumitru, 2006).

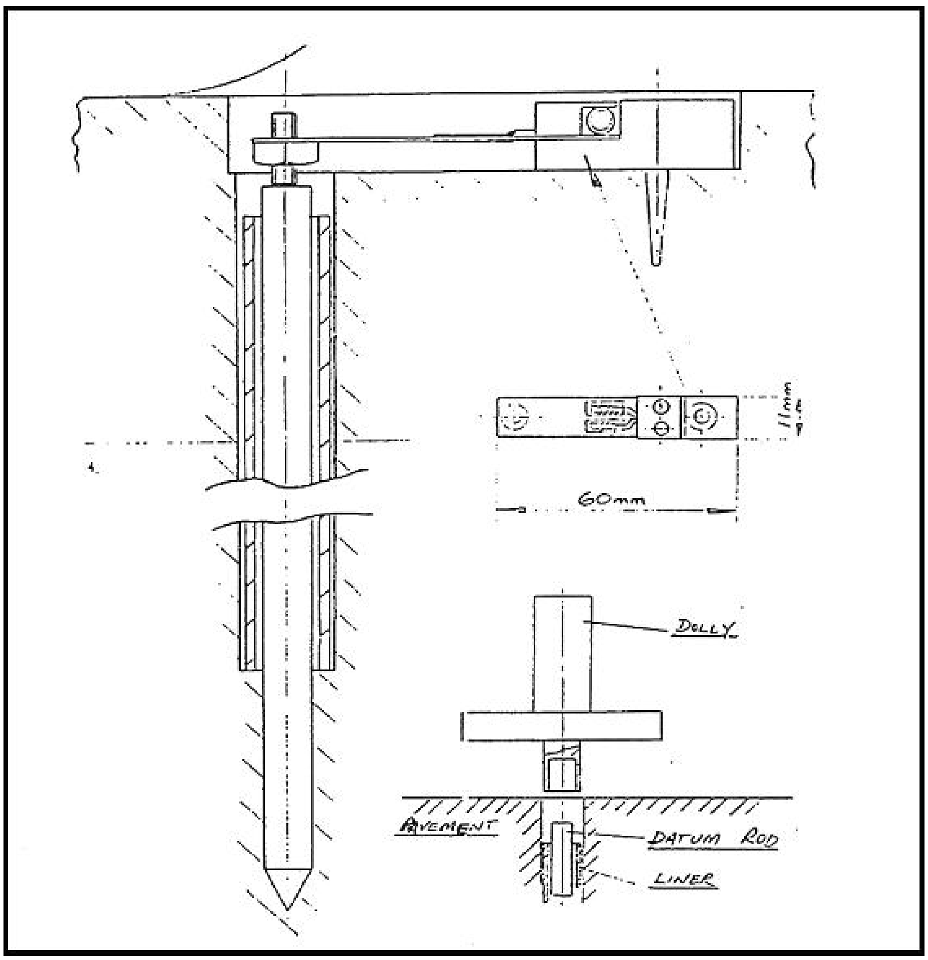


Figure 2-6: Spring Deflection Gauge (Metcalf, 1996)

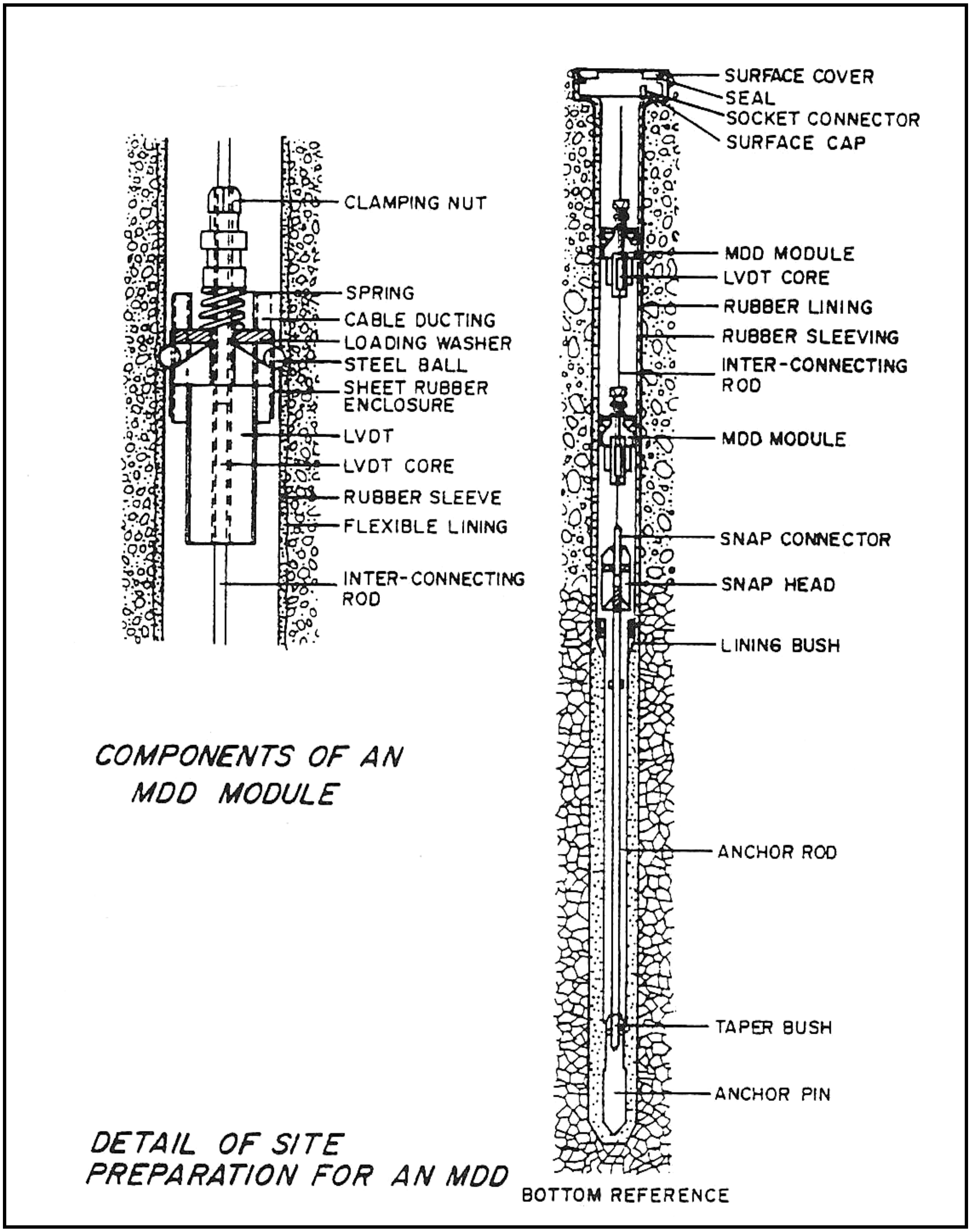


Figure 2-7: Multiple Depth Deflection Gauge (Metcalf, 1996)

### *2.2.4 Pressure Cells*

Pressure cells are used to measure changes in stresses in the overlying layers and also to capture the increase in vertical pressure due to dynamic loads from the traffic (Nassar, 2001). Due to their size, they are almost always used to measure vertical pressure. Various types of pressure cells are available in the market. The Kulite type 0234 earth pressure cells, the Carlson type TP-101, the Geokon 3500, and the Geokon 3410S are some pressure cells that have been successfully used in asphalt pavement research in the past. Depending on the pressure cell model, their structure and mechanism varies. Table 2-1 presents the pressure cell models with their respective description.

Table 2-1: Pressure Cells (Nassar, 2001)

| Pressure Cell Model | Description |
|---|---|
| Kulite type 0234 | • 54mm in diameter, thickness of 14.3 mm<br>• Vertical pressure range of 0 to 690 kPa<br>• Consists of a diaphragm that excites a strain gauge upon any deformation of the diaphragm |
| Carlson type TP-101 | • Vertical pressure range of 0 to 690 kPa<br>• Consists of a stainless steel pressure head 114 mm in diameter and 6.4-mm-thick, and is welded to a 16-mm outside diameter stainless steel tube that is attached to a silicon strain gauge transducer |

Table 2-1 - *Continued*

| Pressure Cell Model | Description |
|---|---|
| Geokon 3500 | • Consists of two circular steel plates welded together around their rims<br>• 13-mm-thick with a diameter of 150 mm<br>• Space between plates is filled with liquid<br>• Steel tube connects the liquid to a pressure transducer located away from the cell<br>• Pressure transducer responds to changes in stresses applied to the cell. |
| Geokon 3410S | • It is a pore water pressure cell used in subsurface applications<br>• Follows the same principle as the Geokon 3500<br>• Designed to operate under intense static loads |

### *2.2.5 Temperature and Moisture Sensors*

Mechanical properties of materials used in pavement structures depend on their temperature and moisture content, so it is critical for research projects to monitor these parameters in order to assess their behavior under different conditions.

Thermocouples are the most common instruments used to monitor the temperature at different depths within the pavement. There are different types of thermocouples, but the most widely used in pavement research is the type T. The principle that makes the thermocouples work is called the thermoelectric effect, which states that when a conductor is subjected to a thermal gradient, it generates a voltage. Thermocouples consists of two metal conductors made of different materials that when are subjected to a temperature gradient, they generate different voltages due to the fact that they are made from different materials. This difference increases as the temperature increases, usually 1 to 70 microvolts per degree ºC (www.wikipedia.com). Figure 2-8 shows how the thermocouples look like.

Figure 2-8: Typical thermocouple type-T (www.wikipedia.com)

Moisture levels can be measured using various types of instruments such as time domain reflectometer probes, open standpipes (water table), pore water pressure cells, resistivity probes, and others. Figure 2-9 shows a typical time domain reflectometer. This type of instrument is very sensitive and must be calibrated specifically for the type of soil that is going to be used in.

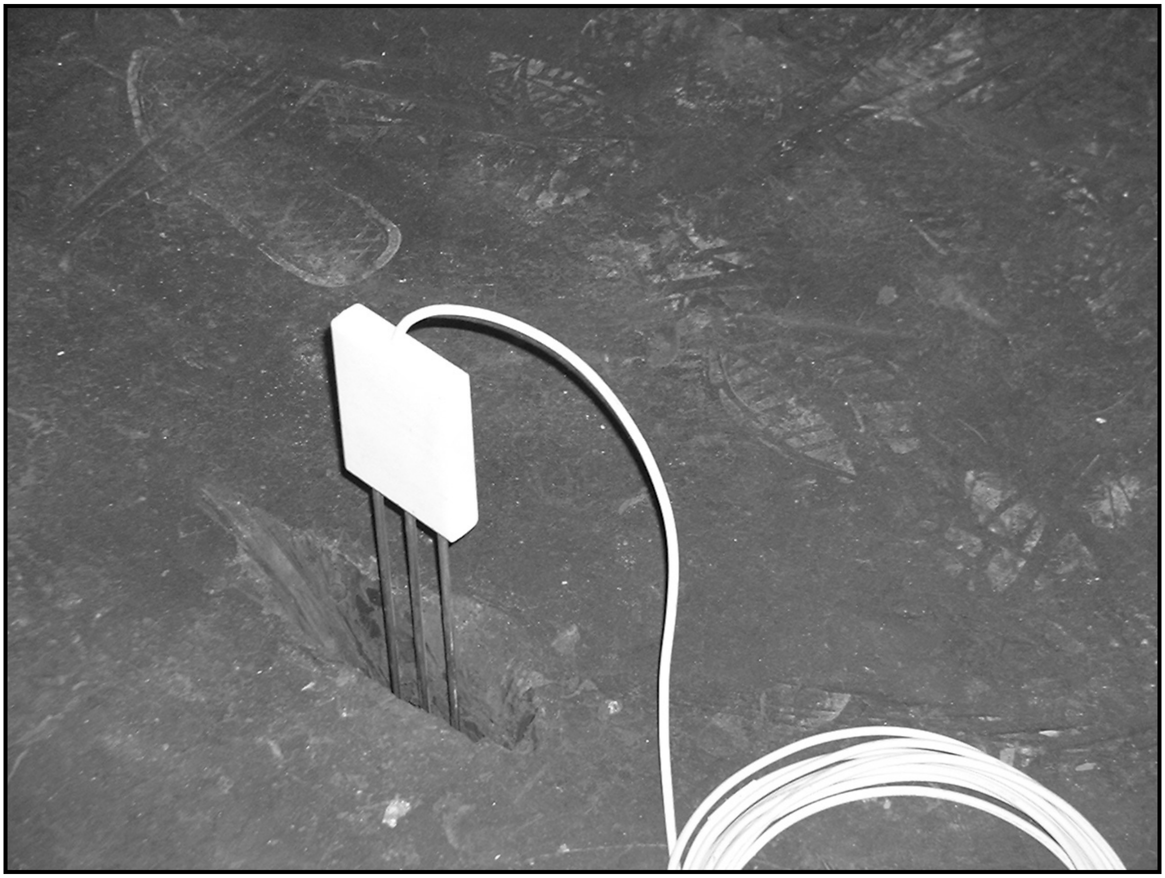

Figure 2-9: Time Domain Reflectometer Probe (Dumitru, 2006)

## 2.3 Linear Elastic Analysis

### *2.3.1 Overview*

Linear elastic analysis of asphalt pavements employs the layered elastic theory. It is the tool most often used to study the behavior of pavements under traffic loading due to the fact that it has been used by engineers since the 1940’s and it is simple to use. In 1943, Burminster came up with a method of solving a two-layer linearly elastic problem for the first time. He then upgraded the model to a three-layer system. Ever since then, taking advantage of the advances in technology, the model has been upgraded to deal with multilayer systems and different software were developed (Amara et al, 2006).

The earliest computer program developed was CHEV, by the Chevron Research Company, which dealt only with linear elastic materials (Huang, 1993). Since then, a number of computer programs such as DAMA, BISAR, ELSYM5, PDMAP, DIPLOMAT, etc were created.

The most important assumptions made in the layered theory are (Amara et al, 2006):

- Each layer is homogenous, with the same properties throughout the layer
- Materials are weightless, so no inertia effects are considered
- Layers are infinite in the lateral direction
- Pavement structures are loaded statically, so no moving loads are considered
- Loading areas are circular
- The layers are fully bonded

*2.3.2 EVERSTRESS Software*

Everstress© has its basis on the WESLEA layered elastic analysis program developed by the US Army Corp of Engineers. The program is capable of determining the stresses, strains, and deflections in a layered elastic system under static loads that are uniform distributed over circular surface areas. The program is limited to analysis of pavement structures including up to five layers, 20 loads, and 50 evaluation points. The program is also capable of considering stress dependent stiffness characteristics of the materials (EVERSERIES©, 2005).

The input data required by the program to run an analysis are the modulus of elasticity, Poisson's ratio, and thickness of each layer, as well as load magnitude, contact pressure or load radius, and location of the loads with respect to a predefined axis. A detailed explanation on how the program runs, the program's structure, and the user's guide is presented elsewhere (EVERSERIES©, 2005).

## 2.4 Visco-elastic Analysis

Hot-mix-asphalt (HMA) is a visco-elastic material because it shares properties from an elastic solid and at the same time from a viscous fluid. For example, if a ball of some material is thrown to the ground and it bounces back, then it is said that the ball is made of an elastic material. On the other hand, if the ball is left on the ground and it begins to deform and flattens gradually, then it is said that the ball is made of a viscous material (Huang, 1993). When HMA is subjected to high temperatures or to slow moving loads, it behaves more as a viscous material. On the other hand, when HMA is subjected to very low temperatures or to fast-moving loads, HMA is more rigid and behaves in a more elastically manner (Elseifi et al., 2006). Early works on asphalt pavement response modeling have used linear elastic programs to study the behavior of asphalt concrete mixtures, but this type of analysis does not consider the time-temperature dependency of HMA.

The main principle of the theory of visco-elasticity is based on the elastic-viscoelastic correspondence principle, which changes a visco-elastic problem to an associated elastic problem through the application of the Laplace transform (Huang, 1993).

*2.4.1 Material Characterization*

Visco-elastic material characterization is done generally in two ways, either by mechanical models or by creep compliance curves (Huang, 1993).

2.4.1.1 Mechanical Models

There are various mechanical models available to characterize visco-elastic materials. They all share two basic components: a spring and a dashpot (Huang, 1993).

2.4.1.1.1 Basic Models

The basic models follow the principles that an elastic material is characterized by a spring (Figure 2-10a) and obeys Hooke's law (Equation 2.1), and a visco-elastic material is characterized by a dashpot (Figure 2-10b) and obeys Newton's law (Equation 2.2). Hooke's law states that stress is proportional to strain. On the other hand, Newton's law states that stress is proportional to the time rate of strain (Huang, 1993).

$$\sigma = E \in \tag{2.1}$$

where:

$\in$ = strain

$\sigma$ = stress

$E$ = elastic modulus

$$\sigma = \lambda \frac{\partial \in}{\partial t} \tag{2.2}$$

where:

$\lambda$ = viscosity

$t$ = time

When there is a constant stress applied, Equation 2.2 is integrated to become:

$$\in = \frac{\sigma \times t}{\lambda} \tag{2.3}$$

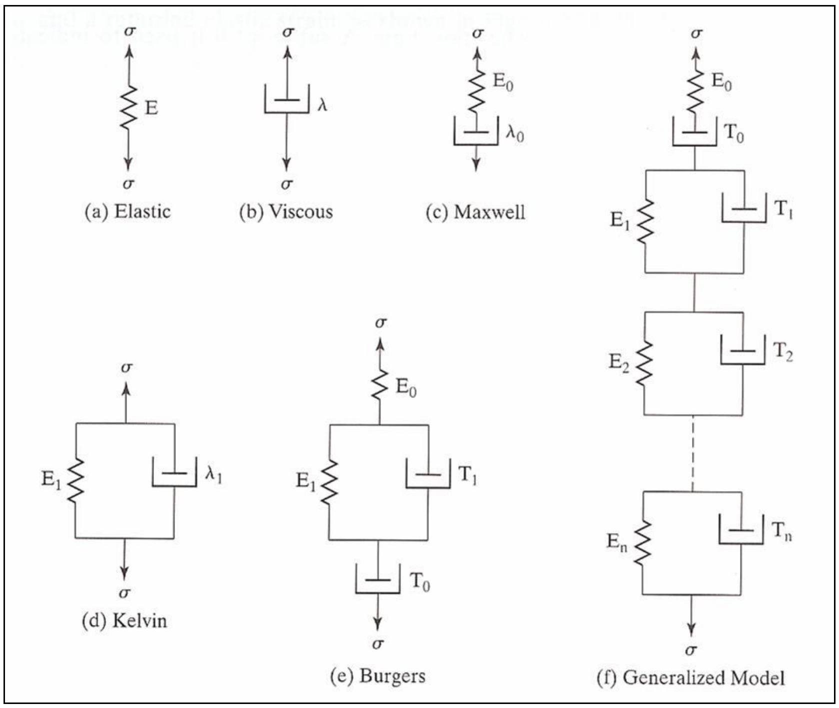


Figure 2-10: Mechanical Models for Viscoelastic Materials (Huang, 1993)

2.4.1.1.2 Maxwell Model

This model is composed by a combination of springs and dashpots arranged in series, as shown in Figure 2-10c. When a constant stress is applied, then the total strain is calculated through Equation 2.4, which in terms is a combination of Equations 2.1 and 2.3 (Huang, 1993).

$$\in = \frac{\sigma}{E_0} + \frac{\sigma \times t}{\lambda_0} = \frac{\sigma}{E_0}\left(1 + \frac{t}{T_0}\right) \tag{2.4}$$

where:

$T_0 = \dfrac{\lambda_0}{E_0} =$ relaxation time

If a stress is applied instantaneously to the system, an instantaneous strain will develop in the spring. If this strain is kept constant, the stress will gradually decrease until it becomes zero, which can be seen after solving the following differential equation (Huang, 1993):

$$\frac{\partial \in}{\partial t} = \frac{1}{E}\frac{\partial \sigma}{\partial t} + \frac{\sigma}{\lambda} \tag{2.5}$$

The solution to Equation 2.5 when the strain is kept constant is as follows:

$$\sigma = \sigma_0 e^{-\frac{t}{T_0}} \tag{2.6}$$

2.4.1.1.3 Kelvin Model

This model is represented by a combination of a spring and a dashpot connected in parallel, as shown in Figure 2-10d. In this model, the spring and the dashpot have the same strain but the total stress in the system is calculated through the summation of the two stresses, as follows (Huang, 1993).

$$\sigma = E \in + \lambda \frac{\partial \in}{\partial t} \tag{2.7}$$

When a constant stress if applied to the system, Equation 2.7 is rearranged and integrated from 0 to $\in$ and from 0 to $t$ to get:

$$\in = \frac{\sigma}{E}\left[1 - e^{-\frac{t}{T}}\right] \tag{2.8}$$

2.4.1.1.4 Burgers Model

This model is a combination of the previous two models connected in series, as shown in Figure 2-10e. When a constant stress is applied to the system, the model is represented by Equation 2.9, which is a combination of Equations 2.7 and 2.8 (Huang, 1993):

$$\in = \frac{\sigma}{E}\left(1 + \frac{t}{T}\right) + \frac{\sigma}{E}\left[1 - e^{-\frac{t}{T}}\right] \tag{2.9}$$

In this model, the total stress is composed of an instantaneous elastic strain, a viscous strain, and a retarded elastic strain, as shown in Figure 2-10e (Huang, 1993).

2.4.1.1.5 Maxwell-Weichert Model

The Maxwell-Weichert model is a combination of sets of springs and dashpots connected in series to each other (Figure 2-11), which is represented by Equation 2.10.

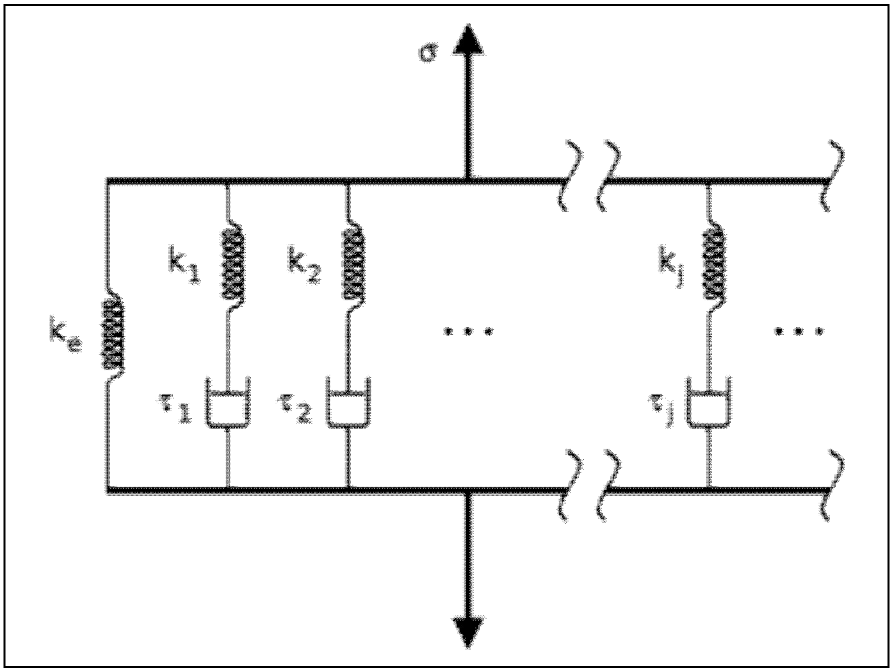


Figure 2-11: Maxwell-Weichert Model (www.wikipedia.com)

$$E(t) = E_\infty + \sum_{1}^{m} E_i e^{-\left(\frac{t}{\rho_i}\right)} \tag{2.10}$$

where:

$E_\infty =$ long-time relaxation modulus

$E_i =$ prony coefficients

$\rho_i =$ relaxation times

The variables shown above are explicit functions of the dashpot viscosities and corresponding spring stiffnesses. This method of expressing the visco-elastic response of the material is widely implemented in the pavement research area due to its computational efficiency and simplicity.

The model has been implemented by many researchers in the past and has proven to closely simulate the behavior of HMA mixes. Mikhail (1996) successfully applied the model in his study to investigate the structural response of flexible pavements under different dynamic loads and pavement roughness conditions, and concluded that the model could be used to expand his research to other truck types and pavement variables, since the study simulated three types of trucks with equal gross weights. Elseifi et al. (2006) implemented the model in their study to accurately simulate pavement responses to different traffic loading and speeds. It was found that the model's predictions were in agreement with field measurements, with an average error in the prediction of less than 15%.

2.4.1.2 Creep Compliance

Creep compliance at various times is another method used to characterize viscoelastic materials (Huang, 1993). The creep compliance is represented as:

$$D(t) = \frac{\in(t)}{\sigma} \tag{2.11}$$

where:

$D(t) =$ creep compliance

$\in(t) =$ time-dependent strain under a constant stress

The creep compliance for the generalized model can be expressed by Equation 2.12, which can be used to compute the creep compliances at various times (Huang, 1993):

$$D(t) = \frac{1}{E_0}\left(1 + \frac{t}{T_0}\right) + \sum_{i=1}^{n} \frac{1}{E_i}\left[1 - e^{-\frac{t}{T_i}}\right] \tag{2.12}$$

## 2.5 Finite Element Method

### *2.5.1 Overview*

The complexity of the problem of modeling the visco-elastic behavior of flexible pavements requires the use of advanced numerical methods, such as finite element methods. The finite element method became widely used thanks to the development of computers. The method was originally created to investigate stresses and strains of aircraft structures, but has extended its applicability to other fields such as continuum mechanics (Dumitru, 2006).

The FEM consists of dividing the model to be analyzed into discrete bodies or finite elements, which have well defined thermal and mechanical properties. It is divided into four major parts, which are the discretization, the element equations, the global stiffness matrix, and the solutions of the problem. (Chapra et al, 1988).

The discretization is the subdivision of the analysis domain into finite elements, which can be characterized by one, two, or three dimensions, depending on the type of problem. The element equations establish the functions applied to approximate the variation of displacement at each nodal point. Generalized forces applied at nodal points are related to the corresponding nodal displacement using a variational principle. This relationship between force and displacement is expressed by the element stiffness matrices [k], which incorporates the geometrical and material properties of each element (Ionnides, 1984). The relationship equation is as follows:

$$[k]\{d\} = \{p\} \tag{2.13}$$

where:

[k] - stiffness matrix of the finite element

{d} - vector of nodal displacements

{p} - vector of nodal forces

The global stiffness matrix [K] is constructed based on the continuity of the structure and the connectivity properties. The solutions of the problem are basically the nodal solutions, and are calculated using Equation 2.14 along with the equations defined by the boundary conditions of the problem.

$$[K]^{-1}\{P\} = \{D\} \tag{2.14}$$

where:

[K] -global stiffness matrix of the finite element

{D} -vector of nodal displacements

{P} -vector of nodal forces

*2.5.2 ABAQUS Software*

ABAQUS is a very powerful finite element modeling software that can solve problems implementing linear and nonlinear analysis. It is able to model virtually any geometry and the behavior of most typical engineering materials using its extensive library of elements and material models (ABAQUS, 2007). Some of the materials that can be modeled with ABAQUS are:

- Metals

- Rubber
- Polymers
- Composites
- Reinforced Concrete
- Crushable and Resilient Foams
- Geotechnical Materials such as Soils and Rocks

In nonlinear analysis such as viscoelastic modeling, ABAQUS automatically selects load increments and convergence tolerances, and keep adjusting these values during the analysis to ensure that an accurate solution is obtained (ABAQUS, 2007). As mentioned in previous sections, HMA is a viscoelastic material, and ABAQUS has the capability of modeling these materials using either the Time-Domain or the Frequency-Domain Viscoelasticity model available in its material models library.

The Time-Domain and the Frequency-Domain Viscoelasticity models describe the viscoelastic material behavior assuming that the shear and volumetric behaviors are independent in multiaxial stress states, except when elastomeric foams are modeled. Both can be used to model problems where large strains are expected. The Time-Domain Viscoelasticity model is active only in analyses such as transient static analysis, implicit and explicit dynamics analyses, steady-state transport analysis, fully coupled thermal-stress analysis, and coupled pore fluid diffusion and stress analysis. On the other hand, the Frequency-Domain Viscoelasticity model is active only in analyses such as the direct-solution steady-state dynamic analysis, subspace-based steady-state dynamic analysis, natural frequency extractions, and the complex eigenvalue extractions (ABAQUS, 2007).

Previous works on HMA finite element modeling have implemented two types of analyses: Quasi-Static and Dynamic analyses. Quasi-Static analyses take into account the dynamic loading effect through material properties with arbitrary time histories. Dynamic analyses, on the other hand, takes into account the inertial effects in the analysis of the pavement structure, which is not considered in the quasi-static analysis (Yin et al., 2007). Dynamic analyses are very complicated because both vehicle-tire and pavement surface have to be modeled, and extensive material properties are needed.

# CHAPTER 3

# THE US-75 PERPETUAL PAVEMENT EXPERIMENT

## 3.1 Background

Kansas Department of Transportation (KDOT) developed a field trial to investigate the suitability of the Perpetual Pavement concept for Kansas highway pavements in 2005. The experiment involved the construction of four thick pavement structures on a new segment of highway US-75 near Sabetha, Kansas, in Brown County. A four-mile long segment connecting Fairview and Sabetha (Figure 3-1) was constructed since the exiting US-75 (a North-South corridor) was overlapping a two mile stretch of US-36 (an East-West corridor). KDOT selected this construction project since it was a new construction in the 2005 construction season, that serves on a corridor with medium to high truck traffic volume and, it is long enough to accommodate four 500 feet-long experimental sections on an uniform natural sub-grade.

The development of the field trial aimed to:

- Validate the two approaches of the Perpetual Pavement Concept, by comparing the endurance limit recommended in the literature with the measured horizontal tensile strains induced in the pavements by a 18,000 lbs single axle load;
- Evaluate the cost effective full-depth asphalt pavements HMA Designs, by comparing four alternate design of long-lasting full-depth asphalt pavements;

- Compare the measured horizontal tensile strains at the bottom of thick full-depth asphalt pavements with those computed with linear elastic and visco-elastic models for flexible pavement structures.

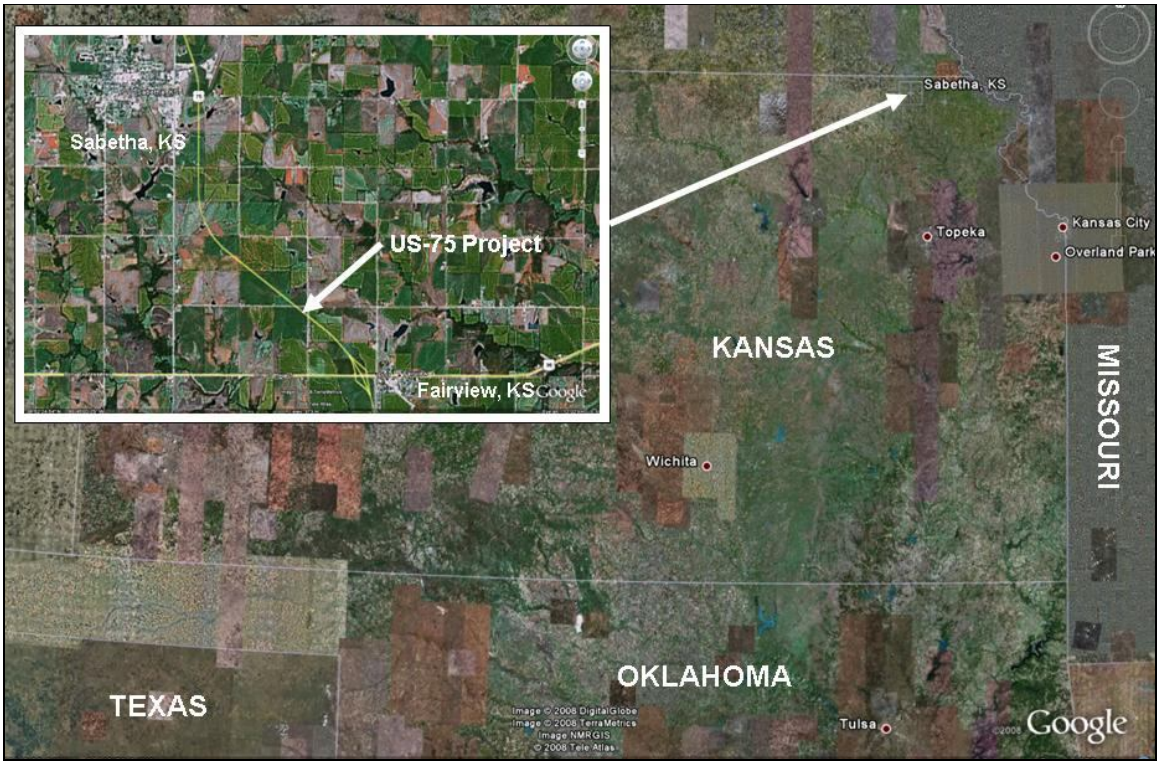


Figure 3-1: Project Location (GoogleEarth, 2008)

## 3.2 Design of Pavement Structures

The pavement structures are given in Table 3-1, the sections are numbered in the order they were constructed, from South going North. The estimated design cumulative traffic for these pavements was 2.6 million (10 years) and 5.7 million (20 years) ESALs per lane. The traffic volume in the initial year was estimated to be 240,000 ESALs per lane. The annual growth rate was estimated to be close to 1.8 percent.

For this traffic data, KDOT provided the design for a long-lasting pavement structure. With an estimated average design resilient modulus for the sub-grade soil of 2,500 psi (17.5MPa), the thickness of asphalt layer obtained for this pavement section (Section 4) was 16 inches (400mm). Kansas Asphalt Pavement Association (KAPA) provided the design of three other pavement structures, for which it was estimated that the tensile strain at the bottom of the asphalt layer is smaller than 70 microstrain, the endurance limit proposed in the literature based on laboratory fatigue tests on asphalt mixes.

Thompson (2006) provided the design for the KAPA standard structure (Section 1) assuming that flexural strains of less than 70 microstrains at the bottom of the HMA layer do not contribute to Cumulative Fatigue Damage, so HMA bottom-up fatigue distress should not occur. He calculated the flexural strains for each month of the year based on the ILLI-PAVE algorithm:

$$\text{Log}(\varepsilon_{HMA}) = 5.746 - 1.589 * \log(T_{HMA}) - 0.774 * \log(E_{HMA}) - 0.097 * \log(E_{Ri}) \qquad (3.1)$$

where:

$\varepsilon_{HMA}$ = HMA flexural strain (micro-strain)

$T_{HMA}$ = HMA thickness (inches)

$E_{HMA}$ = HMA modulus (ksi)

$E_{Ri}$ = Subgarde modulus (ksi)

The HMA modulus for each month was estimated based on the volumetric properties of the HMA mix, binder grade and the Mean Monthly Pavement Temperature

(MMPT) (Thompson, 2006). The 6-inch lime-treated sub-grade layer was not considered in the analysis. The sub-grade modulus, $E_{Ri}$, was assumed to be 5.0 ksi (35MPa).

The following HMA fatigue algorithm was considered in estimating, for each month, the number of load application, $N_a$, to initiate a fatigue crack:

$$N_a = \frac{8.2\times10^{-8}}{\left[ 1/\varepsilon_{HMA} \right]^{3.5}} \tag{3.2}$$

For those months when the HMA strains were less than 70 micro-strain, it was considered than no fatigue damage accumulates.

In order to validate the second approach of the Perpetual Pavement concept, KAPA proposed another pavement structure, that was build in Section 3. This structure has the same thicknesses for the HMA layers as section one. However, a softer binder was used in the construction of the base HMA mix (PG 64-22 instead of PG70-22) and a richer and more ductile HMA mix was used in the bottom lift of the base layer. This mix had a binder content, $P_b$= 6.0%, and different volumetric properties (Design Air Voids = 3%±2%; VFA=77%) than the mix used in the same lift in Section 1 ($P_b$= 5.7%, Design Air Voids = 4%±2%; VFA=72%). It is expected that this mix will have a longer fatigue life.

Thompson also provided the design of a thinner section, with a predicted fatigue life of 30 million ESALs per lane, which corresponds to a reliability factor of about 5.2, or a reliability level of 85%. This section, named the High Reliability Structure, was built in Section 2. It has a total thickness of the HMA layers of 11 inches (280mm).

For the four sections, Andrew Gisi from KDOT, has estimated the life, in years, with the statistical-empirical design method recommended by the 1993 AASHTO Design Guide for Pavement Structures. The estimated life are given in Table 3-1.

Table 3-1: The Configuration and Design Life of the Pavements

<table>
<tr><td>Section</td><td>1</td><td>2</td><td>3</td><td>4</td></tr>
<tr><td>Acronym</td><td>KAPA<br>(Standard)<br>Sta.13+000<br>- 13+305</td><td>High<br>Reliability<br>Sta.13+395<br>- 13+700</td><td>KAPA 2<br>(Modified)<br>Sta.13+790<br>- 14+095</td><td>KDOT<br>Sta.14+185<br>- 14+490</td></tr>
<tr><td colspan="5"></td></tr>
<tr><td>Wearing Course</td><td colspan="4">1.5 inches, SM 9.5A (PG70-28)</td></tr>
<tr><td>Binder Course</td><td colspan="4">2.5 inches, SM 19A (PG70-28)</td></tr>
<tr><td>Base Course</td><td>9.0 inches,<br>SM 19A<br>(PG70-22)</td><td>7.0 inches,<br>SM 19A<br>(PG64-22)</td><td>9.0 inches,<br>SM 19A<br>(PG64-22)*</td><td>12.0 inches,<br>SM 19A<br>(PG64-22)</td></tr>
<tr><td>Chemically Stabilized Embankment Soil</td><td colspan="4">6.0 inches, 6% hydrated lime mixed to the natural soil</td></tr>
<tr><td>Natural Sub-grade</td><td colspan="2">High plasticity clay (A-7-6)</td><td colspan="2">High plasticity clay (A-7-6)</td></tr>
<tr><td>Years of Design Life @ Reliability<br>1993 AASHTO method</td><td>6 @ 85%<br>18 @ 50%</td><td>2.5 @ 85%<br>7 @ 50%</td><td>6 @ 85%<br>18 @ 50%</td><td>10 @ 85%<br>68 @ 50%</td></tr>
</table>

(*) the bottom 3" was designed at 3% air voids for a binder rich layer
(*$P_b$= 6.0%, Design Air Voids = 3%±2%; VFA=77%*)

## 3.3 Construction of the Experimental Sections

The test sections were constructed on a fill and each was approximately 1,300 feet long (390m) with approximately 500 ft (150m) transition zones between them. The contractor, Dobson Brothers, commenced the earthwork in July 2004. The geotechnical investigation identified two natural sub-grade soils along the project, based on their appearance. However, the laboratory tests indicated that they are both high plasticity clays. No significant statistical difference was found between the resilient moduli of the two natural soils.

The embankment on all four pavement sections was brought to grade and the top six inches of soil were stabilized with 6% by weight hydrated lime in May 2005 to ensure proper support to the asphalt concrete layers and to provide a stable support for the construction equipment. Appropriate measures were taken for the proper curing of the lime treated soil.

The asphalt paving work was done in June 2005, according to the schedule given in Table 3-2. The project was completed and the experimental sections were opened to traffic at the beginning of November 2005.

Table 3-2: Construction Dates – HMA Layers

| Lift | Section 1 (KAPA) | Date Placed | Section 2 (High Reliability) | Date Placed |
|---|---|---|---|---|
| Top | 40 mm SM-9.5A PG70-28 | 6/27/05 | 40 mm SM-9.5A PG70-28 | 6/27/05 |
| Mid | 60 mm SM-19A PG70-28 | 6/23/05 | 60 mm SM-19A PG70-28 | 6/23/05 |
| Base | 60 mm SM-19A PG70-22 | 6/18/05 | 75 mm SM-19A PG64-22 | 6/15/05 |
| Base | 65 mm SM-19A PG70-22 | 6/15/05 | 100 mm SM-19A PG64-22 | 6/2/05 |
| Base | 100 mm SM-19A PG70-22 | 6/2/05 | n/a | |
| Base | n/a | | n/a | |
| Lift | Section 3 (KAPA Modified) | Date Placed | Section 4 (KDOT) | Date Placed |
| Top | 40 mm SM-9.5A PG70-28 | 6/27/05 | 40 mm SM-9.5A PG70-28 | 6/27/05 |
| Mid | 60 mm SM-19A PG70-28 | 6/23/05 | 60 mm SM-19A PG70-28 | 6/23/05 |
| Base | 60 mm SM-19A PG64-22 (4%) | 6/20/05 | 75 mm SM-19A PG64-22 | 6/22/05 |
| Base | 65 mm SM-19A PG64-22 (4%) | 6/18/05 | 65 mm SM-19A PG64-22 | 6/20/05 |
| Base | 100 mm SM-19A PG64-22 (3%) | 6/2/05 | 60 mm SM-19A PG64-22 | 6/14/05 |
| Base | n/a | | 100 mm SM-19A PG64-22 | 6/2/05 |

## 3.4 Materials

### *3.4.1 Sub-grade Soil*

The geotechnical investigation conducted by KDOT geotechnical engineers identified two natural sub-grade soils along the project, based on their appearance. The laboratory tests they conducted indicated that the soils are both high plasticity clays. Details of the soil characteristics are given in Table 3-3 while the gradation curves are shown in Figure 3-2 and the moisture-density curves are given in Figures 3-3 and 3-4.

Table 3-3: Characteristics of the Sub-grade Soils

| **Soil** | **A** | **B** |
|---|---|---|
| Location sample was taken | Sta. 13+540 | Sta. 14+385 |
| Liquid Limit (AASTHO T 89-96) | 59 | 57 |
| Plastic Limit (AASHTO T 90-00) | 24 | 25 |
| Plasticity Index | 35 | 32 |
| Specific Gravity (Passing No. 10) | 2.65 | 2.63 |
| Maximum Dry Density (pcf - kg/m3) | 95.0 | 96.5 |
| Optimum Moisture Content (%) | 24 | 22 |
| AASHTO Soil Classification | A-7-6 | A-7-6 |
| KS/ Unified Soil Classification | C-CH | C-CH |

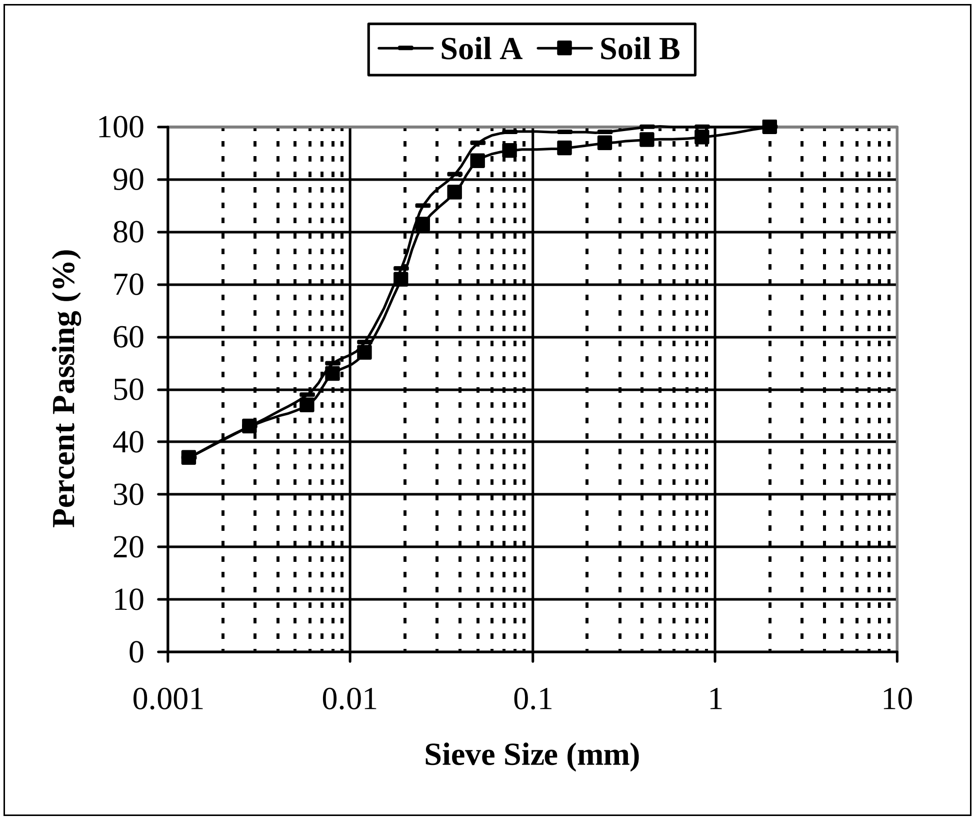


Figure 3-2: Sub-grade Soils – Gradation Analysis Results

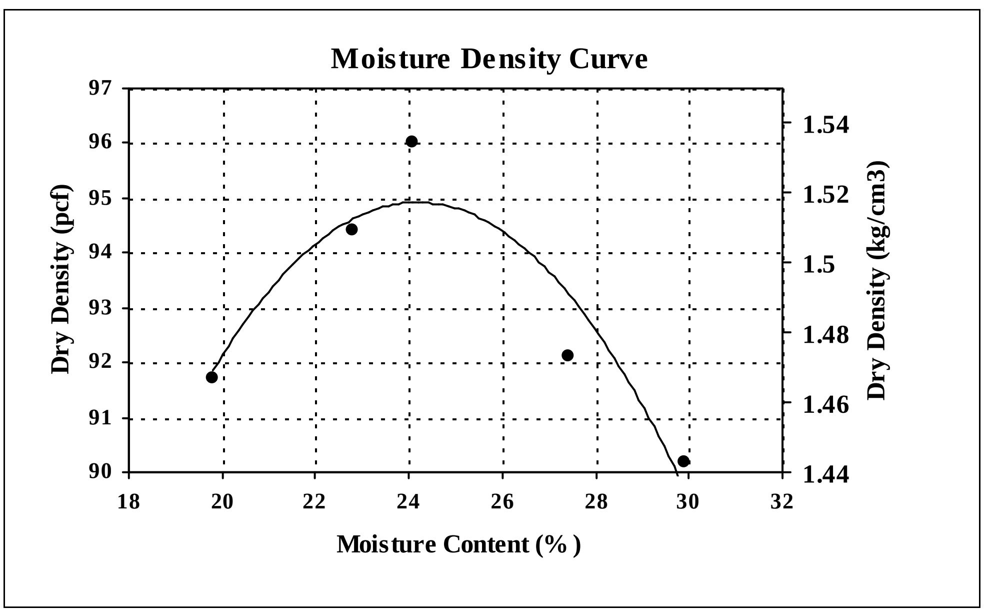


Figure 3-3: Standard Proctor Test Results for Soil A

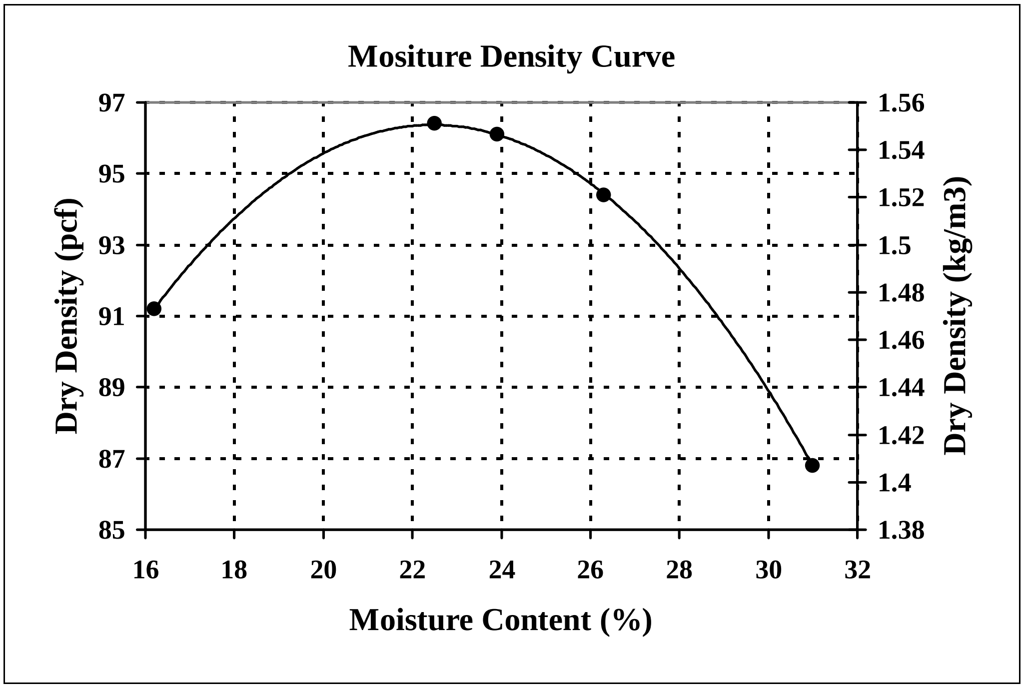


Figure 3-4: Standard Proctor Test for Soil B

Sufficient quantities of the two sub-grade soils were tested to determine their resilient modulus in the Advanced Asphalt Laboratory at Kansas State University. The tests were carried out by graduate students from the department of civil engineering under the guidance of Dr. Stefan Romanoschi. The Triaxial Resilient Modulus tests were performed on an IPC UTM-25 hydraulic testing machine following the AASHTO T 307-99 test protocol. The results of the triaxial resilient modulus tests, given in Table 3-4 and Figures 3-5 and 3-6, show that the resilient modulus decreased with the confining pressure and moisture content and increased with the compaction level. No significant differences were observed between the two soils.

Table 3-4: Triaxial Resilient Modulus (MPa) Test Results

| Relative Density (%) | Moisture Content (%) | Deviator Stress (kPa) | | | | |
|---|---|---|---|---|---|---|
| | | 23.8 | 37.5 | 50.8 | 71.2 | 105.2 |
| Soil A | | | | | | |
| 90 | 19.0 | 104.7 | 95.7 | 86.1 | 79.6 | 70.6 |
| | 21.0 | 100.6 | 89.4 | 81.2 | 71.2 | 70.2 |
| | 24.0 | 70.4 | 62.1 | 58.8 | 57.4 | - |
| | 27.0 | 80.0 | 64.0 | 50.1 | 45.7 | - |
| 95 | 19.0 | 128.2 | 115.3 | 109.1 | 103.6 | 93.6 |
| | 21.0 | 126.6 | 107.6 | 108.8 | 102.0 | 89.2 |
| | 24.0 | 127.2 | 116.5 | 101.3 | 88.9 | 68.0 |
| | 27.0 | 83.8 | 59.7 | 49.4 | 47.5 | - |
| 100 | 19.0 | 167.6 | 160.0 | 155.5 | 146.5 | 132.9 |
| | 21.0 | 155.0 | 140.5 | 130.8 | 114.2 | 92.4 |
| | 24.0 | 149.7 | 148.4 | 134.6 | 121.8 | 98.1 |
| | 27.0 | 93.3 | 78.7 | 58.5 | 45.9 | - |
| Soil B | | | | | | |
| 90 | 17.0 | 113.7 | 107.1 | 97.2 | 88.8 | 69.3 |
| | 19.0 | 118.1 | 111.8 | 111.5 | 98.5 | 84.6 |
| | 22.0 | 94.9 | 88.8 | 77.7 | 66.0 | 54.3 |
| | 25.0 | 94.3 | 73.6 | 62.2 | 59.7 | |
| 95 | 17.0 | 206.2 | 167.1 | 163.0 | 143.5 | 121.8 |
| | 19.0 | 152.8 | 140.1 | 129.4 | 113.8 | 95.9 |
| | 22.0 | 141.6 | 122.8 | 105.7 | 92.0 | 70.8 |
| | 25.0 | 97.4 | 76.3 | 61.3 | 48.9 | 46.1 |
| 100 | 17.0 | 210.8 | 143.1 | 140.1 | 136.7 | 122.7 |
| | 19.0 | 149.1 | 143.1 | 128.9 | 116.2 | 101.1 |
| | 22.0 | 187.0 | 160.6 | 144.3 | 112.0 | 88.2 |
| | 25.0 | 94.0 | 70.6 | 58.5 | 46.5 | 48.5 |

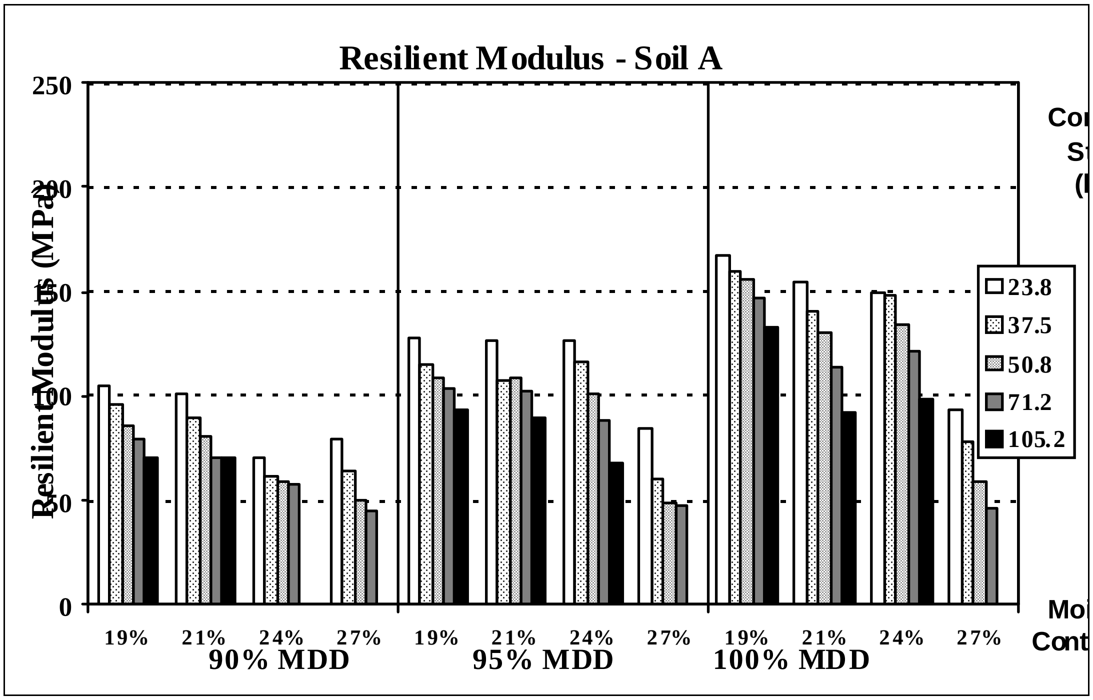


Figure 3-5: Laboratory Resilient Modulus – Untreated Soil A

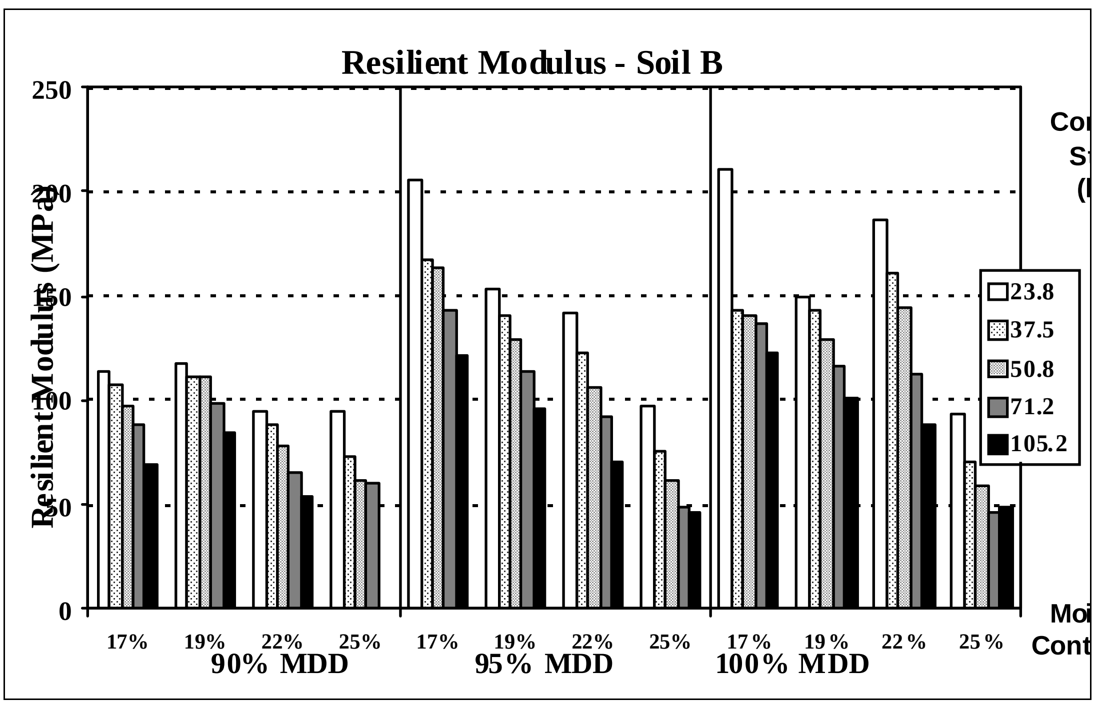


Figure 3-6: Laboratory Resilient Modulus – Untreated Soil B

*3.4.2 Lime Treated Embankment Soil*

In order to reduce the stresses induced by the moving traffic and provide frost protection to the existing sub-grade soils, the top six inches of the sub-grade soils were mixed in-place with six percent lime. Sufficient quantities of lime treated soils were obtained by KDOT personnel from the constructions site. The soils were compacted in the lab at the same density as that recorded in the field, to obtain 6 inch tall by 3 inch diameter test specimens. The specimens were then cured in the moist room.

Triaxial Resilient Modulus tests were performed on samples cured 7, 28, 60 and 90 days using the IPC UTM-25 hydraulic testing machine and following the same test protocol as for the untreated soils. The results of the triaxial resilient modulus tests are provided in Table 3-5 and Figures 3-7. They show that the resilient modulus exhibited some decreased with the curing time. No significant differences were observed between the two lime-treated soils.

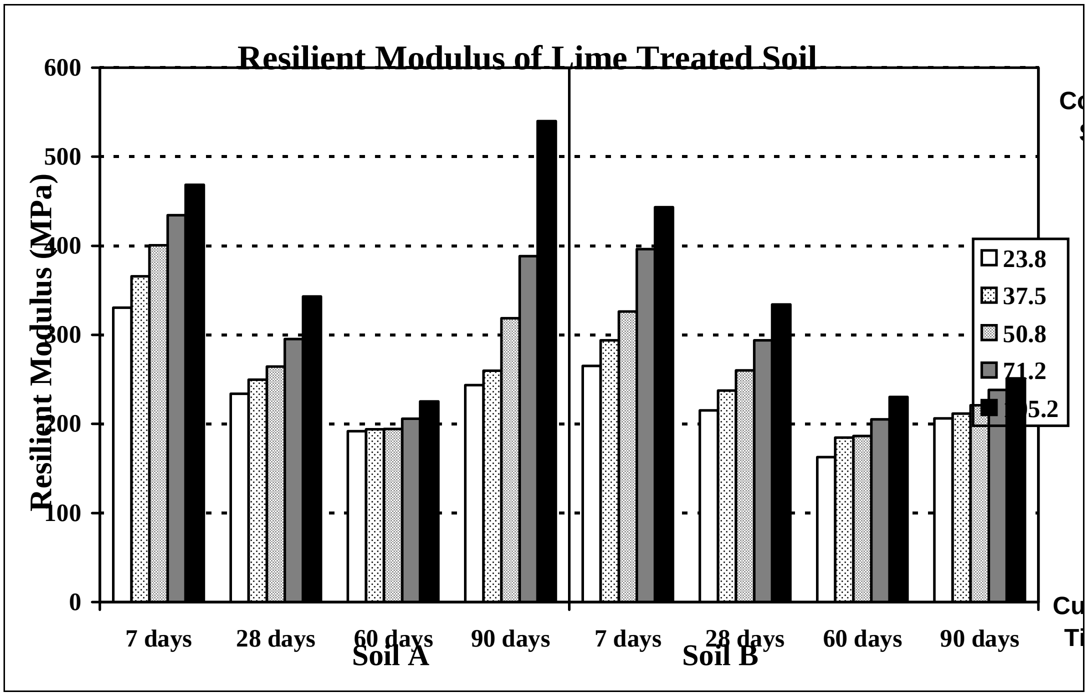


Figure 3-7: Average Resilient Modulus – Lime Treated Soils

Table 3-5: Resilient Modulus (MPa) of Lime Treated Soil

| Curing Time (days) | Deviator Stress (kPa) | Sample # 1 | 2 | 3 | 4 | 5 | 6 | 7 | Mean | CV (%) |
|---|---|---|---|---|---|---|---|---|---|---|
| | | **SOIL A** | | | | | | | | |
| 7 | 23.8 | 254.4 | 464.7 | 457.8 | 201.3 | 273.4 | 242.1 | 421.1 | 330.7 | 34.0 |
| | 37.5 | 291.6 | 607.0 | 462.0 | 205.6 | 274.0 | 251.2 | 467.8 | 365.6 | 40.3 |
| | 50.8 | 329.7 | 683.3 | 496.7 | 207.7 | 295.2 | 275.9 | 515.9 | 400.6 | 42.2 |
| | 71.2 | 340.2 | 771.2 | 550.5 | 220.7 | 323.6 | 294.2 | 540.7 | 434.4 | 44.5 |
| | 105.2 | 361.5 | 875.9 | 668.9 | 251.4 | 338.3 | 333.0 | 450.5 | 468.5 | 47.8 |
| 28 | 23.8 | 228.5 | 216.7 | 355.0 | 180.2 | 194.3 | 281.3 | 180.7 | 233.8 | 27.3 |
| | 37.5 | 255.0 | 219.4 | 375.8 | 181.6 | 218.8 | 305.0 | 192.3 | 249.7 | 27.7 |
| | 50.8 | 279.2 | 213.9 | 380.9 | 195.9 | 230.3 | 308.2 | 242.6 | 264.4 | 24.2 |
| | 71.2 | 319.0 | 227.2 | 405.0 | 219.5 | 256.4 | 359.3 | 280.2 | 295.2 | 23.5 |
| | 105.2 | 376.1 | 255.2 | 463.6 | 247.0 | 295.2 | 429.5 | 335.9 | 343.2 | 24.5 |
| 60 | 23.8 | 277.2 | 138.2 | 169.7 | 113.9 | 151.1 | 257.4 | 235.2 | 191.8 | 33.4 |
| | 37.5 | 259.3 | 132.0 | 169.2 | 121.9 | 184.3 | 264.1 | 227.7 | 194.1 | 29.8 |
| | 50.8 | 149.2 | 136.1 | 211.7 | 129.9 | 208.6 | 281.1 | 245.2 | 194.5 | 29.8 |
| | 71.2 | 153.2 | 143.1 | 223.5 | 145.9 | 239.9 | 273.1 | 261.2 | 205.7 | 27.6 |
| | 105.2 | 142.3 | 158.2 | 253.0 | 169.1 | 265.1 | 291.8 | 297.0 | 225.2 | 29.5 |
| | 37.5 | 301.5 | 130.3 | 261.9 | 197.1 | 498.4 | 242.2 | 186.9 | 259.8 | 45.8 |

Table 3-5 - *Continued*

| Curing Time (days) | Deviator Stress (kPa) | Sample # 1 | 2 | 3 | 4 | 5 | 6 | 7 | Mean | CV (%) |
|---|---|---|---|---|---|---|---|---|---|---|
| | | **SOIL A** | | | | | | | | |
| | 105.2 | 409.4 | 867.7 | 256.1 | 339.6 | 1178.7 | 359.7 | 368.2 | 539.9 | 63.9 |
| | | **SOIL B** | | | | | | | | |
| 7 | 23.8 | 167.2 | 431.3 | 130.8 | 104.5 | 338.8 | 418.3 | | 265.2 | 55.9 |
| | 37.5 | 185.6 | 503.2 | 136.4 | 101.6 | 336.4 | 499.4 | | 293.8 | 61.2 |
| | 50.8 | 208.5 | 589.9 | 154.6 | 112.5 | 369.9 | 521.1 | | 326.1 | 61.1 |
| | 71.2 | 249.3 | 725.3 | 177.1 | 124.2 | 546.0 | 555.5 | | 396.2 | 61.8 |
| | 105.2 | 302.2 | 902.0 | 209.8 | 141.6 | 680.9 | 424.6 | | 443.5 | 66.3 |
| 28 | 23.8 | 265.7 | 252.2 | 146.9 | 183.1 | 185.0 | 258.5 | | 215.2 | 23.1 |
| | 37.5 | 307.1 | 288.1 | 171.4 | 185.8 | 206.7 | 265.3 | | 237.4 | 24.0 |
| | 50.8 | 352.7 | 298.0 | 203.4 | 200.6 | 225.1 | 281.8 | | 260.3 | 23.3 |
| | 71.2 | 411.0 | 275.2 | 253.2 | 240.6 | 266.6 | 316.5 | | 293.9 | 21.4 |
| | 105.2 | 468.4 | 293.0 | 308.1 | 283.4 | 317.6 | 334.6 | | 334.2 | 20.4 |
| 60 | 23.8 | 169.4 | 108.9 | 184.9 | 153.0 | 177.1 | 183.7 | | 162.8 | 17.7 |
| | 37.5 | 182.4 | 151.8 | 194.6 | 194.4 | 185.8 | 199.8 | | 184.8 | 9.4 |
| | 50.8 | 192.5 | 148.4 | 195.5 | 177.6 | 197.7 | 206.2 | | 186.3 | 11.2 |
| | 71.2 | 210.9 | 169.9 | 214.6 | 195.8 | 220.0 | 219.3 | | 205.1 | 9.4 |
| | 105.2 | 245.7 | 191.1 | 228.9 | 219.8 | 250.6 | 246.5 | | 230.4 | 9.8 |
| 90 | 23.8 | 264.7 | 184.9 | 231.2 | 186.7 | 175.6 | 194.5 | | 206.3 | 16.7 |
| | 37.5 | 270.1 | 186.8 | 213.0 | 209.6 | 188.4 | 201.4 | | 211.6 | 14.5 |
| | 50.8 | 288.3 | 197.3 | 212.5 | 214.6 | 196.0 | 216.4 | | 220.9 | 15.5 |
| | 71.2 | 302.6 | 204.1 | 232.5 | 238.0 | 212.2 | 239.9 | | 238.2 | 14.6 |
| | 105.2 | 295.6 | 206.5 | 250.2 | 260.3 | 235.9 | 258.3 | | 251.1 | 11.7 |

### *3.4.3 Hot Mix Asphalt*

As mentioned in Section 3-2 and shown in Table 3-1, five different HMA mixes were used in the construction of the four experimental pavement sections. The mix designs of all five mixes are given in Table 3-6. The aggregate gradation data and volumetric properties, as well as binder grade are provided in Table 3-6 while the gradation curves are shown in Figures 3-8 and 3-9. The mixes were designed following the Superpave mix design method.

On all sections, mixes S and M were used in the construction of the wearing and binder courses, respectively. They had a stiff, polymer modified binder (PG70-28). Mix 1 was used only for the base layer of Section 1 (KAPA); 5.5% of polymer modified binder (PG70-22) was used for this mix. Mixes 3 and 4 had the same aggregate structure and binder (PG64-22). However, Mix 3 had higher binder content than Mix 4, in order to achieve the design air void content of 3%. This was done to obtain a bitumen rich, ductile mix to be used only for the bottom lift of the base layer of Section 3. Mixes M, 1, 3 and 4 had the same aggregate structure (Figure 3-9).

Sufficient quantities of binder and aggregated were obtained from the asphalt plant by KDOT personnel. The materials were transported to the Office of Materials and Research of KDOT where cylindrical specimens, 6 inch in diameter and 8 inch tall, were manufactured using the Superpave Gyratory Compactor. The specimens, compacted at the target air void content of 7.0% were cored and trimmed to obtain cylindrical samples 4 inch in diameter and 6 inch tall. The samples were transported at the Advanced Asphalt Laboratory of Kansas State University to determine the dynamic modulus of the five HMA mixes used n the Perpetual Pavement projects.

Table 3-6: HMA Mix Designs

| | Mix | | | | |
|---|---|---|---|---|---|
| | S | M | 1 | 3 | 4 |
| Lab No. | 1G04057A | 1G04036A | 1G05020A | 1G05021A | 1G05024A |
| Gradation Analysis Percent Passing | | | | | |
| Sieve Size (mm) | | | | | |
| 25.4 (1”) | 100 | 100 | 100 | 100 | 100 |
| 19 (3/4") | 100 | 95 | 95 | 95 | 95 |
| 12.5 (1/2") | 100 | 86.8 | 86.8 | 86.8 | 86.8 |
| 9.5 (3/8") | 97.75 | 81.72 | 81.54 | 81.54 | 81.54 |
| 4.75 (#4) | 81.3 | 70.6 | 69.3 | 69.3 | 69.3 |
| 2.36 (#8) | 50 | 47.08 | 45.16 | 45.16 | 45.16 |
| 1.18 (#16) | 33.75 | 32.44 | 30.68 | 30.68 | 30.68 |
| 0.6 (#30) | 21.3 | 19.16 | 17.82 | 17.82 | 17.82 |
| 0.3 (#50) | 10.35 | 9.28 | 8.76 | 8.76 | 8.76 |
| 0.15 (#100) | 4.35 | 2.98 | 2.96 | 2.96 | 2.96 |
| 0.075(#200) | 3.55 | 2.664 | 2.698 | 2.698 | 2.698 |
| Volumetric Property | | | | | |
| Binder PG grade | PG70-28 | PG70-28 | PG70-22 | PG64-22 | PG64-22 |
| NMAS (mm) | 9.5 | 19 | 19 | 19 | 19 |
| Pb (%) | 6.2 | 5.15 | 5.5 | 6.00 | 5.7 |
| Gmm | 2.421 | 2.440 | 2.424 | 2.399 | 2.417 |
| Gmb | 2.322 | 2.334 | 2.323 | 2.327 | 2.320 |
| Gsb | 2.572 | 2.567 | 2.566 | 2.566 | 2.566 |
| VMA (%) | 15 | 13.5 | 14.2 | 14.5 | 14.5 |
| Va (%) | 4.06 | 4.33 | 4.15 | 2.99 | 4.02 |
| VFA (%) | 73 | 68 | 68 | 77 | 72 |
| TSR (%) | 86 | 80 | 88 | 88 | 88 |
| % Saturation | 55.9 | 59.3 | 56.8 | 56.8 | 56.8 |
| Sand Equivalent | 77 | 75 | 79 | 79 | 79 |
| CAA | 100 | 100 | 100 | 100 | 100 |
| $N_{ini}$ | 8 | 8 | 8 | 8 | 8 |
| $N_{des}$ | 100 | 100 | 100 | 100 | 100 |
| $N_{max}$ | 160 | 160 | 160 | 160 | 160 |
| %Gmm @ Nini | 86.9 | 88 | 86.9 | 87.9 | 86.5 |
| %Gmm @ Ndes | 95.9 | 95.7 | 95.8 | 97.0 | 95.0 |
| %Gmm @ Nmax | 97.1 | 96.7 | 97.1 | 98.4 | 97.4 |

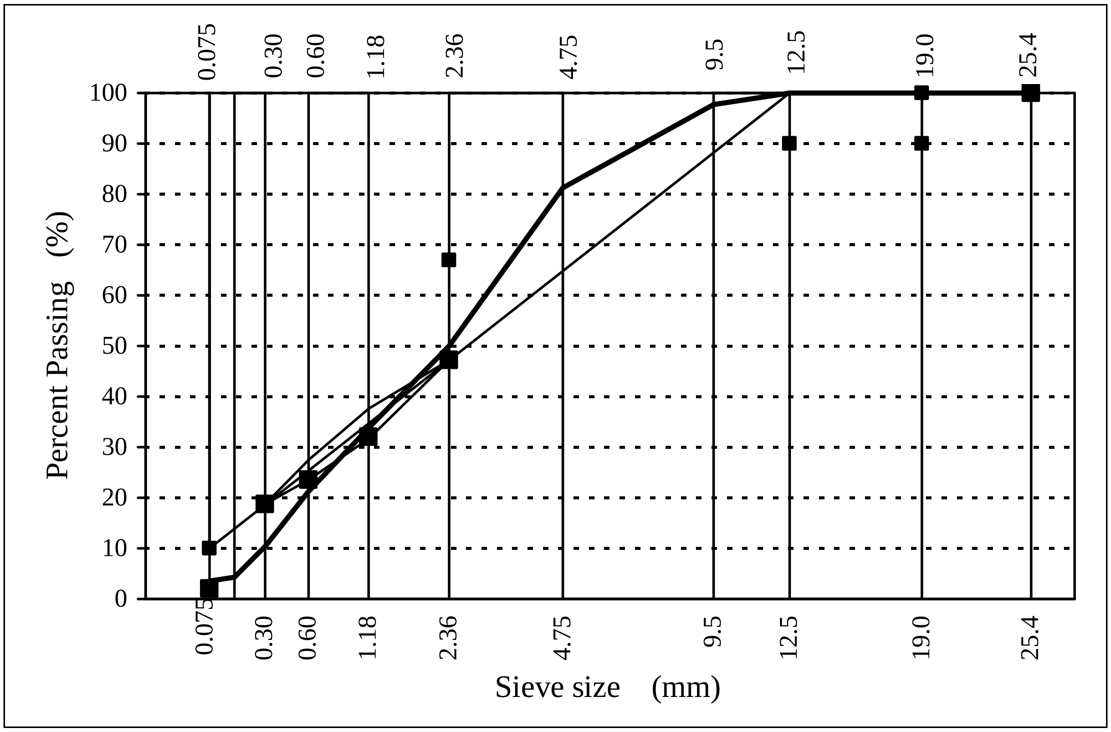


Figure 3-8: Aggregate Gradation Chart for Mix S

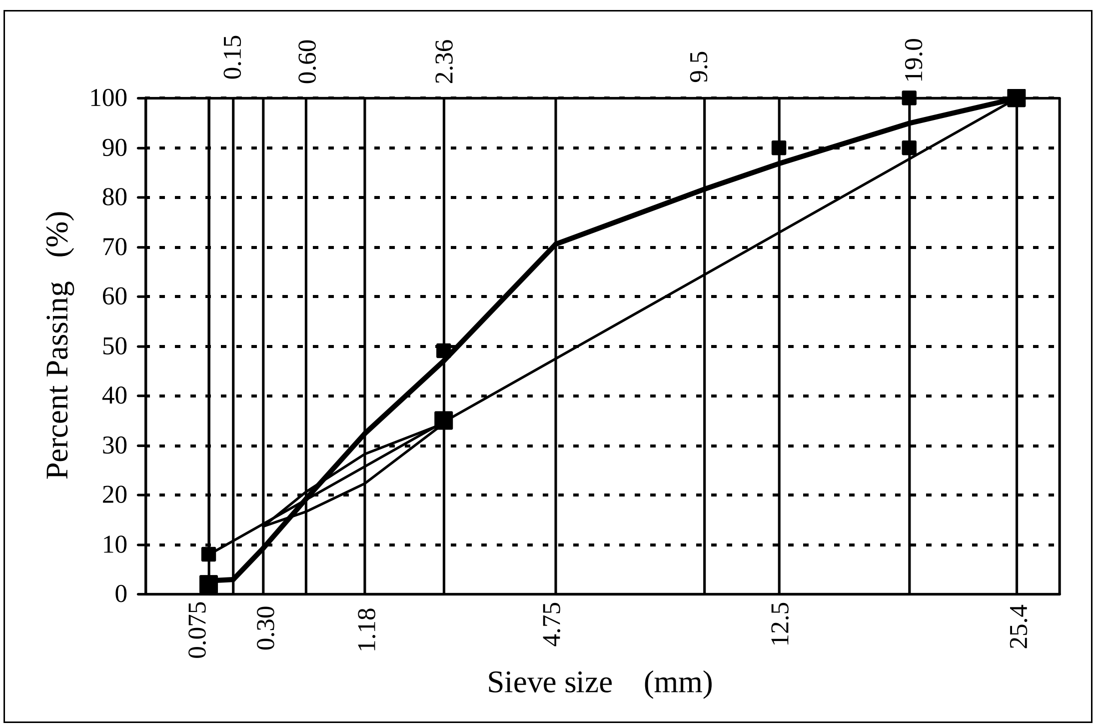


Figure 3-9: Aggregate Gradation Chart for Mixes M, 1, 3, and 4

A Universal Testing Machine (UTM) produced by Industrial Process Controls (IPC), Melbourne, Australia, was used for the asphalt dynamic modulus testing. The UTM system, shown in Figure 3-10 has four main components; the Control and Data Acquisition System (CDAS), the Hydraulic System, the Personal Computer (PC) and the Environmental Chamber.

A hydraulic servo valve that is electrically controlled connects the actuator to the hydraulic pressure system. The magnitude of the load to be applied is controlled by the CDAS and the hydraulic servo valve is adjusted accordingly. The CDAS in turn receives feedback from the load cell that applies the load onto the specimen through the actuator. The strains recorded by the LVDTs mounted on the specimen also sent to the CDAS. The loads and displacements are thus monitored and adjusted by a closed loop mechanism between the hydraulic servo valve, load cell, LVDTs and the CDAS. The loading is precisely controlled by the hydraulic system and therefore the stresses and strains are accurately generated and measured.

The environmental chamber controls and maintains the temperature in the testing frame so that the specimens are tested at desired temperature. Temperatures ranging from -15° to 60° C can be maintained in the chamber with a precision of ±0.5°C.

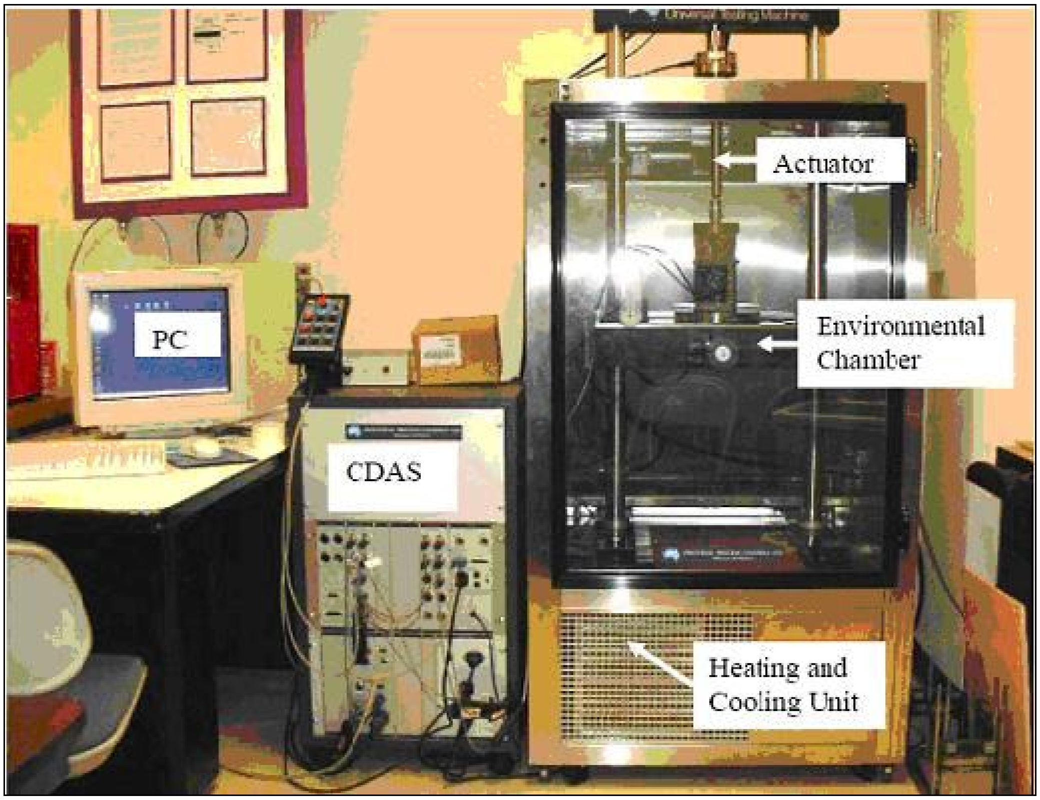


Figure 3-10: Universal Testing Machine Set Up

The dynamic modulus test is a cyclic test performed on cylindrical asphalt specimens of 100 mm diameter and 150 mm height. During the test, a sinusoidal (haversine) axial compressive load is applied to a specimen at a given temperature and loading frequency. The asphalt specimens were tested at five temperatures (4, 10, 20, 30, and 35°C) and six load frequencies (25, 10, 5, 1, 0.5, and 0.1 Hz). The specimens were conditioned in the environmental chamber for at least two hours before testing.

Three linear variable differential transducers (LVDTs) were mounted along the circumference of the specimen using a system of screws and nuts glued with epoxy. The distance from the center line of the two horizontal screws glued to the specimen to hold the LVDT is set at 100 mm and is termed as gage length. The specimen is centered on the bottom of a steel plate. A second steel plate is centered on the top of specimen to ensure centric loading. A specimen with LVDTs mounted and centered between top and bottom steel plates is shown in Figure 3-11.


Figure 3-11: Dynamic Modulus Specimen with Mounted LVDTs

The actuator is gradually lowered to touch the top steel plate. Then, the test software is run and the testing process is executed and controlled entirely by the CDAS. The cyclic loading is applied to the specimen by the actuator, through the top steel plate in the decreasing order of frequencies 25, 10, 5, 1, 0.5, and 0.1 Hz.

As the test progresses, the following data are recorded periodically: dynamic load and stress, microstrain, dynamic modulus, Poisson’s ratio, maximum and minimum load displacement, temperature, duration of test and the phase angle. The data for each test are saved in the computer binary files and then in ASCII text files, which are further imported into Microsoft Excel for analysis.

The dynamic resilient modulus E* is the ratio of peak-to-peak stress to the recoverable axial strain under a repeated sinusoidal loading. The dynamic modulus value for each frequency is computed as:

$$E^* = \frac{\sigma_o}{\varepsilon_o} \tag{3.3}$$

where:

E* = dynamic resilient modulus (MPa)

$\sigma_o$ = applied stress (kN)

$\varepsilon_o$ = recoverable strain

The recoverable strain, $\varepsilon_o$, is calculated as:

$$\varepsilon_o = \frac{d}{GL} \tag{3.4}$$

where:

d = average deformation amplitude (mm)

GL = gage length (100mm for all the samples)

The results of the dynamic modulus test are given in Table 3-7 to 3-11, along with the air void content of each sample tested. As expected, the dynamic modulus decreased with temperature and increased with loading frequency. The few exceptions that were observed, for this trend, may be because of the variability in aggregate structure, compaction levels and measurement errors.

Table 3-7: Dynamic Modulus Results for Mix S

| Mix | Sample | Air Voids (%) | Temp. (°C) | Frequency | | | | | |
|---|---|---|---|---|---|---|---|---|---|
| | | | | 25 | 10 | 5 | 1 | 0.5 | 0.1 |
| Dynamic Modulus (MPa) | | | | | | | | | |
| S | 1 | 6.6 | 4 | 14,183 | 13,009 | 12,100 | 9,955 | 9,491 | 7,236 |
| S | 8 | 6.6 | 4 | 11,862 | 10,974 | 10,020 | 8,499 | 7,713 | 6,170 |
| S | 3 | 6.8 | 10 | 9,055 | 7,864 | 7,204 | 5,783 | 5,289 | 4,089 |
| S | 7 | 6.6 | 10 | 11,646 | 9,935 | 9,263 | 7,526 | 6,944 | 5,413 |
| S | 7 | 6.6 | 20 | 8,358 | 6,493 | 5,511 | 3,767 | 3,238 | 2,052 |
| S | 9 | 6.6 | 30 | 3,661 | 2,758 | 2,328 | 1,476 | 1,213 | 807 |
| S | 10 | 6.3 | 30 | 4,202 | 3,155 | 2,594 | 1,722 | 1,447 | 999 |
| S | 6 | 6.9 | 35 | 2,776 | 1,923 | 1,618 | 1,046 | 855 | 608 |
| Phase Angle (degrees) | | | | | | | | | |
| S | 1 | 6.6 | 4 | 5.35 | 5.88 | 9.96 | 12.05 | 15.5 | 17.9 |
| S | 8 | 6.6 | 4 | 5.88 | 7.75 | 9.64 | 12.82 | 16.39 | 18.84 |
| S | 3 | 6.8 | 10 | 8.38 | 11.21 | 13.3 | 16.86 | 21.33 | 27.37 |
| S | 7 | 6.6 | 10 | 9.19 | 8.99 | 11.93 | 15.22 | 18.92 | 23.64 |
| S | 5 | 6.7 | 20 | 16.53 | 19.66 | 22.52 | 25.97 | 31.7 | 32.51 |
| S | 7 | 6.6 | 20 | 14.69 | 16.45 | 19.97 | 24.4 | 29.97 | 33.28 |
| S | 9 | 6.6 | 30 | 19.51 | 21.71 | 24.75 | 28.13 | 34.45 | 33.84 |
| S | 10 | 6.3 | 30 | 21.16 | 23.56 | 26.14 | 28.95 | 35.63 | 34.33 |
| S | 6 | 6.9 | 35 | 23.56 | 24.8 | 26.73 | 27.91 | 33.27 | 30.45 |

Table 3-8: Dynamic Modulus Results for Mix M

| Mix | Sample | Air Voids (%) | Temp. (°C) | Frequency | | | | | |
|---|---|---|---|---|---|---|---|---|---|
| | | | | 25 | 10 | 5 | 1 | 0.5 | 0.1 |
| Dynamic Modulus (MPa) | | | | | | | | | |
| M | 8 | 7.3 | 4 | 13,508 | 12,094 | 11,628 | 9,709 | 9,166 | 7,934 |
| M | 9 | 6.7 | 4 | 15,351 | 14,417 | 13,629 | 11,756 | 11,076 | 9,116 |
| M | 1 | 6.9 | 10 | 14,115 | 12,654 | 11,538 | 9,495 | 8,778 | 6,590 |
| M | 6 | 7.1 | 10 | 13,638 | 12,642 | 11,536 | 9,174 | 8,401 | 6,232 |
| M | 5 | 7.0 | 20 | 6,389 | 4,994 | 4,425 | 3,193 | 2,830 | 1,911 |
| M | 10 | 6.8 | 20 | 8,465 | 7,408 | 6,610 | 5,060 | 4,537 | 3,226 |
| M | 2 | 7.2 | 30 | 5,411 | 4,064 | 3,372 | 2,225 | 1,846 | 1,247 |
| M | 4 | 7.1 | 30 | 5,090 | 3,985 | 3,310 | 2,163 | 1,814 | 1,219 |

Table 3-8 - *Continued*

| Mix | Sample | Air Voids (%) | Temp. (°C) | Frequency | | | | | |
|---|---|---|---|---|---|---|---|---|---|
| | | | | 25 | 10 | 5 | 1 | 0.5 | 0.1 |
| Dynamic Modulus (MPa) | | | | | | | | | |
| M | 3 | 7.5 | 35 | 3,995 | 3,176 | 2,569 | 1,631 | 1,339 | 918 |
| M | 7 | 6.9 | 35 | 5,048 | 3,958 | 3,273 | 2,090 | 1,728 | 1,204 |
| Phase Angle (degrees) | | | | | | | | | |
| M | 8 | 7.3 | 4 | 7.61 | 6.84 | 9.67 | 12.16 | 13.74 | 18.76 |
| M | 9 | 6.7 | 4 | 5.65 | 7.18 | 8.61 | 9.55 | 11.66 | 12.74 |
| M | 1 | 6.9 | 10 | 8.21 | 10.4 | 11.86 | 15.17 | 19.11 | 22 |
| M | 6 | 7.1 | 10 | 9.57 | 10.44 | 13.37 | 16.89 | 19.96 | 23.85 |
| M | 5 | 7.0 | 20 | 10.05 | 12.62 | 15.04 | 18.16 | 23.04 | 25.51 |
| M | 10 | 6.8 | 20 | 14.14 | 15.67 | 18.48 | 22.1 | 26.58 | 27.15 |
| M | 2 | 7.2 | 30 | 19.89 | 21.73 | 24.49 | 26.78 | 32.44 | 30.69 |
| M | 4 | 7.1 | 30 | 19.14 | 21.76 | 25.03 | 27.04 | 32.66 | 31.31 |
| M | 3 | 7.5 | 35 | 21.74 | 22.8 | 25.56 | 27.34 | 33.44 | 32.32 |
| M | 7 | 6.9 | 35 | 19.85 | 22.86 | 25.09 | 27.57 | 33.65 | 32.66 |

Table 3-9: Dynamic Modulus Results for Mix 1

| Mix | Sample | Air Voids (%) | Temp. (°C) | Frequency | | | | | |
|---|---|---|---|---|---|---|---|---|---|
| | | | | 25 | 10 | 5 | 1 | 0.5 | 0.1 |
| Dynamic Modulus (MPa) | | | | | | | | | |
| 1 | 1 | 6.7 | 4 | 18,352 | 16,701 | 15,617 | 13,499 | 12,420 | 9,895 |
| 1 | 2 | 6.8 | 4 | 19,837 | 18,090 | 16,609 | 14,151 | 13,312 | 10,655 |
| 1 | 3 | 6.7 | 10 | 15,579 | 14,000 | 12,693 | 10,163 | 9,449 | 6,915 |
| 1 | 4 | 6.8 | 10 | 16,109 | 14,340 | 13,344 | 11,091 | 10,344 | 7,972 |
| 1 | 5 | 6.8 | 20 | 10,080 | 8,744 | 7,755 | 5,766 | 5,091 | 3,559 |
| 1 | 6 | 7.1 | 20 | 10,668 | 9,380 | 8,247 | 5,993 | 5,336 | 3,540 |
| 1 | 7 | 6.9 | 30 | 6,366 | 5,343 | 4,419 | 2,991 | 2,563 | 1,624 |
| 1 | 8 | 6.6 | 30 | 6,781 | 5,741 | 4,781 | 3,210 | 2,743 | 1,763 |
| 1 | 9 | 6.6 | 35 | 5,657 | 4,413 | 3,671 | 2,405 | 1,998 | 1,317 |
| 1 | 10 | 6.5 | 35 | 5,701 | 4,407 | 3,652 | 2,400 | 2,002 | 1,327 |
| Phase Angle (degrees) | | | | | | | | | |
| 1 | 1 | 6.7 | 4 | 5.8 | 6.12 | 8.19 | 12.24 | 13.61 | 16.32 |
| 1 | 2 | 6.8 | 4 | 6.2 | 6.78 | 9.43 | 12.03 | 13.77 | 16.58 |

Table 3-9 - *Continued*

| Mix | Sample | Air Voids (%) | Temp. (°C) | Frequency | | | | | |
|---|---|---|---|---|---|---|---|---|---|
| | | | | 25 | 10 | 5 | 1 | 0.5 | 0.1 |
| Dynamic Modulus (MPa) | | | | | | | | | |
| 1 | 3 | 6.7 | 10 | 7.2 | 9.91 | 13.2 | 15.54 | 19.83 | 23.44 |
| 1 | 4 | 6.8 | 10 | 6.5 | 9.06 | 10.99 | 14.01 | 16.68 | 20.22 |
| 1 | 5 | 6.8 | 20 | 12.0 | 14.01 | 16.75 | 21.7 | 27.29 | 33.42 |
| 1 | 6 | 7.1 | 20 | 13.7 | 15.85 | 18.38 | 23.09 | 28.11 | 34.4 |
| 1 | 7 | 6.9 | 30 | 16.8 | 20.34 | 23.91 | 27.72 | 35.01 | 37.33 |
| 1 | 8 | 6.6 | 30 | 16.99 | 20.44 | 23.67 | 28.1 | 35.15 | 37.71 |
| 1 | 9 | 6.6 | 35 | 19.85 | 22.32 | 25.37 | 29.07 | 36.14 | 36.54 |
| 1 | 10 | 6.5 | 35 | 19.79 | 22 | 24.5 | 27.27 | 33.48 | 32.39 |

Table 3-10: Dynamic Modulus Results for Mix 3

| Mix | Sample | Air Voids (%) | Temp. (°C) | Frequency | | | | | |
|---|---|---|---|---|---|---|---|---|---|
| | | | | 25 | 10 | 5 | 1 | 0.5 | 0.1 |
| Dynamic Modulus (MPa) | | | | | | | | | |
| 3 | 3 | 6.4 | 4 | 15,466 | 14,024 | 13,056 | 11,104 | 10,466 | 8,585 |
| 3 | 4 | 6.9 | 4 | 16,574 | 15,106 | 14,029 | 11,971 | 11,132 | 9,274 |
| 3 | 1 | 6.7 | 10 | 15,345 | 13,109 | 11,881 | 9,559 | 8,844 | 6,547 |
| 3 | 2 | 7.0 | 10 | 19,488 | 17,486 | 15,989 | 12,730 | 11,801 | 8,605 |
| 3 | 5 | 6.6 | 20 | 10,552 | 10,247 | 8,759 | 6,011 | 5,298 | 3,376 |
| 3 | 6 | 6.3 | 20 | 12,940 | 11,831 | 10,517 | 7,649 | 6,768 | 4,594 |
| 3 | 7 | 6.5 | 30 | 7,459 | 6,191 | 5,084 | 3,255 | 2,772 | 1,736 |
| 3 | 8 | 6.5 | 30 | 7,253 | 5,929 | 4,871 | 3,174 | 2,659 | 1,639 |
| 3 | 9 | 6.5 | 35 | 4,827 | 3,990 | 3,149 | 1,880 | 1,532 | 947 |
| 3 | 10 | 6.5 | 35 | 2,727 | 2,224 | 1,905 | 1,332 | 1,135 | 781 |
| Phase Angle (degrees) | | | | | | | | | |
| 3 | 3 | 6.4 | 4 | 4.73 | 8.05 | 9.68 | 12.83 | 14.64 | 18.56 |
| 3 | 4 | 6.9 | 4 | 5.34 | 7.02 | 9.36 | 11.43 | 12.26 | 15.52 |
| 3 | 1 | 6.7 | 10 | 9.33 | 11.57 | 14.41 | 17.47 | 21.36 | 26.7 |
| 3 | 2 | 7.0 | 10 | 7.8 | 12.45 | 14.65 | 17.61 | 21.14 | 27.19 |
| 3 | 5 | 6.6 | 20 | 12.03 | 17.04 | 20.32 | 26.01 | 33.05 | 41.13 |
| 3 | 6 | 6.3 | 20 | 11.93 | 14.7 | 17.27 | 24.28 | 30.13 | 38.37 |
| 3 | 7 | 6.5 | 30 | 17.12 | 21.07 | 25 | 29.97 | 37.94 | 40.47 |

Table 3-10 - *Continued*

| Mix | Sample | Air Voids (%) | Temp. (°C) | Frequency | | | | | |
|---|---|---|---|---|---|---|---|---|---|
| | | | | 25 | 10 | 5 | 1 | 0.5 | 0.1 |
| Dynamic Modulus (MPa) | | | | | | | | | |
| 3 | 8 | 6.5 | 30 | 18.56 | 23.72 | 25.94 | 31.98 | 39.91 | 42.64 |
| 3 | 9 | 6.5 | 35 | 21.95 | 26.19 | 28.37 | 31.49 | 37.81 | 34.86 |
| 3 | 10 | 6.5 | 35 | 16.35 | 19.28 | 22.52 | 26.83 | 33.84 | 34.96 |

Table 3-11: Dynamic Modulus Results for Mix 4

| Mix | Sample | Air Voids (%) | Temp. (°C) | Frequency | | | | | |
|---|---|---|---|---|---|---|---|---|---|
| | | | | 25 | 10 | 5 | 1 | 0.5 | 0.1 |
| Dynamic Modulus (MPa) | | | | | | | | | |
| 4 | 7 | | 4 | 16,964 | 15,816 | 15,058 | 13,135 | 12,320 | 10,315 |
| 4 | 8 | | 4 | 17,123 | 15,976 | 15,190 | 13,170 | 12,590 | 10,411 |
| 4 | 5 | | 10 | 17,914 | 15,521 | 13,839 | 10,980 | 10,275 | 7,782 |
| 4 | 6 | | 10 | 15,193 | 14,352 | 13,218 | 10,818 | 10,195 | 7,882 |
| 4 | 9 | | 20 | 9,677 | 8,292 | 7,445 | 5,456 | 4,929 | 3,362 |
| 4 | 10 | | 20 | 8,618 | 7,220 | 6,422 | 4,850 | 4,347 | 3,057 |
| 4 | 3 | | 30 | 4,684 | 3,791 | 3,047 | 1,783 | 1,459 | 864 |
| 4 | 4 | | 30 | 6,043 | 4,496 | 3,630 | 2,230 | 1,855 | 1,113 |
| 4 | 3b | | 30 | 4,289 | 3,442 | 2,756 | 1,714 | 1,375 | 882 |
| 4 | 1 | | 35 | 3,283 | 2,371 | 1,874 | 1,148 | 942 | 638 |
| 4 | 2 | | 35 | 3,163 | 2,304 | 1,856 | 1,119 | 898 | 570 |
| Phase Angle (degrees) | | | | | | | | | |
| 4 | 7 | | 4 | 6.27 | 7.4 | 7.68 | 12.84 | 11.87 | 14.6 |
| 4 | 8 | | 4 | 3.14 | 5.53 | 7.96 | 9.42 | 11.35 | 14.07 |
| 4 | 5 | | 10 | 12.92 | 12.23 | 13.66 | 17.44 | 19.14 | 24.99 |
| 4 | 6 | | 10 | 6.45 | 8.39 | 10.07 | 13.08 | 15.29 | 19.07 |
| 4 | 9 | | 20 | 12.05 | 14.07 | 17.49 | 22.9 | 28.84 | 35.45 |
| 4 | 10 | | 20 | 10.08 | 14.44 | 16.9 | 21.6 | 27.13 | 33.15 |
| 4 | 3 | | 30 | 22.45 | 25.24 | 29.58 | 33.37 | 40.23 | 38.9 |
| 4 | 4 | | 30 | 20.29 | 25.45 | 27.94 | 31.17 | 38.14 | 36.64 |
| 4 | 3b | | 30 | 20.59 | 25.91 | 29.96 | 34.52 | 42.68 | 43.4 |
| 4 | 1 | | 35 | 24.81 | 27.54 | 28.8 | 28.93 | 34.48 | 29.65 |

Figure 3-12 shows for each of the five mixes the variation of the average dynamic modulus with the temperature for the loading frequency of 25 Hz. The values obtained for mixes 1, 3 and 4 are very close, even though Mix 3 had a slightly higher binder content than mixes 1 and 4 and, mix 1 had a stiffer binder (PG70-22) than mixes 3 and 4 (PG64-22). Overall, mix S, used in the wearing course exhibited the lowest average dynamic modulus. This was expected since mix S had a finer aggregate structure (nominal maximum aggregate size of 9.5 mm) than did all four other mixes (nominal maximum aggregate size of 19.0 mm).

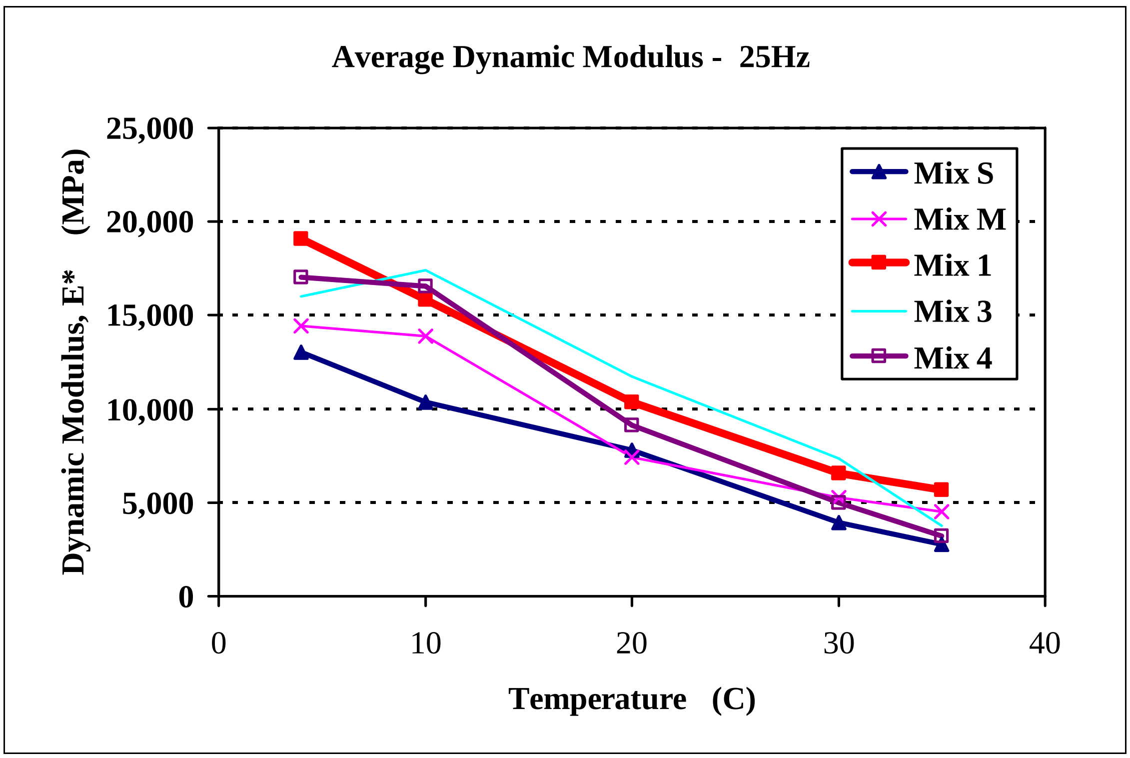


Figure 3-12: Average Dynamic Modulus at 25 Hz Loading Frequency

## 3.5 Response Monitoring Instrumentation and Measuring Procedure

To verify the approach of designing perpetual pavements, based on an endurance strain limit, the four pavements were instrumented with gages for measuring the tensile strains at the bottom of the asphalt base layers. The instrumentation systems were placed in the four pavement structures during their construction, in June 2005.

The configuration of the instrumentation was the same in sections 1, 2 and 4. The gages were placed on top of the lime treated sub-grade soil layer; the first bottom lift of asphalt concrete was placed directly on these gages. A schematic diagram of the layout of the response measuring instrumentation is shown in Figure 3-13. The instrumentation was designed to obtain accurate and multiple measurements of the longitudinal and transverse strains under a single pass of the load vehicle, while minimizing the cost of the instrumentation.

The pavement response measuring instrumentation was composed of:

- *Eight pairs of strain gages*. In each pair, one gage was placed to measure the longitudinal strain and the other to measure the transverse strain. Texas Measurements gage model PML-120-2L (Figure 3-14) were employed, due to their low cost and acceptable performance. Aluminum bars were glued at the ends of each strain gage to form H-bar gages. This significantly improves the bond between the gages and the surrounding asphalt concrete. Four pairs of gages were placed in the outside wheel path while the remaining four pairs were placed on a straight line six inches to the right of the outside wheel path, to determine the effect of the lateral position of the loading wheel on the measured pavement response.

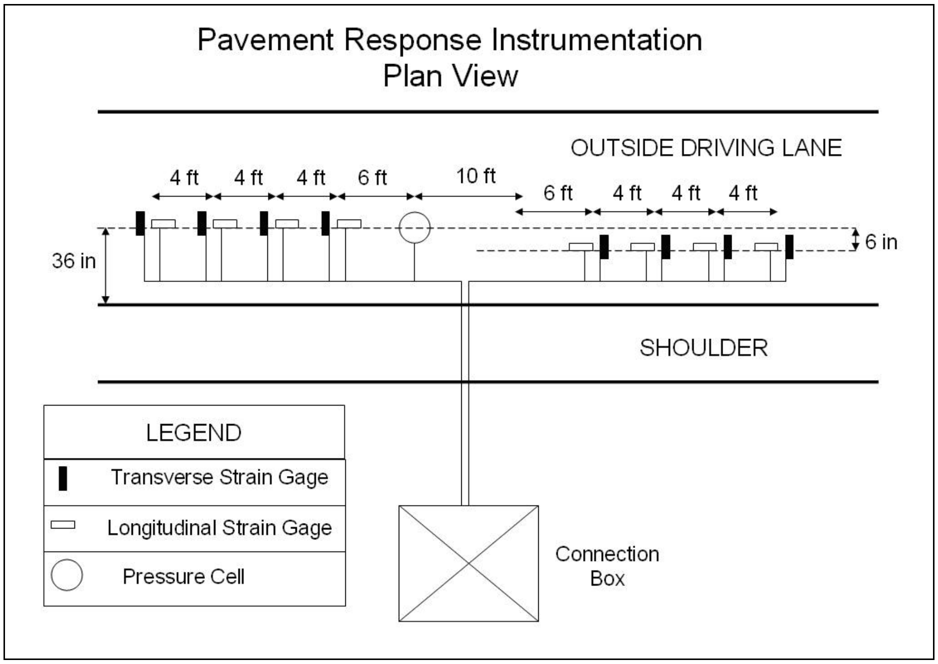


Figure 3-13: Plan View of the Instrumentation Installed in Sections 1, 2, and 4

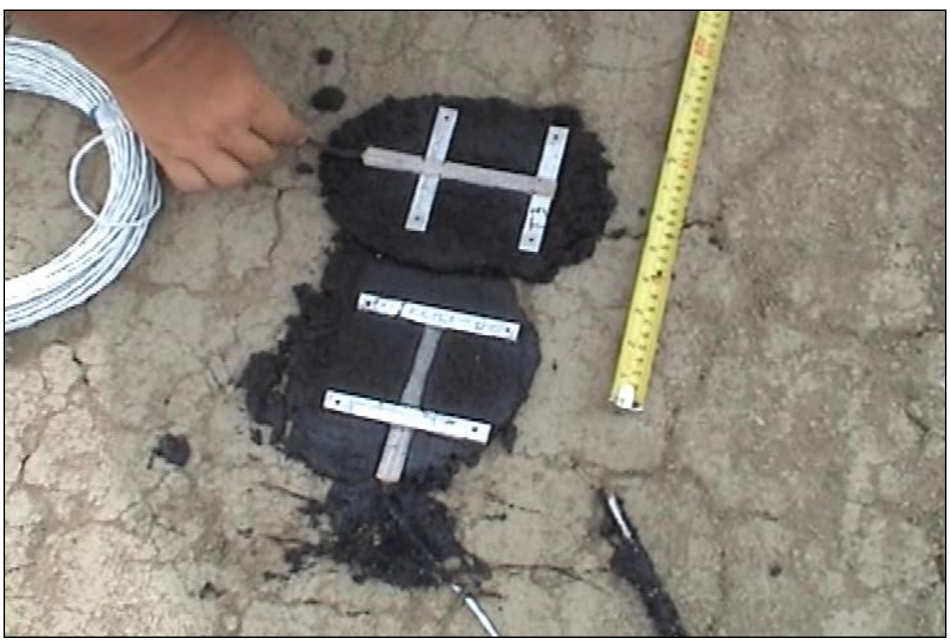

Figure 3-14: Texas Measurement Gauges Model PML-120-2L

- *One stress cell.* A Geokon stress cell, with a range of 0 to15 psi (Figure 3-15) was placed centered in the outside wheel path.

The instrumentation was placed on the top of the compacted lime-treated embankment soil one day prior to the placement of the first lift of HMA. First, the location of the gages was marked relative to the centerline of the road and trenches were cut to bring the cables to a connection box mounted on a pole 15 feet away from the shoulder. The stress cells were placed in circular holes dug into the lime-soil embankment and filled with wet sand. They were seated in the wet sand so that they have a stable and horizontal position.

Figure 3-15: Geokon Stress Cell

For each strain gage, a base of asphalt mortar, consisting of sand mixed with high grade asphalt cement, was placed first on top of the lime-soil layer. The gage was then pushed slowly into the mortar base and placed in position. The day of the HMA placing operation, hot loose asphalt mix was screened above the gage and compacted lightly by hand using a roller pin. The paver placed the first lift of asphalt mix on top of the gages, followed by the compaction of the mix done with vibratory steel and pneumatic rollers. When passing above the gages, the vibration was turned off to reduce the probability of damaging the gages during construction. Field density measurements with a nuclear density gage proved that the stopping of the vibration did not affect the density of the compacted asphalt concrete.

The paving operation was done by unloading the hot asphalt mix in a windrow in front of the paver and then feeding it into the hopper of the paver with a pick-up machine. This operation affected the survivability of the gages; the survival rate was between 50 and 70 percent.

The pick up machine removed all the strain gages placed in Section 3 (KAPA2); the stress cell buried in the lime treated embankment layer in Section 3 was not affected. Therefore, eight strain gages (Figure 3-16) were retrofitted in Section 3 in the bottom lift of HMA by cutting four 12 inch diameter cores from the bottom lift of asphalt concrete and fixing the strain gages to the bottom of the cores with epoxy.  Of the eight gages, four were positioned to measure transverse strain and four were positioned to measure longitudinal strain. The cores with the gages at their bottom were placed back in the same location and glued to the walls of the holes with a thick layer of epoxy. The wires were re-routed to the connection box thru grooves cut into the bottom lift of HMA and then thru a plastic conduit buried into the soil at a depth of about 3 feet.

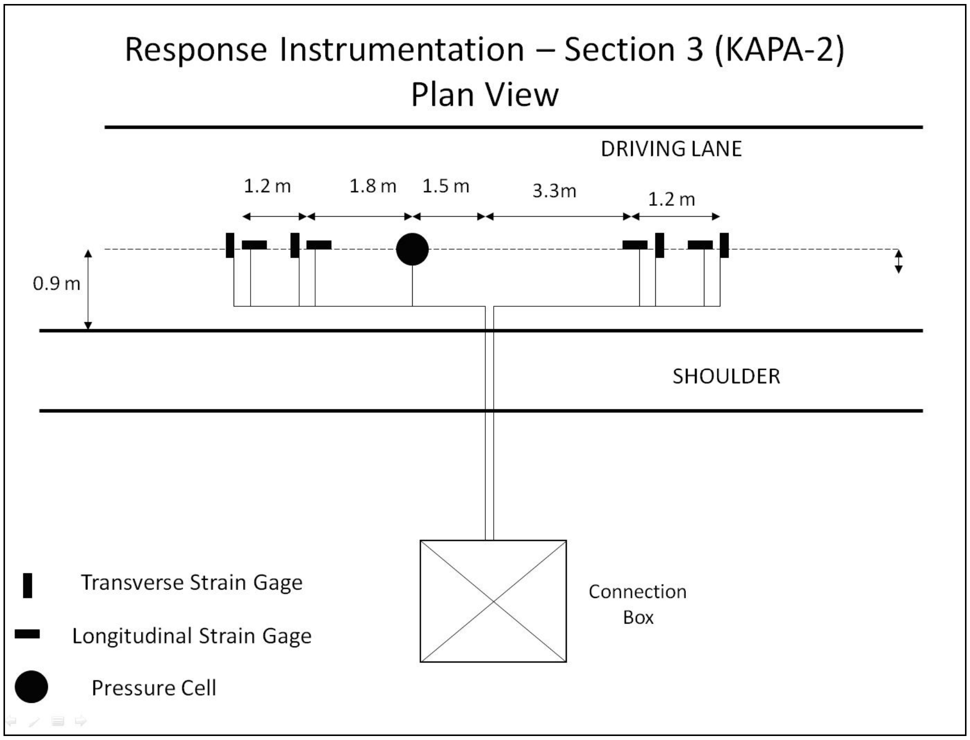


Figure 3-16: Plan View of the Instrumentation Installed in Section 3

Seven sessions of pavement response measurements under known vehicle load were performed between July 2005 and October 2007, before and after the pavement sections were opened to traffic. In each session, a single axle dump truck owned by KDOT was used as the loading vehicle. According to the FHWA vehicle classification system, this truck is a class 5 vehicle.

The same loading vehicle was used for all sessions. Before the runs were performed the static weight of each wheel was measured by the Kansas Highway Patrol using calibrated scales. The dimensions of the tire imprints as well as the distance between tires were also measured. The dimensions of the tire imprints as well as the wheel weights are given in Table 3-12.

On each pavement, three sets of five passes of the loading vehicle were performed. Five passes each were performed with the truck passing at 20-25 mph, 40-45mph and 55-60mph, in order to determine the effect of vehicle speed on the magnitude of pavement response. Using reflective squares glued on the pavement surface as guides, the driver aimed to position the truck with the right wheels above the instrumentation. However, the lateral position of the wheels varied between passes; higher variability was observed at higher speeds.

Table 3-12: Dimensions and Weight of the Tire

| | Steering Front Left | Steering Front Right | Tractor Rear Left | Tractor Rear Right | Trailer Rear Left | Trailer Rear Right |
|---|---|---|---|---|---|---|
| Inflation pressure (psi) | 90 | 96 | | | 101 | 97 |
| Imprint Length (inches) | 7.7 | 7.3 | | | 6 | 6 |
| Imprint Width (inches) | 8.25 | 8.25 | | | 8.9 | 8.9 |
| Space between double tires (inches) | - | - | | | 4.25 | 4.25 |
| Wheel Load (lbs.) | | | | | | |
| July 14, 2005 | 5,200 | 5,600 | - | - | 8,100 | 9,200 |
| September 29, 2005 | 5,400 | 5,800 | - | - | 10,000 | 10,400 |
| April 13, 2006 | 4,900 | 4,800 | - | - | 12,000 | 10,400 |
| August 1, 2006 | 5,500 | 5,400 | - | - | 11,400 | 11,200 |
| | 4,600* | 4,300* | 9,700* | 9,500* | 9,000* | 9,000* |
| October 13, 2006 | 5,400 | 5,300 | - | - | 9,800 | 10,000 |
| May 10, 2007 | 5,000 | 5,300 | - | - | 9,500 | 9,300 |
| October 5, 2007 | 5,500 | 5,100 | - | - | 10,400 | 10,000 |

* RWD truck

Before the response measurements were performed two air rubber hoses connected to a triggering relay system were places across the pavement at a distance of

52.5 ft (16 m). When the front tire of the loading vehicle hit the rubber hoses, the system triggered an electronic switch connected to the same data acquisition system as the strain gages and the stress cell. The system was used to locate the position of the loading vehicle and to estimate its speed.

Putty strips were placed across the outer wheel path. The locations of the imprints made by the tires on the strips were recorded and used to determine the lateral position of the loading vehicle when it passed above the instrumentation.

The thermocouple of a temperature gage was lowered in holes drilled in the HMA layers and filled with oil to measure the temperature at the mid-depth of each HMA layer at the time of response measurements. The values of the recorded temperatures recorded are given in Table 3-13. However, it is important to notice that the recorded temperatures at the mid-depth of the HMA layers were higher for the July 2005 and August 2006 sessions than the corresponding temperatures recorded on all the remaining five sessions. Also, for all sessions, the temperature in the surface layers were the lowest in Section 1 and increased to the highest in Section 4, since the response measurements were done for Sections 1 and 2 in the morning, Sections 3 around noon and, Section 4 in the early afternoon.

Sections 1, 2 and 4 were loaded with an additional vehicle on the August 1, 2006 measurement session. The FHWA's Rolling Wheel Deflectometer (RWD) performed deflection measurements on the experimental sections as well as on several other sections of state highways that day. The RWD truck has an 8,900 lbs single axle single tire steering axle, a 19,200 lbs dual tire tandem axle at the back of the tractor and an 18,000 lbs dual tire single axle in the rear of the trailer. Only five runs of the RWD truck, all at the speed of approximately 60 mph, were performed on each of three sections.

The horizontal strains and the vertical stress at the bottom of the asphalt concrete layer, as well as the position of the loading vehicle, were recorded with a National Instruments data acquisition system at a rate of 300 records per second. A sampling rate of 3,000 Hz was used and the average value for ten samples was recorded. The data was recorded in text format in separate files for each pass of the vehicle and then was processed using Microsoft Excel. Each strain signal was plotted and the peak values of the longitudinal and transverse strains were manually extracted. Appendix A presents charts plotting the peak values corrected to 20 C for all sections and all measurement dates. Appendix D presents the raw tabulated peak values extracted from the output charts.

Table 3-13: Temperature at the Mid-Depth of Asphalt Concrete Layers

| DATE | Layer | Mid-Depth Temperature (°F) | | | | Mid-Depth Temperature (°C) | | | |
|---|---|---|---|---|---|---|---|---|---|
| | | 1 | 2 | 3 | 4 | 1 | 2 | 3 | 4 |
| 7/14/2005 | S | 96.2 | 104.8 | 116.6 | 121.0 | 35.7 | 40.4 | 47.0 | 49.4 |
| | M | 90.0 | 95.6 | 103.9 | 109.5 | 32.2 | 35.3 | 39.9 | 43.1 |
| | Base | 88.0 | 89.1 | 93.5 | 96.6 | 31.1 | 31.7 | 34.2 | 35.9 |
| 9/29/2005 | S | 58.0 | 76.0 | 90.0 | 92.0 | 14.4 | 24.4 | 32.2 | 33.3 |
| | M | 60.0 | 70.0 | 79.0 | 86.0 | 15.6 | 21.1 | 26.1 | 30.0 |
| | Base | 67.0 | 66.0 | 67.0 | 70.0 | 19.4 | 18.9 | 19.4 | 21.1 |
| 4/13/2006 | S | 67.4 | 79.0 | 90.0 | 86.0 | 19.7 | 26.1 | 32.2 | 30.0 |
| | M | 67.5 | 75.0 | 96.0 | 88.0 | 19.7 | 23.9 | 35.6 | 31.1 |
| | Base | 65.8 | 76.0 | 107.0 | 89.0 | 18.8 | 24.4 | 41.7 | 31.7 |
| 8/1/2006 | S | 96.0 | 118.0 | N/A | 123.0 | 35.6 | 47.8 | N/A | 50.6 |
| | M | 99.0 | 111.0 | N/A | 113.0 | 37.2 | 43.9 | N/A | 45.0 |
| | Base | 97.0 | 99.0 | N/A | 101.0 | 36.1 | 37.2 | N/A | 38.3 |
| 8/1/2006 RWD | S | 104.0 | 122.0 | N/A | 129.0 | 40.0 | 50.0 | N/A | 53.9 |
| | M | 100.0 | 112.0 | N/A | 115.0 | 37.8 | 44.4 | N/A | 46.1 |
| | Base | 95.0 | 101.0 | N/A | 101.0 | 35.0 | 38.3 | N/A | 38.3 |

Table 3-13 - *Continued*

| DATE | Layer | Mid-Depth Temperature (°F) | | | | Mid-Depth Temperature (°C) | | | |
|---|---|---|---|---|---|---|---|---|---|
| | | 1 | 2 | 3 | 4 | 1 | 2 | 3 | 4 |
| 10/13/2006 | S | 61.0 | 59.0 | 64.0 | 59.0 | 16.1 | 15.0 | 17.8 | 15.0 |
| | M | 56.0 | 52.0 | 57.0 | 54.0 | 13.3 | 11.1 | 13.9 | 12.2 |
| | Base | 51.0 | 49.0 | 53.0 | 50.0 | 10.6 | 9.4 | 11.7 | 10.0 |
| 5/1/2007 | S | 70.0 | 72.0 | 72.0 | 73.0 | 21.1 | 22.2 | 22.2 | 22.8 |
| | M | 70.0 | 71.0 | 73.0 | 72.0 | 21.1 | 21.7 | 22.8 | 22.2 |
| | Base | 72.0 | 71.0 | 72.0 | 71.0 | 22.2 | 21.7 | 22.2 | 21.7 |
| 10/5/2007 | S | 71.8 | 73.3 | N/A | 80.9 | 22.1 | 22.9 | N/A | 27.2 |
| | M | 72.1 | 71.6 | N/A | 72.0 | 22.3 | 22.0 | N/A | 22.2 |
| | Base | 73.8 | 72.1 | N/A | 69.6 | 23.2 | 22.3 | N/A | 20.9 |

CHAPTER 4

# THEORETICAL RESPONSE OF US-75 PAVEMENT

## 4.1 Linear Elastic Analysis

### *4.1.1 Description*

Linear elastic analyses using the EVERSTRESS© software were performed for Sections 1 through 4 of the US-75 project for 3 of the total of 7 dates that field measurements were carried out. In order to see the seasonal variation of the pavement response, three different field measurement dates were modeled to compare them later with the field measured values. Table 4-1 presents the dates that were modeled, and the temperatures of each pavement layer on the respective date. It is assumed that the findings of the comparison are valid for the remaining four measuring dates, since the temperatures recorded in the asphalt layers were similar.

Table 4-1: Section 1 - Pavement Layer Temperatures

| Field Measurement Date | Temperature, ºC | | |
|---|---|---|---|
| | Layer 1 | Layer 2 | Layer 3 |
| 08/01/2006 | 35.6 | 37.2 | 36.1 |
| 10/13/2006 | 16.1 | 13.3 | 10.6 |
| 05/01/2007 | 21.1 | 21.1 | 22.2 |

As mentioned in Section 2.3.2, the input data needed to run the linear elastic analysis using EVERSTRESS© are: the modulus of elasticity, Poisson's ratio, thickness of each layer, load magnitude, contact pressure or load radius, and location of the loads. The Poisson's ratio was set to 0.3 for the asphalt layers, 0.35 for the sub-base layer, and

0.4 for the sub-grade layer. Layer thicknesses were set according to the values shown in Figure 4-18. The load magnitude and contact pressure used in the calculation of the contact area for each date are given in Table 4-2.

Table 4-2: Tire Pressures and Truck Loads

| | Steering Front Left | Steering Front Right | Trailer Rear Left | Trailer rear Right |
|---|---|---|---|---|
| Inflation Pressure (psi) | 90 | 96 | 101 | 97 |
| Date | Wheel Loads (lbs) | | | |
| 08/01/2006 | 5500 | 5400 | 11400 | 11200 |
| 10/13/2006 | 5400 | 5300 | 9800 | 10000 |
| 05/01/2007 | 5000 | 5300 | 9500 | 9300 |

### *4.1.2 Determination of Dynamic (Elastic) Modulus*

Calculation of the elastic modulus used in this analysis required more work. The moduli were taken from the dynamic modulus laboratory tests performed on each mix used in the project. Results from these tests at 25 and 10 Hz were then fitted to Equation 4-1 to develop a dynamic modulus prediction equation as a function of temperature. This was done in order to convert $E^*$ values obtained from the laboratory tests at the tests temperatures to the values corresponding to the temperatures experienced in the field at the time that the pavement response measurements were taken. Figure 4-1 shows the comparison between measured and predicted $E^*$ values using Equation 4-1 for Mix 1. The same chart, but for mixes 3, 4, S, and M are presented in Appendix D.

$$\log(E^*) = a + \frac{b}{1 + c \times 10^{d \times T^v}} \tag{4-1}$$

where:

$E^*$ = dynamic modulus, MPa

$a$, $b$, $c$, $d$, $v$ = regression coefficients

$T$ = temperature, °C

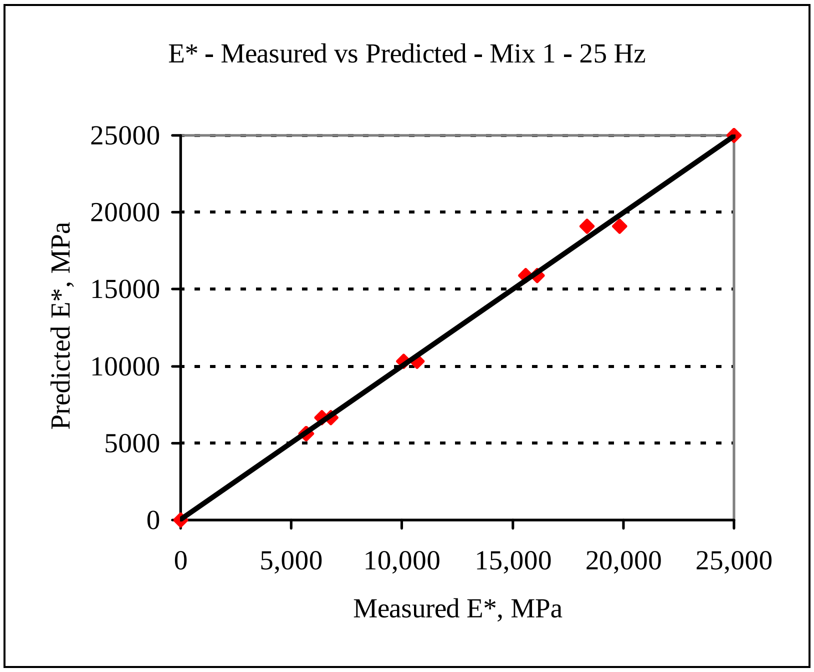


Figure 4-1: E* - Measured vs Predicted – Mix 1

Pavement response values are affected by the speed of the loading vehicle; the greater the vehicle speed, the smaller the values of the strains and stresses applied to the pavement structure. Similarly, in the dynamic modulus laboratory tests, the bigger the frequency at which the load is applied on the mixes, the smaller the moduli will be. The influence of vehicle speed was included in linear elastic analyses by selecting moduli values corresponding to the loading frequency. Based on the recommendation found in the literature, it was considered that the loading frequency the asphalt concrete experience under the passing of a vehicle, in hertz, equals to half the vehicle speed in miles-per-hour. Therefore, in order to model a vehicle moving at 20 mph, the moduli assigned to the asphalt concrete correspond to those measured at 10 Hz loading frequency.

One may realize that dynamic modulus tests were performed at 25, 10, 5, 1, 0.5, and 0.1 Hz only, and not at either 20 or 30 Hz, values that were used to simulate 40 and 60 mph speeds respectively. Values of the moduli at 20 Hz were interpolated from the values measured at 25 and 10 Hz. On the other hand, values of the moduli at 30 Hz were extrapolated from the values measured at 25 and 10 Hz. Figure 4-2 shows a typical curve of the relationship between $E^*$ and frequency. As it is seen in Figure 4-2, from 10 Hz up, the relationship between $E^*$ and frequency becomes very close to be linear, which proves that the interpolation and extrapolation performed to calculate moduli values at 20 and 30 Hz are acceptable. Table 4-3 presents the measured moduli values at 10 and 25 Hz, and the calculated moduli values at 20 and 30 Hz.

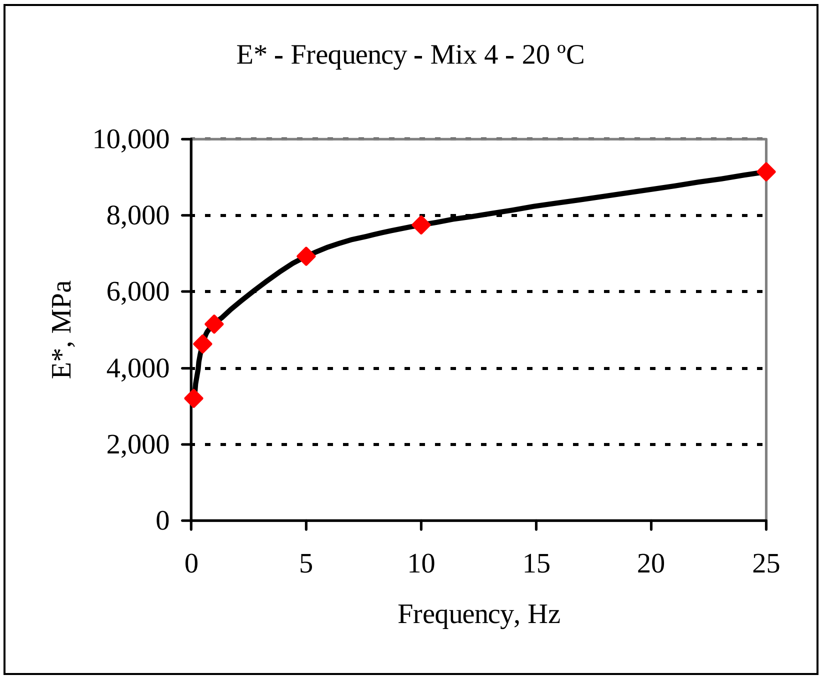


Figure 4-2: *E** vs Frequency – Mix 4 – 20 ºC

Table 4-3: Moduli Values (MPa) Calculated at 20 and 30 Hz

| | | Frequency, Hz | | | | Frequency, Hz | | | |
|---|---|---|---|---|---|---|---|---|---|
| | | 25 | 10 | 20 | 30 | 25 | 10 | 20 | 30 |
| | Date | Section 1 - Moduli (MPa) | | | | Section 2 - Moduli (MPa) | | | |
| Layer 1 | 7/14/2005 | 2,621 | 1,943 | 2,395 | 2,847 | 1,646 | 1,251 | 1,514 | 1,777 |
| | 9/29/2005 | 9,313 | 7,832 | 8,819 | 9,806 | 5,858 | 4,534 | 5,416 | 6,299 |
| | 4/13/2006 | 7,489 | 6,022 | 7,000 | 7,979 | 5,312 | 4,063 | 4,896 | 5,729 |
| | 8/1/2006 | 2,647 | 1,962 | 2,418 | 2,875 | 669 | 583 | 640 | 698 |
| | *8/1/2006 | 1,725 | 1,305 | 1,585 | 1,865 | 484 | 454 | 474 | 494 |
| | 10/13/2006 | 8,732 | 7,238 | 8,234 | 9,230 | 9,119 | 7,632 | 8,624 | 9,615 |
| | 5/1/2007 | 6,989 | 5,552 | 6,510 | 7,468 | 6,607 | 5,201 | 6,139 | 7,076 |
| | 10/5/2007 | 6,645 | 5,236 | 6,175 | 7,115 | 6,361 | 4,979 | 5,901 | 6,822 |
| Layer 2 | 7/14/2005 | 4,637 | 3,779 | 4,351 | 4,923 | 3,920 | 3,757 | 3,865 | 3,974 |
| | 9/29/2005 | 10,341 | 9,850 | 10,177 | 10,504 | 8,112 | 5,536 | 7,253 | 8,971 |
| | 4/13/2006 | 8,644 | 6,410 | 7,900 | 9,389 | 7,108 | 4,464 | 6,227 | 7,990 |
| | 8/1/2006 | 3,534 | 3,752 | 3,607 | 3,461 | 2,436 | 3,748 | 2,873 | 1,998 |
| | *8/1/2006 | 3,427 | 3,751 | 3,535 | 3,319 | 2,361 | 3,748 | 2,823 | 1,898 |
| | 10/13/2006 | 11,285 | 11,350 | 11,306 | 11,263 | 12,233 | 12,306 | 12,257 | 12,208 |
| | 5/1/2007 | 8,112 | 5,536 | 7,253 | 8,971 | 7,905 | 5,253 | 7,021 | 8,788 |
| | 10/5/2007 | 7,680 | 4,985 | 6,782 | 8,579 | 7,782 | 5,101 | 6,888 | 8,675 |

Table 4-3 - *Continued*

| | | Frequency, Hz | | | | Frequency, Hz | | | |
|---|---|---|---|---|---|---|---|---|---|
| | | 25 | 10 | 20 | 30 | 25 | 10 | | |
| | Date | Section 1 - Moduli (MPa) | | | | Section 2 - Moduli (MPa) | | | |
| Layer 3 | 7/14/2005 | 6,384 | 5,249 | 6,006 | 6,762 | 3,876 | 3,213 | 3,655 | 4,096 |
| | 9/29/2005 | 10,600 | 9,317 | 10,172 | 11,028 | 10,206 | 8,764 | 9,725 | 10,687 |
| | 4/13/2006 | 10,937 | 9,624 | 10,499 | 11,375 | 6,163 | 5,348 | 5,892 | 6,435 |
| | 8/1/2006 | 5,461 | 4,220 | 5,047 | 5,875 | 3,265 | 2,571 | 3,034 | 3,496 |
| | *8/1/2006 | 5,631 | 4,418 | 5,227 | 6,036 | 3,192 | 2,490 | 2,958 | 3,426 |
| | 10/13/2006 | 15,556 | 13,862 | 14,991 | 16,120 | 16,558 | 14,941 | 16,019 | 17,097 |
| | 5/1/2007 | 9,301 | 8,121 | 8,908 | 9,695 | 7,913 | 6,847 | 7,558 | 8,269 |
| | 10/5/2007 | 8,878 | 7,724 | 8,493 | 9,263 | 7,477 | 6,478 | 7,144 | 7,810 |
| | | Frequency, Hz | | | | Frequency, Hz | | | |
| | | 25 | 10 | 20 | 30 | 25 | 10 | 20 | 30 |
| | Date | Section 3 - Moduli (MPa) | | | | Section 4 - Moduli (MPa) | | | |
| Layer 1 | 7/14/2005 | 745 | 635 | 708 | 782 | 526 | 483 | 512 | 540 |
| | 9/29/2005 | 3,489 | 2,591 | 3,190 | 3,788 | 3,195 | 2,368 | 2,919 | 3,470 |
| | 4/13/2006 | 3,489 | 2,591 | 3,190 | 3,788 | 4,114 | 3,079 | 3,769 | 4,459 |
| | 8/1/2006 | N/A | N/A | N/A | N/A | 444 | 426 | 438 | 450 |
| | *8/1/2006 | N/A | N/A | N/A | N/A | 257 | 288 | 267 | 246 |
| | 10/13/2006 | 8,149 | 6,658 | 7,652 | 8,646 | 9,119 | 7,632 | 8,624 | 9,615 |
| | 5/1/2007 | 6,607 | 5,201 | 6,139 | 7,076 | 6,418 | 5,030 | 5,955 | 6,880 |
| | 10/5/2007 | N/A | N/A | N/A | N/A | 4,976 | 3,780 | 4,577 | 5,374 |
| Layer 2 | 7/14/2005 | 3,038 | 3,750 | 3,275 | 2,801 | 2,553 | 3,749 | 2,951 | 2,154 |
| | 9/29/2005 | 6,369 | 4,070 | 5,603 | 7,135 | 5,216 | 3,822 | 4,751 | 5,681 |
| | 4/13/2006 | 3,872 | 3,756 | 3,834 | 3,911 | 4,920 | 3,796 | 4,545 | 5,294 |
| | 8/1/2006 | N/A | N/A | N/A | N/A | 2,288 | 3,748 | 2,775 | 1,801 |
| | *8/1/2006 | N/A | N/A | N/A | N/A | 2,149 | 3,748 | 2,682 | 1,616 |
| Layer 2 | 5/1/2007 | 7,500 | 4,796 | 6,598 | 8,401 | 7,700 | 5,007 | 6,803 | 8,598 |
| | 10/5/2007 | N/A | N/A | N/A | N/A | 7,700 | 5,007 | 6,803 | 8,598 |
| Layer 3 | 7/14/2005 | 4,459 | 3,613 | 4,177 | 4,741 | 3,370 | 2,685 | 3,141 | 3,598 |
| | 9/29/2005 | 12,776 | 11,617 | 12,390 | 13,163 | 8,334 | 7,200 | 7,956 | 8,712 |
| | 4/13/2006 | 1,345 | 1,152 | 1,281 | 1,409 | 3,885 | 3,222 | 3,664 | 4,106 |
| | 8/1/2006 | N/A | N/A | N/A | N/A | 3,192 | 2,490 | 2,958 | 3,426 |
| | *8/1/2006 | N/A | N/A | N/A | N/A | 3,192 | 2,490 | 2,958 | 3,426 |
| | 10/13/2006 | 15,644 | 14,151 | 15,146 | 16,142 | 16,400 | 14,723 | 15,841 | 16,959 |
| | 5/1/2007 | 11,381 | 10,297 | 11,020 | 11,742 | 7,913 | 6,847 | 7,558 | 8,269 |
| | 10/5/2007 | N/A | N/A | N/A | N/A | 8,508 | 7,346 | 8,121 | 8,896 |

*4.1.3 Linear Elastic Analysis Results*

Figures 4-3, 4-4, and 4-5 show the calculated pavement response (strains and vertical pressure) at 20, 40, and 60 miles-per-hour for May 1st, 2007 and Section 1 only. Charts for Sections 2, 3, and 4 and for August 1st, 2006 and October 13th, 2007 are presented in Appendix C. Table 4-4 presents the calculated maximum response values for the front and rear axle of the modeled passing truck used in the EVERSTRESS© program. Table 4-5 presents the maximum and minimum measured pavement response values for the rear axle only of the actual truck, which is the one that causes the biggest strains and stresses. Finally, Figures 4-6 through 4-17 show the minimum and maximum measured longitudinal and transverse strains and vertical pressures values against the predicted values for 20, 40, and 60 miles-per-hour and for the three dates modeled in this linear elastic analysis respectively.

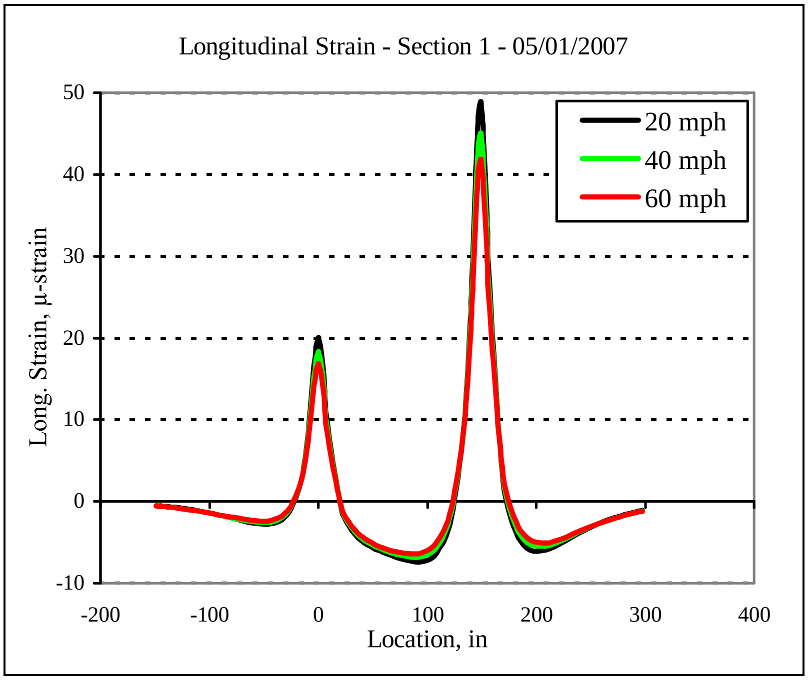


Figure 4-3: Longitudinal Strain – Section 1 – 05/01/2007

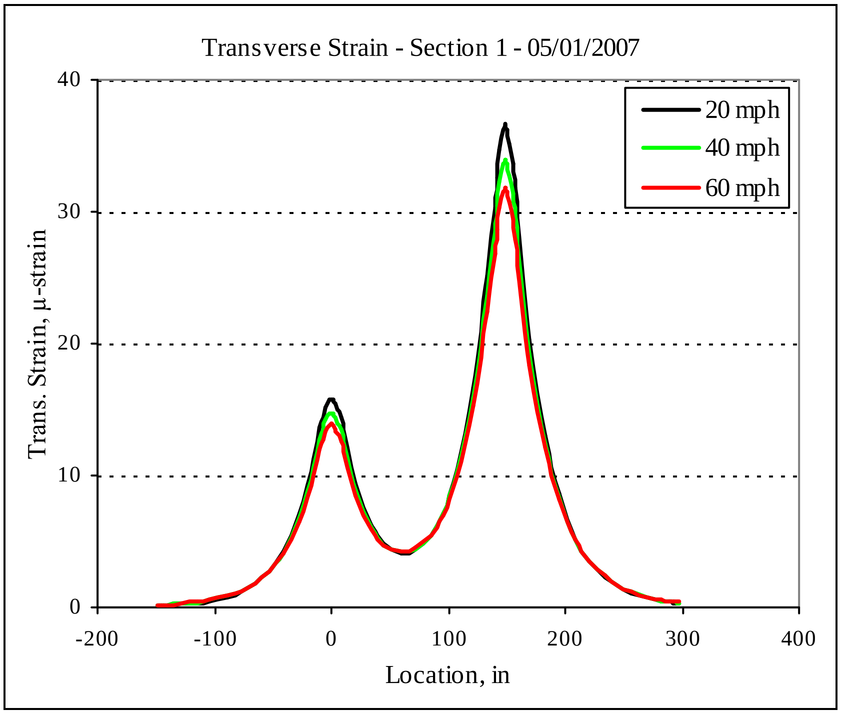


Figure 4-4: Transverse Strain – Section 1 – 05/01/2007

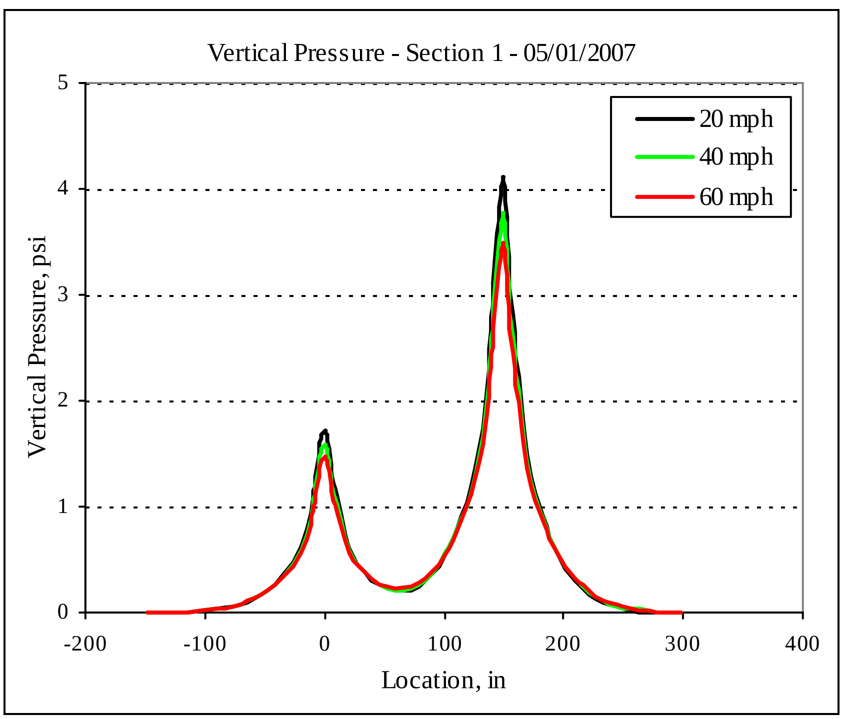


Figure 4-5: Vertical Pressure – Section 1 – 05/01/2007

Table 4-4: Predicted Pavement Response Values (Linear Elastic)

| | Date | Nominal Speed (mph) | Long. Strain (μ-strain) | | Trans. Strain (μ-strain) | | Pressure (psi) | |
|---|---|---|---|---|---|---|---|---|
| | | | Front | Rear | Front | Rear | Front | Rear |
| Section 1 | 8/1/2006 | 20 | 31.21 | 74.17 | 23.05 | 53.49 | 2.53 | 6.00 |
| | | 40 | 28.16 | 67.26 | 21.08 | 48.95 | 2.32 | 5.52 |
| | | 60 | 25.74 | 61.76 | 19.38 | 45.28 | 2.16 | 5.14 |
| | 10/13/2006 | 20 | 15.32 | 34.97 | 16.89 | 26.09 | 1.58 | 2.97 |
| | | 40 | 14.40 | 33.02 | 15.97 | 24.75 | 1.50 | 2.84 |
| | | 60 | 13.59 | 31.31 | 15.16 | 23.56 | 1.43 | 2.72 |
| | 5/1/2007 | 20 | 20.04 | 48.93 | 15.82 | 36.59 | 1.72 | 4.12 |
| | | 40 | 18.29 | 45.04 | 14.69 | 34.01 | 1.58 | 3.77 |
| | | 60 | 16.86 | 41.83 | 13.80 | 31.84 | 1.46 | 3.50 |
| Section 2 | 8/1/2006 | 20 | 49.60 | 115.02 | 31.56 | 78.36 | 4.01 | 9.67 |
| | | 40 | 46.79 | 108.61 | 29.64 | 74.27 | 3.89 | 9.39 |
| | | 60 | 44.87 | 104.17 | 28.42 | 71.34 | 3.84 | 9.29 |
| | 10/13/2006 | 20 | 18.46 | 40.25 | 19.78 | 28.29 | 1.96 | 3.55 |
| | | 40 | 17.47 | 38.24 | 18.80 | 27.00 | 1.88 | 3.40 |
| | | 60 | 16.58 | 36.45 | 17.93 | 25.73 | 1.78 | 3.27 |
| | 5/1/2007 | 20 | 27.20 | 64.86 | 19.18 | 46.84 | 2.32 | 5.62 |
| | | 40 | 24.85 | 59.66 | 17.96 | 43.56 | 2.12 | 5.13 |
| | | 60 | 22.93 | 55.39 | 16.92 | 40.82 | 1.95 | 4.74 |
| Section 3 | 10/13/2006 | 20 | 15.21 | 34.66 | 16.76 | 25.65 | 1.57 | 2.96 |
| | | 40 | 14.32 | 32.81 | 15.88 | 24.53 | 1.50 | 2.83 |
| | | 60 | 13.53 | 31.16 | 15.09 | 23.40 | 1.43 | 2.72 |
| | 5/1/2007 | 20 | 20.65 | 50.40 | 16.22 | 37.77 | 1.73 | 4.13 |
| | | 40 | 18.78 | 46.22 | 15.06 | 34.95 | 1.58 | 3.77 |
| | | 60 | 17.27 | 42.83 | 14.12 | 32.64 | 1.46 | 3.49 |
| Section 4 | 8/1/2006 | 20 | 30.96 | 74.39 | 24.60 | 54.55 | 2.41 | 5.56 |
| | | 40 | 29.14 | 70.10 | 23.10 | 51.65 | 2.31 | 5.36 |
| | | 60 | 27.91 | 67.17 | 22.25 | 49.65 | 2.26 | 5.26 |
| | 10/13/2006 | 20 | 8.41 | 22.57 | 8.54 | 18.50 | 0.79 | 1.88 |
| | | 40 | 7.92 | 21.37 | 8.14 | 17.58 | 0.77 | 1.80 |
| | | 60 | 7.49 | 20.30 | 7.78 | 16.77 | 0.74 | 1.72 |
| | 5/1/2007 | 20 | 15.47 | 39.23 | 13.91 | 30.67 | 1.30 | 3.03 |
| | | 40 | 14.00 | 35.89 | 12.90 | 28.32 | 1.18 | 2.77 |
| | | 60 | 12.81 | 33.17 | 12.06 | 26.39 | 1.07 | 2.56 |

Table 4-5: Measured Pavement Response Values

| | Date | Nominal Speed (mph) | Long. Strain (μ-strain) | | Trans. Strain (μ-strain) | | Pressure (psi) | |
|---|---|---|---|---|---|---|---|---|
| | | | Min | Max | Min | Max | Min | Max |
| Section 1 | 8/1/2006 | 20 | 37.00 | 75.40 | 71.00 | 106.80 | 3.62 | 4.21 |
| | | 40 | 19.20 | 29.00 | 24.40 | 57.80 | 2.40 | 2.65 |
| | | 60 | 18.40 | 26.80 | 29.00 | 58.00 | 2.03 | 2.10 |
| | 10/13/2006 | 20 | 15.80 | 19.60 | 9.00 | 23.40 | 0.53 | 0.64 |
| | | 40 | 8.20 | 10.40 | 12.00 | 17.60 | 0.41 | 0.44 |
| | | 60 | 7.00 | 9.00 | 12.00 | 16.40 | 0.34 | 0.36 |
| | 5/1/2007 | 20 | 21.00 | 30.20 | 18.00 | 42.80 | 2.16 | 2.29 |
| | | 40 | 12.40 | 15.00 | 12.80 | 29.00 | 1.48 | 1.72 |
| | | 60 | 12.60 | 14.20 | 16.40 | 30.40 | 1.25 | 1.42 |
| Section 2 | 8/1/2006 | 20 | 66.20 | 157.00 | 130.80 | 199.80 | 4.14 | 6.01 |
| | | 40 | 51.60 | 58.00 | 103.40 | 141.20 | 3.61 | 3.64 |
| | | 60 | 32.60 | 41.00 | 81.80 | 113.20 | 2.17 | 2.87 |
| | 10/13/2006 | 20 | 20.20 | 26.60 | 20.80 | 33.00 | 1.35 | 1.45 |
| | | 40 | 10.40 | 14.40 | 13.40 | 24.80 | 1.07 | 1.09 |
| | | 60 | 7.80 | 10.00 | 9.60 | 20.80 | 0.97 | 1.02 |
| | 5/1/2007 | 20 | 29.60 | 44.40 | 24.20 | 70.60 | 1.77 | 2.51 |
| | | 40 | 26.00 | 40.80 | 12.60 | 124.40 | 1.54 | 2.13 |
| | | 60 | 18.00 | 21.80 | 39.00 | 100.60 | 1.67 | 2.39 |
| Section 3 | 10/13/2006 | 20 | ---- | ---- | ---- | ---- | 1.17 | 1.24 |
| | | 40 | 6.60 | 7.00 | 7.80 | 13.60 | 0.73 | 0.77 |
| | | 60 | 2.40 | 5.00 | 5.60 | 11.80 | 0.54 | 0.62 |
| Section 4 | 8/1/2006 | 20 | 49.60 | 66.60 | 29.20 | 89.00 | 2.39 | 3.85 |
| | | 40 | 18.60 | 26.20 | 19.80 | 58.40 | 1.67 | 2.11 |
| | | 60 | 11.80 | 18.20 | 24.00 | 42.40 | 1.47 | 1.71 |
| | 10/13/2006 | 20 | 12.80 | 15.00 | 17.40 | 22.00 | 0.46 | 0.53 |
| | | 40 | 7.40 | 9.60 | 15.00 | 18.00 | 0.35 | 0.40 |
| | | 60 | 5.40 | 8.00 | 9.00 | 14.80 | 0.30 | 0.36 |
| | 5/1/2007 | 20 | 16.20 | 24.60 | 27.00 | 44.00 | 0.91 | 1.08 |
| | | 40 | 8.80 | 12.80 | 19.80 | 27.60 | 0.62 | 0.68 |
| | | 60 | 3.80 | 11.40 | 12.60 | 27.60 | 0.63 | 0.73 |

Figures 4-6 through 4-17 clearly show the seasonal variation effect on the pavement response values. August 1st, 2006 was the high-temperature measurement date, May 1st, 2007 the mid-temperature, and October 13th, 2006 was the low-temperature measurement date. This temperature variation is shown in the pavement responses through the fact that the highest strains and stresses the pavement sections experienced were on 08/01/2001, and the lowest strain levels were on 10/13/2006.

It is seen in Figure 4-6 that the calculated longitudinal strain is within the measured longitudinal minimum-maximum range only for 08/01/2006. For 10/13/2006 and 05/01/2007, the calculated longitudinal strain values are 1.5 to 2 times bigger than the measured values. The same observation is true for Sections 2, 3, and 4 as well (Figures 4-9, 4-12, and 4-15).

These differences may be due to the fact that asphalt concrete mixes tend to become stiffer with time. To carry out the linear elastic analysis, the dynamic modulus values were used. These dynamic modulus values were obtained immediately after the construction of the pavement and the HMA mixes were not likely to experience any stiffening due to aging at the time of the test.

Another explanation to this difference between measured and calculated longitudinal strains could be that the dynamic modulus test is carried out in compression, while in the field, pavements may be loaded in flexure. Romanoschi et al. (2005) compared the dynamic modulus and bending stiffness of very similar HMA mixes. The NCHRP Design Guide assumes that these two values should be equal for the same mix. Yet, Romanoschi et al. (2005) found that the dynamic modulus values were more than twice the value for the bending stiffness for the same mix. This may explain the big discrepancy between the calculated and measured longitudinal strain values.

Figures 4-7, 4-10, 4-13, and 4-16 show the minimum and maximum measured transverse strains against the calculated values for Sections 1 through 4 and for the three dates chosen for the analysis. As shown in these figures, in the case of transverse strains, the calculated values are either within the minimum-maximum range of measured values, or very close to be within the range, except for Section 3. Calculated transverse strains are definitely closer to the measured values than calculated longitudinal values were to the measured longitudinal strains.

In the case of vertical pressures (Figures 4-8, 4-11, 4-14, and 4-17) the calculated values tend to be 2 to 3 times bigger than the measured values. This statement is true for all four sections of the project. The reason for these discrepancies may again be the stiffening due aging of the pavement. The stiffer the pavement is, the less pressure the base will experience as the vehicles pass on top of the surface layer. Since just after construction the pavement was still relatively less stiff, pressures were bigger at that time than what they are sometime after the pavement suffered some stiffening due to aging.

Another observation to make about the results of the linear elastic modeling is that even though pavement response values decrease as the speed increases, the changes are not as big as it was expected. As it is shown in Figures 4-6 through 4-17, calculated response values decrease at a slow and steady rate as the vehicle speed increases. On the other hand, there is a very noticeable difference between response values measured at 20 and 40 miles-per-hour, but there is almost no-difference between 40 and 60 miles-per-hour. These results suggest that the implementation of dynamic modulus measured at different frequencies to take into account the effect of speed of vehicles in pavement responses did not work properly.

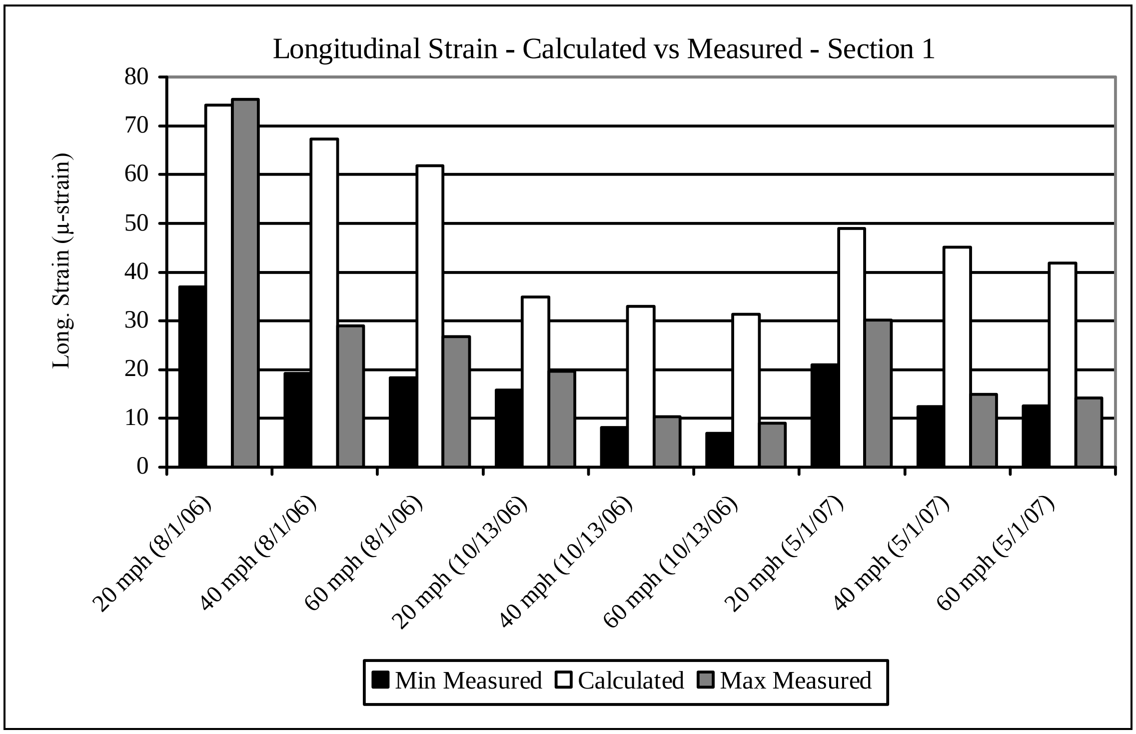


Figure 4-6: Longitudinal Strain – Predicted vs Measured – Section 1

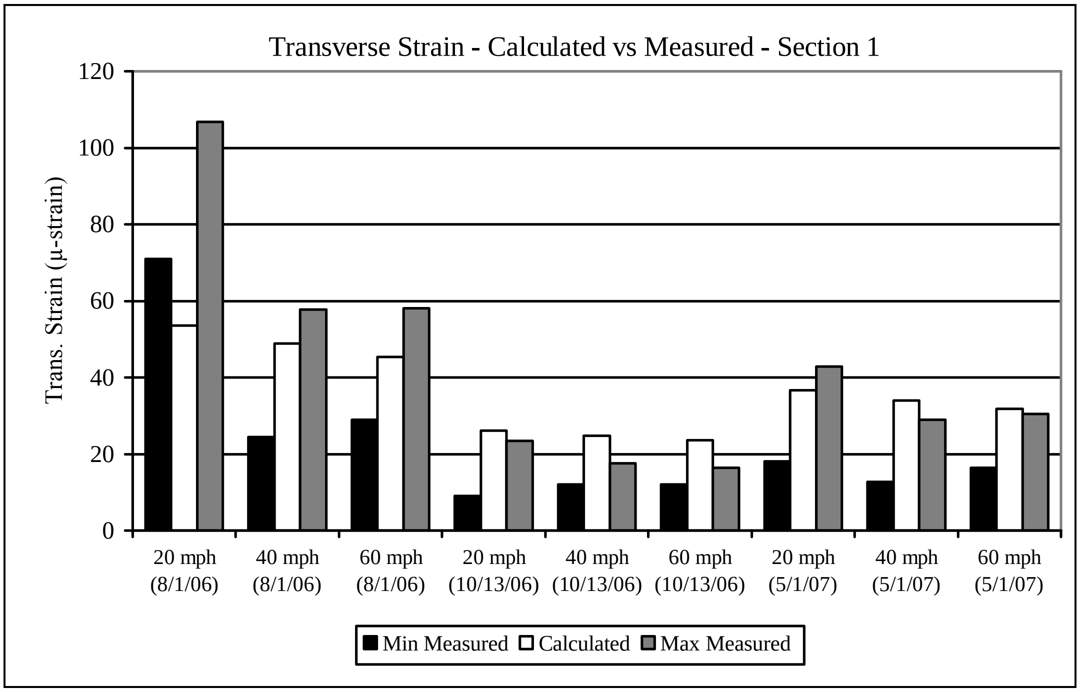


Figure 4-7: Transverse Strain – Predicted vs Measured – Section 1

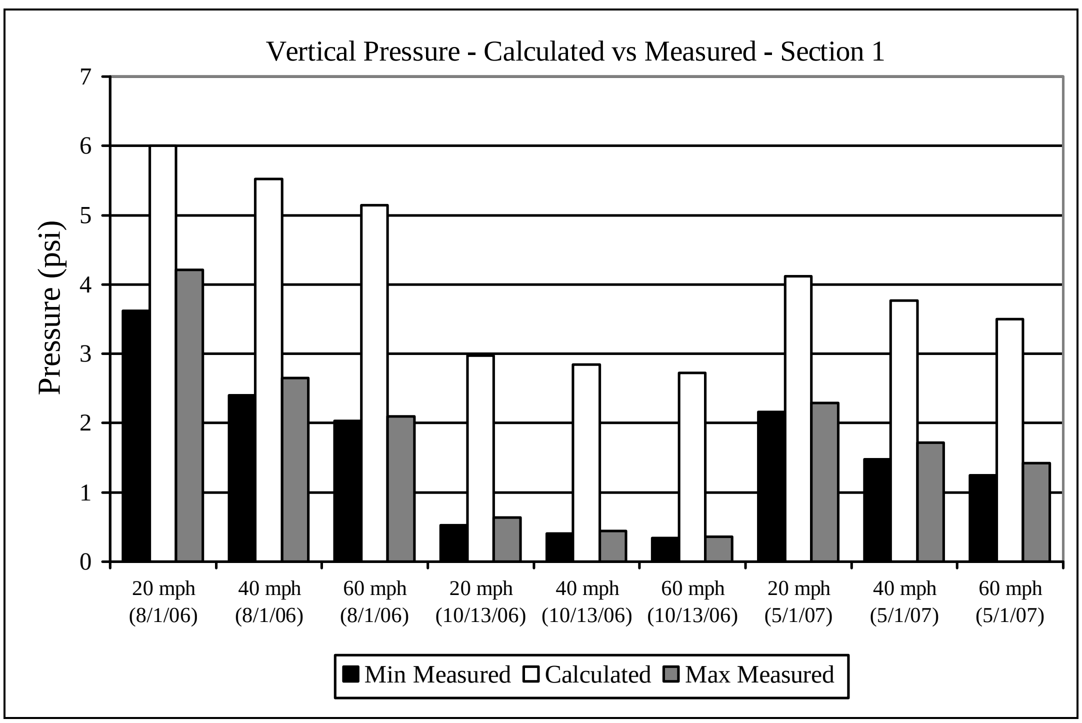


Figure 4-8: Vertical Pressure – Predicted vs Measured – Section 1

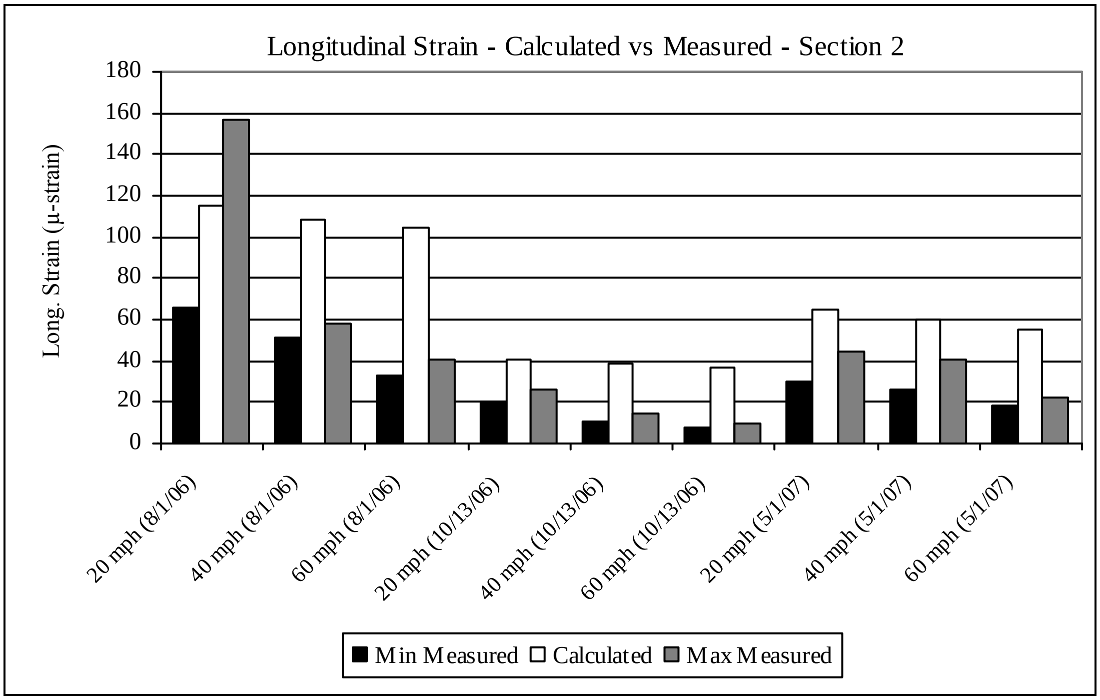


Figure 4-9: Longitudinal Strain – Predicted vs Measured – Section 2

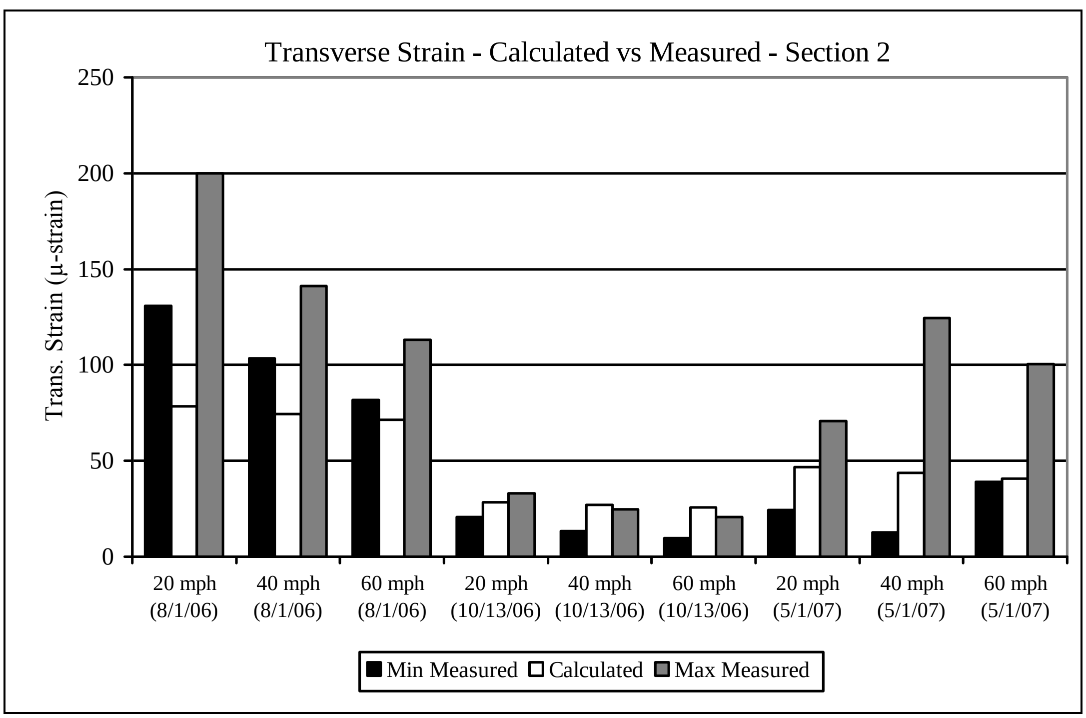


Figure 4-10: Transverse Strain – Predicted vs Measured – Section 2

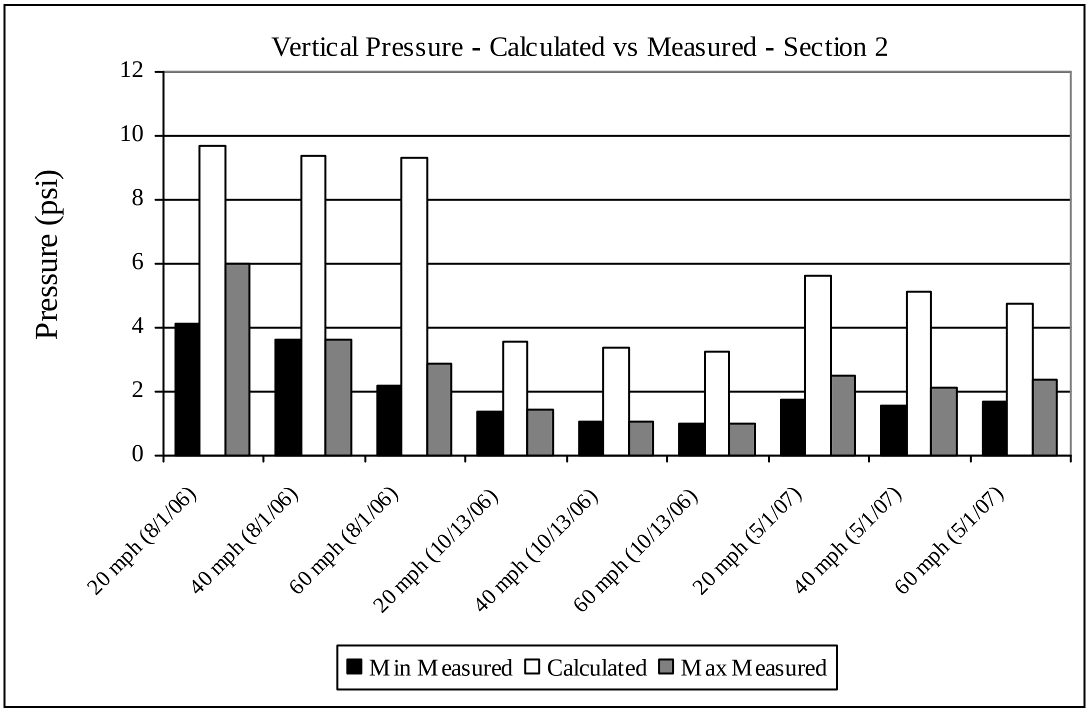


Figure 4-11: Vertical Pressure – Predicted vs Measured – Section 2

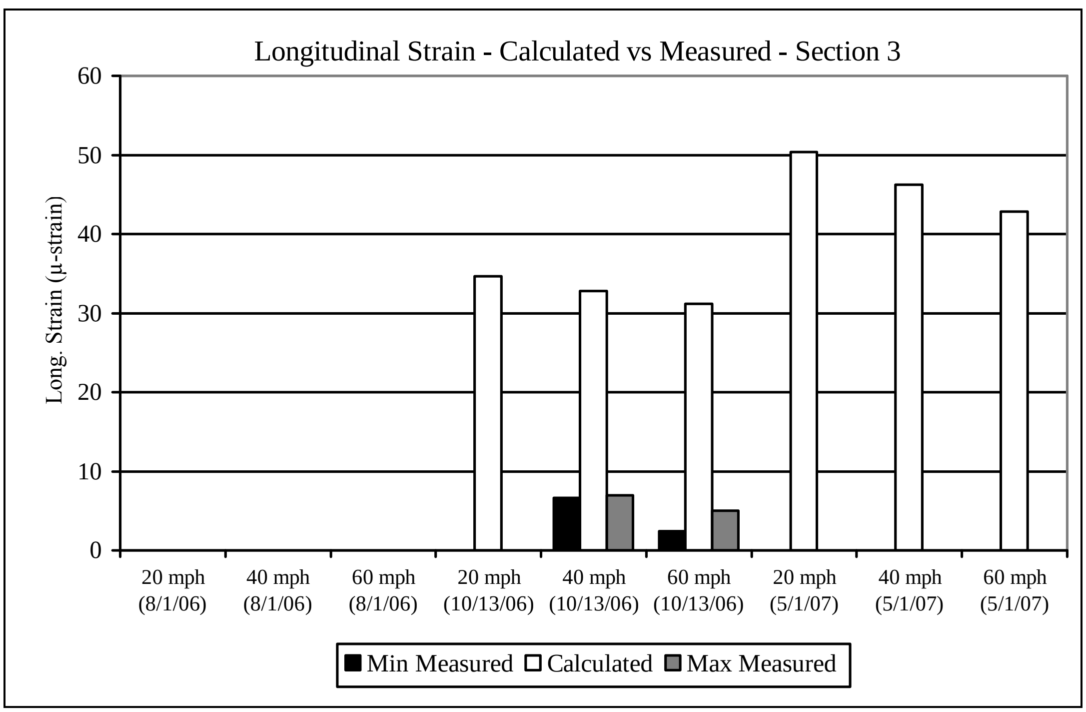


Figure 4-12: Longitudinal Strain – Predicted vs Measured – Section 3

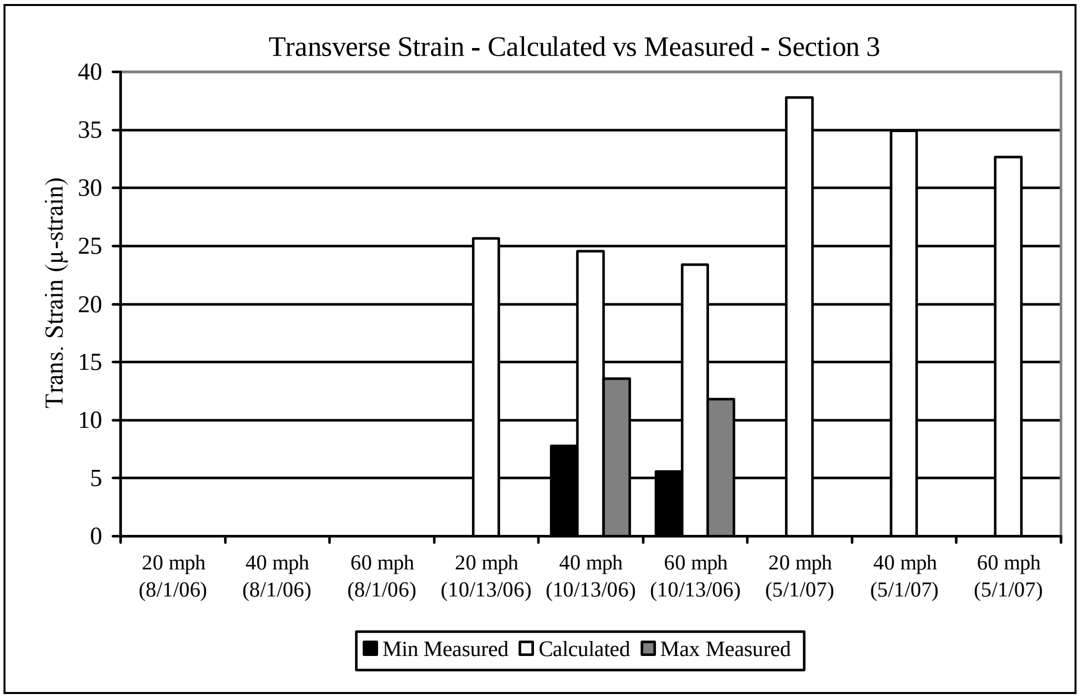


Figure 4-13: Transverse Strain – Predicted vs Measured – Section 3

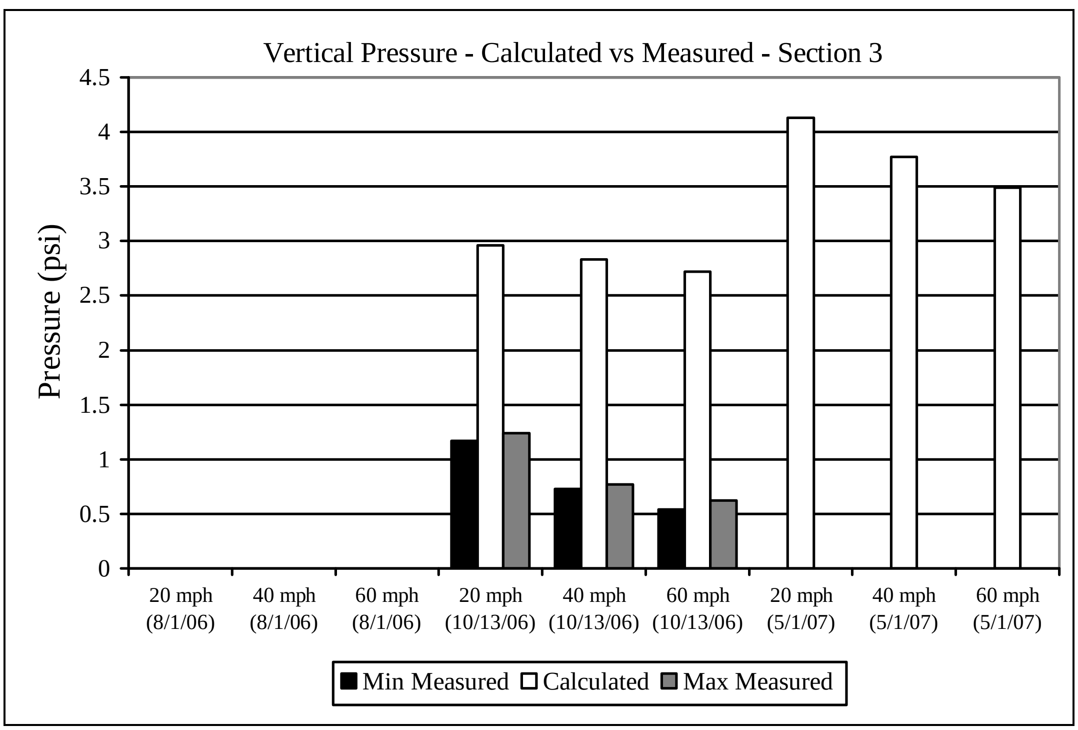


Figure 4-14: Vertical Pressure – Predicted vs Measured – Section 3

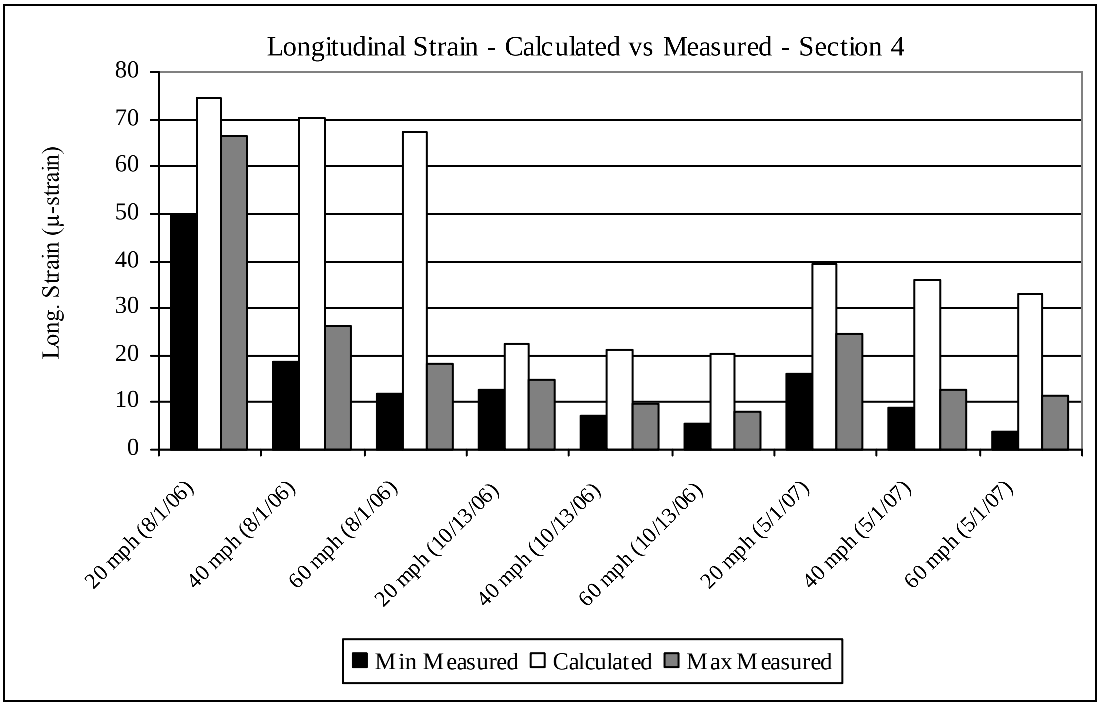


Figure 4-15: Longitudinal Strain – Predicted vs Measured – Section 4

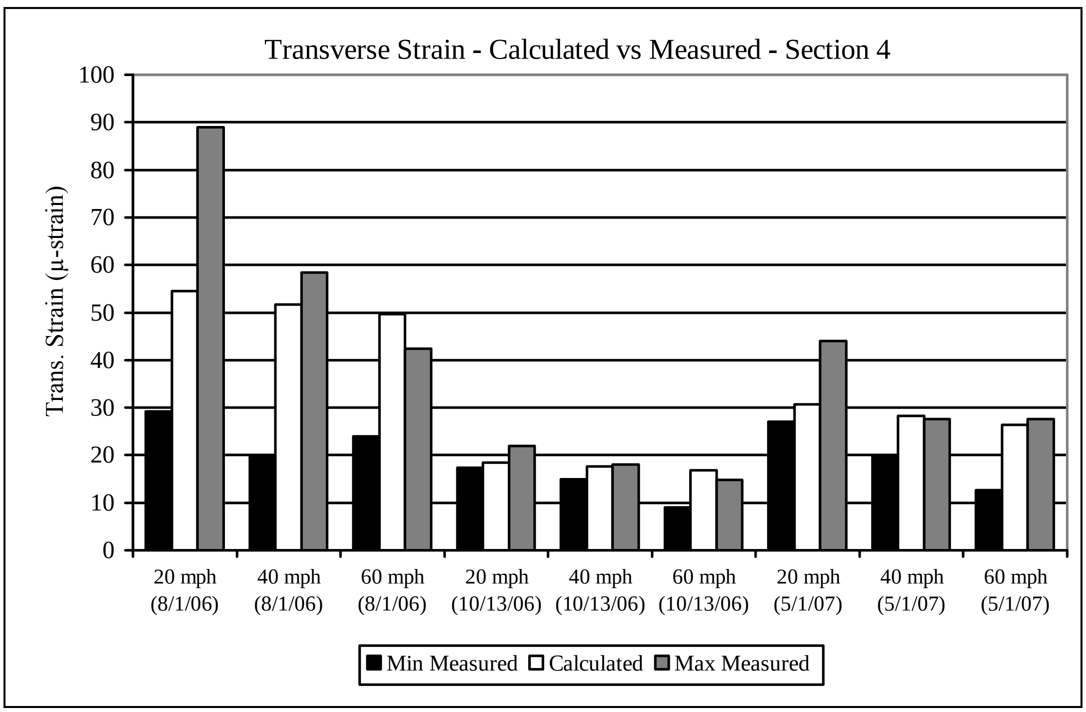


Figure 4-16: Transverse Strain – Predicted vs Measured – Section 4

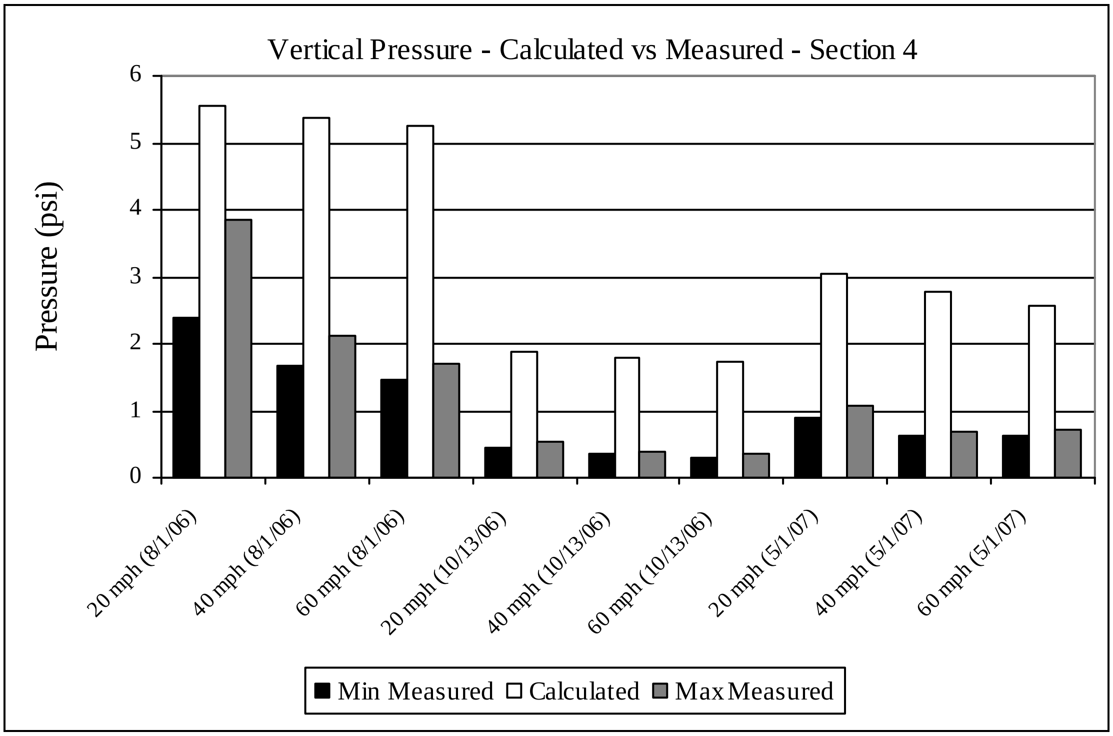


Figure 4-17: Vertical Pressure – Predicted vs Measured – Section 4

## 4.2 Finite Element Analysis

### *4.2.1 Description*

In this thesis work, a three dimensional finite element model was developed by the author of this work, to simulate the behavior of the first section of the US-75 project. The pavement structure dimensions and materials are shown in Figure 4-18, which also includes sections 2 through 4. Critical strains and stresses tend to developed around the loading areas; they are small and sometimes negligible in the far field areas. In order to optimize the model, an analysis was carried out using a coarser mesh first, and then the areas of interest were refined with a finer mesh. This procedure was done to decrease the computational time without affecting the accuracy of the results.

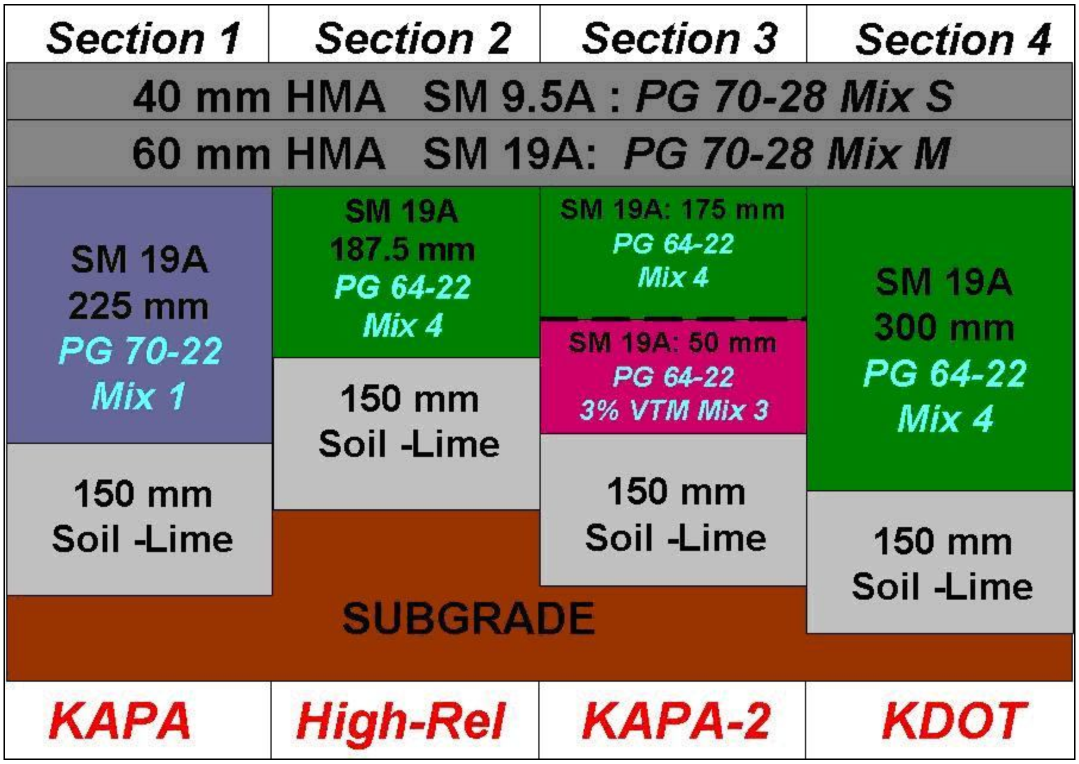


Figure 4-18: Pavement Sections of US-75 Project

*4.2.2 Model Geometry*

As stated in Section 4.2.1, a mesh was developed for Section 1 of the US-75 project. Based on suggestions from the literature review and also after performing a brief sensitivity analysis of the models, it was decided to make the model 270-inch long, 144-inch wide and 90 inches deep (Figure 4-19). These measurements, aside from allowing the pavement models to be long and wide enough to yield reliable results, they allow both axles of the loading truck be present simultaneously on the pavement when modeling one complete pass over the pavement. The nominal thickness of each material layer was used in the model. Table 4-6 provides the thicknesses and materials used in the model developed for the analysis.

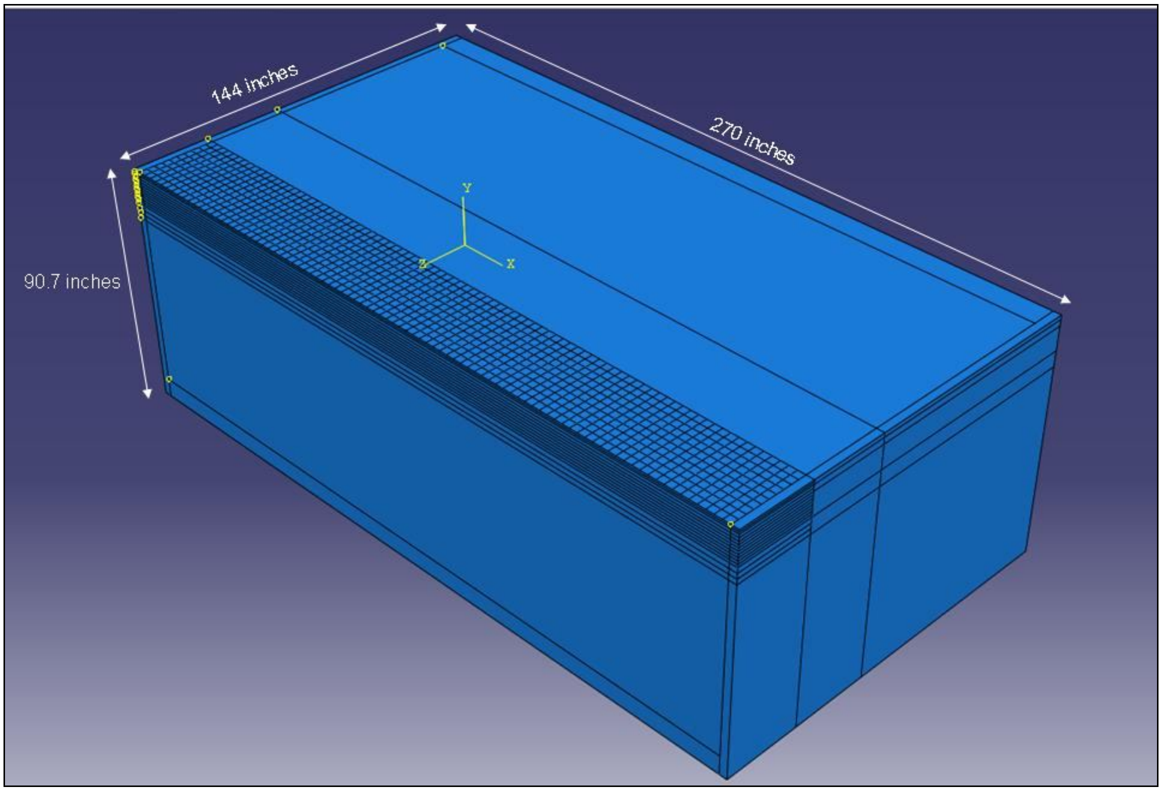


Figure 4-19: Pavement Model Dimensions

Table 4-6: Section 1

| Layer | Thickness (mm) | Material | Mix Code |
|---|---|---|---|
| Surface | 40 | HMA SM 9.5A: PG 70-28 | S |
| Binder | 60 | HMA SM 19A: PG 70-28 | M |
| Base | 225 | HMA SM 19A: PG 70-22 | 1 |
| Sub-base | 150 | Lime Treated Soil | |
| Sub-grade | Infinite | Clayey Soil | |

### *4.2.3 Material Properties*

#### 4.2.3.1 Visco-elastic Materials

Modeling of visco-elastic materials is generally done using the Weichert model mentioned in Section 2.4.1.6. However, the relaxation modulus test is rarely conducted in the laboratory due to experimental constraints. It is well accepted that all linear visco-elastic material functions are mathematically equivalent. Therefore, one material function can be converted into other material functions through corresponding mathematical operations (Yin, 2007). In this study, dynamic modulus data obtained on five different asphalt concrete mixes used in the project were converted into shear and bulk relaxation modulus using the numerical method proposed by Schapery and Park (1999):

$$K(t) = \frac{|E^*|\cos\phi}{3\Gamma(1-n)\cos\left(\frac{n\pi}{2}\right)(1-2\nu)} \tag{4.1}$$

$$G(t) = \frac{|E^*|\cos\phi}{2\Gamma(1-n)\cos\left(\frac{n\pi}{2}\right)(1+\nu)} \tag{4.2}$$

where:

$G(t)$ = shear relaxation modulus

$K(t)$ = bulk relaxation modulus

|E*| = dynamic Modulus

$\phi$ = phase angle

$\Gamma$ = gamma function

$\nu$ = Poisson’s ratio

$n$ = slope of the $|E^*|$ master curve in log-log domain

The dynamic modulus and phase angle values are obtained directly from the complex modulus test. The Γ(1-n) can be obtained implementing the function that comes built in Microsoft Excel as GAMMALN, which yields the natural logarithm of the gamma function. The Poisson's ratio was set to 0.3 as recommended by the MEPDG guide (ERES 2004). The *n*-values calculation will be explained following the explanation of the development of the master curves.

4.2.3.1.1 HMA Dynamic Modulus Master Curves

In order to perform the conversions, master curves of dynamic modulus were developed for each of the asphalt concrete mixes. Master curves describe the time dependency of the mixes and are developed to obtain modulus of HMA at different levels of temperature and loading speed. They are constructed using the principle of time-temperature superposition, where dynamic modulus data obtained at different temperatures are shifted with respect to frequency until the curves merge into a single smooth function (Yin, 2007). The amount of shifting needed to create a smooth curve describes the temperature dependency of the asphalt concrete mixes.

The shifting of the dynamic modulus data is done by first selecting a reference temperature, which in this study was 20 ºC. Frequency-temperature combinations that yielded similar dynamic modulus values were then determined. The shift factors were calculated as follows:

$$a(T) = \frac{f_{ref}}{f_q} \tag{4.3}$$

where:

$a(T)$ = shift factor

$f_{ref}$ = frequency at the reference temperature

$f_q =$ frequency at the temperature in question

Figure 4-20 shows a Shift Factor versus Temperature curve obtained for Mix 1. All the curves showing the relationship between shift factor and temperature for the HMA mixes used in this study are presented in Appendix E.

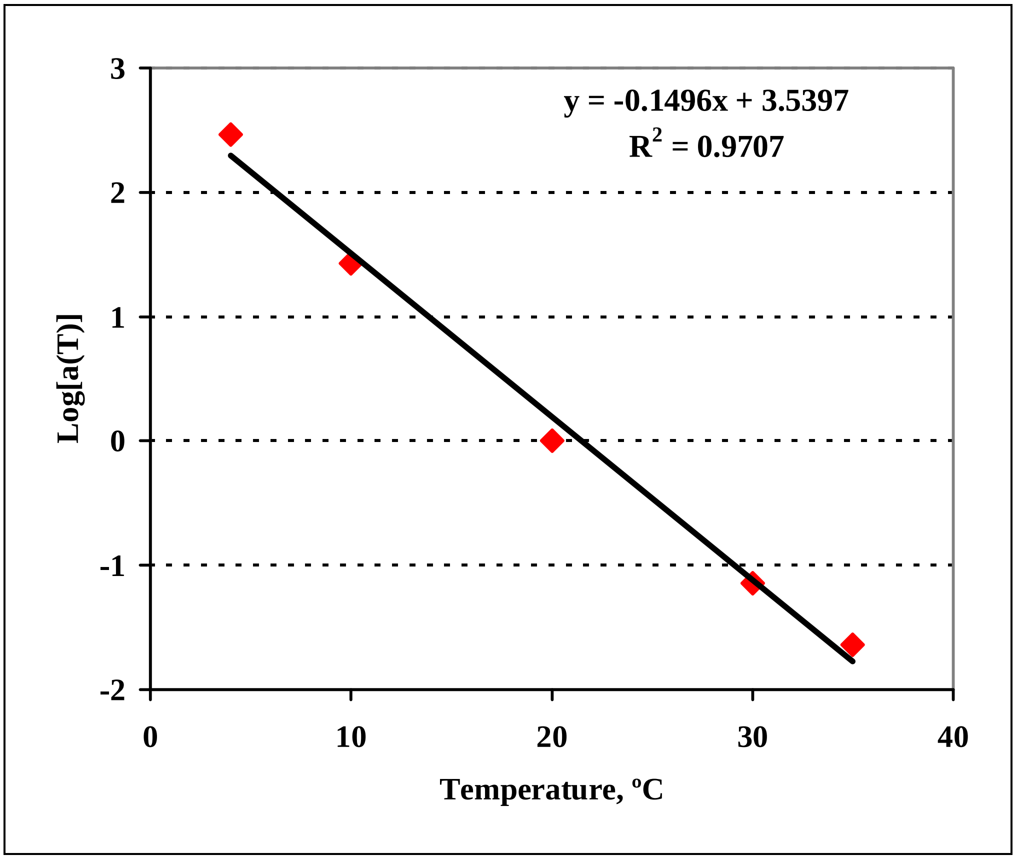


Figure 4-20: Shift Factor vs Temperature Curve – Mix 1

Finally, the reduced frequencies were obtained from as follows:

$$f_r = a(T) \times f \tag{4.4}$$

where:

$f_r =$ reduced frequency, Hz

$a(T)$ = shift factor, dependent on the temperature T

$f$ = original frequency, Hz

The dynamic modulus values were plotted against the reduced frequency and the master curves were mathematically modeled by fitting to the data the following sigmoidal function recommended by AASHTO TP-62:

$$Log|E^*| = a + \frac{b}{1 + \frac{1}{e^{d+e[Log(f_r)]}}} \tag{4.5}$$

where:

$|E^*|$ = dynamic modulus

a, b, d, e = regression coefficients

$f_r$ = reduced frequency

The curve fitting was performed using Microsoft Excel solver. A master curve for Mix 1 is presented in the Figure 4-21. All the master curves for the mixes used in this study are presented in Appendix F. Notice that the master curves include only the reduced frequency range for which dynamic modulus values were obtained from the laboratory tests. For this reason, the sigmoidal curve does not show the plateaus at very low and very high reduced frequency values.

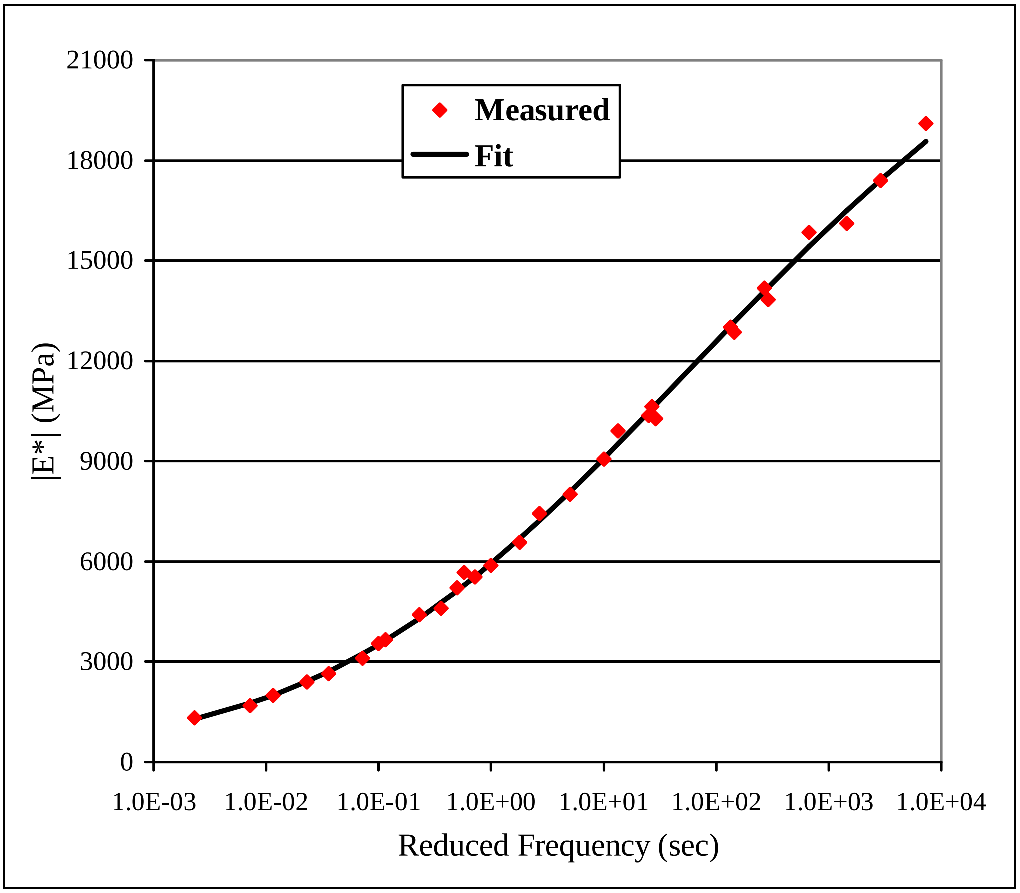


Figure 4-21: Dynamic Modulus Master Curve

4.2.3.1.2 Shear and Bulk Relaxation Master Curves

The *n*-values used in the conversion of |E*| data to shear and bulk relaxation modulus were obtained from the first derivative of the dynamic modulus master curves sigmoidal function with respect to $Log(f_r)$:

$$n = \frac{dLog|E^*|}{dLog(f_r)} \tag{4.6}$$

Once all parameters mentioned above were obtained, the conversions were carried out using a Microsoft Excel spreadsheet that was developed for this purpose only, and the shear and bulk relaxation master curves were plotted for each mix used in the project. For these master curves, reduced frequency was converted to reduced time as follows:

$$t_r = \frac{1}{f_r} \tag{4.7}$$

where:

$t_r$ = reduced time, sec

$f_r$ = reduced frequency, Hz

Following the same steps previously implemented for the construction of dynamic modulus master curves, sigmoidal fitting curves were developed for the calculated shear and bulk relaxation modulus of each asphalt concrete mix. Figures 4-22 and 4-23 show the shear and bulk relaxation master curves for Mix 1. Appendices G and H show the shear and bulk relaxation master curves for all five HMA mixes used in the project.

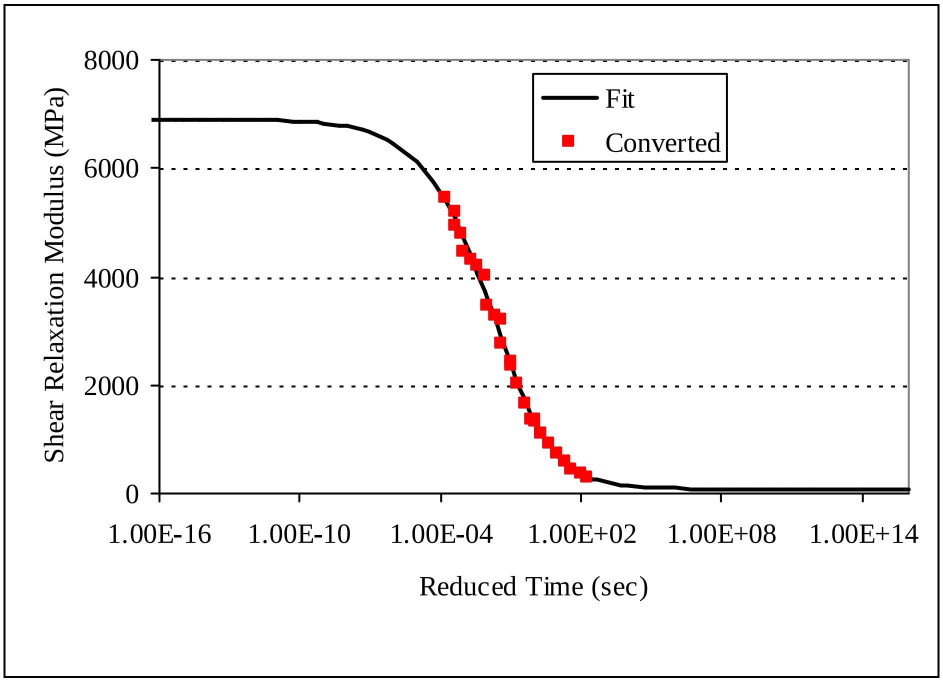


Figure 4-22: Shear Relaxation Modulus Master Curve

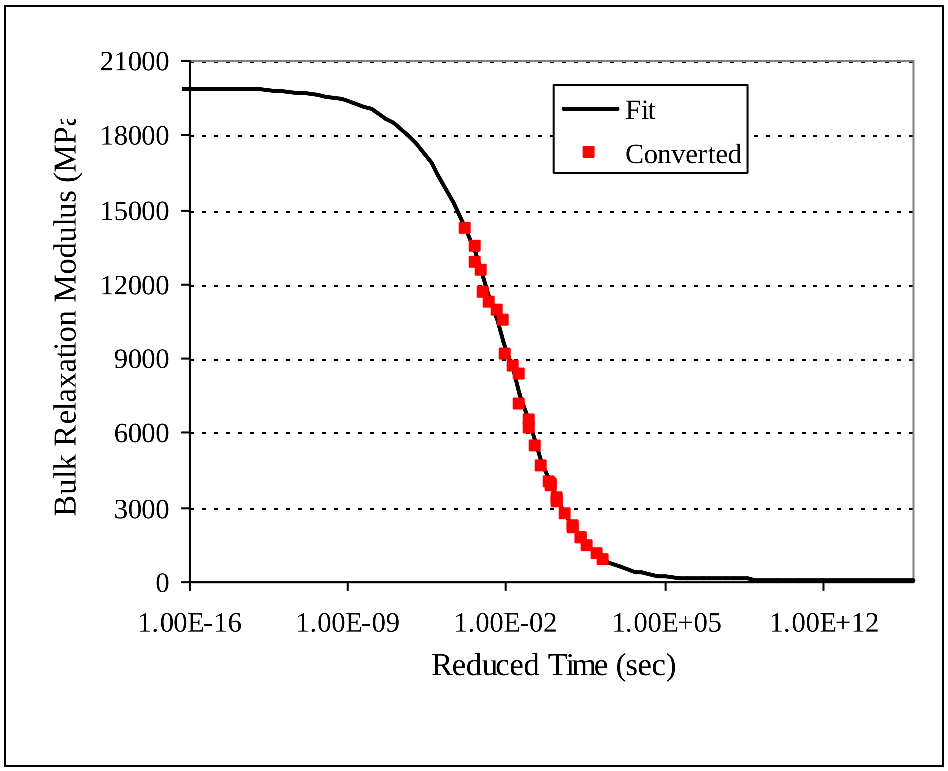


Figure 4-23: Bulk Relaxation Modulus Master Curve

4.2.3.1.3 Calculation of Prony Series Parameters

Two different options for visco-elastic material models are available in ABAQUS: the Time Domain Viscoelasticity and the Frequency Domain Viscoelasticity. The Time Domain Viscoelasticity was implemented in this research since the model is analyzed as a quasi-static problem, and it is the only option that runs with this type of analysis.

The Time Domain Viscoelasticity requires the input of three prony series parameters in order to be able to run the analysis. These parameters are the dimensionless shear relaxation modulus ($g_i$), the dimensionless bulk relaxation modulus ($k_i$), and the reduced relaxation time ($t_i$). These parameters are represented by the following equations:

$$g_i = \frac{G_i}{G_0} \tag{4.8}$$

where:

$g_i$ = dimensionless shear relaxation modulus at time $i$

$G_i$ = shear relaxation modulus at time $i$

$G_0$ = initial shear relaxation modulus

$$k_i = \frac{K_i}{K_0} \tag{4.9}$$

where:

$k_i$ = dimensionless bulk relaxation modulus at time $i$

$K_i$ = bulk relaxation modulus at time $i$

$K_0$ = initial bulk relaxation modulus

The prony series parameters were calculated by developing a Microsoft Excel spreadsheet to fit curves representing Equations 4.10 and 4.11 to the measured or converted shear and bulk relaxation modulus data.

$$G_R(t) = G_0\left(1 - \sum_{k=1}^{N} g_k^P\left(1 - e^{-t/\tau_k}\right)\right) \tag{4.10}$$

$$K_R(t) = K_0\left(1 - \sum_{k=1}^{N} k_k^P\left(1 - e^{-t/\tau_k}\right)\right) \tag{4.11}$$

where:

| | |
|---|---|
| $G_0$ , $K_0$ = | Instantaneous shear and bulk relaxation modulus |
| $g_k^P$ , $k_k^P$ = | Prony series coefficients |
| $t$ = | Time, sec |
| $\tau_k$ = | Relaxation or reduced time, sec |

Table 4-7 presents the calculated prony series parameters for the asphalt concrete mixes used in this research.

Table 4-7: Prony Series Parameters

| | $g_i$ | $k_i$ | $t_i$ |
|---|---|---|---|
| Mix S | 0.308954 | 0.38104 | 0.001 |
| | 0.103362 | 0.119207 | 0.01 |
| | 0.213567 | 0.151703 | 0.1 |
| | 0.155012 | 0.160324 | 1 |
| | 0.127155 | 0.117885 | 10 |
| Mix M | 0.677686 | 0.59063 | 0.001 |
| | 0.000000 | 0.000000 | 0.01 |
| | 0.104582 | 0.164675 | 0.1 |
| | 0.073812 | 0.082773 | 1 |
| | 0.074241 | 0.093324 | 10 |
| Mix 1 | 0.432905 | 0.479071 | 0.001 |
| | 0.04744 | 0.044055 | 0.01 |

Table 4-7 - *Continued*

| | gi | ki | ti |
|---|---|---|---|
| | 0.183055 | 0.181144 | 0.1 |
| | 0.115363 | 0.107065 | 1 |
| | 0.119419 | 0.106327 | 10 |
| Mix 3 | 0.202177 | 0.203267 | 0.001 |
| | 0.092143 | 0.10902 | 0.01 |
| | 0.206384 | 0.223547 | 0.1 |
| | 0.189619 | 0.198801 | 1 |
| | 0.177037 | 0.142907 | 10 |
| Mix 4 | 0.385022 | 0.386497 | 0.001 |
| | 0.069513 | 0.088042 | 0.01 |
| | 0.191603 | 0.197838 | 0.1 |
| | 0.13052 | 0.132064 | 1 |
| | 0.12557 | 0.115278 | 10 |

### *4.2.4 Element Type*

Selection of the element type is critical for any FE analysis in order for the model to yield correct results and at the same time reduce the computation time. Finite elements normally used in analyses involving stress follow a specific mathematical theory that describes how they behave. Even though quadratic elements require more computational time, they provide more accurate results. After reviewing previous works on finite element modeling of flexible pavements, it was decided to implement the C3D8R and CIN3D8 elements in this analysis.

C3D8R elements are eight-node linear brick elements with reduced integration. This type of elements have only one integration point, which is in the middle of the element, as shown in Figure 4-24. Number 1 at the center of the element is the integration point of the element, and numbers 1 through 8 at the corners are the nodal points or nodes. The advantage of implementing this type of element relies on its ability to reduce the costs of computational time without largely affecting the accuracy of the results (Yoo, 2007). On the other hand, since there is only one integration point, smaller elements are needed to capture stresses and strains at the boundary of a structure.

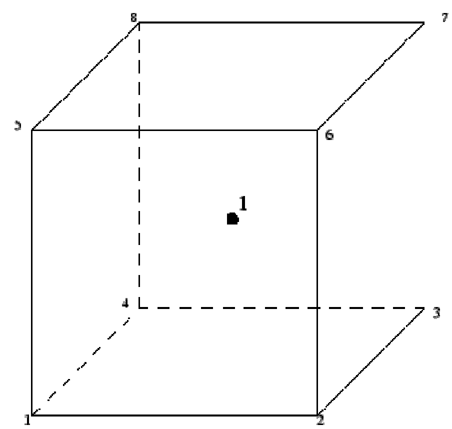


Figure 4-24: C3D8R Element

CIN3D8 elements are eight-node linear brick elements with a one-way infinite face, as shown in Figure 4-25. This type of element is used generally used to simulate far-field regions in the pavement. ABAQUS does not currently support CIN3D8 elements in its ABAQUS CAE platform, but these elements can be included in the input file through the use of a text editor. At first, it is particularly challenging to have the infinite faces pointing in the right direction, but this is easily accomplished by implementing a sweep mesh technique and redefining the sweeping path.

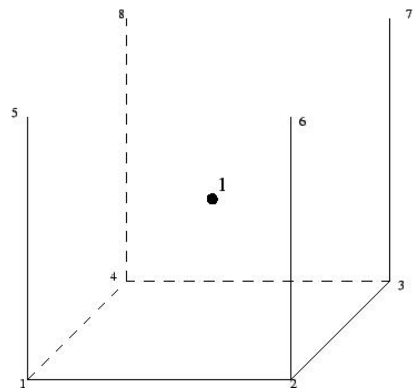


Figure 4-25: CIN3D8 Infinite Element

*4.2.5 Model Meshing*

As previously stated, meshing is a critical step in finite element modeling because it influences greatly the results of the analysis. ABAQUS has a variety of meshing tools and techniques that simplify the meshing process.

The first step in the meshing process is the seeding of the parts in the model. Seeding is the process of assigning sizes to the elements that will later make up the entire model. Seeding is an important step in the meshing process due to the fact that the results of the FE analysis highly depend on the mesh characteristics. In order to get valid results without excessively increasing the calculation time needed, different element sizes are assigned through the model depending on how close the elements are to the loading area. Elements that are close to the loading areas are assigned smaller sizes, leading to finer meshes around the areas of interest. After the seeding is done, the model is meshed.

Figure 4-26 shows the meshed pavement model developed for this study. A fine mesh was developed around the wheel path; the mesh was made gradually coarser in the far field areas. Elements on and around the wheel path are 3 inch by 3 inch with varying thicknesses. Elements in the far field areas are 3 by 9.33 inches, and elements in between are 3 by 6 inches. It is very important to keep in mind that in order to get reliable results, the aspect ratio of the elements should be 10 to 3 or less.

Thicknesses of elements were set depending on the critical location for the measurements needed. For instance, the base layer was subdivided into eight subsections in order to get accurate strain values at the bottom of the base layer. Element thickness at the surface, binder, sub-base and sub-grade layers were arbitrarily set after a brief sensitivity analysis. The surface and binder layer were subdivided into two subsections each. The sub-base was subdivided into three subsections, since it is closer to the critical locations.

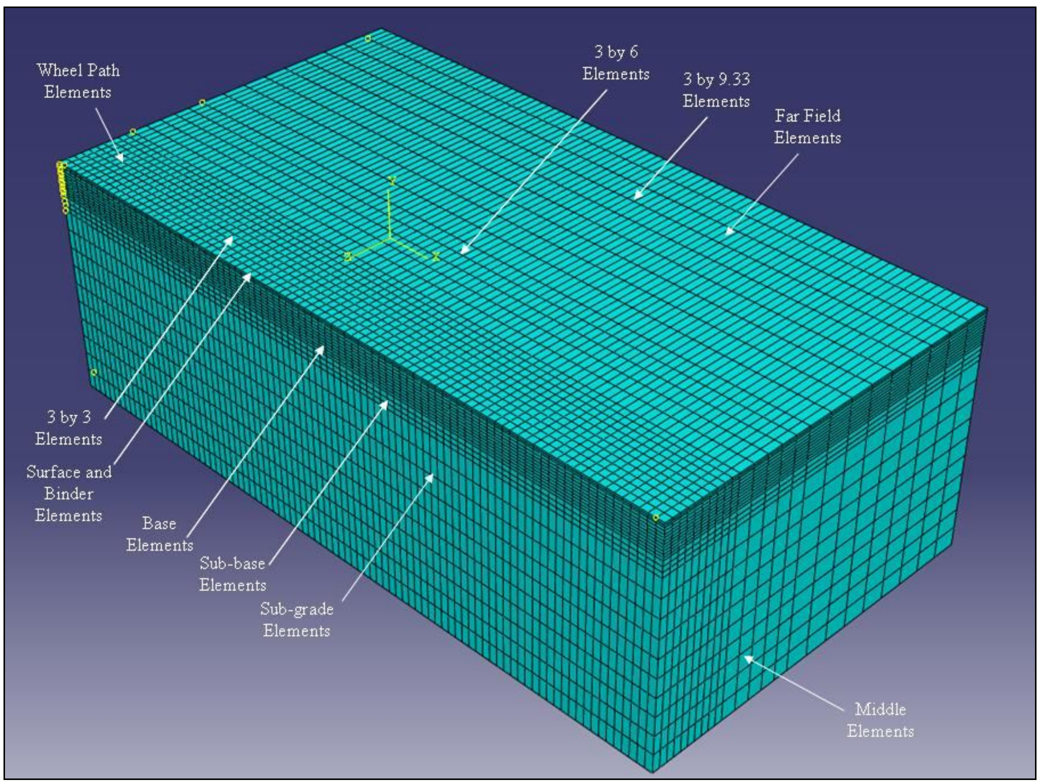


Figure 4-26: Meshed Model

*4.2.6 Boundary Conditions*

In this study, infinite elements boundaries were placed at both ends, on the far field side, and at the bottom of the model (Figure 4-21) in order to simulate the influence of far field areas in the pavement and to avoid fixation of the nodes at the bottom of the model. A symmetry boundary condition on the transverse direction was placed on the wheel path side of the model, along the line of symmetry, as shown in Figure 4-27.

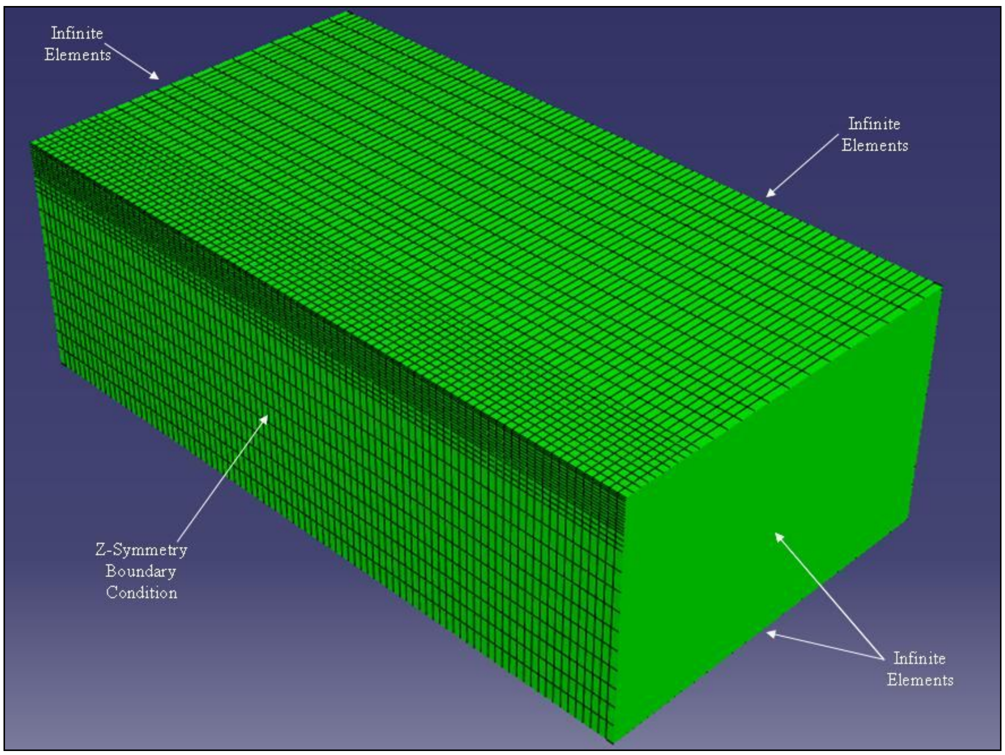


Figure 4-27: Boundary Conditions of the Model

*4.2.7 Simulation of Moving Loads*

Moving vehicle loads were modeled implementing the concept of step loading with trapezoidal loading amplitude. There are three main components of this concept: the entrance element, the elements within the tire imprint, and the leaving element. For instance, element three (Nº 3) in Figure 4-28 is the entrance element, the element where the loading amplitude will increase linearly from 0 at $T_0$ to 1 at $T_1$. Similarly, element one (Nº 1) is the leaving element, the element where the loading amplitude decreases linearly from 1 at $T_0$ to 0 at $T_1$. The elements within the tire imprint, element two (Nº 2 in Figure 4-22, experience a constant loading amplitude of 1 from $T_0$ to $T_1$. The transition from $T_0$ to $T_1$ completes one step in the model, and the load moves one element on each step.

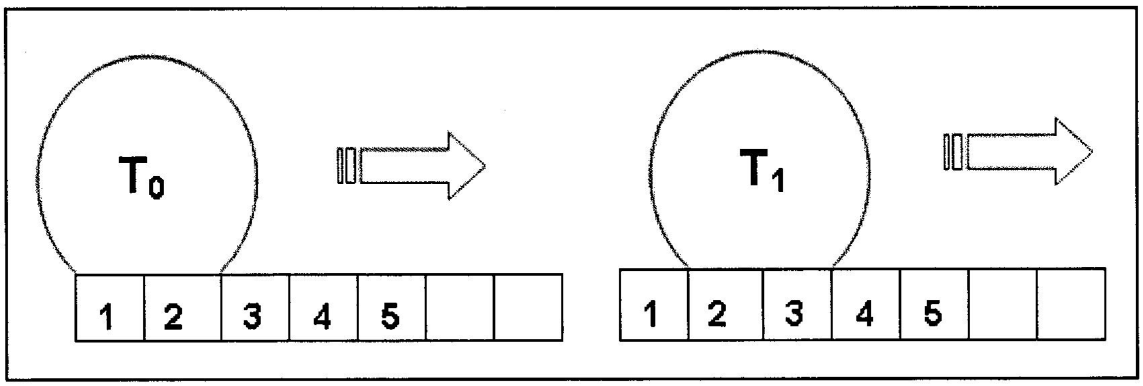


Figure 4-28: Step Loading Diagram (Yoo, 2007)

The duration of each step or step time was calculated depending on the speed that was modeled. For instance, the speed was converted from miles per hour into inches per second. Then the size of each element on the wheel path was divided by the speed in inches per second to obtain the time required for each step to move the load at the desired speed. In this model, the size of the elements on the wheel path was 3 inches. To model the load moving at 60 mph, which is equal to 1056 inches per second, the 3 inches was divided by 1,056 inches per second, and a step time of 0.002841 seconds was obtained. Similarly, step time to simulate 20 and 40 mph speeds were calculated to be 0.008523 and 0.007371 seconds, respectively.

Loading amplitudes were created using the tabulated option in ABAQUS. Tables 4-9, 4-10, and 4-11 present the tabular data used to create the loading amplitudes for 20, 40, and 60 mph speeds.

Table 4-8: Loading Amplitude Tabular Data for Entrance Elements

| 20 mph | | 40 mph | | 60 mph | |
|---|---|---|---|---|---|
| Step Time, sec | Amplitude | Step Time, sec | Amplitude | Step Time, sec | Amplitude |
| 0.000E+00 | 0.0 | 0.000E+00 | 0.0 | 0.000E+00 | 0.0 |
| 8.523E-04 | 0.1 | 7.371E-04 | 0.1 | 2.841E-04 | 0.1 |
| 1.705E-03 | 0.2 | 1.474E-03 | 0.2 | 5.682E-04 | 0.2 |
| 2.557E-03 | 0.3 | 2.211E-03 | 0.3 | 8.523E-04 | 0.3 |
| 3.409E-03 | 0.4 | 2.948E-03 | 0.4 | 1.136E-03 | 0.4 |
| 4.262E-03 | 0.5 | 3.686E-03 | 0.5 | 1.421E-03 | 0.5 |
| 5.114E-03 | 0.6 | 4.423E-03 | 0.6 | 1.705E-03 | 0.6 |
| 5.966E-03 | 0.7 | 5.160E-03 | 0.7 | 1.989E-03 | 0.7 |
| 6.818E-03 | 0.8 | 5.897E-03 | 0.8 | 2.273E-03 | 0.8 |
| 7.671E-03 | 0.9 | 6.634E-03 | 0.9 | 2.557E-03 | 0.9 |
| 8.523E-03 | 1.0 | 7.371E-03 | 1.0 | 2.841E-03 | 1.0 |

Table 4-9: Loading Amplitude Data for Elements within the Wheel Path

| 20 mph | | 40 mph | | 60 mph | |
|---|---|---|---|---|---|
| Step Time, sec | Amplitude | Step Time, sec | Amplitude | Step Time, sec | Amplitude |
| 0.000E+00 | 1.0 | 0.000E+00 | 1.0 | 0.000E+00 | 1.0 |
| 8.523E-04 | 1.0 | 7.371E-04 | 1.0 | 2.841E-04 | 1.0 |
| 1.705E-03 | 1.0 | 1.474E-03 | 1.0 | 5.682E-04 | 1.0 |
| 2.557E-03 | 1.0 | 2.211E-03 | 1.0 | 8.523E-04 | 1.0 |
| 3.409E-03 | 1.0 | 2.948E-03 | 1.0 | 1.136E-03 | 1.0 |
| 4.262E-03 | 1.0 | 3.686E-03 | 1.0 | 1.421E-03 | 1.0 |
| 5.114E-03 | 1.0 | 4.423E-03 | 1.0 | 1.705E-03 | 1.0 |
| 5.966E-03 | 1.0 | 5.160E-03 | 1.0 | 1.989E-03 | 1.0 |
| 6.818E-03 | 1.0 | 5.897E-03 | 1.0 | 2.273E-03 | 1.0 |
| 7.671E-03 | 1.0 | 6.634E-03 | 1.0 | 2.557E-03 | 1.0 |
| 8.523E-03 | 1.0 | 7.371E-03 | 1.0 | 2.841E-03 | 1.0 |

Table 4-10: Loading Amplitude Tabular Data for Leaving Elements

| 20 mph | | 40 mph | | 60 mph | |
|---|---|---|---|---|---|
| Step Time, sec | Amplitude | Step Time, sec | Amplitude | Step Time, sec | Amplitude |
| 0.00E+00 | 1.0 | 0.00E+00 | 1.0 | 0.000E+00 | 1.0 |
| 8.52E-04 | 0.9 | 7.37E-04 | 0.9 | 2.841E-04 | 0.9 |
| 1.71E-03 | 0.8 | 1.47E-03 | 0.8 | 5.682E-04 | 0.8 |
| 2.56E-03 | 0.7 | 2.21E-03 | 0.7 | 8.523E-04 | 0.7 |
| 3.41E-03 | 0.6 | 2.95E-03 | 0.6 | 1.136E-03 | 0.6 |
| 4.26E-03 | 0.5 | 3.69E-03 | 0.5 | 1.421E-03 | 0.5 |
| 5.11E-03 | 0.4 | 4.42E-03 | 0.4 | 1.705E-03 | 0.4 |
| 5.97E-03 | 0.3 | 5.16E-03 | 0.3 | 1.989E-03 | 0.3 |
| 6.82E-03 | 0.2 | 5.90E-03 | 0.2 | 2.273E-03 | 0.2 |
| 7.67E-03 | 0.1 | 6.63E-03 | 0.1 | 2.557E-03 | 0.1 |
| 8.52E-03 | 0.0 | 7.37E-03 | 0.0 | 2.841E-03 | 0.0 |

### *4.2.8 Finite Element Analysis Results*

#### 4.2.8.1 Viscoelastic Model

Results for the visco-elastic finite element model are presented in Table 4-12. Figures 4-29, 4-30, and 4-31 compare the values obtained from the visco-elastic FEM with the measured pavement response values. As shown in these charts, the results from the visco-elastic FEM were smaller than the measured values, which suggested that there was a problem either in the model, or in the material properties that were used in the visco-elastic model.

First, the prony series parameters used in the model were compared with prony series parameters published in previous works, just to see if the parameters were similar. It was discovered that the parameters used in this work were 2 to 3 times larger than parameters published in the literature for asphalt concrete mixes, so the steps followed to calculate these parameters were checked, and it was concluded that there was no calculation errors.

The second step was to check the model itself. In order to do this, it was decided to remove all visco-elastic parameters from the model, and run it as a linear elastic finite element model with elastic properties only, the same elastic properties that were used in the visco-elastic FEM. Results of this analysis will be presented in the following section.

Table 4-11: Visco-elastic Finite Element Model Analysis Results

| Date | Nominal Speed (mph) | Longitudinal Strain (μ-strain) | | Transverse Strain (μ-strain) | | Vertical Pressure (psi) | |
|---|---|---|---|---|---|---|---|
| | | Front | Rear | Front | Rear | Front | Rear |
| 5/1/2007 | 20 | 2.66 | 4.81 | 2.60 | 3.76 | 0.78 | 1.46 |
| | 40 | 2.43 | 4.41 | 2.39 | 3.50 | 0.68 | 1.29 |
| | 60 | 2.24 | 4.06 | 2.20 | 3.26 | 0.62 | 1.19 |

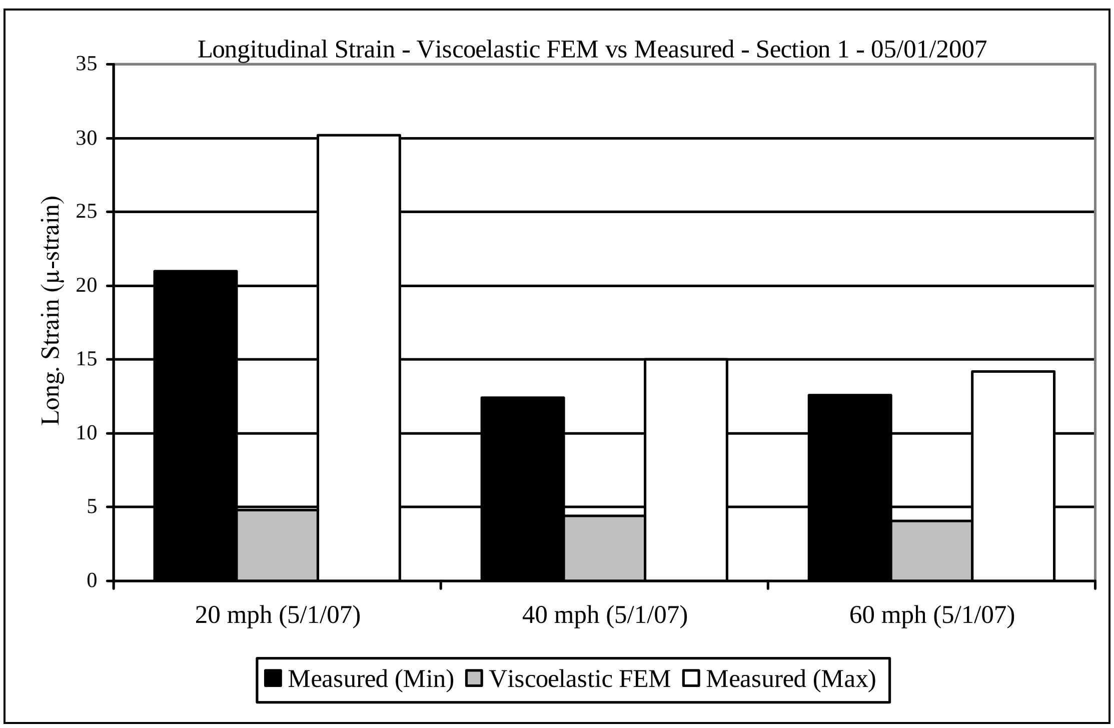


Figure 4-29: Longitudinal Strain – Viscoelastic FEM vs Measured

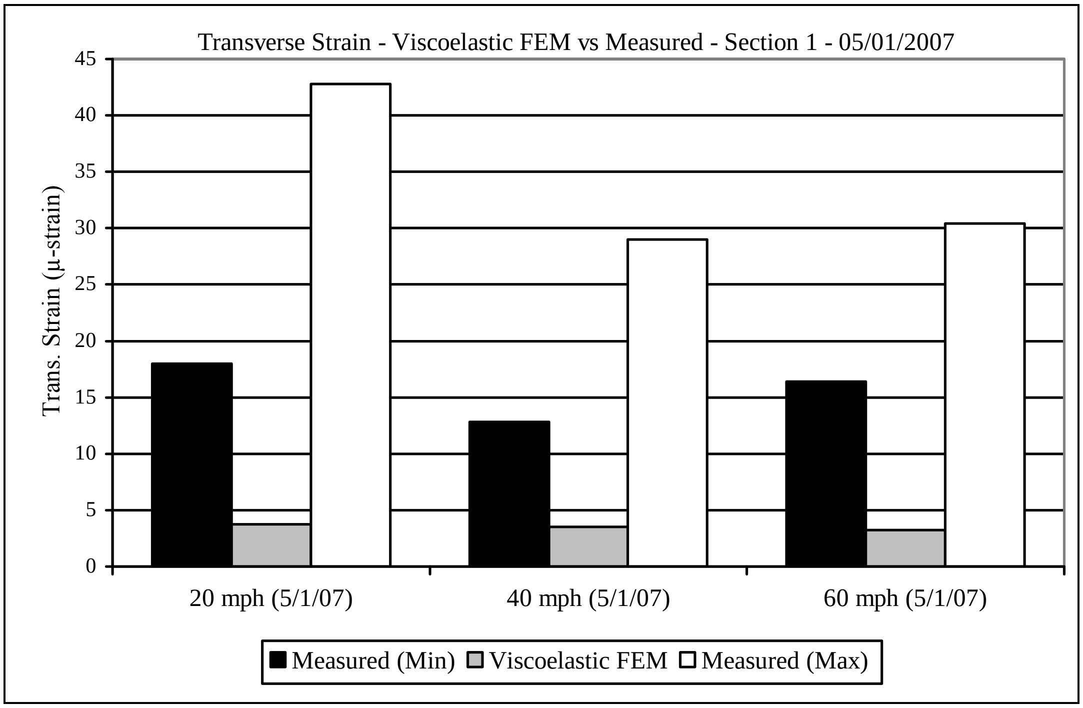


Figure 4-30: Transverse Strain – Visco-elastic FEM vs Measured

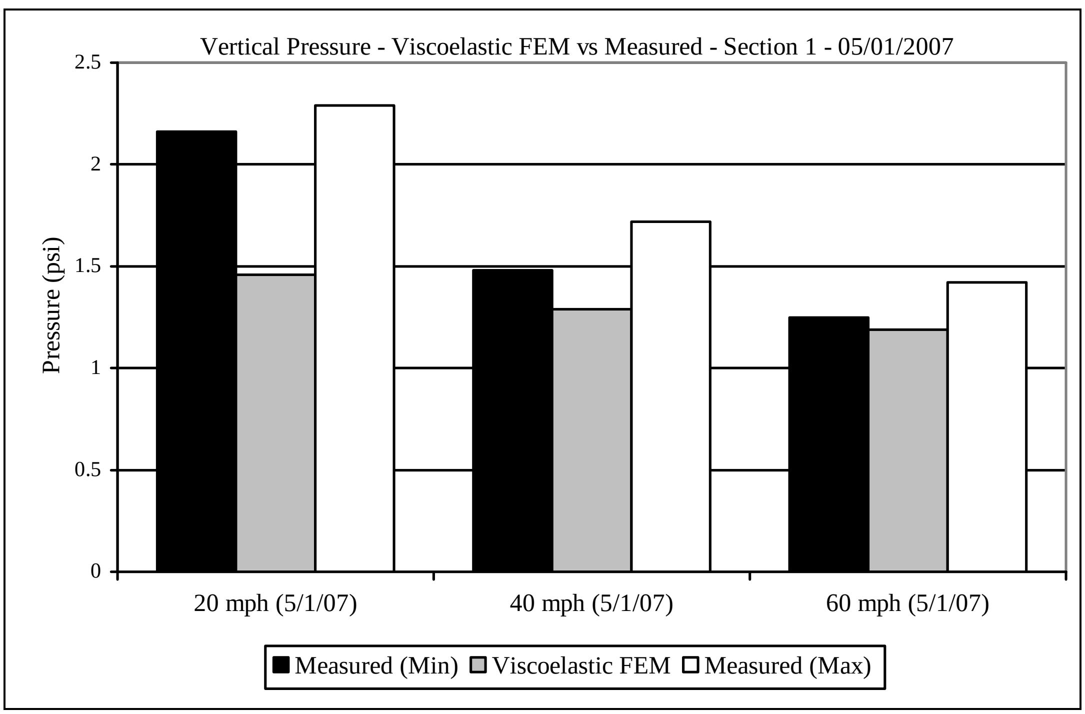


Figure 4-31: Vertical Pressure – Visco-elastic FEM vs Measured

4.2.8.2 Elastic Model

Results of the elastic FEM are presented in Table 4-13. Figures 4-32, 4-33, and 4-34 present a comparison between the elastic FEM results and the results from the linear elastic software EVERSTRESS. These figures were developed to check if the results of the linear elastic finite element model were in accordance with the results from the linear elastic EVERSTRESS software. As it is seen in these charts, results from the elastic finite element model are very similar to the results from the linear elastic EVERSTRESS software. Small discrepancies are still observed, but this may be explained by the fact that in the elastic finite element model, the loaded area is assumed to be rectangular, while in EVERSTRESS, the loaded area is assumed to be circular.

The important outcome of these comparisons between the elastic finite element model and the linear elastic results from EVERSTRESS is that the similarities in the results prove that the mesh, the boundary conditions applied, and the method of loading the model can be assumed to be correct.

Table 4-12: Linear Finite Element Model Analysis Results

| Date | Nominal Speed (mph) | Longitudinal Strain (μ-strain) | | Transverse Strain (μ-strain) | | Vertical Pressure (psi) | |
|---|---|---|---|---|---|---|---|
| | | Front | Rear | Front | Rear | Front | Rear |
| 5/1/2007 | 20 | 20.8 | 36.9 | 20.7 | 28.6 | 2.1 | 3.5 |
| | 40 | 19.1 | 34.0 | 19.0 | 26.5 | 1.9 | 3.3 |
| | 60 | 17.7 | 31.6 | 17.6 | 24.8 | 1.8 | 3.1 |

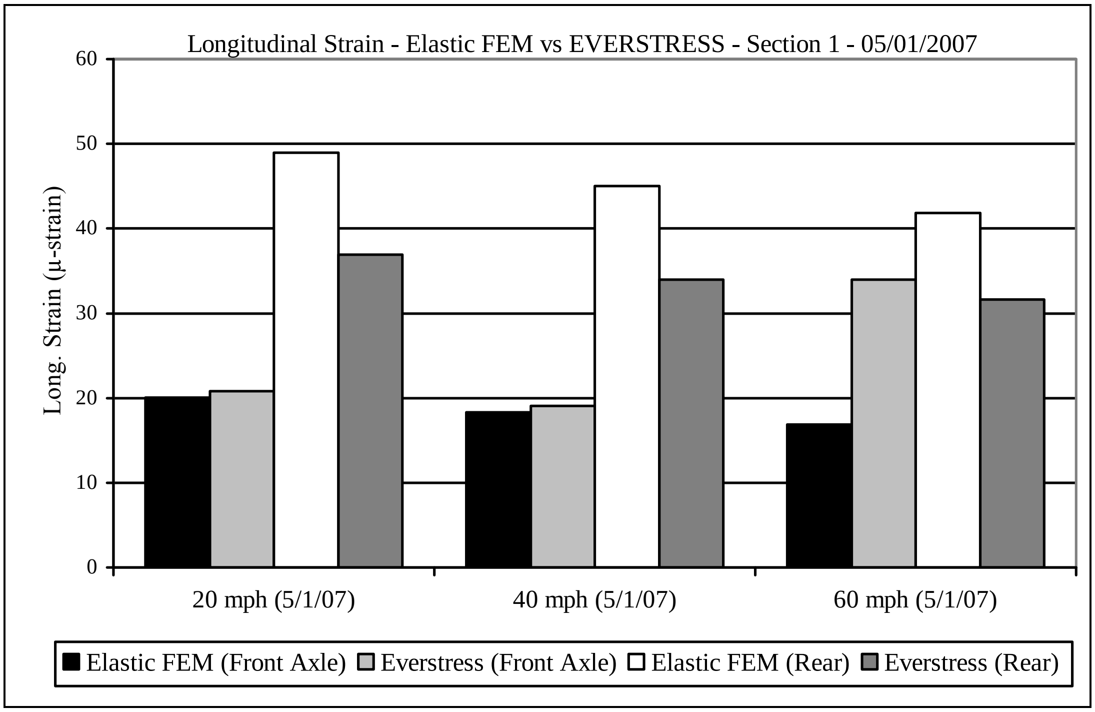


Figure 4-32: Longitudinal Strain – Elastic FEM vs Linear Elastic

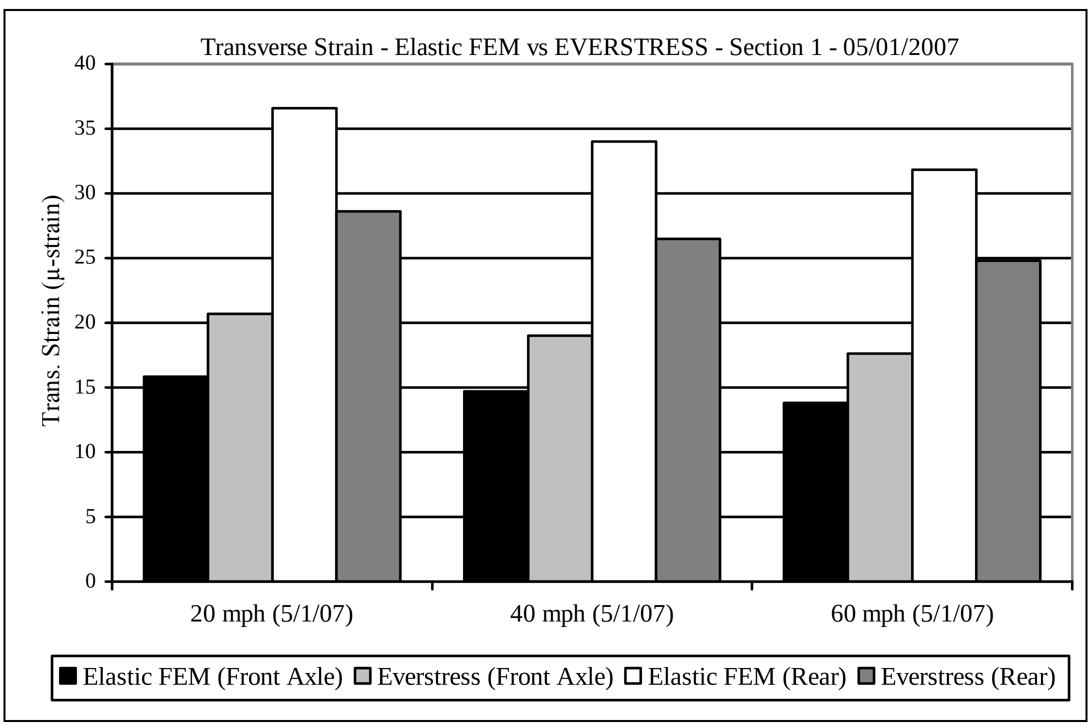


Figure 4-33: Transverse Strain – Elastic FEM vs Linear Elastic

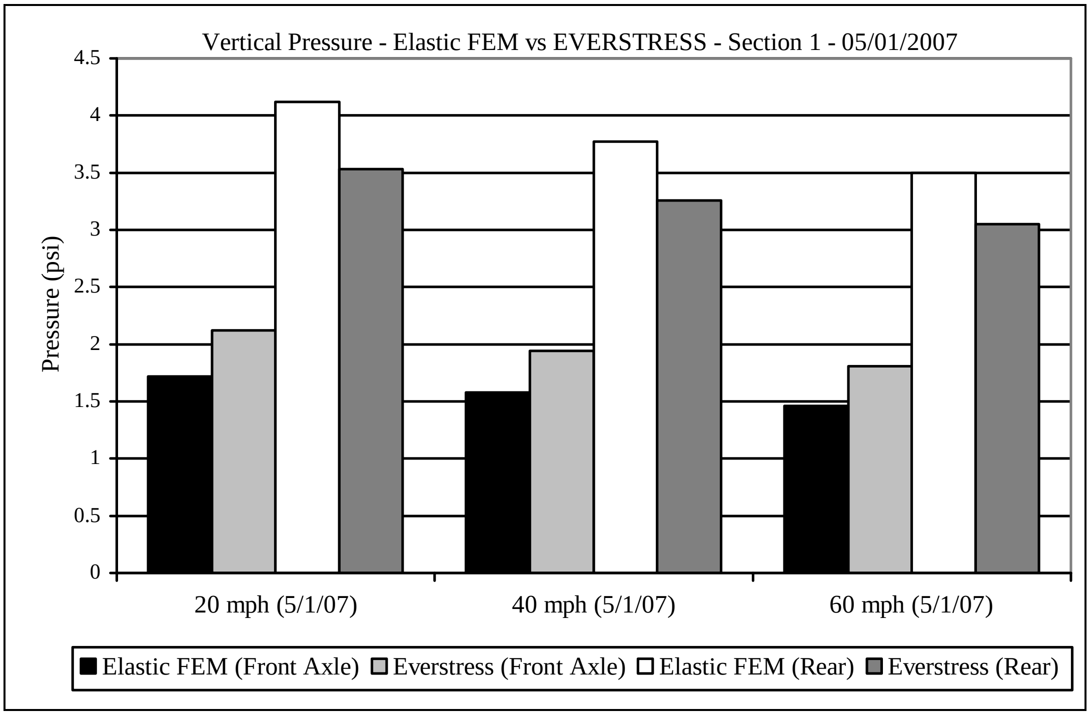


Figure 4-34: Vertical Pressure – Elastic FEM vs Linear Elastic

## 4.3 Comparison: Linear Elastic vs Finite Element

Figures 4-35, 4-36, and 4-37 show the comparison between the three methods used in this work to calculate the theoretical response of the pavement sections in the US-75 project. As it is observed in these figures, results from the linear elastic software EVERSTRESS and the ones from the elastic FEM were similar. As mentioned in Section 4.2.8.2, the small differences may be explained by the fact that different loading areas are assumed in each method, with one being circular and the other rectangular. The important observation to make is that the visco-elastic FEM yielded results that were smaller than the ones calculated using linear elastic methods. The causes of such discrepancies could not be identified for sure, even though the author and his advisor strongly believe that the prony series parameters are the problem.

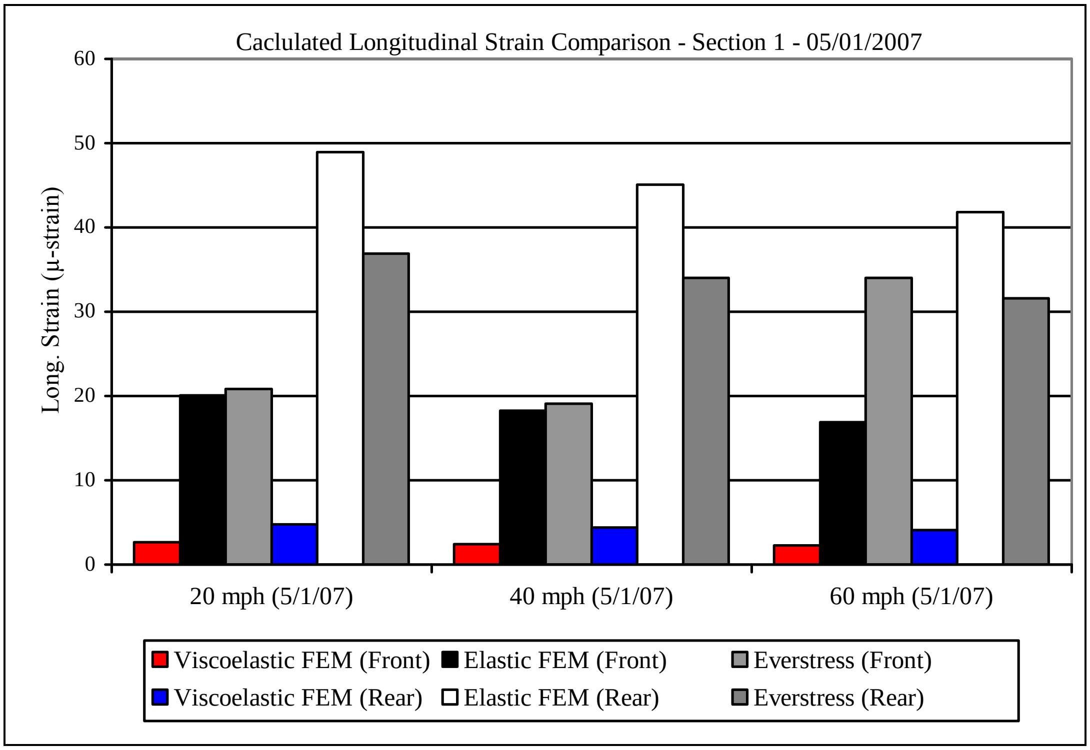


Figure 4-35: Longitudinal Strain – Elastic FEM vs Linear Elastic

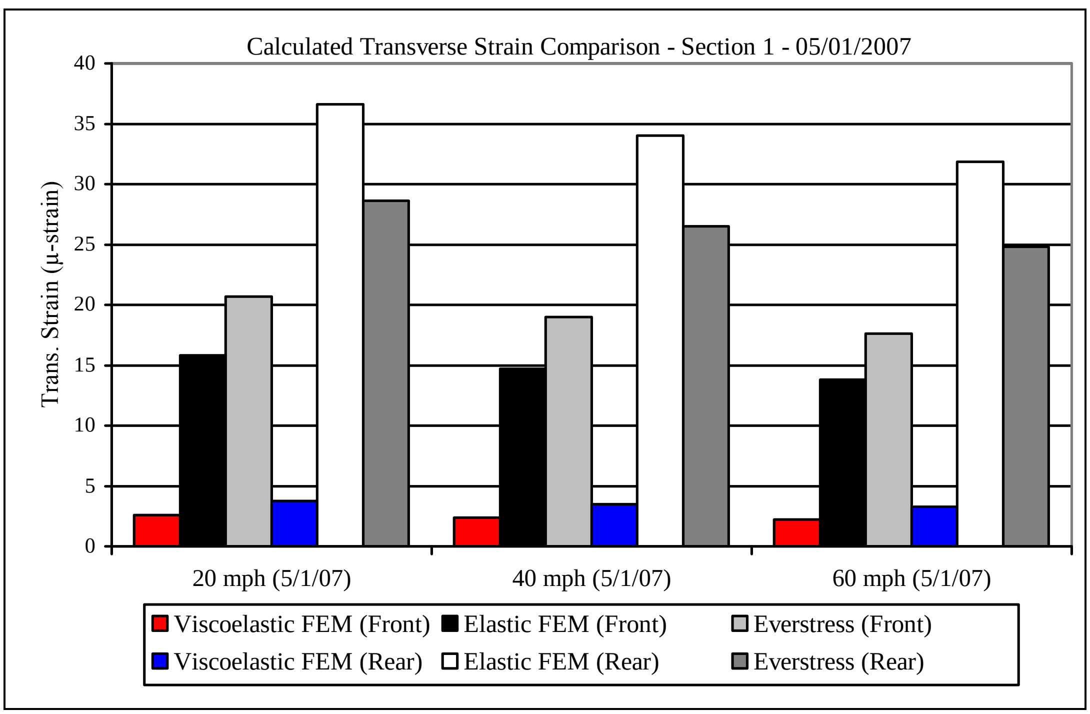


Figure 4-36: Transverse Strain – Elastic FEM vs Linear Elastic

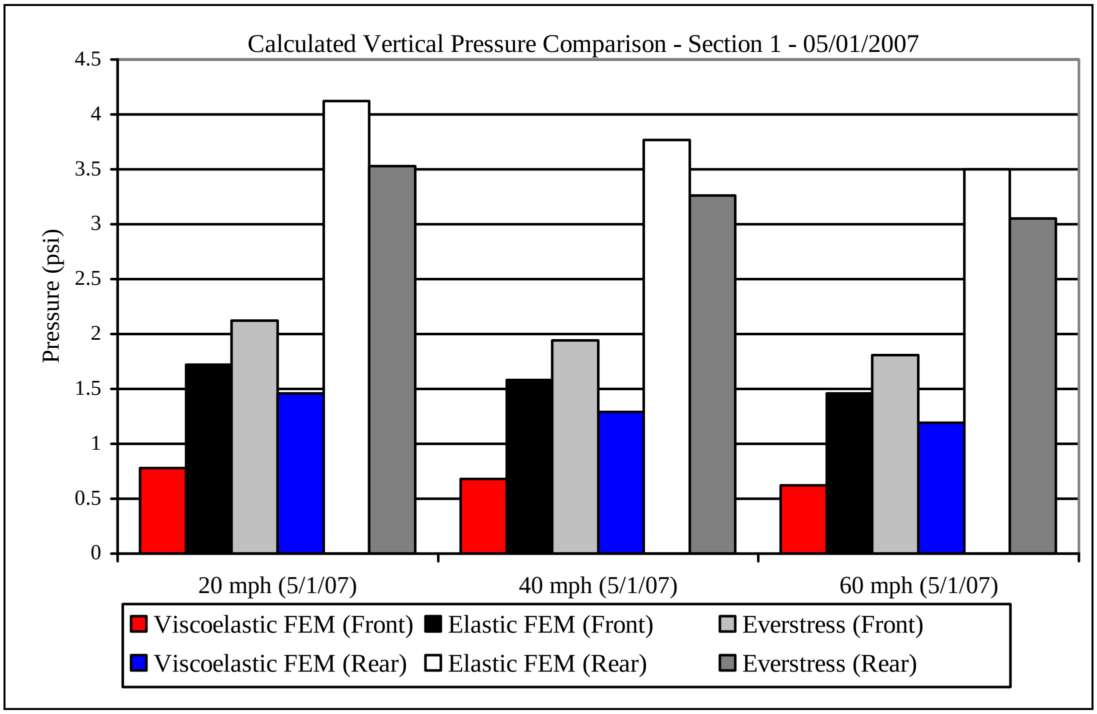


Figure 4-37: Vertical Pressure – Elastic FEM vs Linear Elastic

## 4.4 Comparison: Predicted vs Measured

Figures 4-38, 4-39, and 4-40 present a comparison among measured pavement response values and the different methods implemented to calculate the theoretical response of the perpetual pavement structures in the US-75 project. These figures clearly show that the results from the viscoelastic FEM were far away from the measured values for the longitudinal and transverse strains. The calculated vertical pressure from the viscoelastic FEM was also smaller than the measured, but in this case there was less difference than for the longitudinal and transverse strains.

Results from the linear elastic software and from the elastic FEM were closer to the measured values. As shown in Figure 4-38, calculated longitudinal strains were just outside of the minimum-maximum measured range for the 20 mph nominal speed. For 40 and 60 mph though, the difference between calculated longitudinal strains and measured longitudinal strains were around 2 times higher than the measured values. On the other hand, calculated transverse strains were within the minimum-maximum measured range for all speeds. Calculated vertical pressures were around 2 times higher than the measured values for all speeds (Figure 4-40).

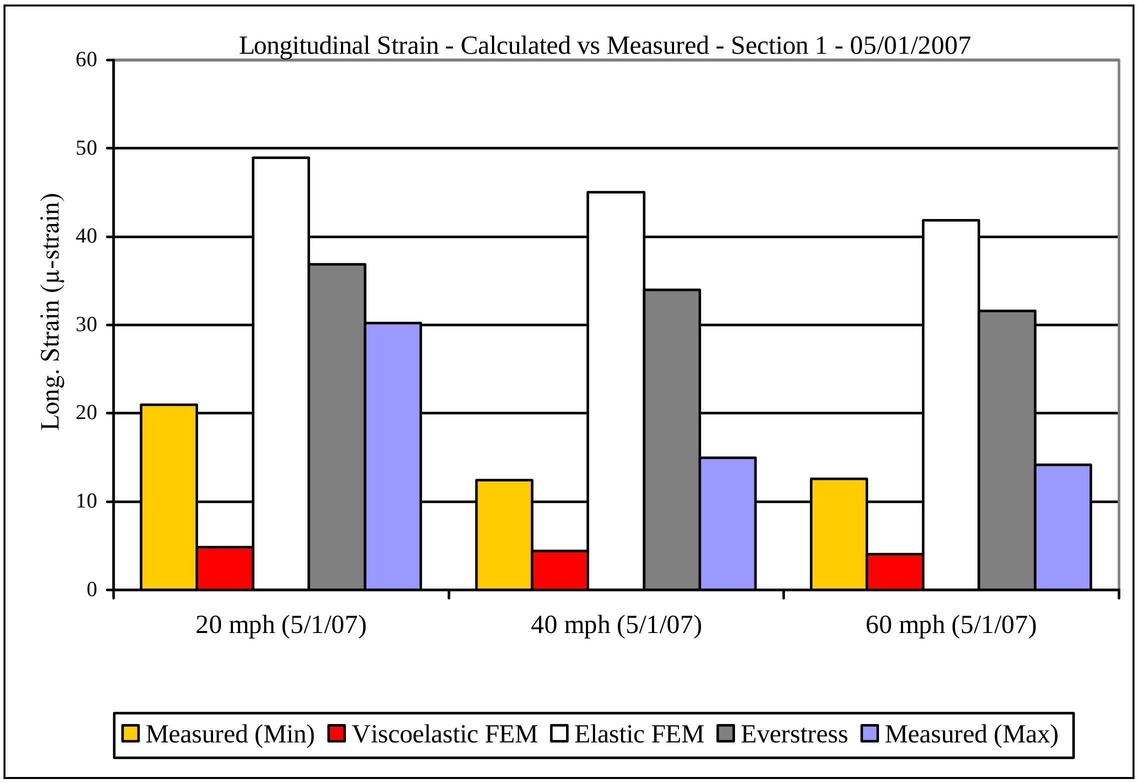


Figure 4-38: Longitudinal Strain – Calculated vs Measured

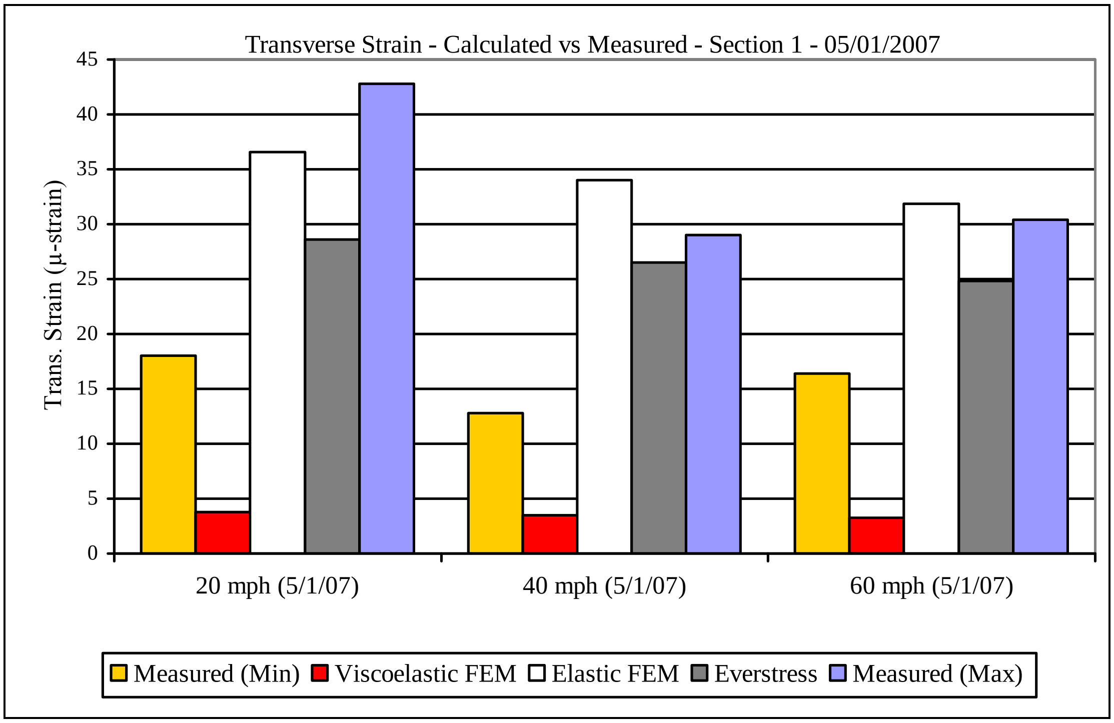


Figure 4-39: Transverse Strain – Calculated vs Measured

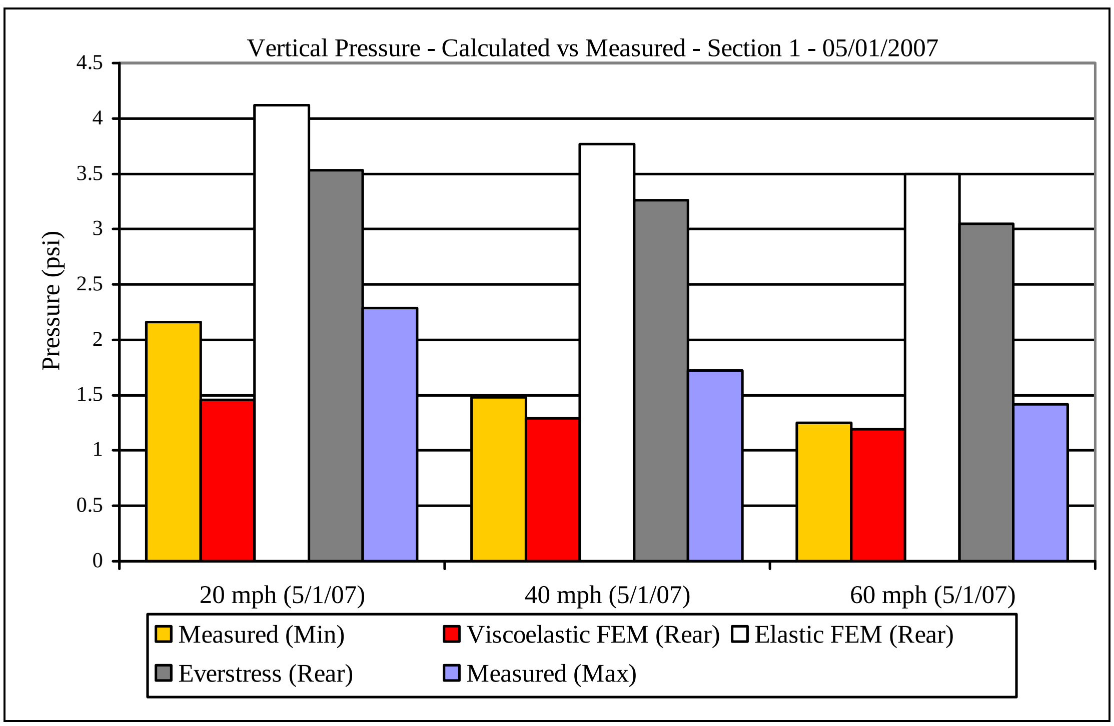


Figure 4-40: Vertical Pressure – Calculated vs Measured

# CHAPTER 5

## CONCLUSIONS AND RECOMMENDATIONS

The Kansas Department of Transportation sponsored a study to investigate the suitability of perpetual pavements for Kansas highway pavements. Four sections with different thick flexible pavement structures were constructed on highway US-75 near Sabetha, Kansas. They were designed to have an infinite fatigue life (Perpetual Pavement Concept) but, at the same time, to have layer thicknesses close to those recommended by the current KDOT's structural design method for flexible pavements.

In this thesis work, the four sections were instrumented with strain gauges to capture longitudinal and transverse strains at the bottom of the base layer. This was done to verify the endurance limit approach implemented in the design. Also, Geokon pressure cells were installed at the top of the lime-treated embankment layer to obtained vertical stresses at this interface. Pavement response measurements under known vehicle load were performed seven times between July 2005 and October 2007.

The analysis of the measured responses led to the following conclusions:

- The measured longitudinal and transverse strains were normally lower than 70 microstrains, which is the average endurance limit value reported in the literature, thus validating the design approach
- Temperature and speed of vehicles are two variables that have a significant influence on the behavior of pavements. Pavement responses at high temperatures

were about 4 times larger than the ones at low temperature, and about 2 times larger than the ones at mid temperature.

- Pavement responses at 20 mph were about 2 times larger than the ones at 40 mph. Responses at 40 mph and 60 mph were generally similar.
- Transverse strains were always larger than longitudinal strains. This observation contradicts what the literature suggests, and the cause may be attributed to what is called the compounding effect.

Linear elastic analyses using the EVERSTRESS software were carried out for all four sections of the US-75 project at three different measurement dates. The dates were chosen to include a hot, a warm, and a cold day. Also, a visco-elastic and an elastic finite element models were developed to compare their results with the ones from the linear elastic software EVERSTRESS. Finally, the calculated responses were compared with the measured responses and the analyses led to the following conclusions:

- Calculated (EVERSTRESS) longitudinal strains were around 1.5 to 2 times larger than the measured values.
- Calculated (EVERSTRESS) transverse strain values were either within the minimum-maximum measured ranged or just outside the range for all sections, except for Section 3.
- Calculated transverse strains were always smaller than the calculated longitudinal strains, which is not in accordance with the field observations.
- In all cases, the calculated (EVERSTRESS) vertical pressures at the top of the lime-treated soil were 2 to 3 times larger than the measured values.

- The use of dynamic modulus at different frequencies to take into account the effect of speed on the pavement responses did not work properly. Even though this method reduced the strains as the loading frequency was increased (which corresponds to speed increase), the differences were not as much as the ones observed in the field measurements.
- The visco-elastic finite element model yielded very small strains and pressures, even though pressures were closer to the measured values than the strains. To check the mesh, the loading, and the boundary conditions, all visco-elastic parameters were removed from the model, and the model was analyzed as an entirely elastic model. Results from this elastic finite element model were similar to the results from the linear elastic analyses using EVERSTRESS.
- All materials parameters used in the visco-elastic models were checked and recalculated, but no errors were encountered.
- The causes that led to very small pavement responses from the visco-elastic FEM compared to the measured response values could not be identified, even though the author and his advisor stringly believe that the problem is in the calculation of the prony series parameters.

The recommendations that are made based on this work are:

- The visco-elastic analysis in the ABAQUS software using dynamic analysis should be performed to compare the results with those obtained with the quasi-static analysis. This may also reveal if the quasi-static modeling in ABAQUS is effective.

- Since the measured vertical stresses at the top of the embankment layer was always 3 to 4 smaller than the theoretical stresses, the method of installing the stress cells should be reviewed.
- The use of dynamic modulus data for visco-elastic modeling of pavement response should be further investigated. It may be possible that indirect tensile resilient modulus may be a better indicator of the visco-elastic behavior of asphalt concrete; it measures the tensile properties of the asphalt concrete, and not the compression properties.

APPENDIX A

MEASURED RESULT CHARTS CORRECTED TO 20 ºC

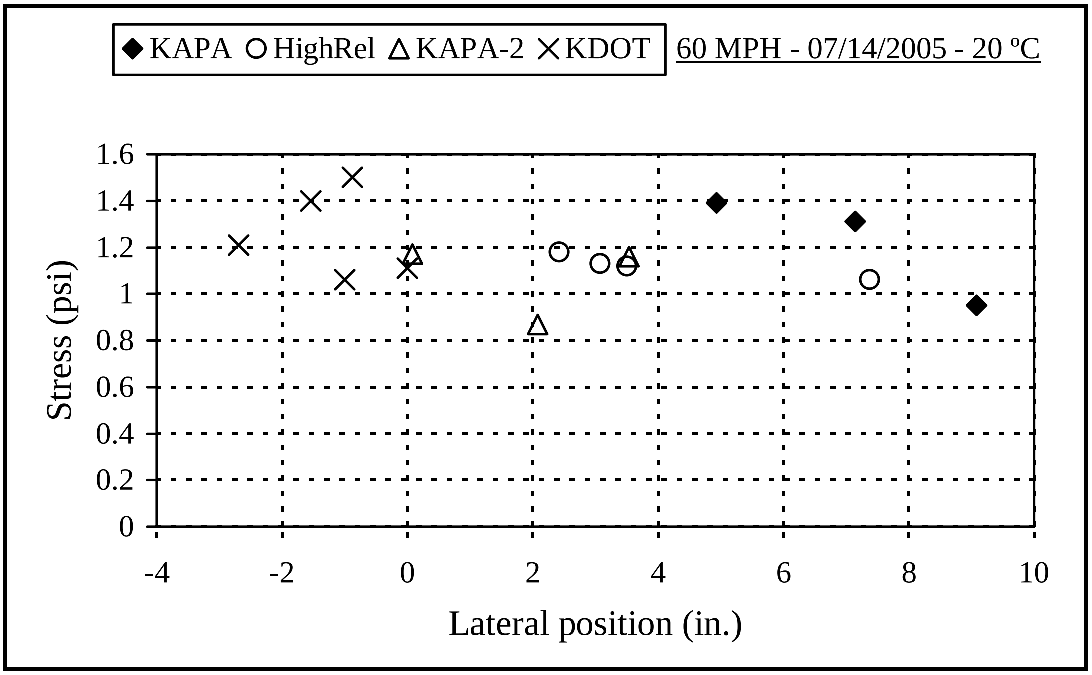


Figure A-1: Vertical Stress - 60 mph – 07/14/2005

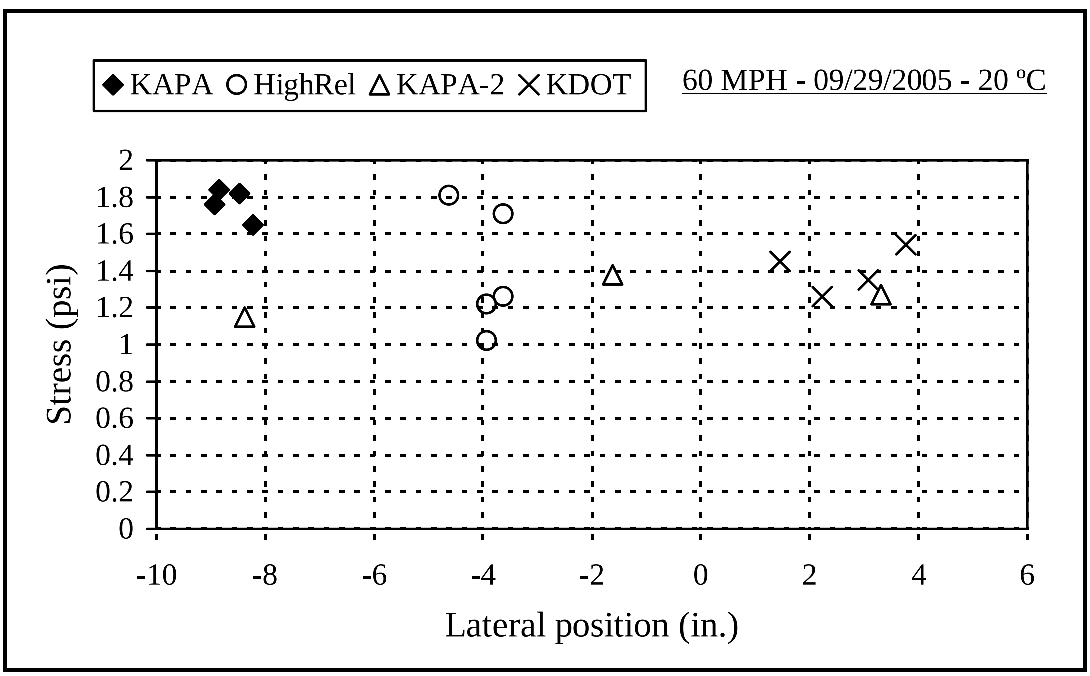


Figure A-2: Vertical Stress - 60 mph – 09/29/2005

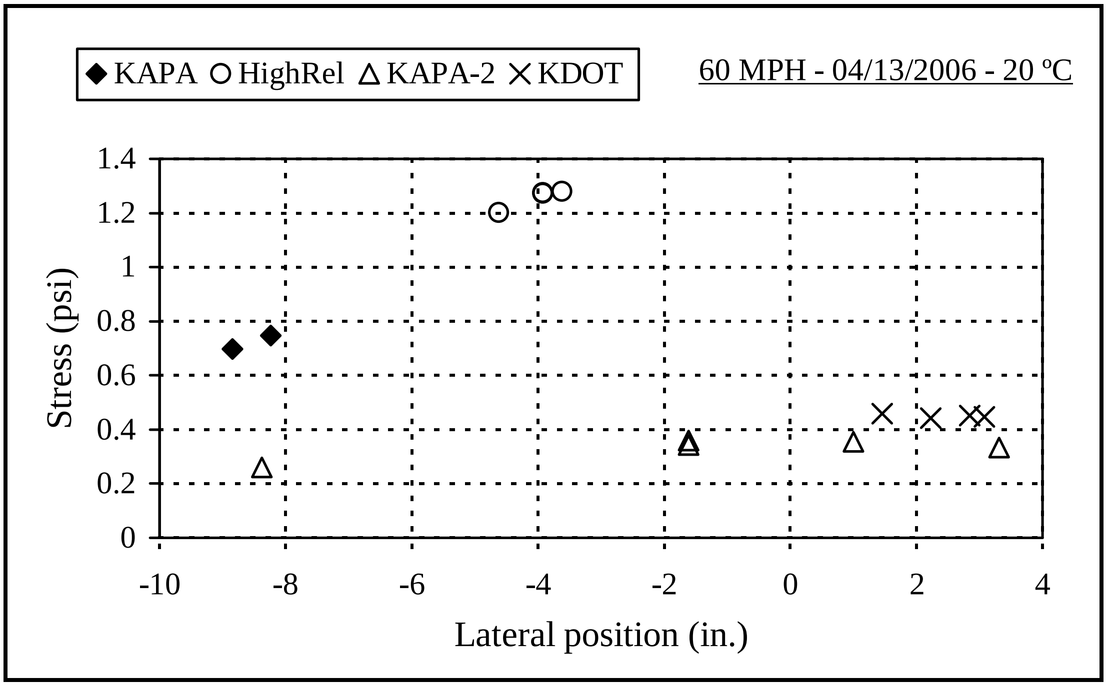


Figure A-3: Vertical Stress - 60 mph – 04/13/2006

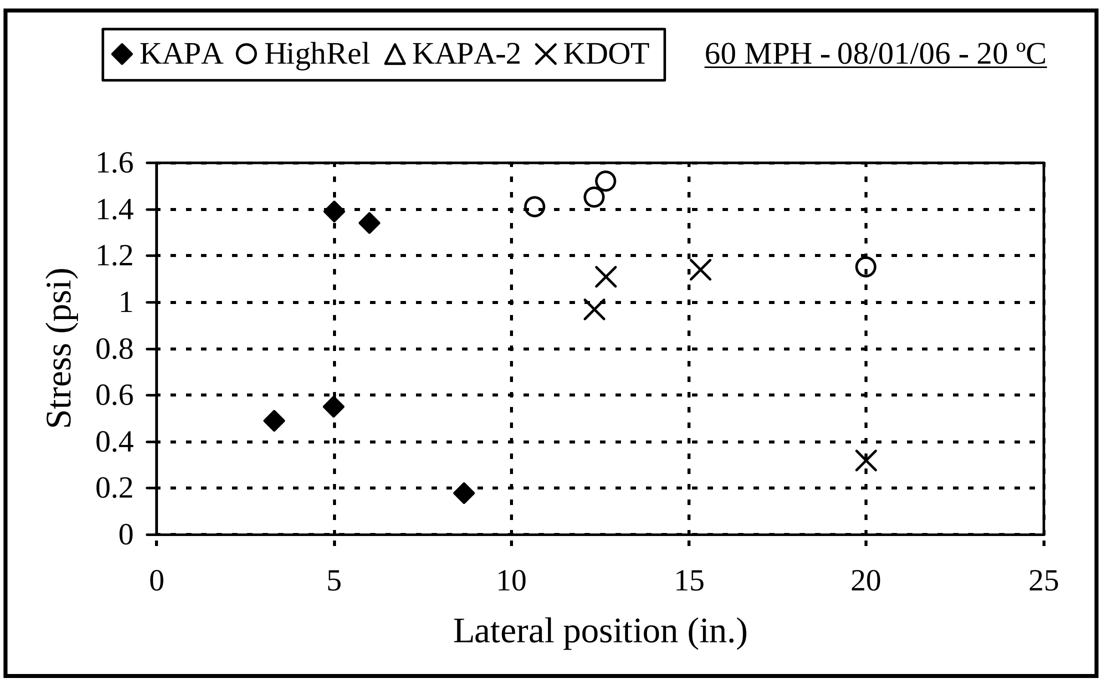


Figure A-4: Vertical Stress - 60 mph – 08/01/2006

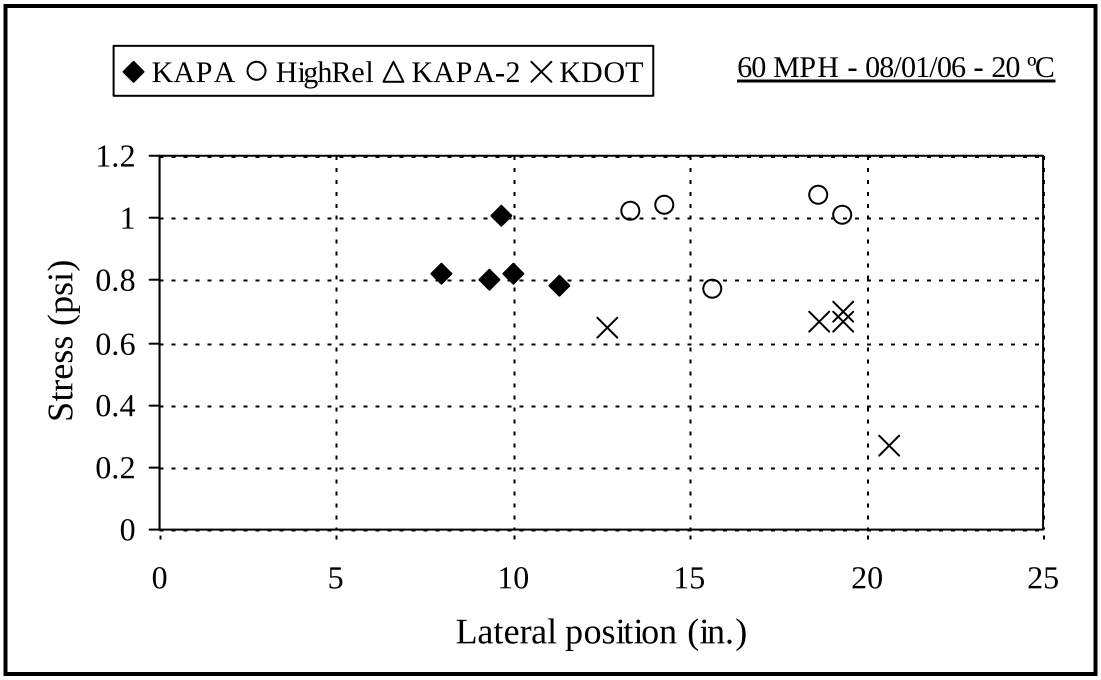


Figure A-5: Vertical Stress – RWD - 60 mph – 08/01/2006

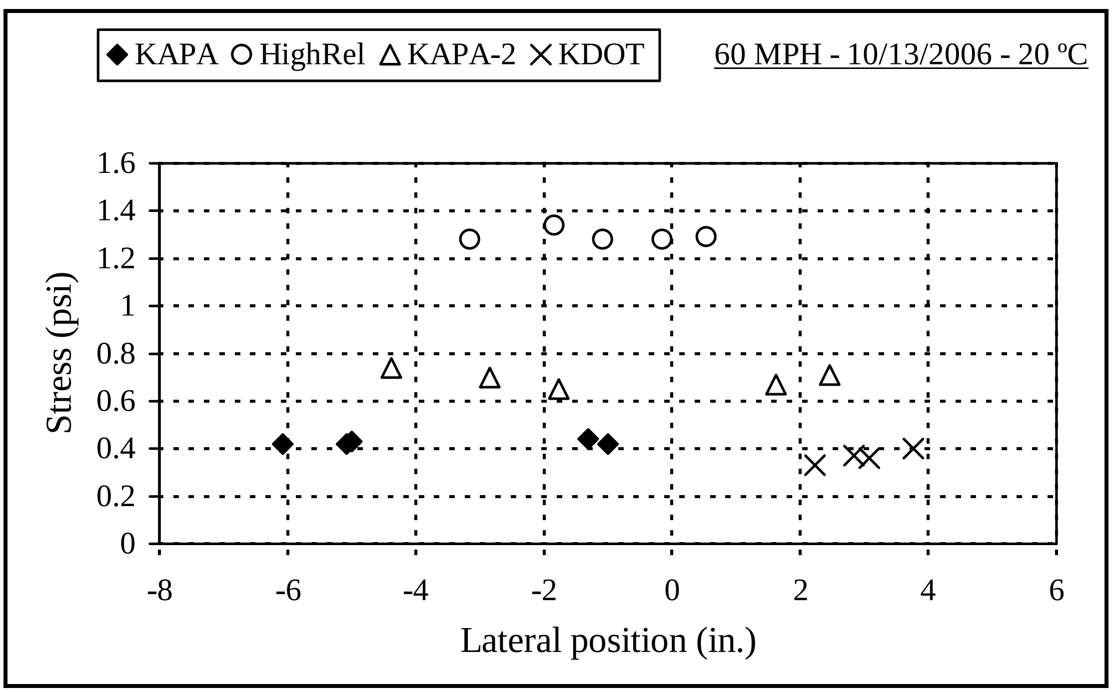


Figure A-6: Vertical Stress - 60 mph – 10/13/2006

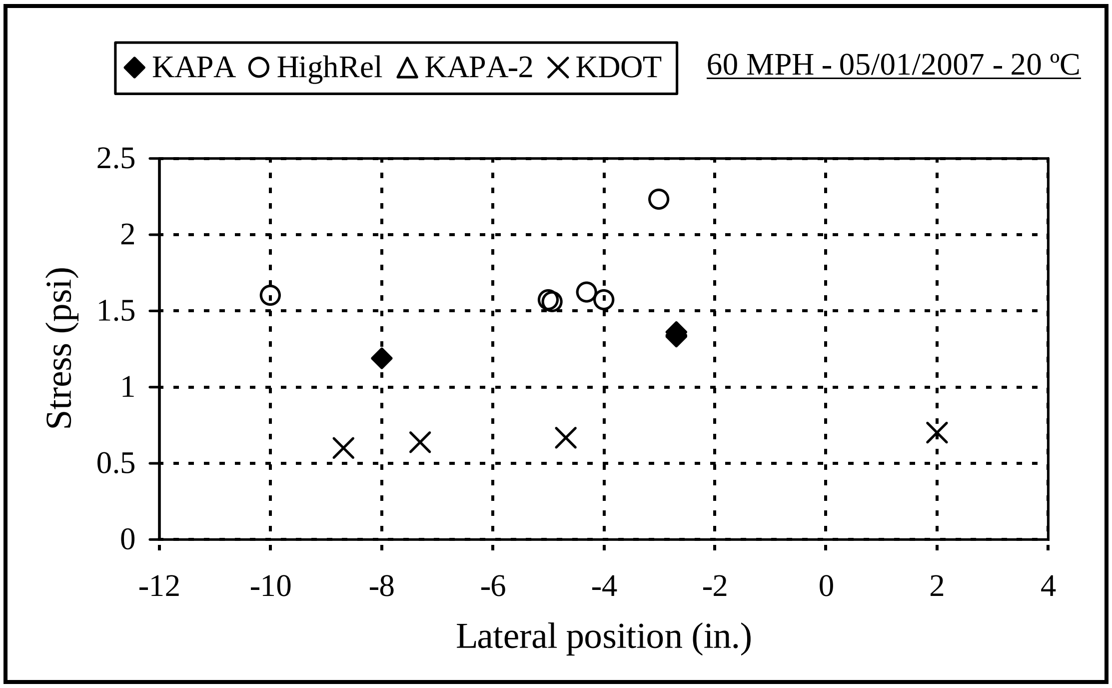


Figure A-7: Vertical Stress - 60 mph – 05/01/2007

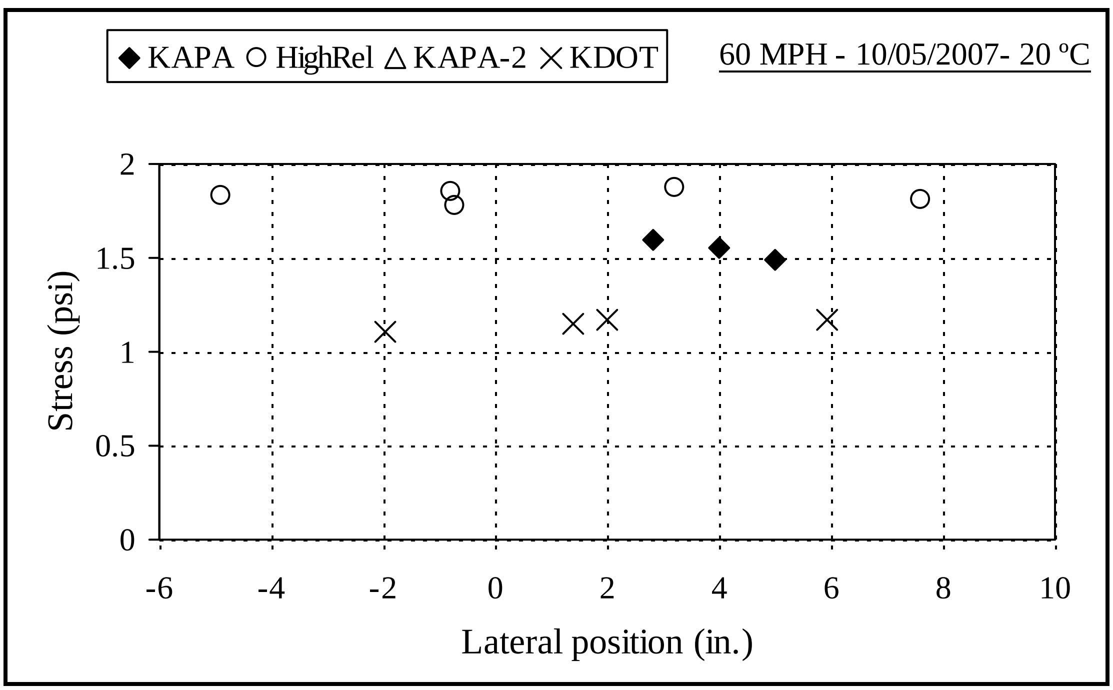


Figure A-8: Vertical Stress - 60 mph – 10/05/2007

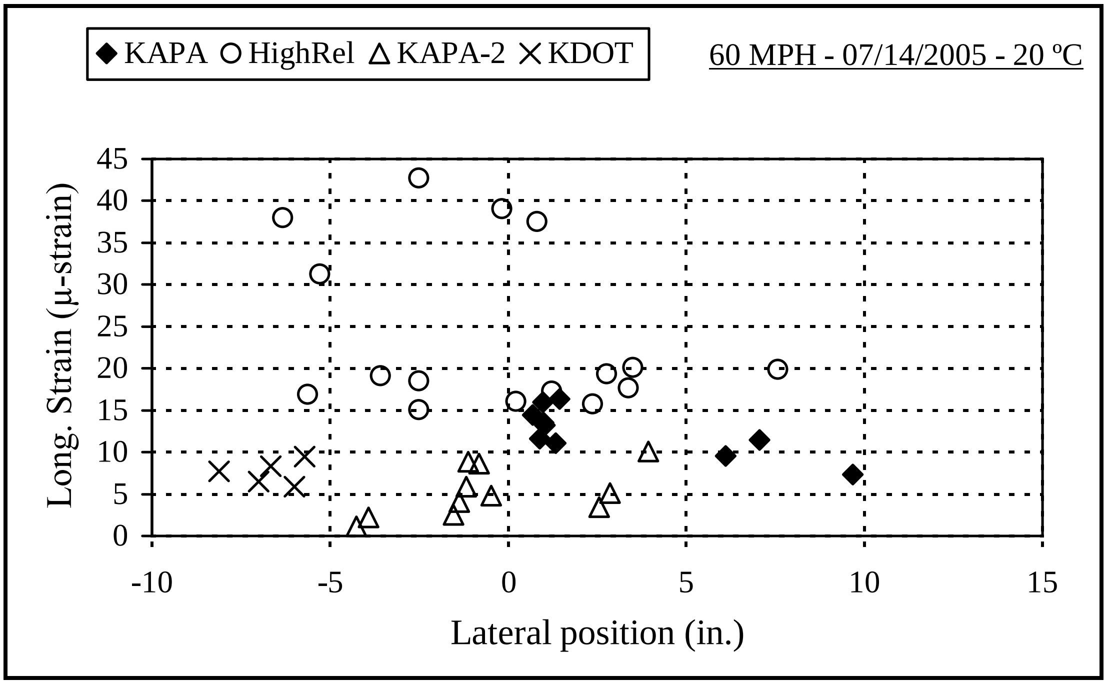


Figure A-9: Longitudinal Strain – 60 mph – 07/14/2005

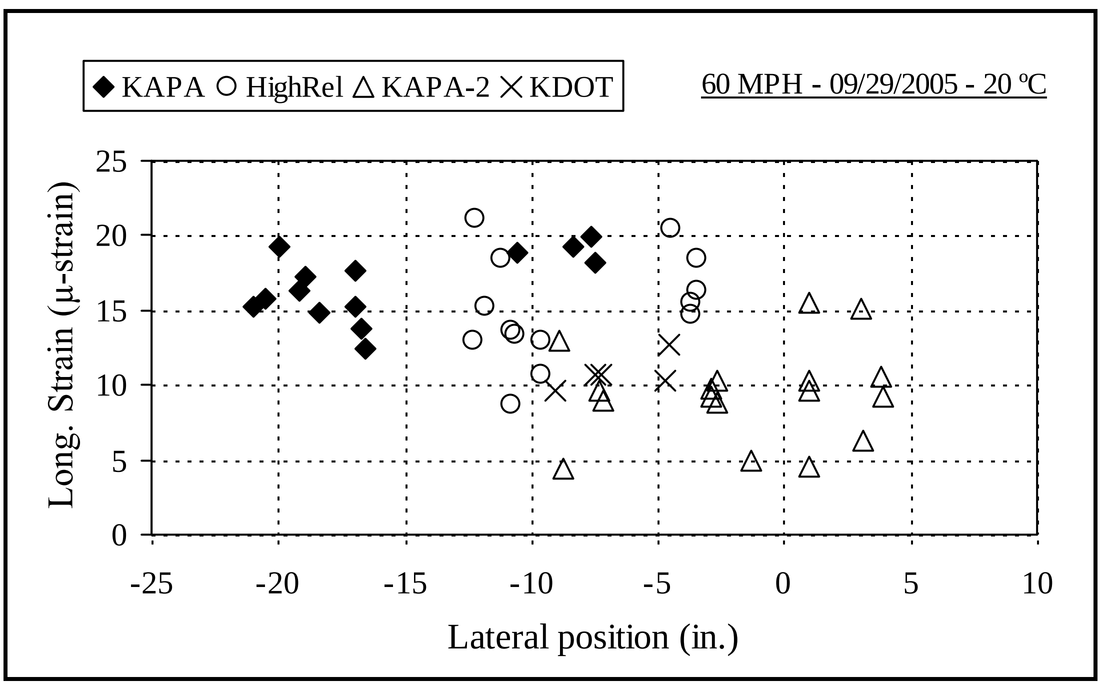


Figure A-10: Longitudinal Strain – 60 mph – 09/29/2005

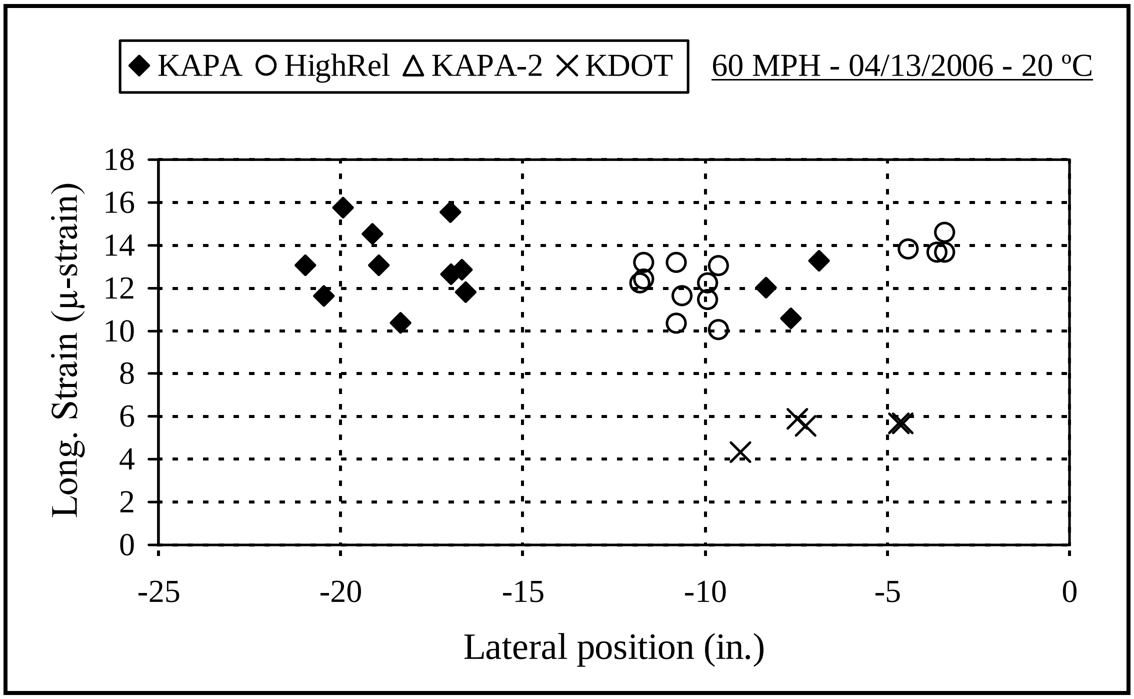


Figure A-11: Longitudinal Strain – 60 mph – 04/13/2006

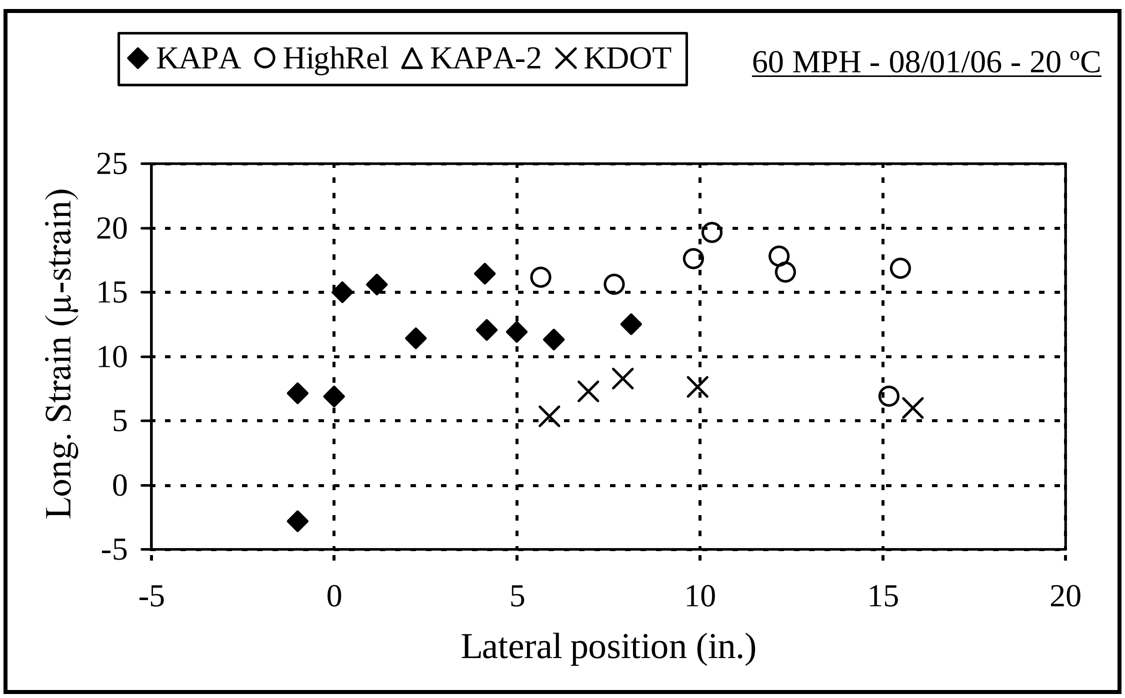


Figure A-12: Longitudinal Strain – 60 mph – 08/01/2006

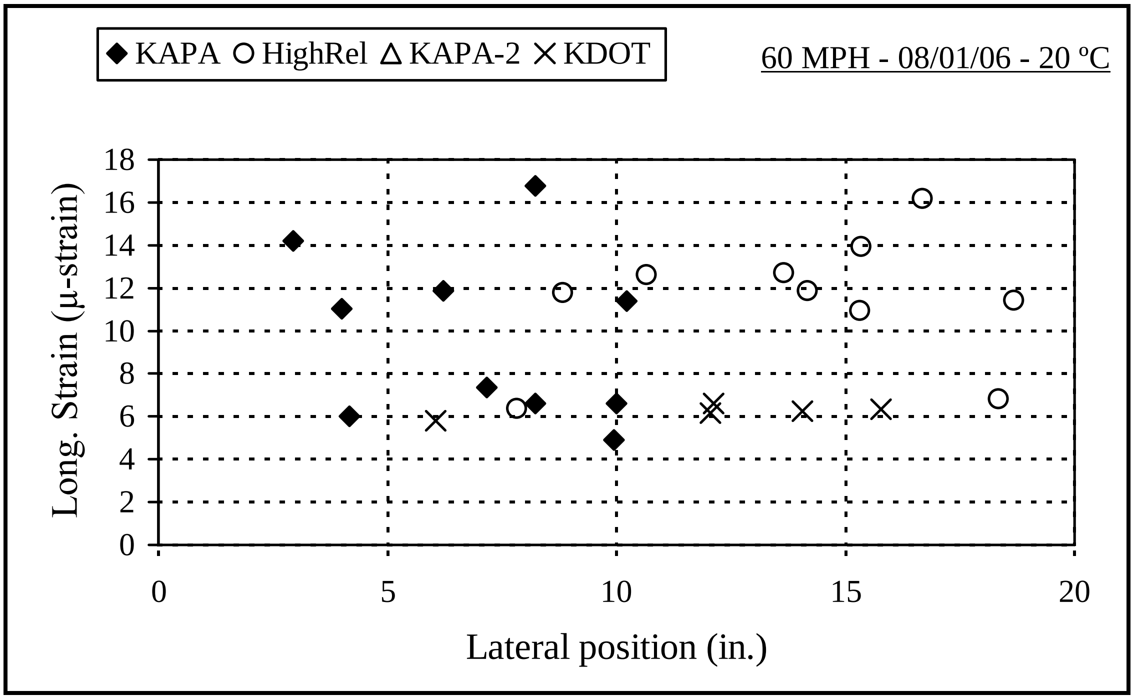


Figure A-13: Longitudinal Strain – RWD - 60 mph – 08/01/2006

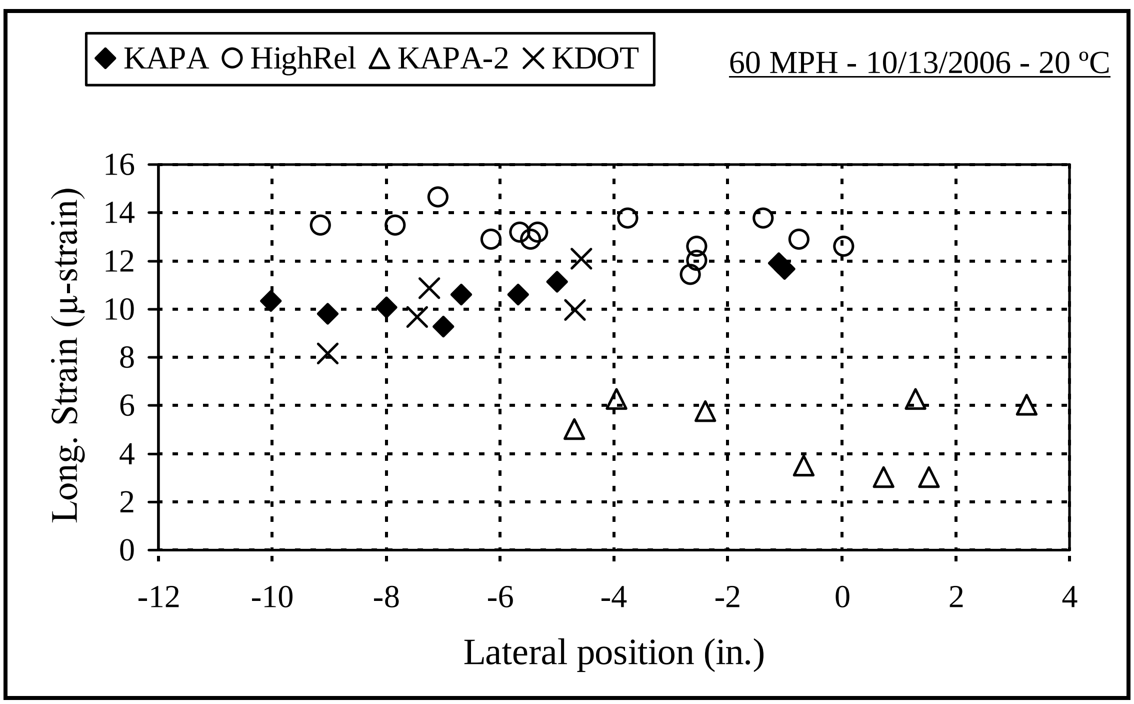


Figure A-14: Longitudinal Strain – 60 mph – 10/13/2006

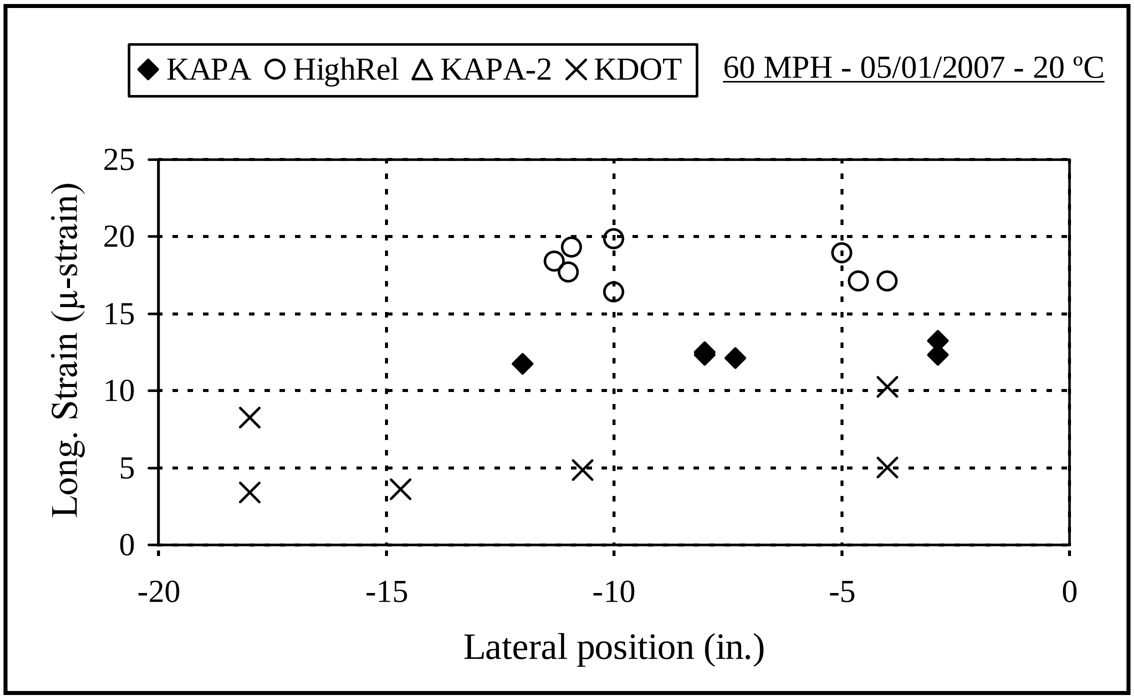


Figure A-15: Longitudinal Strain – 60 mph – 05/01/2007

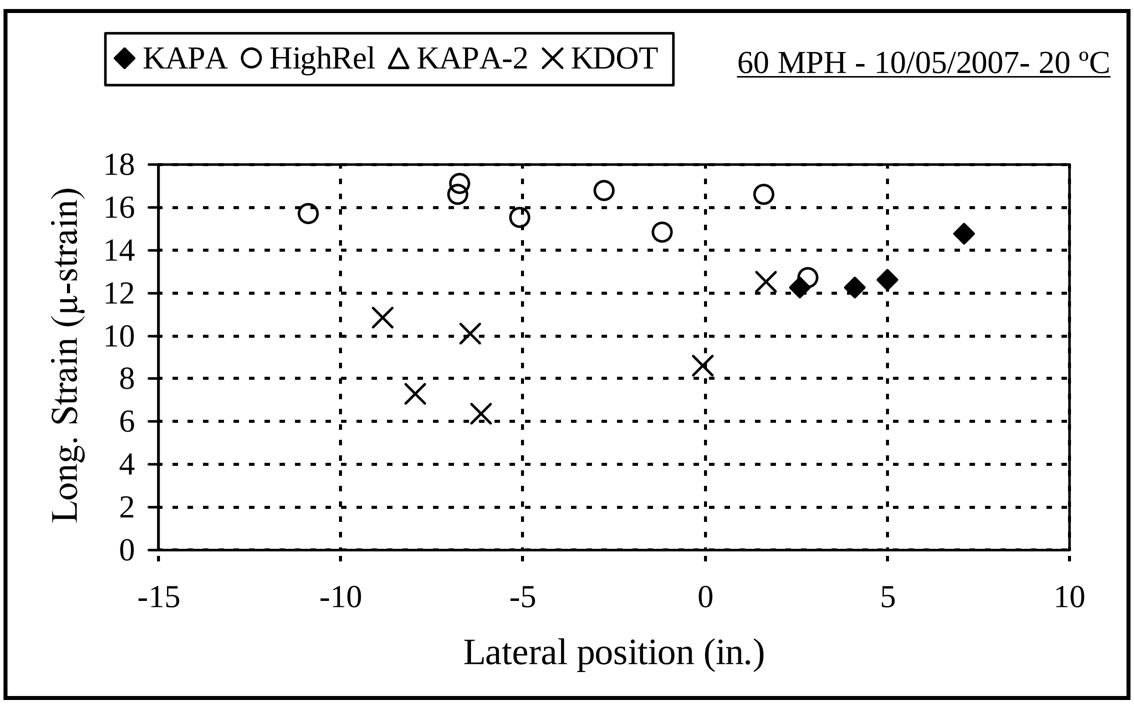


Figure A-16: Longitudinal Strain – 60 mph – 10/05/2007

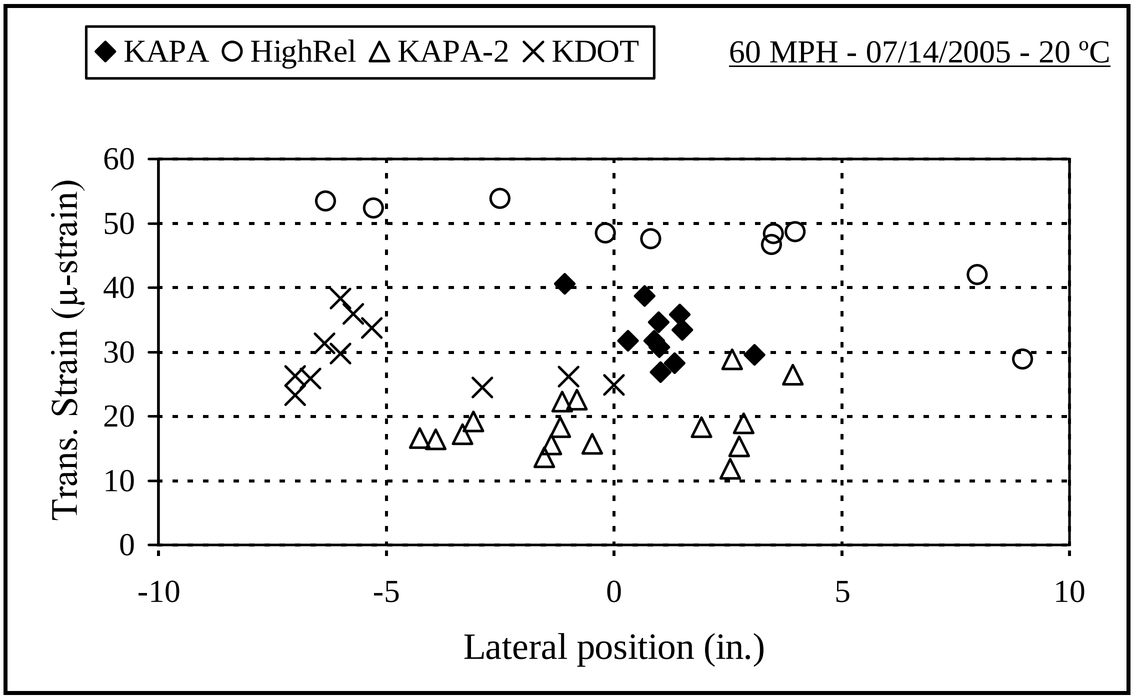


Figure A-17: Transverse Strain – 60 mph – 07/14/2005

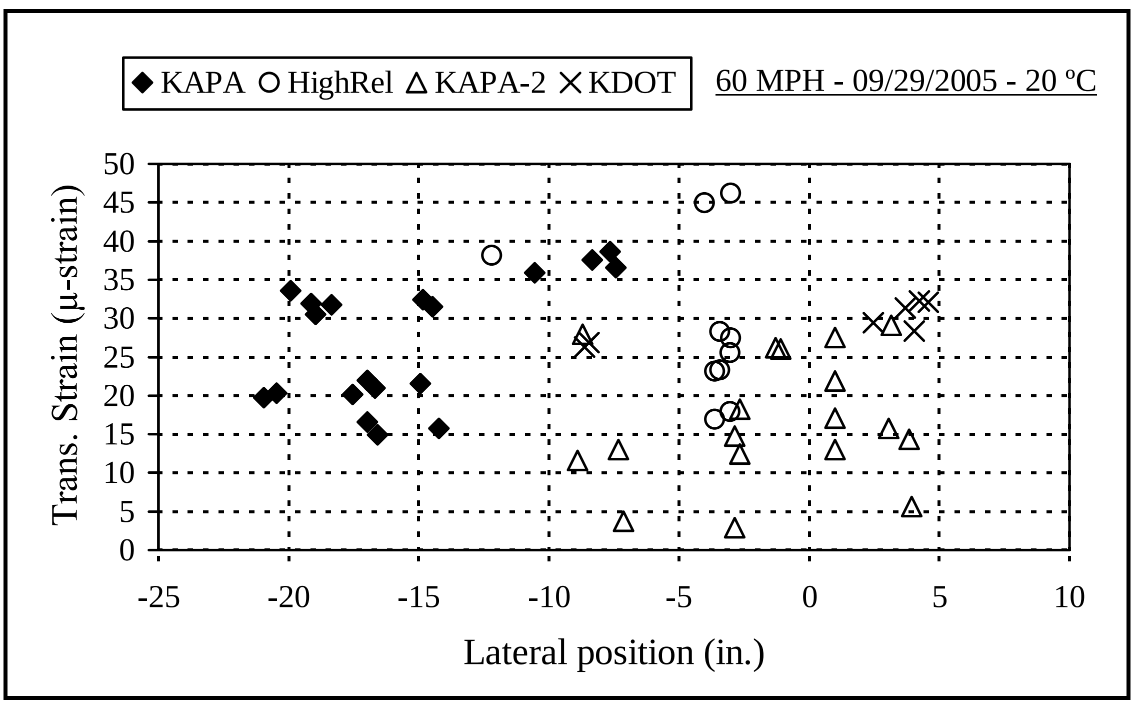


Figure A-18: Transverse Strain – 60 mph – 09/29/2005

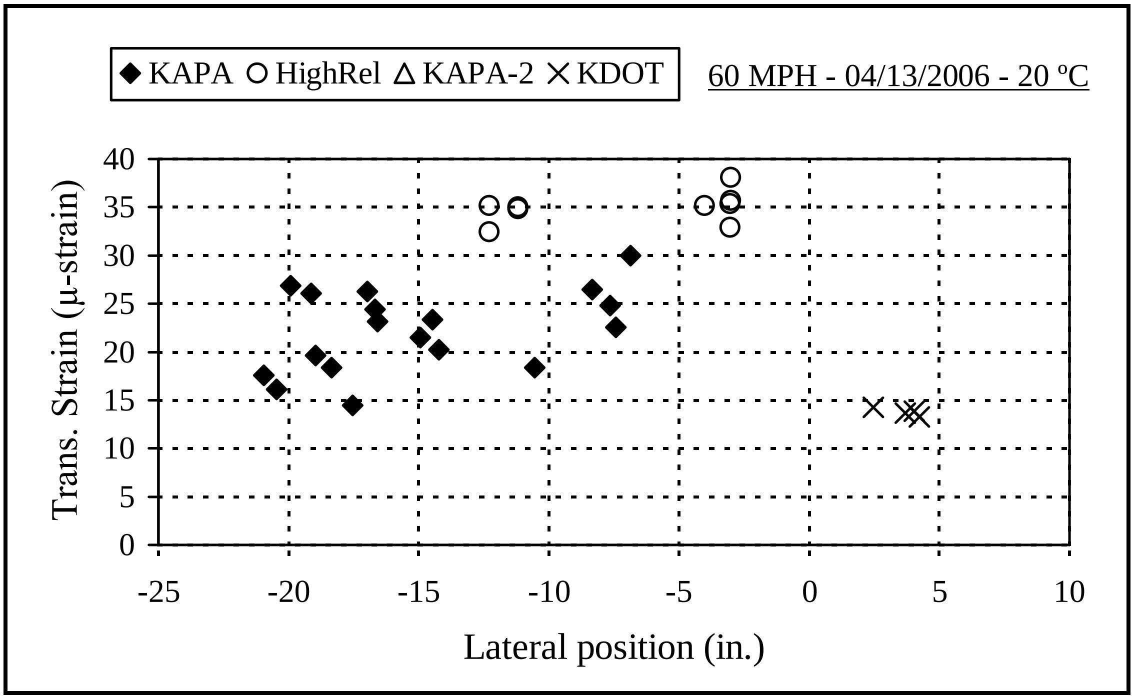


Figure A-19: Transverse Strain – 60 mph – 04/13/2006

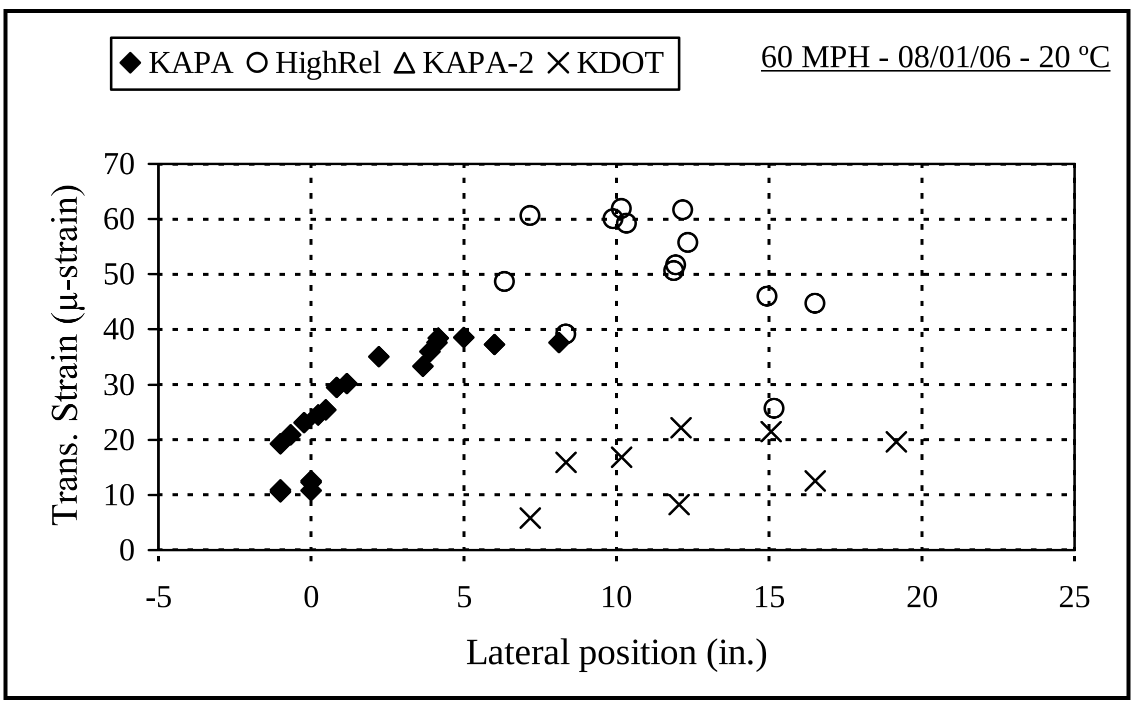


Figure A-20: Transverse Strain – 60 mph – 08/01/2006

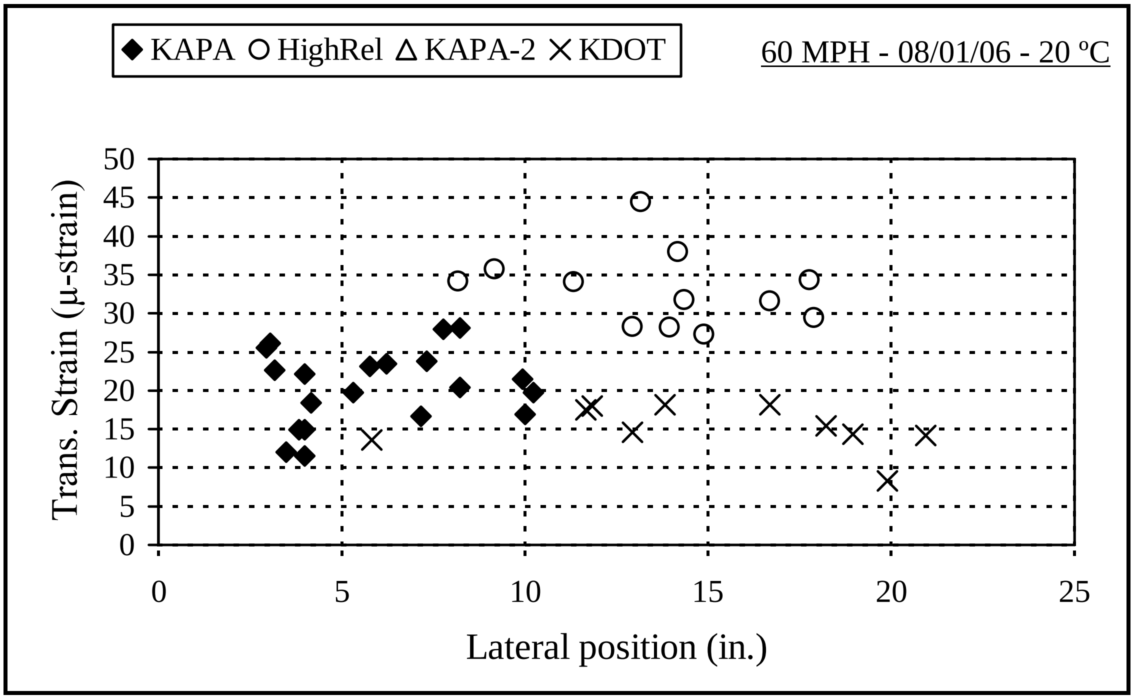


Figure A-21: Transverse Strain – RWD - 60 mph – 08/01/2006

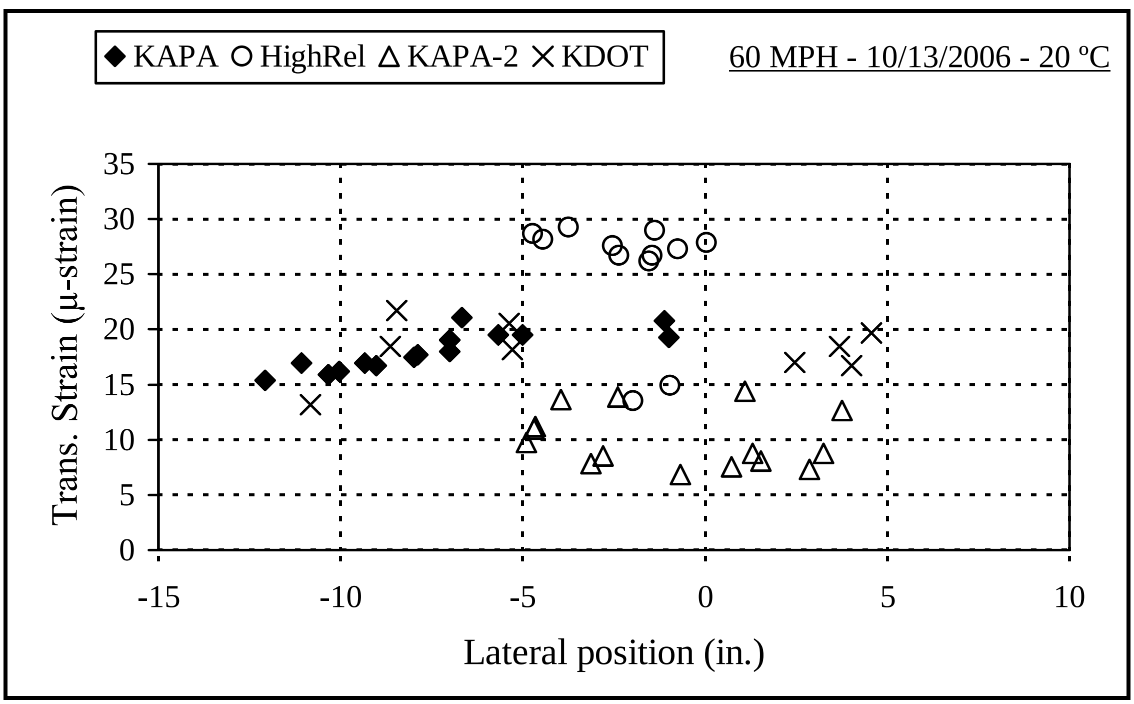


Figure A-22: Transverse Strain – 60 mph – 10/13/2006

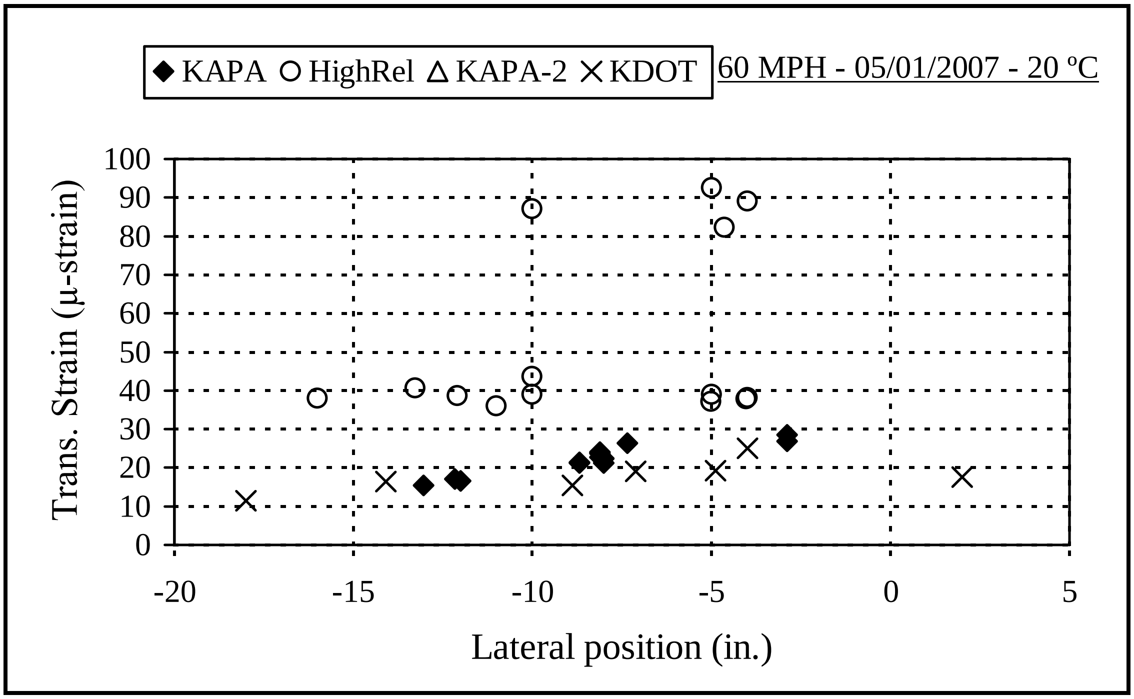


Figure A-23: Transverse Strain – 60 mph – 05/01/2007

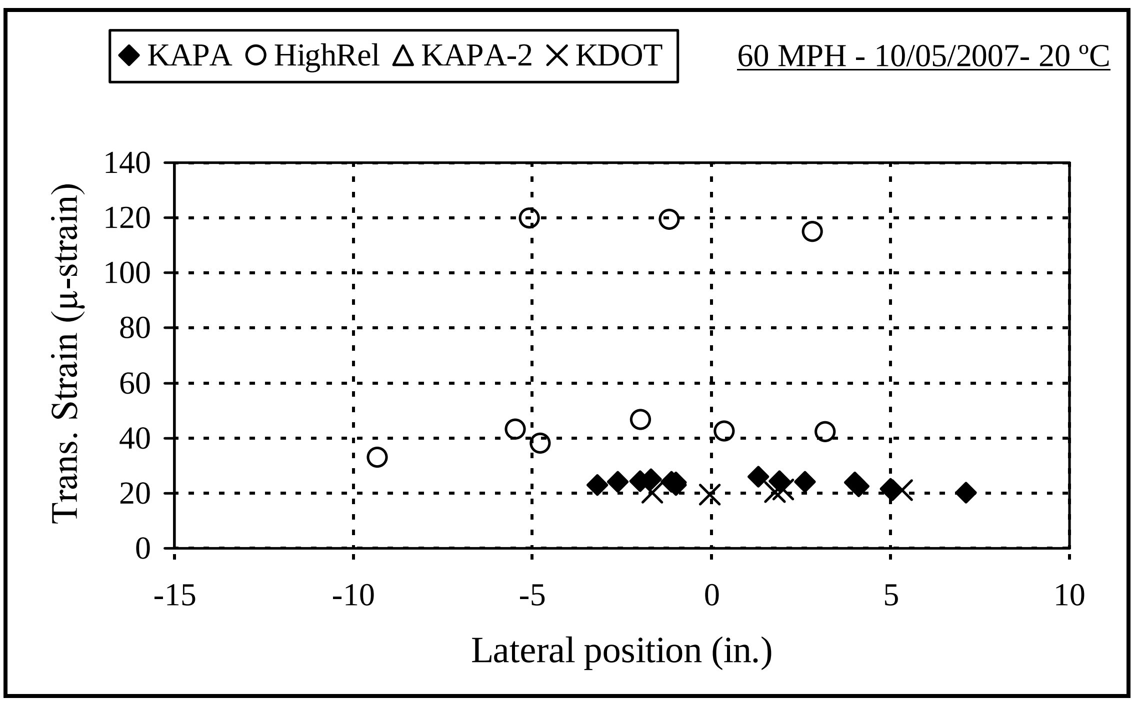


Figure A-24: Transverse Strain – 60 mph – 10/05/2007

# APPENDIX B

# MEASURED PAVEMENT RESPONSE VARIABLES

Table B-1: Vertical Pressure – 07/14/2005

| Nominal Speed (mph) | Section 1 Vertical Pressure (psi) | | | | Nominal Speed (mph) | Section 2 Vertical Pressure (psi) | | | |
|---|---|---|---|---|---|---|---|---|---|
| | Offset (in) | Uncorrected | 20 ºC | 30 ºC | | Offset (in) | Uncorrected | 20 ºC | 30 ºC |
| 20 | 0.8 | 3.28 | 2.34 | 3.11 | 20 | 1.8 | 3.63 | 2.23 | 3.30 |
| 20 | 2.2 | 3.50 | 2.50 | 3.32 | 20 | 4.6 | 3.65 | 2.24 | 3.32 |
| 20 | 3.4 | 3.44 | 2.45 | 3.26 | 45 | 4.0 | 3.63 | 2.23 | 3.30 |
| 45 | 4.5 | 3.16 | 2.26 | 3.00 | 45 | 5.0 | 3.70 | 2.27 | 3.36 |
| 45 | 6.2 | 3.24 | 2.31 | 3.07 | 45 | 7.3 | 3.41 | 2.09 | 3.10 |
| 45 | 6.0 | 1.84 | 1.31 | 1.74 | 45 | 5.9 | 3.30 | 2.03 | 3.00 |
| 45 | 5.3 | 1.89 | 1.35 | 1.80 | 60 | 2.4 | 1.91 | 1.18 | 1.70 |
| 60 | 7.2 | 1.82 | 1.31 | 1.71 | 60 | 3.5 | 1.82 | 1.12 | 1.61 |
| 60 | 4.9 | 1.93 | 1.39 | 1.81 | 60 | 3.1 | 1.84 | 1.13 | 1.64 |
| 60 | 9.1 | 1.31 | 0.95 | 1.24 | 60 | 7.4 | 1.73 | 1.06 | 1.53 |

| Nominal Speed (mph) | Section 3 Vertical Pressure (psi) | | | | Nominal Speed (mph) | Section 4 Vertical Pressure (psi) | | | |
|---|---|---|---|---|---|---|---|---|---|
| | Offset (in) | Uncorrected | 20 ºC | 30 ºC | | Offset (in) | Uncorrected | 20 ºC | 30 ºC |
| 20 | 6.4 | 3.06 | 1.72 | 2.52 | 20 | 10.7 | 2.73 | 1.89 | 2.38 |
| 20 | 5.4 | 3.10 | 1.74 | 2.56 | 20 | 4.1 | 3.21 | 2.22 | 2.79 |
| 20 | 4.5 | 3.20 | 1.80 | 2.64 | 20 | 4.7 | 3.01 | 2.08 | 2.62 |
| 20 | 6.4 | 3.37 | 1.90 | 2.78 | 20 | 3.7 | 3.20 | 2.22 | 2.79 |
| 45 | 3.3 | 2.94 | 1.66 | 2.43 | 20 | 4.7 | 3.26 | 2.26 | 2.84 |
| 45 | 1.7 | 2.09 | 1.18 | 1.73 | 45 | 4.1 | 3.47 | 2.41 | 3.03 |
| 45 | 2.4 | 2.04 | 1.15 | 1.69 | 45 | 3.3 | 3.29 | 2.28 | 2.86 |
| 45 | 2.3 | 2.01 | 1.13 | 1.66 | 45 | -1.0 | 1.81 | 1.26 | 1.58 |
| 60 | 3.5 | 2.11 | 1.16 | 1.65 | 45 | 1.6 | 1.97 | 1.36 | 1.71 |
| 60 | 0.1 | 2.15 | 1.17 | 1.68 | 45 | -1.7 | 1.80 | 1.25 | 1.57 |
| 60 | 2.1 | 1.59 | 0.87 | 1.24 | 60 | -2.7 | 1.78 | 1.21 | 1.48 |
| | | | | | 60 | -0.9 | 2.20 | 1.50 | 1.83 |
| | | | | | 60 | -1.5 | 2.05 | 1.40 | 1.71 |
| | | | | | 60 | -1.0 | 1.56 | 1.06 | 1.30 |
| | | | | | 60 | 0.0 | 1.64 | 1.11 | 1.36 |

Table B-2: Vertical Pressure – 09/29/2005

| Nominal Speed (mph) | Section 1 Vertical Pressure (psi) | | | | Nominal Speed (mph) | Section 2 Vertical Pressure (psi) | | | |
|---|---|---|---|---|---|---|---|---|---|
| | Offset (in) | Uncorrected | 20 ºC | 30 ºC | | Offset (in) | Uncorrected | 20 ºC | 30 ºC |
| 20 | -9.2 | 2.87 | 3.13 | 4.17 | 20 | -6.2 | 2.94 | 2.94 | 4.35 |
| 20 | -0.5 | 2.63 | 2.87 | 3.82 | 20 | -10.7 | 2.77 | 2.76 | 4.10 |
| 20 | -1.9 | 2.93 | 3.19 | 4.25 | 20 | 2.4 | 2.80 | 2.80 | 4.14 |
| 20 | -5.5 | 2.87 | 3.13 | 4.16 | 45 | 6.2 | 1.47 | 1.47 | 2.18 |
| 20 | -4.2 | 2.86 | 3.12 | 4.15 | 45 | -4.9 | 2.25 | 2.25 | 3.33 |
| 45 | -3.9 | 1.63 | 1.78 | 2.37 | 45 | -2.9 | 1.95 | 1.95 | 2.88 |
| 45 | -8.9 | 1.48 | 1.61 | 2.14 | 60 | -4.6 | 1.80 | 1.81 | 2.61 |
| 45 | -10.9 | 1.40 | 1.52 | 2.02 | 60 | -3.9 | 1.21 | 1.22 | 1.76 |
| 45 | -12.2 | 1.38 | 1.50 | 2.00 | 60 | -3.6 | 1.25 | 1.26 | 1.81 |
| 45 | -8.5 | 1.45 | 1.58 | 2.10 | 60 | -3.9 | 1.01 | 1.02 | 1.47 |
| 60 | -8.5 | 1.73 | 1.82 | 2.38 | 60 | -3.6 | 1.70 | 1.71 | 2.46 |
| 60 | -8.9 | 1.74 | 1.84 | 2.41 | | | | | |
| 60 | -8.2 | 1.56 | 1.65 | 2.15 | | | | | |
| 60 | -8.9 | 1.66 | 1.76 | 2.30 | | | | | |

| Nominal Speed (mph) | Section 3 Vertical Pressure (psi) | | | | Nominal Speed (mph) | Section 4 Vertical Pressure (psi) | | | |
|---|---|---|---|---|---|---|---|---|---|
| | Offset (in) | Uncorrected | 20 ºC | 30 ºC | | Offset (in) | Uncorrected | 20 ºC | 30 ºC |
| 20 | -3.9 | 2.98 | 2.71 | 3.98 | 20 | 2.4 | 2.17 | 1.95 | 2.46 |
| 20 | 3.1 | 3.37 | 3.07 | 4.50 | 20 | 2.1 | 2.43 | 2.18 | 2.74 |
| 20 | 3.4 | 2.96 | 2.70 | 3.96 | 20 | 0.2 | 2.18 | 1.96 | 2.46 |
| 20 | 10.7 | 2.71 | 2.47 | 3.62 | 20 | 8.5 | 2.67 | 2.40 | 3.02 |
| 45 | 2.9 | 2.08 | 1.90 | 2.78 | 45 | -0.9 | 1.18 | 1.06 | 1.34 |
| 45 | -5.3 | 2.05 | 1.87 | 2.74 | 45 | -0.6 | 1.54 | 1.39 | 1.74 |
| 45 | 1.4 | 1.93 | 1.76 | 2.58 | 45 | 0.8 | 1.44 | 1.30 | 1.63 |
| 45 | 7.3 | 1.87 | 1.71 | 2.50 | 60 | 1.5 | 1.61 | 1.45 | 1.78 |
| 45 | -3.0 | 2.06 | 1.88 | 2.75 | 60 | 3.8 | 1.71 | 1.54 | 1.89 |
| 60 | -8.4 | 1.24 | 1.15 | 1.64 | 60 | 3.1 | 1.50 | 1.35 | 1.65 |
| 60 | 3.3 | 1.37 | 1.27 | 1.81 | 60 | 2.2 | 1.39 | 1.26 | 1.54 |
| 60 | -1.62 | 1.49 | 1.38 | 1.97 | | | | | |

Table B-3: Vertical Pressure – 04/13/2006

| Nominal Speed (mph) | Section 1 | | | | Nominal Speed (mph) | Section 2 | | | |
|---|---|---|---|---|---|---|---|---|---|
| | Vertical Pressure (psi) | | | | | Vertical Pressure (psi) | | | |
| | Offset (in) | Uncorrected | 20 ºC | 30 ºC | | Offset (in) | Uncorrected | 20 ºC | 30 ºC |
| 20 | -9.2 | 1.02 | 1.04 | 1.39 | 20 | -6.2 | 2.00 | 1.62 | 2.40 |
| 20 | -0.5 | 1.14 | 1.18 | 1.56 | 20 | 2.4 | 2.08 | 1.69 | 2.50 |
| 20 | -1.9 | 1.34 | 1.38 | 1.84 | 20 | -0.6 | 1.89 | 1.53 | 2.27 |
| 20 | -5.5 | 1.58 | 1.62 | 2.16 | 45 | 0.1 | 1.78 | 1.44 | 2.13 |
| 20 | -4.2 | 1.31 | 1.34 | 1.79 | 45 | -4.9 | 1.75 | 1.42 | 2.10 |
| 45 | -8.9 | 0.96 | 0.99 | 1.32 | 45 | -2.9 | 1.79 | 1.45 | 2.15 |
| 45 | -12.2 | 0.81 | 0.83 | 1.10 | 45 | 2.8 | 1.72 | 1.39 | 2.06 |
| 45 | -8.5 | 0.99 | 1.02 | 1.36 | 60 | -4.6 | 1.44 | 1.20 | 1.73 |
| 60 | -8.9 | 0.68 | 0.70 | 0.91 | 60 | -3.9 | 1.53 | 1.28 | 1.84 |
| 60 | -8.2 | 0.73 | 0.75 | 0.98 | 60 | -3.6 | 1.54 | 1.28 | 1.84 |
| | | | | | 60 | -3.9 | 1.53 | 1.27 | 1.83 |

| Nominal Speed (mph) | Section 3 | | | | Nominal Speed (mph) | Section 4 | | | |
|---|---|---|---|---|---|---|---|---|---|
| | Vertical Pressure (psi) | | | | | Vertical Pressure (psi) | | | |
| | Offset (in) | Uncorrected | 20 ºC | 30 ºC | | Offset (in) | Uncorrected | 20 ºC | 30 ºC |
| 20 | 3.1 | 1.35 | 0.71 | 1.04 | 20 | 1.5 | 0.90 | 0.70 | 0.69 |
| 20 | -3.9 | 1.56 | 0.82 | 1.20 | 20 | 2.4 | 0.98 | 0.77 | 0.75 |
| 20 | 3.1 | 1.09 | 0.57 | 0.84 | 20 | 2.1 | 1.06 | 0.83 | 0.81 |
| 20 | 3.4 | 1.59 | 0.83 | 1.22 | 20 | 0.2 | 1.07 | 0.83 | 0.82 |
| 20 | 10.7 | 1.09 | 0.57 | 0.84 | 20 | 8.5 | 0.91 | 0.71 | 0.69 |
| 45 | 2.9 | 1.06 | 0.56 | 0.82 | 45 | -0.9 | 0.64 | 0.50 | 0.49 |
| 45 | -5.3 | 0.92 | 0.48 | 0.71 | 45 | -0.6 | 0.68 | 0.53 | 0.52 |
| 45 | 1.4 | 1.06 | 0.55 | 0.81 | 45 | 1.2 | 0.68 | 0.53 | 0.52 |
| 45 | 7.3 | 0.89 | 0.46 | 0.68 | 60 | 2.8 | 0.56 | 0.45 | 0.55 |
| 45 | -3.0 | 1.10 | 0.58 | 0.84 | 60 | 1.5 | 0.57 | 0.46 | 0.56 |
| 60 | -8.4 | 0.49 | 0.26 | 0.37 | 60 | 3.1 | 0.56 | 0.45 | 0.55 |
| 60 | -1.62 | 0.65 | 0.34 | 0.49 | 60 | 2.2 | 0.55 | 0.44 | 0.54 |
| 60 | 3.31 | 0.63 | 0.33 | 0.48 | | | | | |
| 60 | -1.62 | 0.68 | 0.36 | 0.51 | | | | | |
| 60 | 1.00 | 0.68 | 0.35 | 0.51 | | | | | |

Table B-4: Vertical Pressure – 08/01/2006

| Nominal Speed (mph) | Section 1 | | | | Nominal Speed (mph) | Section 2 | | | |
|---|---|---|---|---|---|---|---|---|---|
| | Vertical Pressure (psi) | | | | | Vertical Pressure (psi) | | | |
| | Offset (in) | Uncorrected | 20 ºC | 30 ºC | | Offset (in) | Uncorrected | 20 ºC | 30 ºC |
| 20 | -5.1 | 4.06 | 2.68 | 3.57 | 20 | -0.4 | 4.62 | 2.55 | 3.78 |
| 20 | -3.1 | 3.62 | 2.39 | 3.18 | 20 | 6.9 | 4.14 | 2.28 | 3.39 |
| 20 | -3.8 | 3.98 | 2.63 | 3.50 | 20 | -5.1 | 4.27 | 2.36 | 3.50 |
| 20 | -3.5 | 4.21 | 2.78 | 3.70 | 20 | 3.3 | 6.01 | 3.32 | 4.92 |
| 45 | -6.7 | 2.40 | 1.58 | 2.11 | 45 | 0.3 | 3.64 | 2.01 | 2.98 |
| 45 | -4.4 | 2.44 | 1.61 | 2.15 | 45 | -2.1 | 3.61 | 1.99 | 2.95 |
| 45 | -8.8 | 2.57 | 1.69 | 2.26 | 45 | -1.0 | 3.61 | 1.99 | 2.95 |
| 45 | -1.9 | 2.65 | 1.75 | 2.33 | 60 | 1.3 | 2.74 | 1.45 | 2.09 |
| 60 | -5.0 | 2.03 | 1.34 | 1.76 | 60 | 8.9 | 2.17 | 1.15 | 1.65 |
| 60 | -6.0 | 2.10 | 1.39 | 1.82 | 60 | -0.4 | 2.67 | 1.41 | 2.04 |
| | | | | | 60 | 1.6 | 2.87 | 1.52 | 2.19 |
| | | | | | | | | | |
| Nominal Speed (mph) | Section 3 | | | | Nominal Speed (mph) | Section 4 | | | |
| | Vertical Pressure (psi) | | | | | Vertical Pressure (psi) | | | |
| | Offset (in) | Uncorrected | 20 ºC | 30 ºC | | Offset (in) | Uncorrected | 20 ºC | 30 ºC |
| | | | | | 20 | 10.7 | 3.85 | 2.61 | 3.28 |
| | | | | | 20 | 18.0 | 2.39 | 1.62 | 2.04 |
| | | | | | 20 | 15.3 | 3.76 | 2.55 | 3.21 |
| | | | | | 20 | 14.3 | 3.75 | 2.55 | 3.20 |
| | | | | | 45 | 11.3 | 2.11 | 1.43 | 1.80 |
| | | | | | 45 | 9.0 | 1.67 | 1.13 | 1.42 |
| | | | | | 45 | 10.0 | 1.90 | 1.29 | 1.62 |
| | | | | | 60 | 15.3 | 1.71 | 1.14 | 1.39 |
| | | | | | 60 | 12.3 | 1.47 | 0.97 | 1.19 |
| | | | | | 60 | 12.7 | 1.68 | 1.11 | 1.36 |

Table B-5: Vertical Pressure – RWD - 08/01/2006

| Nominal Speed (mph) | Section 1 | | | | Nominal Speed (mph) | Section 2 | | | |
|---|---|---|---|---|---|---|---|---|---|
| | Vertical Pressure (psi) | | | | | Vertical Pressure (psi) | | | |
| | Offset (in) | Uncorrected | 20 ºC | 30 ºC | | Offset (in) | Uncorrected | 20 ºC | 30 ºC |
| 60 | -1.3 | 1.55 | 1.01 | 1.32 | 60 | 7.6 | 2.05 | 1.07 | 1.54 |
| 60 | -1.8 | 1.23 | 0.80 | 1.05 | 60 | 8.2 | 1.95 | 1.01 | 1.46 |
| 60 | -1.0 | 1.26 | 0.82 | 1.07 | 60 | 3.3 | 2.00 | 1.04 | 1.50 |
| 60 | -3.1 | 1.26 | 0.82 | 1.07 | 60 | 2.3 | 1.97 | 1.02 | 1.47 |
| | | | | | | | | | |
| Nominal Speed (mph) | Section 3 | | | | Nominal Speed (mph) | Section 4 | | | |
| | Vertical Pressure (psi) | | | | | Vertical Pressure (psi) | | | |
| | Offset (in) | Uncorrected | 20 ºC | 30 ºC | | Offset (in) | Uncorrected | 20 ºC | 30 ºC |
| | | | | | 60 | 8.2 | 1.02 | 0.67 | 0.82 |
| | | | | | 60 | 1.7 | 0.99 | 0.65 | 0.79 |
| | | | | | 60 | 8.4 | 1.07 | 0.70 | 0.86 |
| | | | | | 60 | 7.7 | 1.03 | 0.67 | 0.82 |

Table B-6: Vertical Pressure – 10/13/2006

| Nominal Speed (mph) | Section 1 Vertical Pressure (psi) | | | | Nominal Speed (mph) | Section 2 Vertical Pressure (psi) | | | |
|---|---|---|---|---|---|---|---|---|---|
| | Offset (in) | Uncorrected | 20 ºC | 30 ºC | | Offset (in) | Uncorrected | 20 ºC | 30 ºC |
| 20 | -4.3 | 0.63 | 0.80 | 1.07 | 20 | -2.5 | 1.41 | 1.97 | 2.91 |
| 20 | -2.3 | 0.64 | 0.82 | 1.09 | 20 | -2.7 | 1.35 | 1.89 | 2.80 |
| 20 | -7.2 | 0.53 | 0.68 | 0.91 | 20 | 2.6 | 1.45 | 2.02 | 3.00 |
| 20 | -0.8 | 0.59 | 0.75 | 1.00 | 20 | 2.5 | 1.42 | 1.98 | 2.93 |
| 20 | 2.1 | 0.57 | 0.73 | 0.98 | 45 | 1.2 | 1.11 | 1.56 | 2.31 |
| 45 | -4.1 | 0.44 | 0.56 | 0.74 | 45 | -0.5 | 1.09 | 1.52 | 2.26 |
| 45 | -6.5 | 0.41 | 0.53 | 0.70 | 45 | 3.9 | 1.07 | 1.50 | 2.22 |
| 45 | 5.0 | 0.41 | 0.53 | 0.70 | 45 | 4.7 | 1.08 | 1.52 | 2.25 |
| 45 | -4.8 | 0.42 | 0.53 | 0.71 | 45 | -1.6 | 1.08 | 1.51 | 2.24 |
| 45 | 0.1 | 0.43 | 0.56 | 0.74 | 60 | -3.2 | 0.97 | 1.28 | 1.85 |
| 60 | -6.1 | 0.35 | 0.42 | 0.55 | 60 | -1.1 | 0.97 | 1.28 | 1.84 |
| 60 | -1.0 | 0.34 | 0.42 | 0.55 | 60 | -0.2 | 0.97 | 1.28 | 1.85 |
| 60 | -1.3 | 0.36 | 0.44 | 0.58 | 60 | -1.8 | 1.02 | 1.34 | 1.93 |
| 60 | -5.1 | 0.34 | 0.42 | 0.55 | 60 | 0.5 | 0.98 | 1.29 | 1.86 |
| 60 | -5.0 | 0.35 | 0.43 | 0.56 | | | | | |

| Nominal Speed (mph) | Section 3 Vertical Pressure (psi) | | | | Nominal Speed (mph) | Section 4 Vertical Pressure (psi) | | | |
|---|---|---|---|---|---|---|---|---|---|
| | Offset (in) | Uncorrected | 20 ºC | 30 ºC | | Offset (in) | Uncorrected | 20 ºC | 30 ºC |
| 20 | 3.7 | 1.22 | 1.55 | 2.27 | 20 | 1.5 | 0.53 | 0.62 | 0.78 |
| 20 | 1.0 | 1.17 | 1.50 | 2.19 | 20 | 2.4 | 0.47 | 0.54 | 0.68 |
| 20 | -0.6 | 1.24 | 1.58 | 2.31 | 20 | 2.1 | 0.52 | 0.61 | 0.76 |
| 45 | 1.3 | 0.73 | 0.92 | 1.36 | 20 | 0.2 | 0.46 | 0.53 | 0.67 |
| 45 | 1.0 | 0.77 | 0.98 | 1.44 | 45 | -0.9 | 0.39 | 0.46 | 0.57 |
| 45 | -2.2 | 0.75 | 0.95 | 1.40 | 45 | 1.2 | 0.35 | 0.41 | 0.51 |
| 45 | 5.5 | 0.77 | 0.98 | 1.44 | 45 | 0.1 | 0.40 | 0.46 | 0.58 |
| 45 | 7.8 | 0.74 | 0.94 | 1.39 | 60 | 2.8 | 0.34 | 0.37 | 0.46 |
| 60 | -1.8 | 0.54 | 0.65 | 0.93 | 60 | 3.8 | 0.36 | 0.40 | 0.49 |
| 60 | -2.8 | 0.58 | 0.70 | 0.99 | 60 | 3.1 | 0.32 | 0.36 | 0.44 |
| 60 | 1.6 | 0.55 | 0.67 | 0.95 | 60 | 2.2 | 0.30 | 0.33 | 0.41 |
| 60 | 2.5 | 0.59 | 0.71 | 1.02 | | | | | |
| 60 | -4.4 | 0.62 | 0.74 | 1.06 | | | | | |

Table B-7: Vertical Pressure – 05/01/2007

| Nominal Speed (mph) | Section 1 | | | | Nominal Speed (mph) | Section 2 | | | |
|---|---|---|---|---|---|---|---|---|---|
| | Vertical Pressure (psi) | | | | | Vertical Pressure (psi) | | | |
| | Offset (in) | Uncorrected | 20 ºC | 30 ºC | | Offset (in) | Uncorrected | 20 ºC | 30 ºC |
| 20 | -5.1 | 2.29 | 2.16 | 2.87 | 20 | -9.0 | 2.08 | 1.91 | 2.83 |
| 20 | -3.0 | 2.19 | 2.07 | 2.75 | 20 | -9.0 | 2.51 | 2.31 | 3.42 |
| 20 | -6.0 | 2.16 | 2.03 | 2.71 | 20 | -10.7 | 2.42 | 2.23 | 3.30 |
| 45 | -6.4 | 1.72 | 1.62 | 2.16 | 20 | -9.4 | 1.77 | 1.62 | 2.41 |
| 45 | -3.3 | 1.70 | 1.61 | 2.14 | 20 | -2.3 | 2.04 | 1.88 | 2.78 |
| 45 | -7.7 | 1.48 | 1.39 | 1.85 | 45 | 2.0 | 1.76 | 1.62 | 2.40 |
| 45 | -2.4 | 1.65 | 1.55 | 2.07 | 45 | -0.6 | 2.13 | 1.96 | 2.91 |
| 45 | -8.7 | 1.55 | 1.46 | 1.94 | 45 | 7.7 | 1.54 | 1.41 | 2.09 |
| 60 | -8.0 | 1.25 | 1.19 | 1.55 | 45 | -7.7 | 2.00 | 1.84 | 2.72 |
| 60 | -2.7 | 1.41 | 1.34 | 1.75 | 45 | -9.0 | 2.04 | 1.88 | 2.78 |
| 60 | -2.7 | 1.42 | 1.36 | 1.77 | 60 | -10.0 | 1.72 | 1.60 | 2.31 |
| 60 | -2.7 | 1.40 | 1.33 | 1.74 | 60 | -4.9 | 1.67 | 1.56 | 2.25 |
| | | | | | 60 | -4.3 | 1.74 | 1.62 | 2.34 |
| | | | | | 60 | -4.0 | 1.68 | 1.57 | 2.26 |
| | | | | | 60 | -5.0 | 1.68 | 1.57 | 2.26 |
| | | | | | 60 | -3.0 | 2.39 | 2.23 | 3.21 |
| | | | | | | | | | |
| Nominal Speed (mph) | Section 3 | | | | Nominal Speed (mph) | Section 4 | | | |
| | Vertical Pressure (psi) | | | | | Vertical Pressure (psi) | | | |
| | Offset (in) | Uncorrected | 20 ºC | 30 ºC | | Offset (in) | Uncorrected | 20 ºC | 30 ºC |
| | | | | | 20 | -0.7 | 0.97 | 0.92 | 1.15 |
| | | | | | 20 | -0.6 | 1.08 | 1.03 | 1.29 |
| | | | | | 20 | 6.0 | 0.91 | 0.86 | 1.08 |
| | | | | | 20 | -7.4 | 0.94 | 0.89 | 1.13 |
| | | | | | 20 | -5.7 | 0.99 | 0.94 | 1.19 |
| | | | | | 45 | -4.7 | 0.65 | 0.61 | 0.77 |
| | | | | | 45 | -1.0 | 0.66 | 0.63 | 0.79 |
| | | | | | 45 | -9.0 | 0.62 | 0.59 | 0.75 |
| | | | | | 45 | -3.0 | 0.68 | 0.65 | 0.81 |
| | | | | | 45 | -6.4 | 0.66 | 0.63 | 0.79 |
| | | | | | 60 | -7.3 | 0.67 | 0.64 | 0.78 |
| | | | | | 60 | 2.0 | 0.73 | 0.70 | 0.86 |
| | | | | | 60 | -8.7 | 0.63 | 0.60 | 0.74 |
| | | | | | 60 | -4.7 | 0.69 | 0.67 | 0.82 |

Table B-8: Vertical Pressure – 10/05/2007

| Nominal Speed (mph) | Section 1 Vertical Pressure (psi) | | | | Nominal Speed (mph) | Section 2 Vertical Pressure (psi) | | | |
|---|---|---|---|---|---|---|---|---|---|
| | Offset (in) | Uncorrected | 20 ºC | 30 ºC | | Offset (in) | Uncorrected | 20 ºC | 30 ºC |
| 20 | -0.7 | 2.65 | 2.41 | 3.21 | 20 | 10.9 | 2.39 | 2.14 | 3.16 |
| 20 | 4.8 | 2.74 | 2.50 | 3.32 | 20 | 10.6 | 2.45 | 2.19 | 3.24 |
| 20 | 4.7 | 2.54 | 2.32 | 3.09 | 20 | 6.6 | 2.77 | 2.48 | 3.67 |
| 20 | 7.2 | 2.37 | 2.16 | 2.87 | 45 | 6.3 | 2.10 | 1.88 | 2.79 |
| 45 | 6.0 | 1.98 | 1.80 | 2.40 | 45 | -1.7 | 2.24 | 2.01 | 2.98 |
| 45 | 6.2 | 1.90 | 1.74 | 2.31 | 45 | 0.1 | 2.07 | 1.85 | 2.74 |
| 45 | 8.3 | 1.84 | 1.68 | 2.24 | 45 | 3.6 | 2.05 | 1.84 | 2.73 |
| 45 | 3.7 | 1.84 | 1.68 | 2.23 | 60 | 3.2 | 2.05 | 1.87 | 2.45 |
| 60 | 5.0 | 1.61 | 1.49 | 1.95 | 60 | -0.8 | 2.03 | 1.85 | 2.43 |
| 60 | 4.0 | 1.67 | 1.55 | 2.02 | 60 | -0.7 | 1.95 | 1.78 | 2.33 |
| 60 | 2.8 | 1.73 | 1.60 | 2.09 | 60 | 7.6 | 1.99 | 1.81 | 2.38 |
| | | | | | 60 | -4.9 | 2.01 | 1.83 | 2.40 |

| Nominal Speed (mph) | Section 3 Vertical Pressure (psi) | | | | Nominal Speed (mph) | Section 4 Vertical Pressure (psi) | | | |
|---|---|---|---|---|---|---|---|---|---|
| | Offset (in) | Uncorrected | 20 ºC | 30 ºC | | Offset (in) | Uncorrected | 20 ºC | 30 ºC |
| | | | | | 20 | 0.0 | 1.49 | 1.41 | 1.77 |
| | | | | | 20 | 6.3 | 1.74 | 1.64 | 2.06 |
| | | | | | 20 | -1.2 | 1.74 | 1.64 | 2.07 |
| | | | | | 20 | -1.5 | 1.68 | 1.58 | 1.99 |
| | | | | | 45 | -0.3 | 1.27 | 1.19 | 1.50 |
| | | | | | 45 | 3.3 | 1.34 | 1.26 | 1.59 |
| | | | | | 45 | 1.2 | 1.30 | 1.23 | 1.54 |
| | | | | | 45 | 3.8 | 1.34 | 1.26 | 1.59 |
| | | | | | 45 | 3.7 | 1.32 | 1.25 | 1.57 |
| | | | | | 60 | 5.9 | 1.23 | 1.17 | 1.43 |
| | | | | | 60 | 2.0 | 1.23 | 1.17 | 1.43 |
| | | | | | 60 | -2.0 | 1.16 | 1.11 | 1.35 |
| | | | | | 60 | 1.4 | 1.20 | 1.15 | 1.41 |

Table B-9: Longitudinal Strains – 07/14/2005

| Nominal Speed (mph) | Section 1 Longitudinal Strain (μ-strain) | | | | Nominal Speed (mph) | Section 2 Longitudinal Strain (μ-strain) | | | |
|---|---|---|---|---|---|---|---|---|---|
| | Offset (in) | Uncorrected | 20 ºC | 30 ºC | | Offset (in) | Uncorrected | 20 ºC | 30 ºC |
| 20 | 0.3 | 44.60 | 29.74 | 42.35 | 20 | 11.7 | 76.40 | 41.65 | 69.47 |
| 20 | 3.4 | 44.60 | 29.74 | 42.35 | 20 | 4.4 | 105.80 | 57.67 | 96.20 |
| 20 | 2.2 | 43.80 | 29.20 | 41.59 | 20 | -1.1 | 86.40 | 47.10 | 78.56 |
| 20 | 3.8 | 44.40 | 29.60 | 42.16 | 20 | 3.4 | 84.40 | 46.01 | 76.74 |
| 20 | 4.7 | 42.80 | 28.54 | 40.64 | 20 | -4.2 | 94.80 | 51.68 | 86.20 |
| 20 | -3.8 | 60.00 | 40.00 | 56.98 | 20 | -1.4 | 99.00 | 53.97 | 90.02 |
| 20 | -5.7 | 52.60 | 35.07 | 49.95 | 20 | 1.4 | 70.00 | 38.16 | 63.65 |
| 20 | -3.8 | 60.40 | 40.27 | 57.36 | 20 | 4.7 | 88.00 | 47.97 | 80.02 |
| 20 | -3.7 | 58.60 | 39.07 | 55.65 | 20 | -6.6 | 85.80 | 46.77 | 78.01 |
| 20 | -8.0 | 61.20 | 40.80 | 58.12 | 20 | -0.2 | 92.80 | 50.59 | 84.38 |
| 20 | -6.0 | 64.00 | 42.67 | 60.78 | 20 | -7.4 | 236.20 | 128.75 | 214.77 |
| 20 | -4.0 | 67.00 | 44.67 | 63.63 | 20 | 0.2 | 285.80 | 155.79 | 259.87 |
| 20 | -4.0 | 65.20 | 43.47 | 61.92 | 45 | 5.0 | 107.00 | 58.33 | 97.29 |
| 45 | 4.2 | 43.00 | 28.67 | 40.83 | 45 | 7.4 | 108.20 | 58.98 | 98.38 |
| 45 | 7.4 | 42.00 | 28.00 | 39.89 | 45 | -2.0 | 94.80 | 51.68 | 86.20 |
| 45 | 0.9 | 17.60 | 11.73 | 16.71 | 45 | -1.0 | 109.80 | 59.85 | 99.84 |
| 45 | 6.0 | 15.20 | 10.13 | 14.43 | 45 | 1.3 | 101.40 | 55.27 | 92.20 |
| 45 | 5.1 | 16.60 | 11.07 | 15.76 | 45 | -0.1 | 90.40 | 49.28 | 82.20 |
| 45 | -0.7 | 53.20 | 35.47 | 50.52 | 45 | -3.3 | 27.00 | 14.72 | 24.55 |
| 45 | -3.4 | 54.60 | 36.40 | 51.85 | 45 | -2.0 | 85.80 | 46.77 | 78.01 |
| 45 | -5.4 | 23.20 | 15.47 | 22.03 | 45 | -1.0 | 102.60 | 55.93 | 93.29 |
| 45 | 0.0 | 20.20 | 13.47 | 19.18 | 45 | -1.3 | 75.00 | 40.88 | 68.19 |
| 45 | -0.5 | 60.60 | 40.40 | 57.55 | 45 | -3.9 | 29.20 | 15.92 | 26.55 |
| 45 | -5.5 | 22.60 | 15.07 | 21.46 | 45 | -2.0 | 236.20 | 128.75 | 214.77 |
| 60 | 7.1 | 16.80 | 11.46 | 15.90 | 45 | -1.0 | 306.80 | 167.24 | 278.96 |
| 60 | 6.1 | 14.00 | 9.55 | 13.25 | 45 | 1.0 | 272.40 | 148.49 | 247.68 |
| 60 | 9.7 | 10.80 | 7.37 | 10.22 | 45 | -1.7 | 249.80 | 136.17 | 227.13 |
| 60 | 1.4 | 24.00 | 16.37 | 22.71 | 45 | -4.1 | 80.00 | 43.61 | 72.74 |
| 60 | 0.7 | 21.20 | 14.46 | 20.06 | 60 | 2.8 | 34.60 | 19.30 | 31.06 |
| 60 | 0.9 | 17.00 | 11.60 | 16.09 | 60 | 3.5 | 36.00 | 20.09 | 32.31 |
| 60 | 1.3 | 16.20 | 11.05 | 15.33 | 60 | 3.4 | 31.60 | 17.63 | 28.36 |
| 60 | 1.0 | 23.40 | 15.96 | 22.15 | 60 | 7.6 | 35.60 | 19.86 | 31.95 |
| 60 | 1.0 | 19.80 | 13.50 | 18.74 | 60 | -3.6 | 34.20 | 19.08 | 30.70 |
| 60 | 1.0 | 19.40 | 13.23 | 18.36 | 60 | 2.4 | 28.20 | 15.73 | 25.31 |
| | | | | | 60 | -2.5 | 33.20 | 18.52 | 29.80 |
| | | | | | 60 | -5.6 | 30.20 | 16.85 | 27.11 |
| | | | | | 60 | 1.2 | 31.00 | 17.30 | 27.82 |
| | | | | | 60 | -2.5 | 27.00 | 15.06 | 24.23 |
| | | | | | 60 | 0.2 | 28.80 | 16.07 | 25.85 |
| | | | | | 60 | -6.3 | 68.00 | 37.94 | 61.03 |
| | | | | | 60 | 0.8 | 67.20 | 37.49 | 60.32 |

Table B-10 - *Continued*

| Nominal Speed (mph) | Section 3 Longitudinal Strain (μ-strain) | | | | Nominal Speed (mph) | Section 4 Longitudinal Strain (μ-strain) | | | |
|---|---|---|---|---|---|---|---|---|---|
| | Offset (in) | Uncorrected | 20 ºC | 30 ºC | | Offset (in) | Uncorrected | 20 ºC | 30 ºC |
| 20 | 7.6 | 39.60 | 18.94 | 30.43 | 20 | 4.9 | 45.20 | 20.04 | 36.07 |
| 20 | 4.9 | 43.60 | 20.86 | 33.50 | 20 | -1.9 | 41.20 | 18.27 | 32.88 |
| 20 | 6.9 | 46.60 | 22.29 | 35.81 | 20 | -1.1 | 38.60 | 17.12 | 30.80 |
| 20 | 0.7 | 52.20 | 24.97 | 40.11 | 45 | -3.7 | 47.80 | 21.20 | 38.14 |
| 20 | 6.7 | 31.00 | 14.83 | 23.82 | 45 | -2.9 | 44.20 | 19.60 | 35.27 |
| 20 | 4.8 | 31.00 | 14.83 | 23.82 | 45 | -7.0 | 15.60 | 6.92 | 12.45 |
| 20 | 0.2 | 34.80 | 16.65 | 26.74 | 45 | -3.2 | 16.20 | 7.18 | 12.93 |
| 20 | 0.9 | 26.80 | 12.82 | 20.59 | 45 | -6.3 | 17.00 | 7.54 | 13.57 |
| 20 | 3.8 | 27.20 | 13.01 | 20.90 | 60 | -8.1 | 16.20 | 7.72 | 13.13 |
| 20 | 5.3 | 28.80 | 13.78 | 22.13 | 60 | -5.7 | 19.80 | 9.44 | 16.05 |
| 20 | -3.6 | 34.40 | 16.46 | 26.43 | 60 | -6.7 | 17.40 | 8.29 | 14.10 |
| 20 | 0.1 | 23.80 | 11.38 | 18.29 | 60 | -7.0 | 13.60 | 6.48 | 11.02 |
| 20 | 5.1 | 30.20 | 14.45 | 23.21 | 60 | -6.0 | 12.40 | 5.91 | 10.05 |
| 20 | -4.1 | 31.40 | 15.02 | 24.13 | | | | | |
| 45 | 2.0 | 49.80 | 23.82 | 38.27 | | | | | |
| 45 | 2.0 | 18.80 | 8.99 | 14.45 | | | | | |
| 45 | 2.9 | 34.60 | 16.55 | 26.59 | | | | | |
| 45 | 1.9 | 34.80 | 16.65 | 26.74 | | | | | |
| 45 | 1.9 | 9.60 | 4.59 | 7.38 | | | | | |
| 45 | 3.2 | 11.00 | 5.26 | 8.45 | | | | | |
| 45 | 4.6 | 29.60 | 14.16 | 22.74 | | | | | |
| 45 | 0.6 | 6.60 | 3.16 | 5.07 | | | | | |
| 45 | 1.1 | 30.40 | 14.54 | 23.36 | | | | | |
| 45 | 0.2 | 7.60 | 3.64 | 5.84 | | | | | |
| 60 | 3.9 | 21.00 | 10.09 | 15.72 | | | | | |
| 60 | -0.8 | 18.00 | 8.65 | 13.47 | | | | | |
| 60 | -1.1 | 18.40 | 8.84 | 13.77 | | | | | |
| 60 | -1.2 | 12.20 | 5.86 | 9.13 | | | | | |
| 60 | 2.9 | 10.60 | 5.09 | 7.93 | | | | | |
| 60 | -0.5 | 10.00 | 4.80 | 7.48 | | | | | |
| 60 | -1.4 | 8.40 | 4.04 | 6.29 | | | | | |
| 60 | -1.5 | 5.20 | 2.50 | 3.89 | | | | | |
| 60 | 2.55 | 7.20 | 3.46 | 5.39 | | | | | |
| 60 | -3.92 | 4.60 | 2.21 | 3.44 | | | | | |
| 60 | -4.27 | 2.40 | 1.15 | 1.80 | | | | | |

Table B-11: Longitudinal Strains – 09/29/2005

| Nominal Speed (mph) | Section 1 Longitudinal Strain (μ-strain) | | | | Nominal Speed (mph) | Section 2 Longitudinal Strain (μ-strain) | | | |
|---|---|---|---|---|---|---|---|---|---|
| | Offset (in) | Uncorrected | 20 ºC | 30 ºC | | Offset (in) | Uncorrected | 20 ºC | 30 ºC |
| 20 | 1.1 | 35.80 | 38.34 | 54.61 | 45 | -4.6 | 29.60 | 30.51 | 50.90 |
| 20 | -11.1 | 35.40 | 37.91 | 54.00 | 45 | -2.6 | 28.40 | 29.28 | 48.83 |
| 20 | -11.9 | 39.20 | 41.98 | 59.79 | 45 | 3.5 | 26.00 | 26.80 | 44.71 |
| 20 | -12.0 | 34.60 | 37.06 | 52.78 | 45 | -8.9 | 22.00 | 22.68 | 37.83 |
| 60 | -7.7 | 19.00 | 19.91 | 27.63 | 45 | -3.2 | 18.80 | 19.38 | 32.33 |
| 60 | -10.5 | 18.00 | 18.86 | 26.18 | 45 | -10.7 | 20.60 | 21.24 | 35.42 |
| 60 | -7.4 | 17.40 | 18.24 | 25.30 | 45 | -7.2 | 18.20 | 18.76 | 31.29 |
| 60 | -8.3 | 18.40 | 19.28 | 26.76 | 45 | -13.3 | 26.60 | 27.42 | 45.74 |
| 60 | -19.1 | 15.60 | 16.35 | 22.69 | 45 | -11.3 | 23.40 | 24.12 | 40.24 |
| 60 | -18.4 | 14.20 | 14.88 | 20.65 | 45 | -8.6 | 20.60 | 21.24 | 35.42 |
| 60 | -20.5 | 15.00 | 15.72 | 21.81 | 60 | -4.4 | 19.80 | 20.46 | 32.92 |
| 60 | -16.6 | 11.80 | 12.37 | 17.16 | 60 | -3.6 | 15.00 | 15.50 | 24.94 |
| 60 | -16.7 | 13.20 | 13.83 | 19.20 | 60 | -3.4 | 15.80 | 16.33 | 26.27 |
| 60 | -19.9 | 18.40 | 19.28 | 26.76 | 60 | -3.6 | 14.20 | 14.67 | 23.61 |
| 60 | -19.0 | 16.40 | 17.19 | 23.85 | 60 | -3.4 | 17.80 | 18.40 | 29.59 |
| 60 | -21.0 | 14.60 | 15.30 | 21.23 | 60 | -10.6 | 13.00 | 13.43 | 21.61 |
| 60 | -17.0 | 14.60 | 15.30 | 21.23 | 60 | -9.6 | 10.40 | 10.75 | 17.29 |
| 60 | -17.0 | 16.80 | 17.61 | 24.43 | 60 | -9.6 | 12.60 | 13.02 | 20.95 |
| | | | | | 60 | -11.8 | 14.80 | 15.30 | 24.61 |
| | | | | | 60 | -10.8 | 8.40 | 8.68 | 13.97 |
| | | | | | 60 | -10.8 | 13.20 | 13.64 | 21.95 |
| | | | | | 60 | -12.2 | 20.40 | 21.08 | 33.92 |
| | | | | | 60 | -12.3 | 12.60 | 13.02 | 20.95 |
| | | | | | 60 | -11.2 | 17.80 | 18.40 | 29.59 |

| Nominal Speed (mph) | Section 3 Longitudinal Strain (μ-strain) | | | | Nominal Speed (mph) | Section 4 Longitudinal Strain (μ-strain) | | | |
|---|---|---|---|---|---|---|---|---|---|
| | Offset (in) | Uncorrected | 20 ºC | 30 ºC | | Offset (in) | Uncorrected | 20 ºC | 30 ºC |
| 20 | 3.9 | 37.20 | 35.18 | 56.51 | 20 | -7.5 | 27.40 | 24.71 | 44.47 |
| 20 | -3.2 | 40.00 | 37.83 | 60.76 | 20 | -4.8 | 24.40 | 22.01 | 39.60 |
| 20 | 3.9 | 42.80 | 40.48 | 65.02 | 20 | -5.7 | 31.80 | 28.68 | 51.61 |
| 20 | 3.9 | 36.40 | 34.42 | 55.29 | 20 | -9.4 | 26.40 | 23.81 | 42.85 |
| 20 | 11.0 | 35.20 | 33.29 | 53.47 | 45 | -8.7 | 12.20 | 11.00 | 19.80 |
| 20 | 3.6 | 19.80 | 18.72 | 30.08 | 45 | -7.8 | 14.20 | 12.81 | 23.05 |
| 20 | -3.5 | 18.20 | 17.21 | 27.65 | 45 | -8.4 | 15.20 | 13.71 | 24.67 |
| 20 | 3.6 | 19.00 | 17.97 | 28.86 | 45 | -9.2 | 12.60 | 11.36 | 20.45 |
| 20 | 3.7 | 17.60 | 16.64 | 26.74 | 60 | -7.2 | 11.80 | 10.69 | 18.18 |

Table B -10 - *Continued*

| Nominal Speed (mph) | Section 3 | | | | Nominal Speed (mph) | Section 4 | | | |
|---|---|---|---|---|---|---|---|---|---|
| | Longitudinal Strain (μ-strain) | | | | | Longitudinal Strain (μ-strain) | | | |
| | Offset (in) | Uncorrected | 20 ºC | 30 ºC | | Offset (in) | Uncorrected | 20 ºC | 30 ºC |
| 20 | 1.2 | 29.60 | 27.99 | 44.96 | | | | | |
| 20 | -5.8 | 30.40 | 28.75 | 46.18 | | | | | |
| 20 | 1.2 | 31.60 | 29.88 | 48.00 | | | | | |
| 20 | 2.1 | 28.00 | 26.48 | 42.53 | | | | | |
| 20 | 10.1 | 26.20 | 24.78 | 39.80 | | | | | |
| 45 | -5.1 | 21.00 | 19.86 | 31.90 | | | | | |
| 45 | 1.9 | 19.20 | 18.16 | 29.17 | | | | | |
| 45 | 7.1 | 19.20 | 18.16 | 29.17 | | | | | |
| 45 | -3.0 | 19.60 | 18.54 | 29.77 | | | | | |
| 45 | 2.5 | 7.00 | 6.62 | 10.63 | | | | | |
| 45 | -5.2 | 7.80 | 7.38 | 11.85 | | | | | |
| 45 | 1.7 | 8.20 | 7.75 | 12.46 | | | | | |
| 45 | 7.2 | 7.20 | 6.81 | 10.94 | | | | | |
| 45 | -3.0 | 9.20 | 8.70 | 13.98 | | | | | |
| 45 | 4.5 | 14.20 | 13.43 | 21.57 | | | | | |
| 45 | -5.8 | 13.80 | 13.05 | 20.96 | | | | | |
| 45 | 0.3 | 13.60 | 12.86 | 20.66 | | | | | |
| 45 | -3.00 | 13.20 | 12.48 | 20.05 | | | | | |
| 45 | 4.80 | 14.80 | 14.00 | 22.48 | | | | | |
| 60 | -8.90 | 13.60 | 13.00 | 20.25 | | | | | |
| 60 | 3.05 | 15.80 | 15.10 | 23.53 | | | | | |
| 60 | 1.00 | 16.20 | 15.48 | 24.12 | | | | | |
| 60 | -8.70 | 4.60 | 4.40 | 6.85 | | | | | |
| 60 | 3.15 | 6.60 | 6.31 | 9.83 | | | | | |
| 60 | -1.30 | 5.20 | 4.97 | 7.74 | | | | | |
| 60 | 1.00 | 4.80 | 4.59 | 7.15 | | | | | |
| 60 | -7.33 | 10.00 | 9.56 | 14.89 | | | | | |
| 60 | -2.67 | 9.20 | 8.79 | 13.70 | | | | | |
| 60 | 3.83 | 11.00 | 10.51 | 16.38 | | | | | |
| 60 | -2.67 | 10.80 | 10.32 | 16.08 | | | | | |
| 60 | 1.00 | 10.80 | 10.32 | 16.08 | | | | | |
| 60 | -7.13 | 9.40 | 8.98 | 14.00 | | | | | |
| 60 | -2.87 | 10.20 | 9.75 | 15.19 | | | | | |
| 60 | 3.93 | 9.60 | 9.18 | 14.30 | | | | | |
| 60 | -2.87 | 9.60 | 9.18 | 14.30 | | | | | |
| 60 | 1.00 | 10.00 | 9.56 | 14.89 | | | | | |

Table B-12: Longitudinal Strains – 04/13/2006

| Nominal Speed (mph) | Section 1 Longitudinal Strain (μ-strain) | | | | Nominal Speed (mph) | Section 2 Longitudinal Strain (μ-strain) | | | |
|---|---|---|---|---|---|---|---|---|---|
| | Offset (in) | Uncorrected | 20 ºC | 30 ºC | | Offset (in) | Uncorrected | 20 ºC | 30 ºC |
| 20 | -7.8 | 25.80 | 26.81 | 38.19 | 20 | -5.8 | 36.60 | 27.96 | 46.64 |
| 20 | -3.9 | 32.40 | 33.67 | 47.96 | 20 | -12.1 | 35.20 | 26.89 | 44.85 |
| 20 | -19.2 | 22.80 | 23.69 | 33.75 | 20 | 2.6 | 35.80 | 27.35 | 45.62 |
| 20 | -11.1 | 24.40 | 25.36 | 36.12 | 20 | 2.6 | 41.80 | 31.93 | 53.26 |
| 20 | -16.1 | 26.80 | 27.85 | 39.67 | 20 | -0.4 | 43.40 | 33.15 | 55.30 |
| 20 | -14.2 | 24.40 | 25.36 | 36.12 | 20 | -12.2 | 32.20 | 24.60 | 41.03 |
| 20 | -19.9 | 28.40 | 29.51 | 42.04 | 20 | -16.7 | 28.00 | 21.39 | 35.68 |
| 20 | -11.9 | 31.80 | 33.05 | 47.07 | 20 | -3.6 | 33.40 | 25.51 | 42.56 |
| 20 | -16.9 | 30.20 | 31.39 | 44.70 | 20 | -3.6 | 41.80 | 31.93 | 53.26 |
| 20 | -14.9 | 32.00 | 33.26 | 47.37 | 20 | -14.6 | 37.20 | 28.42 | 47.40 |
| 45 | -2.7 | 14.60 | 15.17 | 21.61 | 20 | -8.5 | 27.60 | 21.08 | 35.17 |
| 45 | -8.3 | 14.60 | 15.17 | 21.61 | 20 | -4.8 | 36.60 | 27.96 | 46.64 |
| 45 | -9.7 | 14.40 | 14.97 | 21.31 | 20 | -4.8 | 42.00 | 32.08 | 53.52 |
| 45 | -10.8 | 12.80 | 13.30 | 18.95 | 45 | 5.5 | 19.40 | 14.82 | 24.72 |
| 45 | -13.4 | 15.60 | 16.21 | 23.09 | 45 | 0.4 | 26.80 | 20.47 | 34.15 |
| 45 | -20.4 | 14.60 | 15.17 | 21.61 | 45 | -4.6 | 24.80 | 18.95 | 31.60 |
| 45 | -22.2 | 14.60 | 15.17 | 21.61 | 45 | -2.6 | 24.40 | 18.64 | 31.09 |
| 45 | -14.0 | 17.80 | 18.50 | 26.35 | 45 | 3.5 | 24.00 | 18.33 | 30.58 |
| 45 | -17.0 | 15.20 | 15.80 | 22.50 | 45 | 0.2 | 21.40 | 16.35 | 27.27 |
| 45 | -21.0 | 17.40 | 18.08 | 25.76 | 45 | -5.9 | 26.00 | 19.86 | 33.13 |
| 45 | -22.9 | 14.80 | 15.38 | 21.91 | 45 | -10.9 | 21.80 | 16.65 | 27.78 |
| 60 | -6.9 | 12.80 | 13.28 | 18.42 | 45 | -8.9 | 23.80 | 18.18 | 30.33 |
| 60 | -7.7 | 10.20 | 10.58 | 14.68 | 45 | -3.2 | 24.00 | 18.33 | 30.58 |
| 60 | -8.3 | 11.60 | 12.03 | 16.69 | 45 | 4.2 | 21.00 | 16.04 | 26.76 |
| 60 | -19.1 | 14.00 | 14.52 | 20.15 | 45 | -7.7 | 21.00 | 16.04 | 26.76 |
| 60 | -18.4 | 10.00 | 10.37 | 14.39 | 45 | -12.7 | 19.40 | 14.82 | 24.72 |
| 60 | -20.5 | 11.20 | 11.62 | 16.12 | 45 | -7.2 | 21.20 | 16.20 | 27.01 |
| 60 | -16.6 | 11.40 | 11.82 | 16.41 | 60 | -4.4 | 17.60 | 13.81 | 22.22 |
| 60 | -16.7 | 12.40 | 12.86 | 17.85 | 60 | -3.6 | 17.40 | 13.66 | 21.97 |
| 60 | -19.9 | 15.20 | 15.76 | 21.87 | 60 | -3.4 | 18.60 | 14.60 | 23.48 |
| 60 | -19.0 | 12.60 | 13.07 | 18.13 | 60 | -3.4 | 17.40 | 13.66 | 21.97 |
| 60 | -21.0 | 12.60 | 13.07 | 18.13 | 60 | -10.6 | 14.80 | 11.62 | 18.69 |
| 60 | -17.0 | 12.20 | 12.65 | 17.56 | 60 | -9.9 | 15.60 | 12.24 | 19.70 |
| 60 | -17.0 | 15.00 | 15.56 | 21.59 | 60 | -9.6 | 16.60 | 13.03 | 20.96 |
| | | | | | 60 | -9.9 | 14.60 | 11.46 | 18.43 |
| | | | | | 60 | -9.6 | 12.80 | 10.05 | 16.16 |
| | | | | | 60 | -11.8 | 15.60 | 12.24 | 19.70 |

Table B-11 - *Continued*

| Nominal Speed (mph) | Section 3 Longitudinal Strain (μ-strain) | | | | Nominal Speed (mph) | Section 4 Longitudinal Strain (μ-strain) | | | |
|---|---|---|---|---|---|---|---|---|---|
| | Offset (in) | Uncorrected | 20 ºC | 30 ºC | | Offset (in) | Uncorrected | 20 ºC | 30 ºC |
| | | | | | 20 | -4.8 | 23.80 | 12.41 | 22.34 |
| | | | | | 20 | -5.7 | 24.60 | 12.83 | 23.09 |
| | | | | | 20 | -9.4 | 24.80 | 12.94 | 23.28 |
| | | | | | 20 | -0.5 | 24.40 | 12.73 | 22.90 |
| | | | | | 45 | -8.7 | 14.40 | 7.51 | 13.52 |
| | | | | | 45 | -8.4 | 15.80 | 8.24 | 14.83 |
| | | | | | 45 | -7.7 | 14.20 | 7.41 | 13.33 |
| | | | | | 45 | -9.2 | 15.80 | 8.24 | 14.83 |
| | | | | | 60 | -7.2 | 10.00 | 5.56 | 9.46 |
| | | | | | 60 | -7.5 | 10.60 | 5.90 | 10.03 |
| | | | | | 60 | -4.6 | 10.20 | 5.67 | 9.65 |
| | | | | | 60 | -4.7 | 10.20 | 5.67 | 9.65 |
| | | | | | 60 | -9.0 | 7.80 | 4.34 | 7.38 |

Table B-13: Longitudinal Strains – 08/01/2006

| Nominal Speed (mph) | Section 1 | | | | Nominal Speed (mph) | Section 2 | | | |
|---|---|---|---|---|---|---|---|---|---|
| | Longitudinal Strain (μ-strain) | | | | | Longitudinal Strain (μ-strain) | | | |
| | Offset (in) | Uncorrected | 20 ºC | 30 ºC | | Offset (in) | Uncorrected | 20 ºC | 30 ºC |
| 20 | -5.7 | 44.80 | 26.57 | 37.84 | 20 | -0.6 | 99.20 | 47.28 | 78.86 |
| 20 | -3.7 | 37.00 | 21.94 | 31.25 | 20 | 6.6 | 105.80 | 50.42 | 84.10 |
| 20 | -4.6 | 42.80 | 25.38 | 36.15 | 20 | -5.4 | 83.60 | 39.84 | 66.46 |
| 20 | -4.5 | 46.40 | 27.52 | 39.19 | 20 | 3.2 | 150.60 | 71.77 | 119.72 |
| 20 | -9.0 | 64.80 | 38.43 | 54.73 | 20 | -6.4 | 92.80 | 44.23 | 73.77 |
| 20 | -7.0 | 58.20 | 34.51 | 49.16 | 20 | 0.9 | 114.60 | 54.61 | 91.10 |
| 20 | -7.0 | 68.80 | 40.80 | 58.11 | 20 | -11.1 | 66.20 | 31.55 | 52.62 |
| 20 | -6.0 | 75.40 | 44.72 | 63.69 | 20 | -2.7 | 157.00 | 74.82 | 124.80 |
| 20 | 0.0 | 20.00 | 11.86 | 16.89 | 45 | 0.2 | 57.40 | 27.35 | 45.63 |
| 20 | -6.9 | 20.40 | 12.10 | 17.23 | 45 | 4.0 | 51.60 | 24.59 | 41.02 |
| 45 | -4.8 | 19.20 | 11.39 | 16.22 | 45 | -5.7 | 58.00 | 27.64 | 46.11 |
| 45 | -9.6 | 22.00 | 13.05 | 18.58 | 45 | -2.0 | 56.20 | 26.78 | 44.68 |
| 45 | -1.3 | 20.60 | 12.22 | 17.40 | 45 | -8.1 | 52.80 | 25.16 | 41.97 |
| 45 | -13.9 | 29.00 | 17.20 | 24.50 | 45 | -7.0 | 55.00 | 26.21 | 43.72 |
| 45 | -12.0 | 27.60 | 16.37 | 23.31 | 45 | -4.0 | 53.80 | 25.64 | 42.77 |
| 45 | -9.0 | 27.80 | 16.49 | 23.48 | 60 | 1.2 | 37.20 | 17.79 | 28.62 |
| 45 | -12.0 | 27.40 | 16.25 | 23.14 | 60 | -0.6 | 41.00 | 19.61 | 31.55 |
| 45 | -10.0 | 28.20 | 16.72 | 23.82 | 60 | 1.4 | 34.60 | 16.55 | 26.62 |
| 60 | -6.7 | 19.60 | 12.04 | 16.71 | 60 | -1.7 | 36.80 | 17.60 | 28.31 |
| 60 | -5.0 | 18.40 | 11.30 | 15.69 | 60 | 2.9 | 35.20 | 16.83 | 27.08 |
| 60 | -8.6 | 18.60 | 11.43 | 15.86 | 60 | -6.4 | 33.80 | 16.17 | 26.01 |
| 60 | -6.0 | 19.40 | 11.92 | 16.54 | 60 | -4.4 | 32.60 | 15.59 | 25.08 |
| 60 | -2.8 | 20.40 | 12.53 | 17.39 | | | | | |
| 60 | -10.0 | 25.40 | 15.60 | 21.65 | | | | | |
| 60 | -11.0 | 24.40 | 14.99 | 20.80 | | | | | |
| 60 | -7.0 | 26.80 | 16.46 | 22.85 | | | | | |

| Nominal Speed (mph) | Section 3 | | | | Nominal Speed (mph) | Section 4 | | | |
|---|---|---|---|---|---|---|---|---|---|
| | Longitudinal Strain (μ-strain) | | | | | Longitudinal Strain (μ-strain) | | | |
| | Offset (in) | Uncorrected | 20 ºC | 30 ºC | | Offset (in) | Uncorrected | 20 ºC | 30 ºC |
| | | | | | 20 | 5.9 | 66.60 | 28.01 | 50.40 |
| | | | | | 20 | 13.8 | 49.60 | 20.86 | 37.54 |
| | | | | | 20 | 13.6 | 66.00 | 27.75 | 49.95 |
| | | | | | 20 | 8.9 | 59.00 | 24.81 | 44.65 |
| | | | | | 45 | 5.9 | 26.20 | 11.02 | 19.83 |
| | | | | | 45 | 9.0 | 21.20 | 8.92 | 16.04 |
| | | | | | 45 | 4.8 | 18.60 | 7.82 | 14.08 |

Table B-13 - *Continued*

| Nominal Speed (mph) | Section 3 Longitudinal Strain (μ-strain) | | | | Nominal Speed (mph) | Section 4 Longitudinal Strain (μ-strain) | | | |
|---|---|---|---|---|---|---|---|---|---|
| | Offset (in) | Uncorrected | 20 ºC | 30 ºC | | Offset (in) | Uncorrected | 20 ºC | 30 ºC |
| | | | | | 60 | 15.8 | 13.20 | 6.01 | 10.22 |
| | | | | | 60 | 5.9 | 11.80 | 5.37 | 9.13 |
| | | | | | 60 | 7.9 | 18.20 | 8.29 | 14.09 |

Table B-14: Longitudinal Strains – RWD - 08/01/2006

| Nominal Speed (mph) | Section 1 Longitudinal Strain (μ-strain) | | | | Nominal Speed (mph) | Section 2 Longitudinal Strain (μ-strain) | | | |
|---|---|---|---|---|---|---|---|---|---|
| | Offset (in) | Uncorrected | 20 ºC | 30 ºC | | Offset (in) | Uncorrected | 20 ºC | 30 ºC |
| 60 | -0.6 | 18.60 | 11.39 | 15.80 | 60 | 4.4 | 29.80 | 13.94 | 22.42 |
| 60 | -2.6 | 10.80 | 6.61 | 9.17 | 60 | 7.8 | 24.40 | 11.41 | 18.36 |
| 60 | -1.0 | 10.80 | 6.61 | 9.17 | 60 | 3.2 | 25.40 | 11.88 | 19.11 |
| 60 | -3.7 | 12.00 | 7.35 | 10.19 | 60 | 2.2 | 29.60 | 13.84 | 22.27 |
| 60 | -3.0 | 27.40 | 16.77 | 23.27 | 60 | -1.4 | 27.00 | 12.63 | 20.31 |
| 60 | -8.0 | 23.20 | 14.20 | 19.71 | 60 | 1.6 | 27.20 | 12.72 | 20.46 |
| 60 | -5.0 | 19.40 | 11.88 | 16.48 | 60 | 2.2 | 23.40 | 10.94 | 17.61 |
| 60 | -7.0 | 18.00 | 11.02 | 15.29 | 60 | -2.7 | 25.20 | 11.79 | 18.96 |

| Nominal Speed (mph) | Section 3 Longitudinal Strain (μ-strain) | | | | Nominal Speed (mph) | Section 4 Longitudinal Strain (μ-strain) | | | |
|---|---|---|---|---|---|---|---|---|---|
| | Offset (in) | Uncorrected | 20 ºC | 30 ºC | | Offset (in) | Uncorrected | 20 ºC | 30 ºC |
| | | | | | 60 | 4.6 | 14.00 | 6.34 | 10.79 |
| | | | | | 60 | -4.9 | 12.80 | 5.80 | 9.86 |
| | | | | | 60 | 3.1 | 13.80 | 6.25 | 10.63 |
| | | | | | 60 | 1.2 | 14.60 | 6.62 | 11.25 |
| | | | | | 60 | 1.1 | 13.60 | 6.16 | 10.48 |

Table B-15: Longitudinal Strains – 10/13/2006

| Nominal Speed (mph) | Section 1 Longitudinal Strain (μ-strain) | | | | Nominal Speed (mph) | Section 2 Longitudinal Strain (μ-strain) | | | |
|---|---|---|---|---|---|---|---|---|---|
| | Offset (in) | Uncorrected | 20 ºC | 30 ºC | | Offset (in) | Uncorrected | 20 ºC | 30 ºC |
| 20 | -4.1 | 19.00 | 25.97 | 36.99 | 20 | -3.0 | 25.20 | 39.29 | 65.55 |
| 20 | -2.1 | 19.40 | 26.52 | 37.77 | 20 | -0.4 | 23.40 | 36.49 | 60.86 |
| 20 | -6.4 | 17.00 | 23.24 | 33.10 | 20 | -2.8 | 24.60 | 38.36 | 63.98 |
| 20 | -1.6 | 16.20 | 22.14 | 31.54 | 20 | 2.4 | 25.80 | 40.23 | 67.11 |
| 20 | 2.7 | 16.80 | 22.96 | 32.71 | 20 | 2.0 | 25.60 | 39.92 | 66.59 |
| 20 | -11.0 | 17.80 | 24.33 | 34.66 | 20 | -6.1 | 20.40 | 31.81 | 53.06 |
| 20 | -9.0 | 19.60 | 26.79 | 38.16 | 20 | -8.7 | 20.20 | 31.50 | 52.54 |
| 20 | -16.0 | 15.80 | 21.60 | 30.76 | 20 | -3.4 | 26.60 | 41.48 | 69.19 |
| 20 | -4.0 | 16.20 | 22.14 | 31.54 | 20 | -3.5 | 24.00 | 37.42 | 62.42 |
| 20 | -6.0 | 17.00 | 23.24 | 33.10 | 20 | -4.3 | 21.20 | 33.06 | 55.14 |
| 45 | -7.5 | 9.60 | 13.12 | 18.69 | 20 | -8.1 | 22.60 | 35.24 | 58.78 |
| 45 | 5.0 | 9.40 | 12.85 | 18.30 | 20 | -2.2 | 26.20 | 40.85 | 68.15 |
| 45 | 0.7 | 9.80 | 13.40 | 19.08 | 45 | 0.8 | 14.40 | 22.45 | 37.45 |
| 45 | -8.0 | 10.40 | 14.22 | 20.25 | 45 | -1.0 | 13.40 | 20.89 | 34.85 |
| 45 | -9.0 | 8.20 | 11.21 | 15.97 | 45 | 3.3 | 14.40 | 22.45 | 37.45 |
| 45 | -1.0 | 9.00 | 12.30 | 17.52 | 45 | 4.8 | 13.40 | 20.89 | 34.85 |
| 45 | -8.0 | 9.20 | 12.58 | 17.91 | 45 | -1.4 | 14.00 | 21.83 | 36.41 |
| 45 | -8.0 | 10.00 | 13.67 | 19.47 | 45 | -4.8 | 13.00 | 20.27 | 33.81 |
| 60 | -6.7 | 8.00 | 10.60 | 14.71 | 45 | -6.5 | 12.40 | 19.34 | 32.25 |
| 60 | -1.0 | 8.80 | 11.66 | 16.18 | 45 | -3.5 | 10.40 | 16.22 | 27.05 |
| 60 | -1.1 | 9.00 | 11.92 | 16.55 | 45 | 1.4 | 10.60 | 16.53 | 27.57 |
| 60 | -5.7 | 8.00 | 10.60 | 14.71 | 60 | -3.8 | 9.40 | 13.77 | 22.16 |
| 60 | -5.0 | 8.40 | 11.13 | 15.44 | 60 | -1.4 | 9.40 | 13.77 | 22.16 |
| 60 | -10.0 | 7.80 | 10.33 | 14.34 | 60 | -0.8 | 8.80 | 12.89 | 20.74 |
| 60 | -7.0 | 7.00 | 9.27 | 12.87 | 60 | -2.5 | 8.20 | 12.01 | 19.33 |
| 60 | -8.0 | 7.60 | 10.07 | 13.97 | 60 | 0.0 | 8.60 | 12.60 | 20.27 |
| 60 | -9.0 | 7.40 | 9.80 | 13.60 | 60 | -9.2 | 9.20 | 13.48 | 21.68 |
| | | | | | 60 | -7.1 | 10.00 | 14.65 | 23.57 |
| | | | | | 60 | -6.2 | 8.80 | 12.89 | 20.74 |
| | | | | | 60 | -7.8 | 9.20 | 13.48 | 21.68 |
| | | | | | 60 | -5.5 | 8.80 | 12.89 | 20.74 |
| | | | | | 60 | -5.7 | 9.00 | 13.19 | 21.21 |
| | | | | | 60 | -5.3 | 9.00 | 13.19 | 21.21 |
| | | | | | 60 | -2.7 | 7.80 | 11.43 | 18.38 |
| | | | | | 60 | -2.5 | 8.60 | 12.60 | 20.27 |

Table B-14 - *Continued*

| Nominal Speed (mph) | Section 3 | | | | Nominal Speed (mph) | Section 4 | | | |
|---|---|---|---|---|---|---|---|---|---|
| | Longitudinal Strain (μ-strain) | | | | | Longitudinal Strain (μ-strain) | | | |
| | Offset (in) | Uncorrected | 20 ºC | 30 ºC | | Offset (in) | Uncorrected | 20 ºC | 30 ºC |
| 45 | 9.0 | 6.60 | 8.59 | 13.80 | 20 | -5.7 | 13.60 | 21.68 | 39.02 |
| 60 | -2.4 | 4.60 | 5.78 | 9.01 | 20 | -9.4 | 13.20 | 21.05 | 37.87 |
| 60 | -4.0 | 5.00 | 6.28 | 9.79 | 20 | -0.5 | 14.40 | 22.96 | 41.32 |
| 60 | 1.3 | 5.00 | 6.28 | 9.79 | 45 | -8.7 | 8.60 | 13.71 | 24.67 |
| 60 | 3.3 | 4.80 | 6.03 | 9.40 | 45 | -7.8 | 8.60 | 13.71 | 24.67 |
| 60 | -4.7 | 4.00 | 5.03 | 7.83 | 45 | -8.4 | 7.40 | 11.80 | 21.23 |
| 60 | 0.7 | 2.40 | 3.02 | 4.70 | 45 | -7.7 | 9.60 | 15.31 | 27.54 |
| 60 | 1.5 | 2.40 | 3.02 | 4.70 | 45 | -9.2 | 8.80 | 14.03 | 25.25 |
| 60 | -0.7 | 2.80 | 3.52 | 5.48 | 60 | -7.2 | 7.20 | 10.88 | 18.51 |
| | | | | | 60 | -7.5 | 6.40 | 9.67 | 16.45 |
| | | | | | 60 | -4.6 | 8.00 | 12.09 | 20.56 |
| | | | | | 60 | -4.7 | 6.60 | 9.98 | 16.96 |
| | | | | | 60 | -9.0 | 5.40 | 8.16 | 13.88 |

Table B-16: Longitudinal Strains – 05/01/2007

| Nominal Speed (mph) | Section 1 Longitudinal Strain (μ-strain) | | | | Nominal Speed (mph) | Section 2 Longitudinal Strain (μ-strain) | | | |
|---|---|---|---|---|---|---|---|---|---|
| | Offset (in) | Uncorrected | 20 ºC | 30 ºC | | Offset (in) | Uncorrected | 20 ºC | 30 ºC |
| 20 | -5.7 | 30.20 | 27.98 | 39.85 | 20 | -9.0 | 50.80 | 45.71 | 76.24 |
| 20 | -3.0 | 28.00 | 25.94 | 36.95 | 20 | -10.8 | 41.60 | 37.43 | 62.44 |
| 20 | -4.8 | 28.00 | 25.94 | 36.95 | 20 | -9.6 | 29.60 | 26.63 | 44.43 |
| 20 | -6.0 | 27.80 | 25.76 | 36.69 | 20 | -2.2 | 41.00 | 36.89 | 61.54 |
| 20 | -2.8 | 21.00 | 19.46 | 27.71 | 20 | -3.0 | 40.60 | 36.53 | 60.93 |
| 20 | -9.0 | 29.00 | 26.87 | 38.27 | 20 | -15.0 | 44.40 | 39.95 | 66.64 |
| 20 | -9.0 | 27.00 | 25.02 | 35.63 | 20 | -16.7 | 35.40 | 31.85 | 53.13 |
| 20 | -9.0 | 28.20 | 26.13 | 37.21 | 20 | -15.4 | 30.20 | 27.17 | 45.33 |
| 20 | -7.0 | 26.80 | 24.83 | 35.37 | 45 | -0.4 | 40.80 | 36.71 | 61.24 |
| 20 | -6.8 | 13.40 | 12.42 | 17.68 | 45 | -7.8 | 26.00 | 23.39 | 39.02 |
| 45 | -3.1 | 15.00 | 13.90 | 19.79 | 45 | -9.0 | 26.80 | 24.11 | 40.22 |
| 45 | -8.9 | 13.20 | 12.23 | 17.42 | 45 | -4.0 | 26.00 | 23.39 | 39.02 |
| 45 | -11.0 | 15.00 | 13.90 | 19.79 | 45 | -6.6 | 36.00 | 32.39 | 54.03 |
| 45 | -10.0 | 14.40 | 13.34 | 19.00 | 45 | 1.7 | 26.20 | 23.57 | 39.32 |
| 45 | -13.0 | 13.60 | 12.60 | 17.95 | 45 | -13.7 | 26.20 | 23.57 | 39.32 |
| 45 | -14.0 | 12.40 | 11.49 | 16.36 | 45 | -15.0 | 27.20 | 24.47 | 40.82 |
| 60 | -7.3 | 13.00 | 12.13 | 16.83 | 60 | -10.0 | 18.00 | 16.40 | 26.39 |
| 60 | -2.9 | 14.20 | 13.25 | 18.39 | 60 | -4.6 | 18.80 | 17.13 | 27.56 |
| 60 | -2.9 | 13.20 | 12.32 | 17.09 | 60 | -4.0 | 18.80 | 17.13 | 27.56 |
| 60 | -8.0 | 13.40 | 12.50 | 17.35 | 60 | -5.0 | 20.80 | 18.95 | 30.49 |
| 60 | -12.0 | 12.60 | 11.76 | 16.32 | 60 | -10.9 | 21.20 | 19.32 | 31.08 |
| 60 | -8.0 | 13.40 | 12.50 | 17.35 | 60 | -11.3 | 20.20 | 18.41 | 29.61 |
| 60 | -8.0 | 13.20 | 12.32 | 17.09 | 60 | -10.0 | 21.80 | 19.86 | 31.96 |
| | | | | | 60 | -11.0 | 19.40 | 17.68 | 28.44 |
| | | | | | | | | | |
| Nominal Speed (mph) | Section 3 Longitudinal Strain (μ-strain) | | | | Nominal Speed (mph) | Section 4 Longitudinal Strain (μ-strain) | | | |
| | Offset (in) | Uncorrected | 20 ºC | 30 ºC | | Offset (in) | Uncorrected | 20 ºC | 30 ºC |
| | | | | | 20 | -6.7 | 18.80 | 16.74 | 30.13 |
| | | | | | 20 | 0.0 | 21.00 | 18.70 | 33.66 |
| | | | | | 20 | -13.4 | 16.20 | 14.43 | 25.96 |
| | | | | | 20 | -11.7 | 16.20 | 14.43 | 25.96 |
| | | | | | 20 | -9.0 | 18.20 | 16.21 | 29.17 |
| | | | | | 20 | -6.1 | 24.20 | 21.55 | 38.79 |
| | | | | | 20 | -7.8 | 24.60 | 21.91 | 39.43 |
| | | | | | 20 | 0.0 | 22.80 | 20.31 | 36.54 |
| | | | | | 20 | -12.2 | 21.00 | 18.70 | 33.66 |

Table B-15 - *Continued*

| Nominal Speed (mph) | Section 3 | | | | Nominal Speed (mph) | Section 4 | | | |
|---|---|---|---|---|---|---|---|---|---|
| | Longitudinal Strain (μ-strain) | | | | | Longitudinal Strain (μ-strain) | | | |
| | Offset (in) | Uncorrected | 20 ºC | 30 ºC | | Offset (in) | Uncorrected | 20 ºC | 30 ºC |
| | | | | | 45 | -15.0 | 9.00 | 8.02 | 14.42 |
| | | | | | 45 | -9.0 | 9.40 | 8.37 | 15.07 |
| | | | | | 45 | -12.4 | 8.80 | 7.84 | 14.10 |
| | | | | | 45 | -10.1 | 12.80 | 11.40 | 20.52 |
| | | | | | 45 | -7.0 | 12.20 | 10.87 | 19.55 |
| | | | | | 45 | -15.0 | 12.20 | 10.87 | 19.55 |
| | | | | | 45 | -9.0 | 12.20 | 10.87 | 19.55 |
| | | | | | 45 | -11.2 | 11.20 | 9.98 | 17.95 |
| | | | | | 60 | -4.0 | 5.60 | 5.04 | 8.57 |
| | | | | | 60 | -14.7 | 4.00 | 3.60 | 6.12 |
| | | | | | 60 | -10.7 | 5.40 | 4.86 | 8.27 |
| | | | | | 60 | -18.0 | 3.80 | 3.42 | 5.82 |
| | | | | | 60 | -4.0 | 11.40 | 10.27 | 17.46 |
| | | | | | 60 | -18.0 | 9.20 | 8.28 | 14.09 |

Table B-17: Longitudinal Strains – 10/05/2007

| Nominal Speed (mph) | Section 1 Longitudinal Strain (μ-strain) | | | | Nominal Speed (mph) | Section 2 Longitudinal Strain (μ-strain) | | | |
|---|---|---|---|---|---|---|---|---|---|
| | Offset (in) | Uncorrected | 20 ºC | 30 ºC | | Offset (in) | Uncorrected | 20 ºC | 30 ºC |
| 20 | -1.8 | 33.60 | 29.90 | 42.59 | 20 | 6.3 | 46.20 | 40.10 | 66.89 |
| 20 | 3.1 | 30.80 | 27.41 | 39.04 | 20 | 8.2 | 55.00 | 47.74 | 79.63 |
| 20 | 5.6 | 32.20 | 28.66 | 40.82 | 20 | 10.6 | 40.20 | 34.89 | 58.20 |
| 20 | 7.7 | 30.40 | 27.06 | 38.54 | 20 | 10.4 | 41.80 | 36.28 | 60.52 |
| 45 | 1.4 | 12.60 | 11.21 | 15.97 | 20 | 6.4 | 43.60 | 37.84 | 63.12 |
| 45 | 6.1 | 14.60 | 12.99 | 18.51 | 20 | 0.5 | 47.20 | 40.97 | 68.34 |
| 45 | 8.1 | 19.40 | 17.27 | 24.59 | 20 | 2.3 | 60.60 | 52.60 | 87.74 |
| 45 | 3.6 | 16.20 | 14.42 | 20.54 | 20 | 4.9 | 48.80 | 42.36 | 70.65 |
| 60 | 7.1 | 16.40 | 14.78 | 20.51 | 20 | 4.6 | 47.60 | 41.31 | 68.91 |
| 60 | 4.1 | 13.60 | 12.26 | 17.01 | 20 | 0.6 | 50.20 | 43.57 | 72.68 |
| 60 | 5.0 | 14.00 | 12.62 | 17.51 | 45 | 9.0 | 20.00 | 17.36 | 28.96 |
| 60 | 2.6 | 13.60 | 12.26 | 17.01 | 45 | 6.2 | 28.60 | 24.82 | 41.41 |
| | | | | | 45 | -1.8 | 30.80 | 26.73 | 44.59 |
| | | | | | 45 | -0.3 | 29.20 | 25.34 | 42.28 |
| | | | | | 45 | 0.3 | 26.60 | 23.09 | 38.51 |
| | | | | | 45 | -7.7 | 25.20 | 21.87 | 36.48 |
| | | | | | 45 | -5.9 | 22.00 | 19.10 | 31.85 |
| | | | | | 45 | -2.4 | 26.60 | 23.09 | 38.51 |
| | | | | | 60 | 2.8 | 14.40 | 12.70 | 20.43 |
| | | | | | 60 | -1.2 | 16.80 | 14.82 | 23.84 |
| | | | | | 60 | -5.1 | 17.60 | 15.52 | 24.97 |
| | | | | | 60 | -2.8 | 19.00 | 16.76 | 26.96 |
| | | | | | 60 | -6.8 | 18.80 | 16.58 | 26.67 |
| | | | | | 60 | -6.7 | 19.40 | 17.11 | 27.53 |
| | | | | | 60 | 1.6 | 18.80 | 16.58 | 26.67 |
| | | | | | 60 | -10.9 | 17.80 | 15.70 | 25.26 |

| Nominal Speed (mph) | Section 3 Longitudinal Strain (μ-strain) | | | | Nominal Speed (mph) | Section 4 Longitudinal Strain (μ-strain) | | | |
|---|---|---|---|---|---|---|---|---|---|
| | Offset (in) | Uncorrected | 20 ºC | 30 ºC | | Offset (in) | Uncorrected | 20 ºC | 30 ºC |
| | | | | | 20 | -0.6 | 24.60 | 22.84 | 41.11 |
| | | | | | 20 | 0.3 | 18.80 | 17.46 | 31.42 |
| | | | | | 20 | -7.2 | 23.40 | 21.73 | 39.10 |
| | | | | | 20 | -7.5 | 24.60 | 22.84 | 41.11 |
| | | | | | 20 | -1.8 | 30.20 | 28.04 | 50.46 |
| | | | | | 20 | 0.9 | 23.00 | 21.36 | 38.43 |
| | | | | | 20 | -5.8 | 29.40 | 27.30 | 49.13 |

Table B-17 - *Continued*

| Nominal Speed (mph) | Section 3 | | | | Nominal Speed (mph) | Section 4 | | | |
|---|---|---|---|---|---|---|---|---|---|
| | Longitudinal Strain (μ-strain) | | | | | Longitudinal Strain (μ-strain) | | | |
| | Offset (in) | Uncorrected | 20 ºC | 30 ºC | | Offset (in) | Uncorrected | 20 ºC | 30 ºC |
| | | | | | 45 | -6.9 | 12.20 | 11.33 | 20.39 |
| | | | | | 45 | -2.9 | 13.20 | 12.26 | 22.06 |
| | | | | | 45 | -2.4 | 14.40 | 13.37 | 24.06 |
| | | | | | 45 | -2.9 | 15.00 | 13.93 | 25.07 |
| | | | | | 60 | -0.1 | 9.20 | 8.60 | 14.63 |
| | | | | | 60 | -6.2 | 6.80 | 6.36 | 10.81 |
| | | | | | 60 | -8.0 | 7.80 | 7.30 | 12.40 |
| | | | | | 60 | 1.7 | 13.40 | 12.53 | 21.31 |
| | | | | | 60 | -6.4 | 10.80 | 10.10 | 17.18 |
| | | | | | 60 | -8.8 | 11.60 | 10.85 | 18.45 |

Table B-18: Transverse Strains – 07/14/2005

| Nominal Speed (mph) | Section 1 Transverse Strain (μ-strain) | | | | Nominal Speed (mph) | Section 2 Transverse Strain (μ-strain) | | | |
|---|---|---|---|---|---|---|---|---|---|
| | Offset (in) | Uncorrected | 20 ºC | 30 ºC | | Offset (in) | Uncorrected | 20 ºC | 30 ºC |
| 20 | 0.3 | 60.80 | 43.11 | 58.18 | 20 | 6.0 | 137.80 | 82.94 | 128.35 |
| 20 | 3.4 | 61.20 | 43.39 | 58.57 | 20 | 10.5 | 74.00 | 44.54 | 68.93 |
| 20 | 2.2 | 59.40 | 42.12 | 56.84 | 20 | 3.0 | 135.00 | 81.26 | 125.75 |
| 20 | 3.8 | 61.20 | 43.39 | 58.57 | 20 | 4.0 | 148.80 | 89.57 | 138.60 |
| 20 | -5.2 | 97.80 | 69.35 | 93.59 | 20 | -3.8 | 125.80 | 75.72 | 117.18 |
| 20 | -2.6 | 86.80 | 61.55 | 83.07 | 20 | -7.4 | 122.00 | 73.43 | 113.64 |
| 20 | -3.8 | 91.80 | 65.09 | 87.85 | 20 | 0.2 | 126.40 | 76.08 | 117.74 |
| 20 | -7.4 | 90.60 | 64.24 | 86.70 | 45 | 4.0 | 135.00 | 81.26 | 125.75 |
| 20 | -5.7 | 91.20 | 64.67 | 87.28 | 45 | 5.0 | 158.40 | 95.34 | 147.54 |
| 20 | -3.8 | 87.20 | 61.83 | 83.45 | 45 | 7.5 | 137.60 | 82.82 | 128.17 |
| 20 | -3.7 | 86.00 | 60.98 | 82.30 | 45 | 6.5 | 140.20 | 84.39 | 130.59 |
| 20 | -8.0 | 87.00 | 61.69 | 83.26 | 45 | 3.0 | 91.80 | 55.26 | 85.51 |
| 20 | -6.0 | 88.20 | 62.54 | 84.41 | 45 | -2.0 | 122.00 | 73.43 | 113.64 |
| 20 | -4.0 | 85.80 | 60.84 | 82.11 | 45 | -1.0 | 137.80 | 82.94 | 128.35 |
| 20 | -1.5 | 89.40 | 63.39 | 85.55 | 45 | 1.0 | 129.20 | 77.77 | 120.34 |
| 45 | 0.1 | 90.00 | 63.82 | 86.13 | 45 | -1.7 | 122.60 | 73.79 | 114.20 |
| 45 | -5.2 | 64.80 | 45.95 | 62.01 | 45 | -4.1 | 69.40 | 41.77 | 64.64 |
| 45 | 0.0 | 55.40 | 39.28 | 53.02 | 60 | 3.5 | 76.20 | 46.66 | 70.49 |
| 45 | -0.7 | 78.40 | 55.59 | 75.03 | 60 | 9.0 | 47.20 | 28.90 | 43.67 |
| 45 | -3.4 | 80.40 | 57.01 | 76.94 | 60 | 3.5 | 79.00 | 48.37 | 73.08 |
| 45 | -5.4 | 62.80 | 44.53 | 60.10 | 60 | 4.0 | 79.40 | 48.62 | 73.45 |
| 45 | 0.0 | 51.00 | 36.16 | 48.81 | 60 | 8.0 | 68.60 | 42.01 | 63.46 |
| 45 | -5.5 | 57.20 | 40.56 | 54.74 | 60 | -6.3 | 87.20 | 53.39 | 80.67 |
| 60 | -1.1 | 56.20 | 40.55 | 53.73 | 60 | 0.8 | 77.60 | 47.52 | 71.79 |
| 60 | 0.3 | 44.00 | 31.75 | 42.07 | 60 | -2.5 | 88.00 | 53.88 | 81.41 |
| 60 | 3.1 | 41.00 | 29.59 | 39.20 | 60 | -5.3 | 85.40 | 52.29 | 79.01 |
| 60 | 1.4 | 49.60 | 35.79 | 47.42 | 60 | -0.2 | 79.20 | 48.50 | 73.27 |
| 60 | 0.7 | 53.60 | 38.68 | 51.24 | | | | | |
| 60 | 0.9 | 44.00 | 31.75 | 42.07 | | | | | |
| 60 | 1.3 | 39.20 | 28.29 | 37.48 | | | | | |
| 60 | 1.5 | 46.40 | 33.48 | 44.36 | | | | | |
| 60 | 1.0 | 48.00 | 34.64 | 45.89 | | | | | |
| 60 | 1.0 | 42.60 | 30.74 | 40.73 | | | | | |
| 60 | 1.0 | 37.20 | 26.84 | 35.57 | | | | | |

Table B-18 - *Continued*

| Nominal Speed (mph) | Section 3 Transverse Strain (μ-strain) | | | | Nominal Speed (mph) | Section 4 Transverse Strain (μ-strain) | | | |
|---|---|---|---|---|---|---|---|---|---|
| | Offset (in) | Uncorrected | 20 ºC | 30 ºC | | Offset (in) | Uncorrected | 20 ºC | 30 ºC |
| 20 | 6.9 | 67.80 | 36.83 | 54.96 | 20 | -1.1 | 394.40 | 198.47 | 332.62 |
| 20 | 0.7 | 61.80 | 33.57 | 50.10 | 20 | 5.0 | 85.00 | 42.77 | 71.68 |
| 20 | 6.7 | 34.20 | 18.58 | 27.72 | 20 | -4.3 | 94.40 | 47.50 | 79.61 |
| 20 | 4.8 | 35.80 | 19.45 | 29.02 | 20 | -2.1 | 88.60 | 44.59 | 74.72 |
| 20 | 0.2 | 39.40 | 21.40 | 31.94 | 20 | -4.2 | 92.20 | 46.40 | 77.76 |
| 20 | 0.9 | 44.40 | 24.12 | 35.99 | 20 | -1.0 | 88.00 | 44.28 | 74.21 |
| 20 | 3.8 | 41.80 | 22.71 | 33.88 | 45 | 3.4 | 81.00 | 40.76 | 68.31 |
| 20 | 5.3 | 41.00 | 22.27 | 33.24 | 45 | -1.0 | 55.40 | 27.88 | 46.72 |
| 20 | 0.1 | 61.00 | 33.13 | 49.45 | 45 | -3.7 | 291.60 | 146.74 | 245.92 |
| 20 | 5.1 | 79.80 | 43.35 | 64.69 | 45 | -2.9 | 342.60 | 172.40 | 288.93 |
| 20 | -4.1 | 46.00 | 24.99 | 37.29 | 45 | -7.0 | 54.80 | 27.58 | 46.22 |
| 45 | 2.0 | 67.40 | 36.61 | 54.64 | 45 | -4.3 | 98.40 | 49.52 | 82.99 |
| 45 | 2.0 | 44.40 | 24.12 | 35.99 | 45 | -3.0 | 94.40 | 47.50 | 79.61 |
| 45 | 2.9 | 36.40 | 19.77 | 29.51 | 45 | -7.0 | 69.40 | 34.92 | 58.53 |
| 45 | 1.9 | 39.40 | 21.40 | 31.94 | 45 | -2.8 | 66.40 | 33.41 | 56.00 |
| 45 | 1.9 | 27.60 | 14.99 | 22.37 | 45 | -5.8 | 58.00 | 29.19 | 48.91 |
| 45 | 4.6 | 41.00 | 22.27 | 33.24 | 60 | -2.9 | 45.20 | 24.51 | 39.36 |
| 45 | 1.2 | 31.40 | 17.06 | 25.45 | 60 | -1.0 | 48.20 | 26.14 | 41.97 |
| 45 | 0.6 | 29.00 | 15.75 | 23.51 | 60 | 0.0 | 45.80 | 24.84 | 39.88 |
| 45 | -0.6 | 33.40 | 18.14 | 27.08 | 60 | -5.7 | 66.20 | 35.90 | 57.64 |
| 45 | 1.1 | 70.60 | 38.35 | 57.23 | 60 | -6.7 | 47.80 | 25.92 | 41.62 |
| 45 | 0.2 | 45.20 | 24.55 | 36.64 | 60 | -7.0 | 43.00 | 23.32 | 37.44 |
| 45 | -1.1 | 44.40 | 24.12 | 35.99 | 60 | -6.0 | 70.60 | 38.29 | 61.47 |
| 60 | 3.9 | 48.40 | 26.43 | 38.73 | 60 | -5.3 | 62.20 | 33.73 | 54.16 |
| 60 | -0.8 | 41.40 | 22.61 | 33.13 | 60 | -6.4 | 57.80 | 31.35 | 50.33 |
| 60 | -1.1 | 40.80 | 22.28 | 32.65 | 60 | -7.0 | 48.40 | 26.25 | 42.14 |
| 60 | -1.2 | 33.60 | 18.35 | 26.89 | 60 | -6.0 | 54.80 | 29.72 | 47.72 |
| 60 | 2.9 | 34.60 | 18.90 | 27.69 | | | | | |
| 60 | -0.5 | 28.80 | 15.73 | 23.05 | | | | | |
| 60 | -1.4 | 28.60 | 15.62 | 22.89 | | | | | |
| 60 | -1.5 | 25.00 | 13.65 | 20.01 | | | | | |
| 60 | 2.6 | 21.60 | 11.80 | 17.29 | | | | | |
| 60 | 2.8 | 28.00 | 15.29 | 22.41 | | | | | |
| 60 | 1.9 | 33.60 | 18.35 | 26.89 | | | | | |
| 60 | -3.1 | 35.20 | 19.22 | 28.17 | | | | | |
| 60 | -3.9 | 30.00 | 16.38 | 24.01 | | | | | |
| 60 | 2.60 | 52.80 | 28.84 | 42.25 | | | | | |
| 60 | -3.33 | 31.60 | 17.26 | 25.29 | | | | | |

Table B-19: Transverse Strains – 09/29/2005

| Nominal Speed (mph) | Section 1 Transverse Strain (μ-strain) | | | | Nominal Speed (mph) | Section 2 Transverse Strain (μ-strain) | | | |
|---|---|---|---|---|---|---|---|---|---|
| | Offset (in) | Uncorrected | 20 ºC | 30 ºC | | Offset (in) | Uncorrected | 20 ºC | 30 ºC |
| 20 | 1.1 | 45.00 | 47.24 | 63.75 | 45 | -4.0 | 54.80 | 56.43 | 87.32 |
| 20 | -6.5 | 27.00 | 28.34 | 38.25 | 45 | -2.0 | 51.80 | 53.34 | 82.54 |
| 20 | -11.1 | 30.40 | 31.91 | 43.07 | 45 | 4.9 | 43.40 | 44.69 | 69.16 |
| 20 | -11.9 | 33.40 | 35.06 | 47.32 | 45 | -13.3 | 51.40 | 52.93 | 81.90 |
| 20 | -12.0 | 43.00 | 45.14 | 60.92 | 45 | -8.6 | 15.20 | 15.65 | 24.22 |
| 60 | -7.7 | 37.20 | 38.60 | 51.14 | 60 | -4.0 | 43.60 | 44.98 | 67.95 |
| 60 | -10.5 | 34.60 | 35.90 | 47.57 | 60 | -3.0 | 24.80 | 25.58 | 38.65 |
| 60 | -7.4 | 35.20 | 36.53 | 48.39 | 60 | -3.0 | 26.60 | 27.44 | 41.46 |
| 60 | -8.3 | 36.20 | 37.56 | 49.77 | 60 | -3.0 | 17.40 | 17.95 | 27.12 |
| 60 | -14.5 | 30.40 | 31.55 | 41.80 | 60 | -3.0 | 44.80 | 46.21 | 69.82 |
| 60 | -14.9 | 31.20 | 32.38 | 42.90 | 60 | -3.6 | 22.40 | 23.11 | 34.91 |
| 60 | -17.5 | 19.40 | 20.13 | 26.67 | 60 | -3.4 | 22.60 | 23.31 | 35.22 |
| 60 | -14.2 | 15.20 | 15.77 | 20.90 | 60 | -3.6 | 16.40 | 16.92 | 25.56 |
| 60 | -14.9 | 20.80 | 21.58 | 28.60 | 60 | -3.4 | 27.40 | 28.26 | 42.70 |
| 60 | -19.1 | 30.80 | 31.96 | 42.35 | 60 | -12.2 | 37.00 | 38.17 | 57.66 |
| 60 | -18.4 | 30.60 | 31.75 | 42.07 | | | | | |
| 60 | -20.5 | 19.60 | 20.34 | 26.95 | | | | | |
| 60 | -16.6 | 14.40 | 14.94 | 19.80 | | | | | |
| 60 | -16.7 | 20.20 | 20.96 | 27.77 | | | | | |
| 60 | -19.9 | 32.40 | 33.62 | 44.55 | | | | | |
| 60 | -19.0 | 29.40 | 30.51 | 40.42 | | | | | |
| 60 | -21.0 | 19.00 | 19.72 | 26.12 | | | | | |
| 60 | -17.0 | 16.00 | 16.60 | 22.00 | | | | | |
| 60 | -17.0 | 21.20 | 22.00 | 29.15 | | | | | |

| Nominal Speed (mph) | Section 3 Transverse Strain (μ-strain) | | | | Nominal Speed (mph) | Section 4 Transverse Strain (μ-strain) | | | |
|---|---|---|---|---|---|---|---|---|---|
| | Offset (in) | Uncorrected | 20 ºC | 30 ºC | | Offset (in) | Uncorrected | 20 ºC | 30 ºC |
| 20 | 3.9 | 35.00 | 33.70 | 50.30 | 20 | 2.5 | 60.80 | 56.52 | 94.73 |
| 20 | -3.2 | 28.80 | 27.73 | 41.39 | 20 | 2.8 | 52.20 | 48.53 | 81.33 |
| 20 | 3.9 | 41.60 | 40.06 | 59.78 | 20 | 2.7 | 52.60 | 48.90 | 81.95 |
| 20 | 3.9 | 27.40 | 26.38 | 39.38 | 20 | 1.4 | 45.20 | 42.02 | 70.42 |
| 20 | 11.0 | 38.40 | 36.98 | 55.18 | 20 | 9.5 | 62.40 | 58.01 | 97.22 |
| 20 | 3.6 | 47.20 | 45.45 | 67.83 | 20 | -8.5 | 47.20 | 43.88 | 73.54 |
| 20 | -3.5 | 49.20 | 47.38 | 70.70 | 20 | -5.2 | 29.40 | 27.33 | 45.80 |
| 20 | 3.6 | 43.40 | 41.79 | 62.37 | 20 | -6.3 | 69.00 | 64.14 | 107.50 |
| 20 | 3.7 | 51.20 | 49.30 | 73.58 | 20 | -10.6 | 36.20 | 33.65 | 56.40 |

Table B-19 - *Continued*

| Nominal Speed (mph) | Section 3 | | | | Nominal Speed (mph) | Section 4 | | | |
|---|---|---|---|---|---|---|---|---|---|
| | Transverse Strain (μ-strain) | | | | | Transverse Strain (μ-strain) | | | |
| | Offset (in) | Uncorrected | 20 ºC | 30 ºC | | Offset (in) | Uncorrected | 20 ºC | 30 ºC |
| 20 | 2.3 | 19.20 | 18.49 | 27.59 | 45 | 2.2 | 34.40 | 31.98 | 53.59 |
| 20 | 10.2 | 25.60 | 24.65 | 36.79 | 45 | -9.3 | 7.60 | 7.07 | 11.84 |
| 20 | 1.2 | 24.20 | 23.30 | 34.78 | 45 | -8.2 | 27.60 | 25.66 | 43.00 |
| 20 | -5.8 | 13.80 | 13.29 | 19.83 | 45 | -9.6 | 33.60 | 31.24 | 52.35 |
| 20 | 1.2 | 30.80 | 29.66 | 44.26 | 60 | 4.2 | 34.60 | 32.25 | 51.78 |
| 20 | 10.1 | 30.40 | 29.27 | 43.69 | 60 | 2.5 | 31.60 | 29.46 | 47.29 |
| 45 | -5.1 | 25.20 | 24.27 | 36.21 | 60 | 4.6 | 34.40 | 32.07 | 51.49 |
| 45 | 1.9 | 17.80 | 17.14 | 25.58 | 60 | 3.7 | 33.60 | 31.32 | 50.29 |
| 45 | 7.1 | 18.20 | 17.53 | 26.15 | 60 | 4.0 | 30.40 | 28.34 | 45.50 |
| 45 | -3.0 | 20.20 | 19.45 | 29.03 | 60 | -8.6 | 28.20 | 26.29 | 42.21 |
| 45 | 2.5 | 32.60 | 31.39 | 46.85 | 60 | -8.5 | 28.80 | 26.85 | 43.10 |
| 45 | -5.2 | 31.40 | 30.24 | 45.12 | | | | | |
| 45 | 1.7 | 32.00 | 30.81 | 45.99 | | | | | |
| 45 | 7.2 | 31.40 | 30.24 | 45.12 | | | | | |
| 45 | -3.0 | 32.00 | 30.81 | 45.99 | | | | | |
| 45 | 4.5 | 17.40 | 16.76 | 25.00 | | | | | |
| 45 | -5.8 | 18.40 | 17.72 | 26.44 | | | | | |
| 45 | 0.3 | 16.20 | 15.60 | 23.28 | | | | | |
| 45 | -3.0 | 17.80 | 17.14 | 25.58 | | | | | |
| 45 | 4.8 | 9.20 | 8.86 | 13.22 | | | | | |
| 60 | -8.9 | 12.00 | 11.65 | 17.07 | | | | | |
| 60 | 3.1 | 16.20 | 15.72 | 23.04 | | | | | |
| 60 | -1.1 | 26.80 | 26.01 | 38.12 | | | | | |
| 60 | 1.0 | 22.60 | 21.93 | 32.14 | | | | | |
| 60 | -8.7 | 28.80 | 27.95 | 40.96 | | | | | |
| 60 | 3.15 | 30.00 | 29.12 | 42.67 | | | | | |
| 60 | -1.30 | 27.00 | 26.21 | 38.40 | | | | | |
| 60 | 1.00 | 28.40 | 27.56 | 40.39 | | | | | |
| 60 | -7.33 | 13.40 | 13.01 | 19.06 | | | | | |
| 60 | -2.67 | 12.80 | 12.42 | 18.20 | | | | | |
| 60 | 3.83 | 14.80 | 14.36 | 21.05 | | | | | |
| 60 | -2.67 | 18.80 | 18.25 | 26.74 | | | | | |
| 60 | 1.00 | 17.60 | 17.08 | 25.03 | | | | | |
| 60 | -7.13 | 3.80 | 3.69 | 5.40 | | | | | |
| 60 | -2.87 | 3.00 | 2.91 | 4.27 | | | | | |
| 60 | 3.93 | 5.80 | 5.63 | 8.25 | | | | | |
| 60 | -2.87 | 15.20 | 14.75 | 21.62 | | | | | |

Table B-20: Transverse Strains – 04/13/2006

| Nominal Speed (mph) | Section 1 Transverse Strain (μ-strain) | | | | Nominal Speed (mph) | Section 2 Transverse Strain (μ-strain) | | | |
|---|---|---|---|---|---|---|---|---|---|
| | Offset (in) | Uncorrected | 20 ºC | 30 ºC | | Offset (in) | Uncorrected | 20 ºC | 30 ºC |
| 20 | -7.8 | 41.80 | 43.23 | 58.34 | 20 | -14.9 | 62.00 | 49.28 | 76.26 |
| 20 | 1.1 | 19.00 | 19.65 | 26.52 | 20 | 3.0 | 57.80 | 45.94 | 71.10 |
| 20 | -0.7 | 21.40 | 22.13 | 29.87 | 20 | 0.0 | 61.60 | 48.96 | 75.77 |
| 20 | -3.9 | 44.80 | 46.33 | 62.53 | 20 | -5.2 | 58.40 | 46.42 | 71.83 |
| 20 | -15.2 | 21.60 | 22.34 | 30.15 | 20 | -5.2 | 69.60 | 55.32 | 85.61 |
| 20 | -7.9 | 36.60 | 37.85 | 51.08 | 20 | -8.2 | 66.00 | 52.46 | 81.18 |
| 20 | -11.5 | 26.20 | 27.09 | 36.57 | 45 | 1.0 | 45.20 | 35.93 | 55.60 |
| 20 | -19.2 | 21.40 | 22.13 | 29.87 | 45 | -4.0 | 50.60 | 40.22 | 62.24 |
| 20 | -11.1 | 41.00 | 42.40 | 57.22 | 45 | -2.0 | 47.60 | 37.84 | 58.55 |
| 20 | -16.1 | 34.40 | 35.57 | 48.01 | 45 | 4.9 | 40.40 | 32.11 | 49.69 |
| 20 | -14.2 | 38.00 | 39.30 | 53.04 | 45 | 5.6 | 21.00 | 16.69 | 25.83 |
| 20 | -11.9 | 46.20 | 47.78 | 64.48 | 45 | -11.3 | 43.60 | 34.66 | 53.63 |
| 20 | -16.9 | 35.00 | 36.19 | 48.85 | 45 | -8.6 | 46.60 | 37.04 | 57.32 |
| 20 | -14.9 | 44.20 | 45.71 | 61.69 | 60 | -4.0 | 43.60 | 35.17 | 53.14 |
| 45 | -2.7 | 31.60 | 32.68 | 44.10 | 60 | -3.0 | 43.80 | 35.33 | 53.38 |
| 45 | -8.3 | 29.00 | 29.99 | 40.48 | 60 | -3.0 | 47.20 | 38.08 | 57.53 |
| 45 | -9.7 | 28.20 | 29.16 | 39.36 | 60 | -3.0 | 40.80 | 32.91 | 49.73 |
| 45 | -10.8 | 25.20 | 26.06 | 35.17 | 60 | -3.0 | 44.20 | 35.66 | 53.87 |
| 45 | -9.9 | 29.60 | 30.61 | 41.31 | 60 | -12.3 | 43.60 | 35.17 | 53.14 |
| 45 | -16.9 | 20.40 | 21.10 | 28.47 | 60 | -11.2 | 43.20 | 34.85 | 52.65 |
| 45 | -18.2 | 11.40 | 11.79 | 15.91 | 60 | -12.3 | 40.20 | 32.43 | 49.00 |
| 45 | -13.4 | 31.80 | 32.89 | 44.38 | 60 | -11.2 | 43.40 | 35.01 | 52.90 |
| 45 | -20.4 | 24.20 | 25.03 | 33.78 | | | | | |
| 45 | -22.2 | 12.60 | 13.03 | 17.59 | | | | | |
| 45 | -14.0 | 33.00 | 34.13 | 46.06 | | | | | |
| 45 | -17.0 | 28.20 | 29.16 | 39.36 | | | | | |
| 45 | -21.0 | 27.00 | 27.92 | 37.68 | | | | | |
| 45 | -22.9 | 13.40 | 13.86 | 18.70 | | | | | |
| 45 | -19.9 | 24.00 | 24.82 | 33.50 | | | | | |
| 60 | -6.9 | 29.00 | 29.96 | 39.70 | | | | | |
| 60 | -7.7 | 24.00 | 24.80 | 32.86 | | | | | |
| 60 | -10.5 | 17.80 | 18.39 | 24.37 | | | | | |
| 60 | -7.4 | 21.80 | 22.53 | 29.84 | | | | | |
| 60 | -8.3 | 25.60 | 26.45 | 35.05 | | | | | |
| 60 | -14.5 | 22.60 | 23.35 | 30.94 | | | | | |
| 60 | -17.5 | 14.00 | 14.47 | 19.17 | | | | | |
| 60 | -14.2 | 19.60 | 20.25 | 26.83 | | | | | |

Table B-20 - *Continued*

| Nominal Speed (mph) | Section 1 Transverse Strain (μ-strain) | | | | Nominal Speed (mph) | Section 2 Transverse Strain (μ-strain) | | | |
|---|---|---|---|---|---|---|---|---|---|
| | Offset (in) | Uncorrected | 20 ºC | 30 ºC | | Offset (in) | Uncorrected | 20 ºC | 30 ºC |
| 60 | -16.6 | 22.40 | 23.15 | 30.67 | | | | | |
| 60 | -16.7 | 23.60 | 24.39 | 32.31 | | | | | |
| 60 | -19.9 | 26.00 | 26.87 | 35.59 | | | | | |
| 60 | -19.0 | 19.00 | 19.63 | 26.01 | | | | | |
| 60 | -21.0 | 17.00 | 17.57 | 23.27 | | | | | |
| 60 | -17.0 | 25.40 | 26.25 | 34.77 | | | | | |

| Nominal Speed (mph) | Section 3 Transverse Strain (μ-strain) | | | | Nominal Speed (mph) | Section 4 Transverse Strain (μ-strain) | | | |
|---|---|---|---|---|---|---|---|---|---|
| | Offset (in) | Uncorrected | 20 ºC | 30 ºC | | Offset (in) | Uncorrected | 20 ºC | 30 ºC |
| | | | | | 20 | 2.5 | 32.40 | 18.25 | 30.59 |
| | | | | | 20 | 2.7 | 43.60 | 24.56 | 41.16 |
| | | | | | 20 | 1.4 | 42.00 | 23.66 | 39.65 |
| | | | | | 20 | 9.5 | 31.00 | 17.46 | 29.27 |
| | | | | | 20 | -8.5 | 39.40 | 22.20 | 37.20 |
| | | | | | 45 | -0.2 | 33.20 | 18.70 | 31.35 |
| | | | | | 45 | 0.7 | 31.00 | 17.46 | 29.27 |
| | | | | | 45 | 2.2 | 31.80 | 17.91 | 30.02 |
| | | | | | 60 | 4.2 | 22.40 | 13.28 | 21.32 |
| | | | | | 60 | 2.5 | 24.00 | 14.23 | 22.85 |
| | | | | | 60 | 3.7 | 23.00 | 13.64 | 21.89 |
| | | | | | 60 | 4.0 | 23.40 | 13.87 | 22.28 |

Table B-21: Transverse Strains – 08/01/2006

| Nominal Speed (mph) | Section 1 Transverse Strain (μ-strain) | | | | Nominal Speed (mph) | Section 2 Transverse Strain (μ-strain) | | | |
|---|---|---|---|---|---|---|---|---|---|
| | Offset (in) | Uncorrected | 20 ºC | 30 ºC | | Offset (in) | Uncorrected | 20 ºC | 30 ºC |
| 20 | -5.7 | 81.60 | 52.38 | 70.70 | 20 | -1.0 | 148.60 | 80.61 | 124.75 |
| 20 | -3.7 | 71.00 | 45.58 | 61.52 | 20 | 6.0 | 134.20 | 72.80 | 112.66 |
| 20 | -4.6 | 81.00 | 52.00 | 70.18 | 20 | -6.0 | 145.00 | 78.66 | 121.73 |
| 20 | -4.5 | 81.60 | 52.38 | 70.70 | 20 | 3.0 | 178.00 | 96.56 | 149.43 |
| 20 | -11.1 | 77.20 | 49.56 | 66.89 | 20 | -0.6 | 172.20 | 93.42 | 144.56 |
| 20 | -9.1 | 87.00 | 55.85 | 75.38 | 20 | 6.6 | 1555.00 | 843.57 | 1305.41 |
| 20 | -9.8 | 83.80 | 53.80 | 72.61 | 20 | -5.4 | 154.80 | 83.98 | 129.95 |
| 20 | -9.5 | 96.00 | 61.63 | 83.18 | 20 | 3.2 | 159.20 | 86.36 | 133.65 |
| 20 | -7.3 | 91.20 | 58.55 | 79.02 | 20 | 3.3 | 167.80 | 91.03 | 140.87 |
| 20 | -6.5 | 106.00 | 68.05 | 91.84 | 20 | -8.7 | 130.80 | 70.96 | 109.81 |
| 20 | -9.0 | 92.80 | 59.57 | 80.40 | 20 | -1.9 | 199.80 | 108.39 | 167.73 |
| 20 | -7.0 | 88.80 | 57.01 | 76.94 | 45 | 0.0 | 120.80 | 65.53 | 101.41 |
| 20 | -7.0 | 97.80 | 62.78 | 84.74 | 45 | 4.0 | 103.40 | 56.09 | 86.80 |
| 20 | -6.0 | 106.80 | 68.56 | 92.53 | 45 | -3.0 | 121.20 | 65.75 | 101.75 |
| 45 | 0.0 | 51.20 | 32.87 | 44.36 | 45 | 2.0 | 112.80 | 61.19 | 94.69 |
| 45 | -6.9 | 55.40 | 35.56 | 48.00 | 45 | 0.2 | 120.80 | 65.53 | 101.41 |
| 45 | -4.8 | 53.80 | 34.54 | 46.61 | 45 | 4.0 | 114.40 | 62.06 | 96.04 |
| 45 | -9.6 | 56.60 | 36.33 | 49.04 | 45 | 2.0 | 107.20 | 58.15 | 89.99 |
| 45 | -1.3 | 57.80 | 37.10 | 50.08 | 45 | -4.9 | 141.20 | 76.60 | 118.54 |
| 45 | -7.8 | 24.40 | 15.66 | 21.14 | 45 | -2.0 | 133.80 | 72.58 | 112.32 |
| 45 | -12.7 | 33.60 | 21.57 | 29.11 | 45 | -5.7 | 138.60 | 75.19 | 116.35 |
| 45 | -10.4 | 42.40 | 27.22 | 36.74 | 45 | -4.0 | 138.40 | 75.08 | 116.19 |
| 45 | -7.9 | 45.80 | 29.40 | 39.68 | 60 | 4.0 | 84.00 | 45.95 | 69.42 |
| 45 | -13.0 | 27.80 | 17.85 | 24.09 | 60 | 1.0 | 94.40 | 51.63 | 78.01 |
| 45 | -12.1 | 37.20 | 23.88 | 32.23 | 60 | -1.0 | 109.60 | 59.95 | 90.57 |
| 45 | -9.2 | 53.80 | 34.54 | 46.61 | 60 | 1.0 | 92.60 | 50.65 | 76.52 |
| 45 | -12.4 | 34.20 | 21.95 | 29.63 | 60 | 1.2 | 112.60 | 61.59 | 93.05 |
| 45 | -9.7 | 52.80 | 33.90 | 45.75 | 60 | -0.6 | 108.20 | 59.18 | 89.42 |
| 45 | -13.9 | 27.40 | 17.59 | 23.74 | 60 | 1.4 | 101.80 | 55.68 | 84.13 |
| 45 | -9.0 | 52.40 | 33.64 | 45.40 | 60 | -0.9 | 113.20 | 61.92 | 93.55 |
| 45 | -12.0 | 35.20 | 22.60 | 30.50 | 60 | -3.9 | 110.80 | 60.60 | 91.56 |
| 45 | -10.0 | 51.20 | 32.87 | 44.36 | 60 | 5.3 | 81.80 | 44.74 | 67.60 |
| 60 | -6.7 | 57.80 | 38.38 | 50.86 | | | | | |
| 60 | -5.0 | 56.20 | 37.32 | 49.45 | | | | | |
| 60 | -8.6 | 52.80 | 35.06 | 46.46 | | | | | |
| 60 | -6.0 | 58.00 | 38.52 | 51.03 | | | | | |
| 60 | -2.8 | 56.60 | 37.59 | 49.80 | | | | | |

Table B-21 - *Continued*

| Nominal Speed (mph) | Section 1 | | | | Nominal Speed (mph) | Section 2 | | | |
|---|---|---|---|---|---|---|---|---|---|
| | Transverse Strain ($\mu$-strain) | | | | | Transverse Strain ($\mu$-strain) | | | |
| | Offset (in) | Uncorrected | 20 ºC | 30 ºC | | Offset (in) | Uncorrected | 20 ºC | 30 ºC |
| 60 | -10.3 | 44.40 | 29.48 | 39.07 | | | | | |
| 60 | -11.4 | 34.80 | 23.11 | 30.62 | | | | | |
| 60 | -7.2 | 54.20 | 35.99 | 47.69 | | | | | |
| 60 | -10.0 | 45.40 | 30.15 | 39.95 | | | | | |
| 60 | -11.0 | 36.80 | 24.44 | 32.38 | | | | | |
| 60 | -7.0 | 56.60 | 37.59 | 49.80 | | | | | |

| Nominal Speed (mph) | Section 3 | | | | Nominal Speed (mph) | Section 4 | | | |
|---|---|---|---|---|---|---|---|---|---|
| | Transverse Strain ($\mu$-strain) | | | | | Transverse Strain ($\mu$-strain) | | | |
| | Offset (in) | Uncorrected | 20 ºC | 30 ºC | | Offset (in) | Uncorrected | 20 ºC | 30 ºC |
| | | | | | 20 | 17.2 | 29.20 | 14.06 | 23.56 |
| | | | | | 20 | 13.4 | 74.40 | 35.83 | 60.04 |
| | | | | | 20 | 14.1 | 83.60 | 40.26 | 67.46 |
| | | | | | 20 | 6.3 | 86.20 | 41.51 | 69.56 |
| | | | | | 20 | 14.5 | 49.80 | 23.98 | 40.19 |
| | | | | | 20 | 15.2 | 89.00 | 42.86 | 71.82 |
| | | | | | 20 | 9.2 | 85.40 | 41.12 | 68.92 |
| | | | | | 45 | 15.0 | 45.20 | 21.76 | 36.48 |
| | | | | | 45 | 8.2 | 45.60 | 21.96 | 36.80 |
| | | | | | 45 | 10.0 | 53.40 | 25.71 | 43.09 |
| | | | | | 45 | 13.0 | 54.60 | 26.29 | 44.06 |
| | | | | | 45 | 6.2 | 58.40 | 28.12 | 47.13 |
| | | | | | 45 | 9.0 | 25.40 | 12.23 | 20.50 |
| | | | | | 45 | 5.5 | 19.80 | 9.53 | 15.98 |
| | | | | | 45 | 4.0 | 34.60 | 16.66 | 27.92 |
| | | | | | 60 | 15.1 | 41.00 | 21.47 | 34.47 |
| | | | | | 60 | 19.2 | 37.40 | 19.59 | 31.45 |
| | | | | | 60 | 12.1 | 42.40 | 22.21 | 35.65 |
| | | | | | 60 | 10.2 | 32.20 | 16.86 | 27.07 |
| | | | | | 60 | 16.5 | 24.00 | 12.57 | 20.18 |
| | | | | | 60 | 8.3 | 30.40 | 15.92 | 25.56 |

Table B-22: Transverse Strains – RWD - 08/01/2006

| Nominal Speed (mph) | Section 1 Transverse Strain (μ-strain) | | | | Nominal Speed (mph) | Section 2 Transverse Strain (μ-strain) | | | |
|---|---|---|---|---|---|---|---|---|---|
| | Offset (in) | Uncorrected | 20 ºC | 30 ºC | | Offset (in) | Uncorrected | 20 ºC | 30 ºC |
| 60 | -0.6 | 26.20 | 17.34 | 22.98 | 60 | 4.0 | 44.40 | 23.88 | 36.08 |
| 60 | -2.6 | 23.60 | 15.62 | 20.70 | 60 | 7.0 | 63.80 | 34.31 | 51.84 |
| 60 | -1.0 | 22.20 | 14.70 | 19.47 | 60 | 2.0 | 41.80 | 22.48 | 33.96 |
| 60 | -3.7 | 23.80 | 15.76 | 20.88 | 60 | 3.2 | 60.20 | 32.38 | 48.92 |
| 60 | -5.8 | 34.60 | 22.91 | 30.35 | 60 | 2.2 | 58.20 | 31.30 | 47.29 |
| 60 | -7.3 | 34.20 | 22.64 | 30.00 | 60 | 0.2 | 45.00 | 24.20 | 36.57 |
| 60 | -7.8 | 29.80 | 19.73 | 26.14 | 60 | 3.2 | 46.00 | 24.74 | 37.38 |
| 60 | -3.4 | 42.20 | 27.94 | 37.01 | 60 | -1.9 | 49.80 | 26.78 | 40.47 |
| 60 | -7.9 | 39.40 | 26.08 | 34.56 | 60 | -2.9 | 53.40 | 28.72 | 43.39 |
| 60 | -5.4 | 35.00 | 23.17 | 30.70 | | | | | |
| 60 | -3.0 | 41.20 | 27.28 | 36.14 | | | | | |
| 60 | -8.0 | 38.60 | 25.55 | 33.86 | | | | | |
| 60 | -5.0 | 35.40 | 23.44 | 31.05 | | | | | |
| 60 | -7.0 | 33.40 | 22.11 | 29.30 | | | | | |
| 60 | -7.0 | 27.80 | 18.40 | 24.38 | | | | | |

| Nominal Speed (mph) | Section 3 Transverse Strain (μ-strain) | | | | Nominal Speed (mph) | Section 4 Transverse Strain (μ-strain) | | | |
|---|---|---|---|---|---|---|---|---|---|
| | Offset (in) | Uncorrected | 20 ºC | 30 ºC | | Offset (in) | Uncorrected | 20 ºC | 30 ºC |
| | | | | | 60 | 7.4 | 26.60 | 13.93 | 22.37 |
| | | | | | 60 | 1.9 | 21.40 | 11.21 | 17.99 |
| | | | | | 60 | 9.9 | 27.00 | 14.14 | 22.70 |
| | | | | | 60 | 7.9 | 25.60 | 13.41 | 21.53 |
| | | | | | 60 | 5.4 | 26.80 | 14.04 | 22.53 |
| | | | | | 60 | -5.1 | 26.00 | 13.62 | 21.86 |
| | | | | | 60 | 2.9 | 26.00 | 13.62 | 21.86 |
| | | | | | 60 | 0.8 | 25.40 | 13.30 | 21.36 |
| | | | | | 60 | 0.9 | 26.60 | 13.93 | 22.37 |

Table B-23: Transverse Strains – 10/13/2006

| Nominal Speed (mph) | Section 1 Transverse Strain (μ-strain) | | | | Nominal Speed (mph) | Section 2 Transverse Strain (μ-strain) | | | |
|---|---|---|---|---|---|---|---|---|---|
| | Offset (in) | Uncorrected | 20 ºC | 30 ºC | | Offset (in) | Uncorrected | 20 ºC | 30 ºC |
| 20 | -4.1 | 22.80 | 29.83 | 40.27 | 20 | -4.0 | 28.80 | 42.40 | 65.61 |
| 20 | -2.1 | 23.00 | 30.10 | 40.62 | 20 | -1.0 | 20.80 | 30.62 | 47.39 |
| 20 | -6.4 | 20.40 | 26.69 | 36.03 | 20 | -3.0 | 22.00 | 32.39 | 50.12 |
| 20 | -1.6 | 21.00 | 27.48 | 37.09 | 20 | 2.0 | 30.00 | 44.17 | 68.35 |
| 20 | 2.7 | 19.60 | 25.65 | 34.61 | 20 | 1.0 | 29.60 | 43.58 | 67.43 |
| 20 | -10.3 | 14.20 | 18.58 | 25.08 | 20 | -3.0 | 32.00 | 47.11 | 72.90 |
| 20 | -13.2 | 9.00 | 11.78 | 15.89 | 20 | -0.4 | 30.80 | 45.34 | 70.17 |
| 20 | -6.8 | 18.20 | 23.81 | 32.14 | 20 | -2.8 | 33.00 | 48.58 | 75.18 |
| 20 | -10.9 | 15.80 | 20.67 | 27.90 | 20 | 2.4 | 32.80 | 48.29 | 74.72 |
| 20 | -8.9 | 20.20 | 26.43 | 35.67 | 20 | 2.0 | 32.80 | 48.29 | 74.72 |
| 20 | -15.6 | 10.20 | 13.35 | 18.01 | 20 | -4.5 | 31.60 | 46.52 | 71.99 |
| 20 | -4.4 | 23.40 | 30.62 | 41.32 | 20 | -3.7 | 30.40 | 44.75 | 69.26 |
| 20 | -5.7 | 21.40 | 28.00 | 37.79 | 20 | -7.9 | 32.00 | 47.11 | 72.90 |
| 20 | -11.0 | 18.20 | 23.81 | 32.14 | 20 | -1.8 | 29.80 | 43.87 | 67.89 |
| 20 | -9.0 | 19.60 | 25.65 | 34.61 | 20 | 0.5 | 32.60 | 47.99 | 74.27 |
| 20 | -16.0 | 10.40 | 13.61 | 18.37 | 45 | -2.0 | 14.20 | 20.90 | 32.35 |
| 20 | -4.0 | 19.60 | 25.65 | 34.61 | 45 | 2.1 | 13.80 | 20.32 | 31.44 |
| 20 | -6.0 | 21.20 | 27.74 | 37.44 | 45 | 5.0 | 13.40 | 19.73 | 30.53 |
| 45 | -7.5 | 15.20 | 19.89 | 26.84 | 45 | 0.8 | 23.40 | 34.45 | 53.31 |
| 45 | 5.0 | 12.80 | 16.75 | 22.61 | 45 | -1.0 | 23.00 | 33.86 | 52.40 |
| 45 | 0.7 | 16.20 | 21.20 | 28.61 | 45 | 3.3 | 21.60 | 31.80 | 49.21 |
| 45 | -10.1 | 14.80 | 19.37 | 26.14 | 45 | 4.8 | 20.40 | 30.03 | 46.47 |
| 45 | -12.5 | 13.00 | 17.01 | 22.96 | 45 | -1.4 | 24.80 | 36.51 | 56.50 |
| 45 | -1.0 | 17.60 | 23.03 | 31.08 | 45 | -1.6 | 23.80 | 35.04 | 54.22 |
| 45 | -10.8 | 15.00 | 19.63 | 26.49 | 45 | -2.5 | 23.40 | 34.45 | 53.31 |
| 45 | -5.9 | 14.00 | 18.32 | 24.72 | 45 | 2.6 | 23.00 | 33.86 | 52.40 |
| 45 | -8.3 | 15.80 | 20.67 | 27.90 | 45 | -2.1 | 20.80 | 30.62 | 47.39 |
| 45 | -9.5 | 13.80 | 18.06 | 24.37 | 45 | -9.2 | 24.00 | 35.33 | 54.68 |
| 45 | -1.0 | 15.40 | 20.15 | 27.20 | 60 | -2.0 | 9.60 | 13.50 | 20.40 |
| 45 | -8.4 | 14.40 | 18.84 | 25.43 | 60 | -1.0 | 10.60 | 14.91 | 22.53 |
| 45 | -7.7 | 15.00 | 19.63 | 26.49 | 60 | -3.8 | 20.80 | 29.26 | 44.20 |
| 45 | -8.0 | 14.00 | 18.32 | 24.72 | 60 | -1.4 | 20.60 | 28.98 | 43.78 |
| 45 | -9.0 | 12.00 | 15.70 | 21.19 | 60 | -0.8 | 19.40 | 27.29 | 41.23 |
| 45 | -1.0 | 16.20 | 21.20 | 28.61 | 60 | -2.5 | 19.60 | 27.57 | 41.65 |
| 45 | -8.0 | 15.40 | 20.15 | 27.20 | 60 | 0.0 | 19.80 | 27.85 | 42.08 |
| 45 | -8.0 | 14.20 | 18.58 | 25.08 | 60 | -4.5 | 20.00 | 28.13 | 42.50 |
| 60 | -6.7 | 16.40 | 21.06 | 27.90 | 60 | -4.7 | 20.40 | 28.69 | 43.35 |

Table B-23 - *Continued*

| Nominal Speed (mph) | Section 1 | | | | Nominal Speed (mph) | Section 2 | | | |
|---|---|---|---|---|---|---|---|---|---|
| | Transverse Strain (μ-strain) | | | | | Transverse Strain (μ-strain) | | | |
| | Offset (in) | Uncorrected | 20 ºC | 30 ºC | | Offset (in) | Uncorrected | 20 ºC | 30 ºC |
| 60 | -12.1 | 12.00 | 15.41 | 20.42 | | | | | |
| 60 | -7.0 | 14.80 | 19.01 | 25.18 | | | | | |
| 60 | -11.1 | 13.20 | 16.95 | 22.46 | | | | | |
| 60 | -10.3 | 12.40 | 15.92 | 21.10 | | | | | |
| 60 | -7.0 | 14.80 | 19.01 | 25.18 | | | | | |
| 60 | -7.9 | 13.80 | 17.72 | 23.48 | | | | | |
| 60 | -9.3 | 13.20 | 16.95 | 22.46 | | | | | |
| 60 | -10.0 | 12.60 | 16.18 | 21.44 | | | | | |
| 60 | -7.0 | 14.00 | 17.98 | 23.82 | | | | | |
| 60 | -8.0 | 13.60 | 17.47 | 23.14 | | | | | |
| 60 | -9.0 | 13.00 | 16.69 | 22.12 | | | | | |

| Nominal Speed (mph) | Section 3 | | | | Nominal Speed (mph) | Section 4 | | | |
|---|---|---|---|---|---|---|---|---|---|
| | Transverse Strain (μ-strain) | | | | | Transverse Strain (μ-strain) | | | |
| | Offset (in) | Uncorrected | 20 ºC | 30 ºC | | Offset (in) | Uncorrected | 20 ºC | 30 ºC |
| 45 | 1.0 | 10.00 | 12.48 | 18.62 | 20 | 2.5 | 21.40 | 32.59 | 54.61 |
| 45 | -1.2 | 10.40 | 12.98 | 19.37 | 20 | 2.8 | 19.80 | 30.15 | 50.53 |
| 45 | 4.3 | 11.20 | 13.98 | 20.86 | 20 | 2.7 | 22.00 | 33.50 | 56.14 |
| 45 | 9.7 | 12.60 | 15.72 | 23.46 | 20 | 1.4 | 20.40 | 31.06 | 52.06 |
| 45 | 1.0 | 13.40 | 16.72 | 24.95 | 20 | 9.5 | 21.40 | 32.59 | 54.61 |
| 45 | -1.6 | 13.60 | 16.97 | 25.33 | 20 | -8.5 | 20.00 | 30.45 | 51.04 |
| 45 | 4.8 | 13.60 | 16.97 | 25.33 | 20 | -5.2 | 17.40 | 26.50 | 44.40 |
| 45 | 9.0 | 12.20 | 15.22 | 22.72 | 20 | -6.3 | 17.80 | 27.10 | 45.42 |
| 45 | -4.7 | 8.00 | 9.98 | 14.90 | 20 | -10.6 | 19.00 | 28.93 | 48.49 |
| 45 | 8.7 | 7.80 | 9.73 | 14.53 | 20 | -1.5 | 18.80 | 28.63 | 47.98 |
| 60 | -2.8 | 7.00 | 8.54 | 12.51 | 45 | -0.3 | 16.00 | 24.36 | 40.83 |
| 60 | -4.7 | 9.20 | 11.22 | 16.44 | 45 | -0.2 | 16.40 | 24.97 | 41.85 |
| 60 | 1.1 | 11.80 | 14.39 | 21.09 | 45 | 2.4 | 15.00 | 22.84 | 38.28 |
| 60 | 3.8 | 10.40 | 12.68 | 18.59 | 45 | 0.7 | 16.40 | 24.97 | 41.85 |
| 60 | -4.9 | 8.00 | 9.76 | 14.30 | 45 | -9.3 | 15.40 | 23.45 | 39.30 |
| 60 | -2.4 | 11.40 | 13.90 | 20.37 | 45 | -8.2 | 15.40 | 23.45 | 39.30 |
| 60 | -4.0 | 11.20 | 13.66 | 20.02 | 45 | -8.3 | 18.00 | 27.41 | 45.94 |
| 60 | 1.3 | 7.20 | 8.78 | 12.87 | 45 | -10.6 | 17.20 | 26.19 | 43.89 |
| 60 | 3.3 | 7.20 | 8.78 | 12.87 | 60 | 2.5 | 11.60 | 17.01 | 27.32 |
| 60 | -4.7 | 9.00 | 10.98 | 16.08 | 60 | 4.6 | 13.40 | 19.65 | 31.56 |
| 60 | 0.7 | 6.20 | 7.56 | 11.08 | 60 | 3.7 | 12.60 | 18.48 | 29.67 |
| 60 | 1.5 | 6.60 | 8.05 | 11.80 | 60 | 4.0 | 11.40 | 16.72 | 26.85 |
| 60 | 2.9 | 6.00 | 7.32 | 10.72 | 60 | -8.6 | 12.60 | 18.48 | 29.67 |

Table B-24: Transverse Strains – 05/01/2007

| Nominal Speed (mph) | Section 1 Transverse Strain (μ-strain) | | | | Nominal Speed (mph) | Section 2 Transverse Strain (μ-strain) | | | |
|---|---|---|---|---|---|---|---|---|---|
| | Offset (in) | Uncorrected | 20 ºC | 30 ºC | | Offset (in) | Uncorrected | 20 ºC | 30 ºC |
| 20 | -5.7 | 42.80 | 40.09 | 54.11 | 20 | -9.0 | 70.60 | 64.53 | 99.87 |
| 20 | -3.0 | 42.80 | 40.09 | 54.11 | 20 | -11.0 | 67.40 | 61.61 | 95.34 |
| 20 | -4.8 | 40.80 | 38.22 | 51.58 | 20 | -10.0 | 24.20 | 22.12 | 34.23 |
| 20 | -6.0 | 41.00 | 38.40 | 51.83 | 20 | -2.0 | 47.60 | 43.51 | 67.33 |
| 20 | -2.8 | 33.00 | 30.91 | 41.72 | 20 | -15.0 | 64.80 | 59.23 | 91.66 |
| 20 | -11.1 | 29.80 | 27.91 | 37.67 | 20 | -15.0 | 70.00 | 63.99 | 99.02 |
| 20 | -9.0 | 30.60 | 28.66 | 38.68 | 20 | -15.9 | 57.20 | 52.29 | 80.91 |
| 20 | -10.4 | 26.20 | 24.54 | 33.12 | 20 | -13.8 | 48.40 | 44.24 | 68.46 |
| 20 | -12.0 | 18.00 | 16.86 | 22.76 | 20 | -9.1 | 59.20 | 54.11 | 83.74 |
| 20 | -8.4 | 28.40 | 26.60 | 35.90 | 45 | 2.0 | 12.60 | 11.52 | 17.82 |
| 20 | -9.3 | 36.00 | 33.72 | 45.51 | 45 | 0.0 | 67.20 | 61.43 | 95.06 |
| 20 | -9.0 | 33.20 | 31.10 | 41.97 | 45 | -8.0 | 41.80 | 38.21 | 59.13 |
| 20 | -9.2 | 32.20 | 30.16 | 40.71 | 45 | -9.0 | 45.80 | 41.87 | 64.79 |
| 20 | -12.0 | 21.00 | 19.67 | 26.55 | 45 | -0.4 | 124.40 | 113.71 | 175.97 |
| 20 | -7.2 | 27.80 | 26.04 | 35.14 | 45 | -7.8 | 117.40 | 107.31 | 166.07 |
| 20 | -9.0 | 35.80 | 33.53 | 45.26 | 45 | -9.0 | 108.60 | 99.27 | 153.62 |
| 20 | -9.0 | 33.60 | 31.47 | 42.48 | 45 | -4.0 | 31.40 | 28.70 | 44.42 |
| 20 | -9.0 | 34.40 | 32.22 | 43.49 | 45 | -8.2 | 59.40 | 54.30 | 84.02 |
| 20 | -7.0 | 34.20 | 32.03 | 43.24 | 45 | -12.9 | 37.20 | 34.00 | 52.62 |
| 45 | -6.8 | 28.00 | 26.23 | 35.40 | 45 | -15.0 | 40.40 | 36.93 | 57.15 |
| 45 | -3.1 | 29.00 | 27.16 | 36.66 | 60 | -10.0 | 47.40 | 43.64 | 65.93 |
| 45 | -12.4 | 21.60 | 20.23 | 27.31 | 60 | -4.0 | 41.00 | 37.75 | 57.03 |
| 45 | -14.7 | 14.20 | 13.30 | 17.95 | 60 | -5.0 | 40.40 | 37.20 | 56.20 |
| 45 | -11.2 | 22.60 | 21.17 | 28.57 | 60 | -4.0 | 41.40 | 38.12 | 57.59 |
| 45 | -9.9 | 23.80 | 22.29 | 30.09 | 60 | -5.0 | 42.40 | 39.04 | 58.98 |
| 45 | -14.1 | 14.00 | 13.11 | 17.70 | 60 | -10.0 | 94.60 | 87.10 | 131.59 |
| 45 | -11.0 | 19.20 | 17.98 | 24.27 | 60 | -4.6 | 89.40 | 82.31 | 124.35 |
| 45 | -10.0 | 25.40 | 23.79 | 32.11 | 60 | -4.0 | 96.80 | 89.12 | 134.65 |
| 45 | -14.0 | 12.80 | 11.99 | 16.18 | 60 | -5.0 | 100.60 | 92.62 | 139.93 |
| 60 | -7.3 | 28.00 | 26.32 | 34.87 | 60 | -16.0 | 41.20 | 37.93 | 57.31 |
| 60 | -2.9 | 30.40 | 28.58 | 37.86 | 60 | -13.3 | 44.20 | 40.69 | 61.48 |
| 60 | -2.9 | 28.60 | 26.88 | 35.62 | 60 | -12.1 | 42.00 | 38.67 | 58.42 |
| 60 | -8.7 | 22.60 | 21.24 | 28.15 | 60 | -10.0 | 42.40 | 39.04 | 58.98 |
| 60 | -13.0 | 16.40 | 15.42 | 20.43 | 60 | -11.0 | 39.00 | 35.91 | 54.25 |
| 60 | -8.7 | 22.80 | 21.43 | 28.40 | | | | | |
| 60 | -8.1 | 25.20 | 23.69 | 31.39 | | | | | |
| 60 | -12.2 | 18.20 | 17.11 | 22.67 | | | | | |

Table B-24 - *Continued*

| Nominal Speed (mph) | Section 1 | | | | Nominal Speed (mph) | Section 2 | | | |
|---|---|---|---|---|---|---|---|---|---|
| | Transverse Strain (μ-strain) | | | | | Transverse Strain (μ-strain) | | | |
| | Offset (in) | Uncorrected | 20 ºC | 30 ºC | | Offset (in) | Uncorrected | 20 ºC | 30 ºC |
| 60 | -8.0 | 23.80 | 22.37 | 29.64 | | | | | |
| 60 | -8.0 | 22.60 | 21.24 | 28.15 | | | | | |

| Nominal Speed (mph) | Section 3 | | | | Nominal Speed (mph) | Section 4 | | | |
|---|---|---|---|---|---|---|---|---|---|
| | Transverse Strain (μ-strain) | | | | | Transverse Strain (μ-strain) | | | |
| | Offset (in) | Uncorrected | 20 ºC | 30 ºC | | Offset (in) | Uncorrected | 20 ºC | 30 ºC |
| | | | | | 20 | -0.9 | 37.60 | 34.04 | 57.05 |
| | | | | | 20 | -0.2 | 41.00 | 37.12 | 62.21 |
| | | | | | 20 | 6.0 | 27.00 | 24.45 | 40.97 |
| | | | | | 20 | -7.8 | 36.60 | 33.14 | 55.54 |
| | | | | | 20 | -3.0 | 37.80 | 34.22 | 57.36 |
| | | | | | 20 | -5.9 | 44.00 | 39.84 | 66.76 |
| | | | | | 20 | -8.2 | 39.60 | 35.85 | 60.09 |
| | | | | | 20 | -11.8 | 27.20 | 24.63 | 41.27 |
| | | | | | 20 | -10.9 | 33.80 | 30.60 | 51.29 |
| | | | | | 45 | -4.9 | 26.80 | 24.26 | 40.67 |
| | | | | | 45 | -1.0 | 27.00 | 24.45 | 40.97 |
| | | | | | 45 | -9.0 | 24.40 | 22.09 | 37.02 |
| | | | | | 45 | -3.0 | 27.60 | 24.99 | 41.88 |
| | | | | | 45 | -6.8 | 27.60 | 24.99 | 41.88 |
| | | | | | 45 | -9.9 | 27.40 | 24.81 | 41.58 |
| | | | | | 45 | -7.0 | 27.40 | 24.81 | 41.58 |
| | | | | | 45 | -15.0 | 19.80 | 17.93 | 30.04 |
| | | | | | 45 | -10.8 | 21.20 | 19.19 | 32.17 |
| | | | | | 60 | -7.1 | 21.00 | 19.11 | 30.68 |
| | | | | | 60 | 2.0 | 19.40 | 17.65 | 28.34 |
| | | | | | 60 | -8.9 | 17.00 | 15.47 | 24.84 |
| | | | | | 60 | -4.9 | 21.20 | 19.29 | 30.97 |
| | | | | | 60 | -14.1 | 18.00 | 16.38 | 26.30 |
| | | | | | 60 | -4.0 | 27.60 | 25.12 | 40.32 |
| | | | | | 60 | -18.0 | 12.60 | 11.47 | 18.41 |

Table B-25: Transverse Strains – 10/05/2007

| Nominal Speed (mph) | Section 1 Transverse Strain (μ-strain) | | | | Nominal Speed (mph) | Section 2 Transverse Strain (μ-strain) | | | |
|---|---|---|---|---|---|---|---|---|---|
| | Offset (in) | Uncorrected | 20 ºC | 30 ºC | | Offset (in) | Uncorrected | 20 ºC | 30 ºC |
| 20 | -1.8 | 45.00 | 40.79 | 55.05 | 20 | 6.0 | 59.00 | 52.27 | 80.88 |
| 20 | 3.1 | 37.80 | 34.26 | 46.24 | 20 | 8.0 | 58.00 | 51.38 | 79.51 |
| 20 | 5.6 | 35.60 | 32.27 | 43.55 | 20 | 10.0 | 25.20 | 22.32 | 34.55 |
| 20 | 5.9 | 30.00 | 27.19 | 36.70 | 20 | 10.0 | 34.60 | 30.65 | 47.43 |
| 20 | 7.7 | 23.80 | 21.57 | 29.12 | 20 | 6.0 | 54.20 | 48.02 | 74.30 |
| 20 | -7.5 | 43.80 | 39.70 | 53.58 | 20 | 6.3 | 135.20 | 119.77 | 185.35 |
| 20 | -3.6 | 36.80 | 33.36 | 45.02 | 20 | 8.2 | 150.00 | 132.89 | 205.64 |
| 20 | -1.2 | 43.80 | 39.70 | 53.58 | 20 | 10.6 | 86.00 | 76.19 | 117.90 |
| 20 | -1.4 | 41.20 | 37.34 | 50.40 | 20 | 10.4 | 102.20 | 90.54 | 140.11 |
| 20 | 1.2 | 43.20 | 39.16 | 52.85 | 20 | 6.4 | 131.00 | 116.05 | 179.59 |
| 20 | -6.9 | 38.40 | 34.81 | 46.98 | 20 | 3.1 | 82.00 | 72.64 | 112.42 |
| 20 | -5.6 | 38.20 | 34.63 | 46.73 | 20 | 7.3 | 64.60 | 57.23 | 88.56 |
| 20 | -4.9 | 41.20 | 37.34 | 50.40 | 20 | 6.2 | 73.20 | 64.85 | 100.35 |
| 20 | -0.2 | 42.60 | 38.61 | 52.11 | 20 | 2.2 | 74.20 | 65.73 | 101.72 |
| 45 | 1.4 | 26.00 | 23.57 | 31.81 | 45 | 8.5 | 23.80 | 21.08 | 32.63 |
| 45 | 6.1 | 21.40 | 19.40 | 26.18 | 45 | 6.0 | 45.40 | 40.22 | 62.24 |
| 45 | 8.1 | 21.00 | 19.03 | 25.69 | 45 | 3.0 | 50.40 | 44.65 | 69.09 |
| 45 | 3.6 | 26.20 | 23.75 | 32.05 | 45 | 9.0 | 93.40 | 82.74 | 128.04 |
| 45 | -3.9 | 29.40 | 26.65 | 35.97 | 45 | 6.2 | 132.60 | 117.47 | 181.78 |
| 45 | 0.0 | 27.80 | 25.20 | 34.01 | 45 | -1.8 | 143.80 | 127.39 | 197.14 |
| 45 | 0.2 | 25.60 | 23.20 | 31.32 | 45 | -0.3 | 156.40 | 138.56 | 214.41 |
| 45 | 2.3 | 28.20 | 25.56 | 34.50 | 45 | 5.2 | 41.00 | 36.32 | 56.21 |
| 45 | -2.3 | 27.40 | 24.84 | 33.52 | 45 | 1.1 | 59.60 | 52.80 | 81.71 |
| 45 | -1.9 | 28.80 | 26.10 | 35.23 | 45 | -3.2 | 60.00 | 53.15 | 82.26 |
| 45 | 0.4 | 27.80 | 25.20 | 34.01 | 45 | -0.8 | 59.80 | 52.98 | 81.98 |
| 45 | -2.1 | 30.80 | 27.92 | 37.68 | 60 | -2.0 | 52.20 | 46.67 | 70.52 |
| 60 | 7.1 | 22.20 | 20.26 | 26.84 | 60 | -5.5 | 48.20 | 43.10 | 65.11 |
| 60 | 4.1 | 24.80 | 22.63 | 29.98 | 60 | 2.8 | 128.40 | 114.81 | 173.45 |
| 60 | 5.0 | 23.60 | 21.53 | 28.53 | 60 | -1.2 | 133.40 | 119.28 | 180.21 |
| 60 | 4.0 | 26.20 | 23.90 | 31.67 | 60 | -5.1 | 134.00 | 119.81 | 181.02 |
| 60 | 2.6 | 26.40 | 24.09 | 31.91 | 60 | 0.4 | 47.60 | 42.56 | 64.30 |
| 60 | 1.3 | 28.60 | 26.09 | 34.57 | 60 | -4.8 | 42.60 | 38.09 | 57.55 |
| 60 | -1.7 | 27.60 | 25.18 | 33.36 | 60 | 3.2 | 47.20 | 42.20 | 63.76 |
| 60 | -1.0 | 26.20 | 23.90 | 31.67 | 60 | -9.3 | 37.00 | 33.08 | 49.98 |
| 60 | -2.0 | 26.80 | 24.45 | 32.40 | | | | | |
| 60 | -3.2 | 25.20 | 22.99 | 30.46 | | | | | |
| 60 | 1.9 | 26.60 | 24.27 | 32.16 | | | | | |

Table B-25 - *Continued*

| Nominal Speed (mph) | Section 3 Transverse Strain (μ-strain) | | | | Nominal Speed (mph) | Section 4 Transverse Strain (μ-strain) | | | |
|---|---|---|---|---|---|---|---|---|---|
| | Offset (in) | Uncorrected | 20 ºC | 30 ºC | | Offset (in) | Uncorrected | 20 ºC | 30 ºC |
| | | | | | 20 | 0.3 | 44.40 | 41.94 | 70.29 |
| | | | | | 20 | 5.8 | 42.60 | 40.24 | 67.44 |
| | | | | | 20 | 6.1 | 41.80 | 39.48 | 66.17 |
| | | | | | 20 | -1.7 | 35.00 | 33.06 | 55.41 |
| | | | | | 20 | -1.2 | 43.20 | 40.81 | 68.39 |
| | | | | | 45 | 3.4 | 28.20 | 26.64 | 44.64 |
| | | | | | 45 | 1.1 | 28.00 | 26.45 | 44.33 |
| | | | | | 45 | 3.9 | 28.40 | 26.83 | 44.96 |
| | | | | | 60 | 5.3 | 22.40 | 21.19 | 34.02 |
| | | | | | 60 | 2.0 | 22.60 | 21.38 | 34.32 |
| | | | | | 60 | -0.1 | 20.60 | 19.49 | 31.28 |
| | | | | | 60 | -1.7 | 21.40 | 20.24 | 32.50 |
| | | | | | 60 | 1.8 | 21.60 | 20.43 | 32.80 |

# APPENDIX C

# PREDICTED (LINEAR ELASTIC) VS MEASURED PAVEMENT RESPONSE VALUES

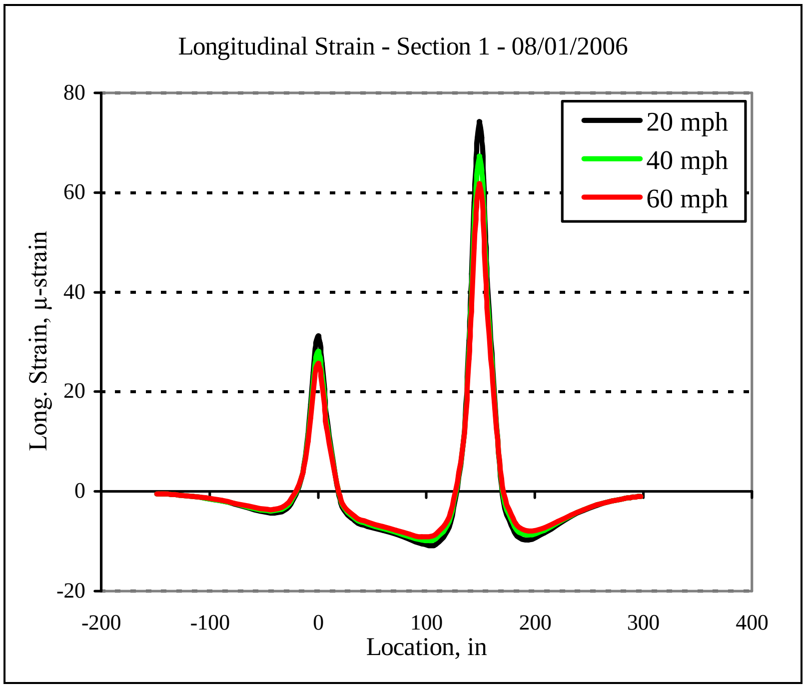


Figure C-1: Longitudinal Strain – Section 1 – 08/01/2006

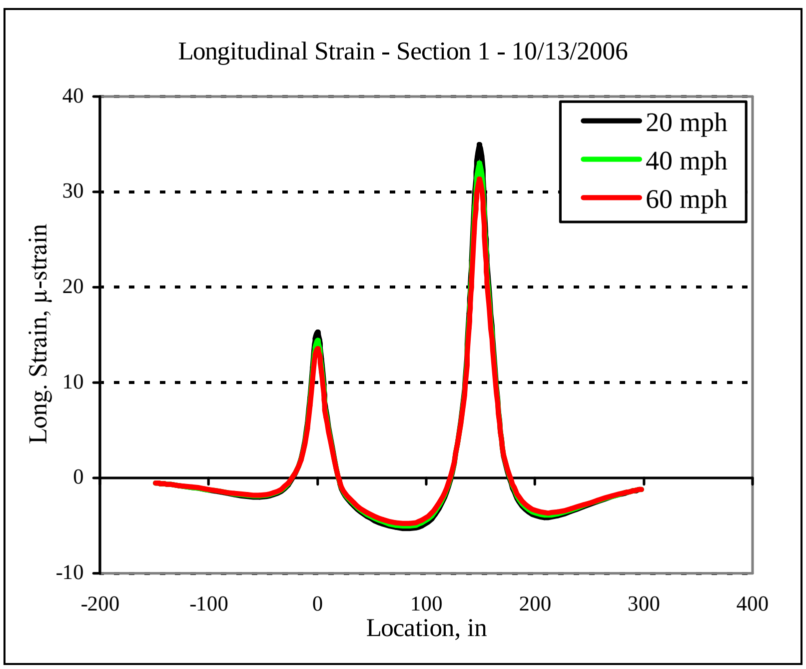


Figure C-2: Longitudinal Strain – Section 1 – 10/13/2006

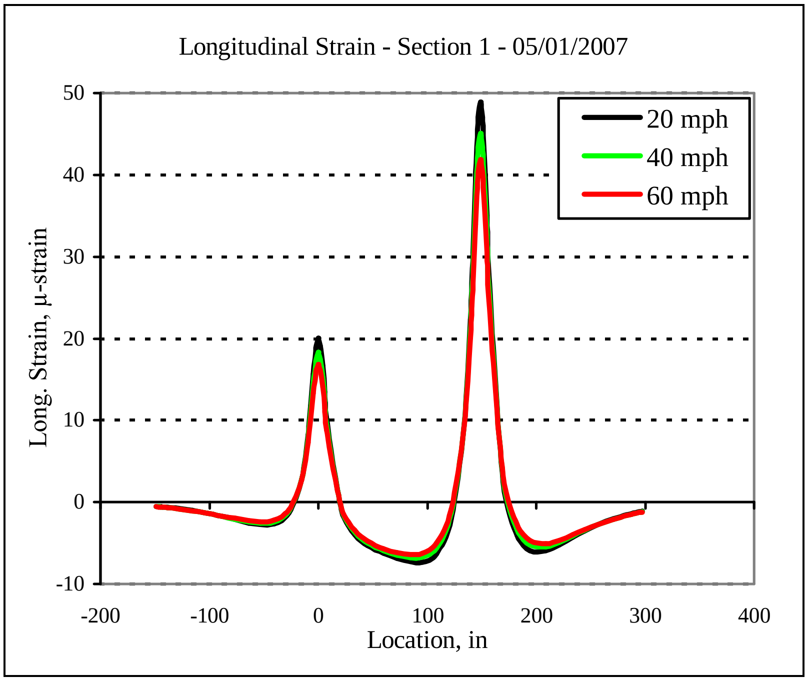


Figure C-3: Longitudinal Strain – Section 1 – 05/01/2007

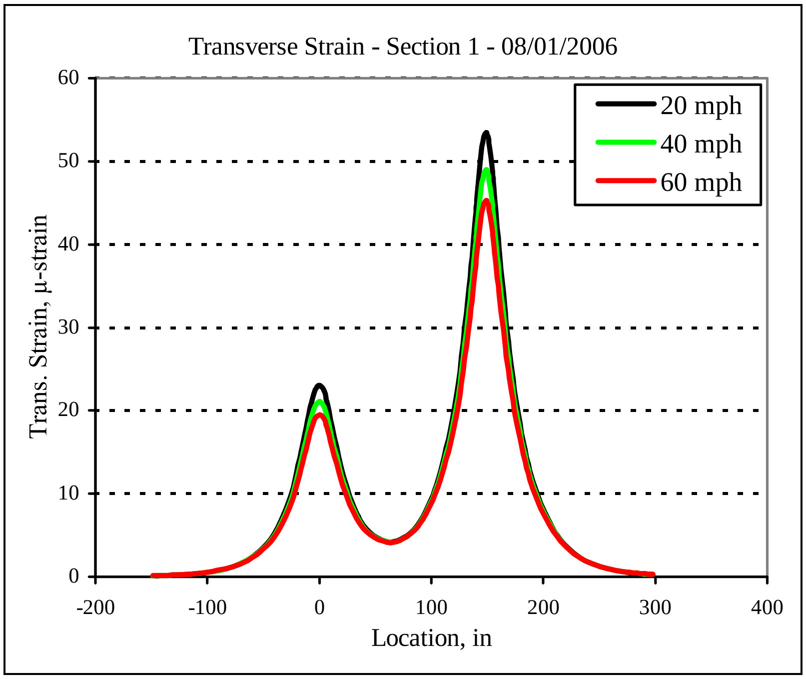


Figure C-4: Transverse Strain – Section 1 – 08/01/2006

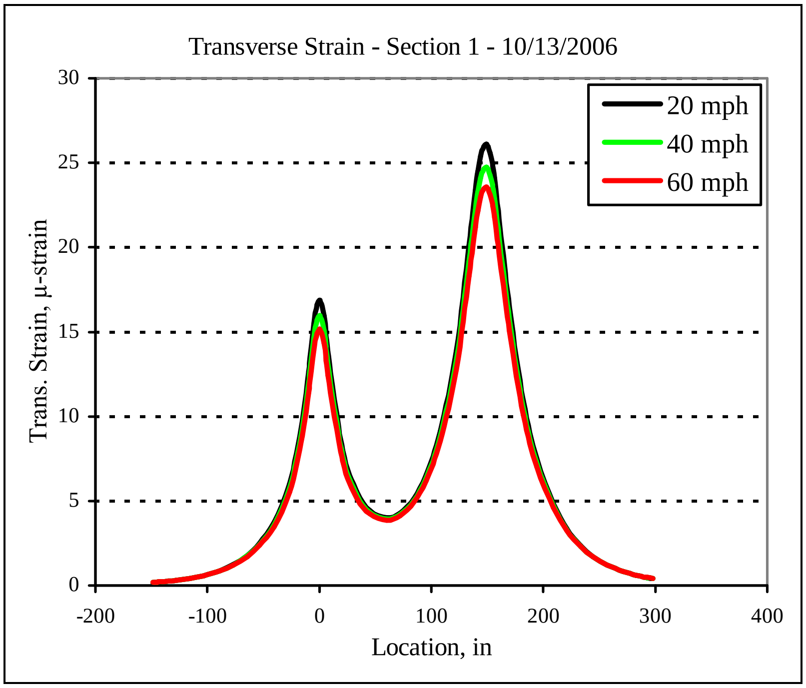


Figure C-5: Transverse Strain – Section 1 – 10/13/2006

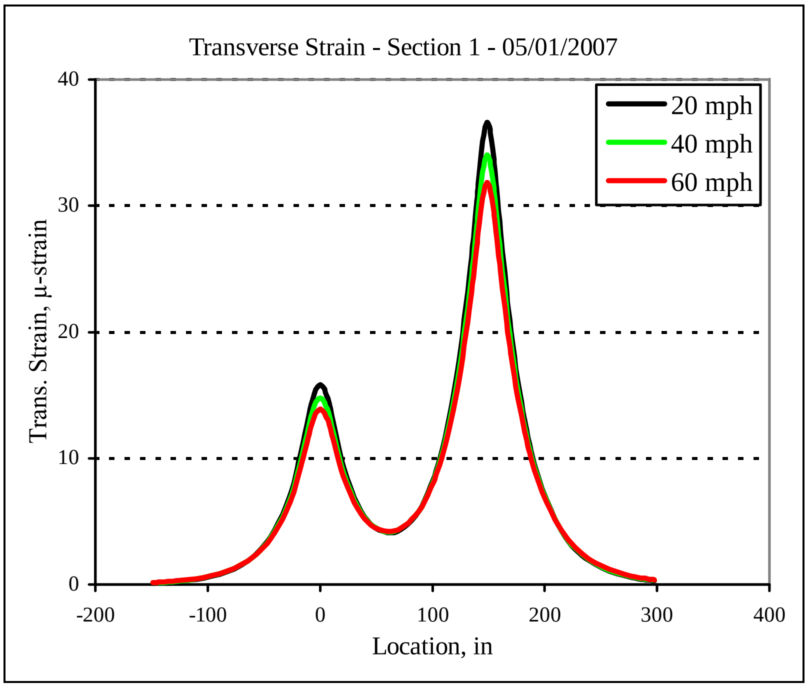


Figure C-6: Transverse Strain – Section 1 – 05/01/2007

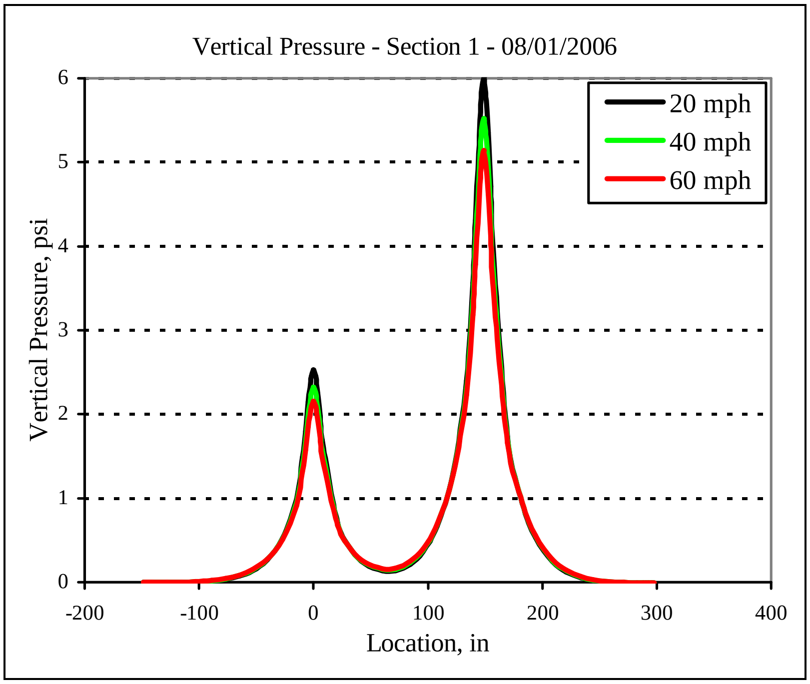


Figure C-7: Vertical Pressure – Section 1 – 08/01/2006

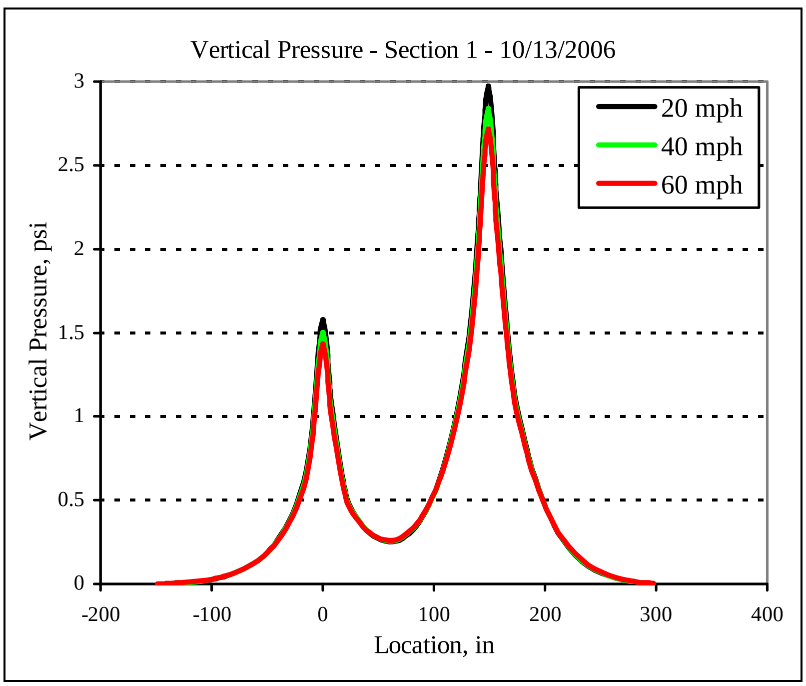


Figure C-8: Vertical Pressure – Section 1 – 10/13/2006

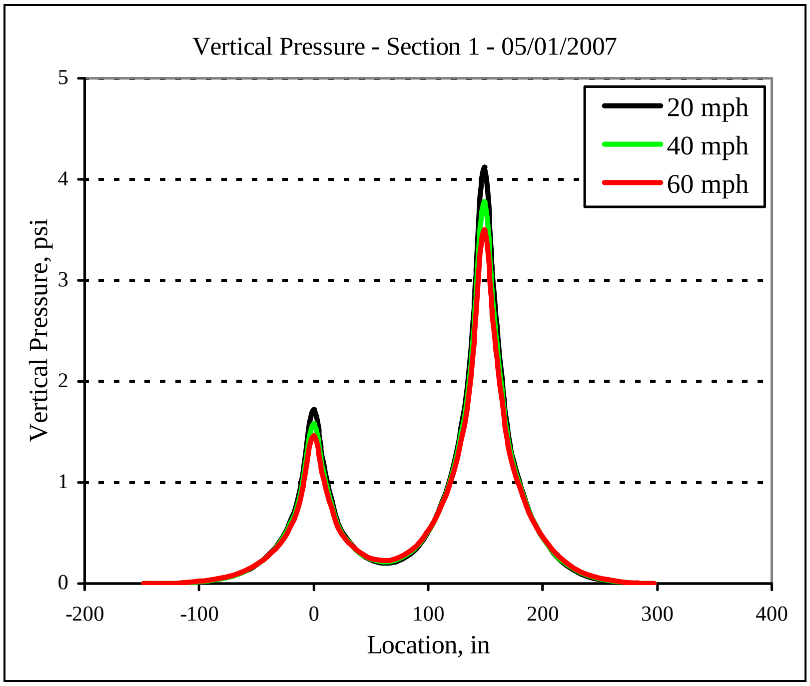


Figure C-9: Vertical Pressure – Section 1 – 05/01/2007

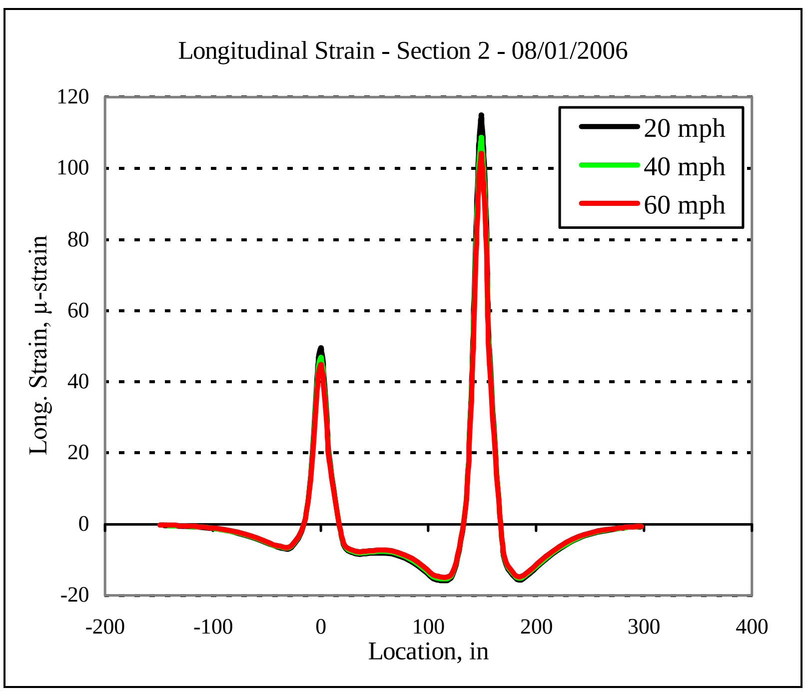


Figure C-10: Longitudinal Strain – Section 2 – 08/01/2006

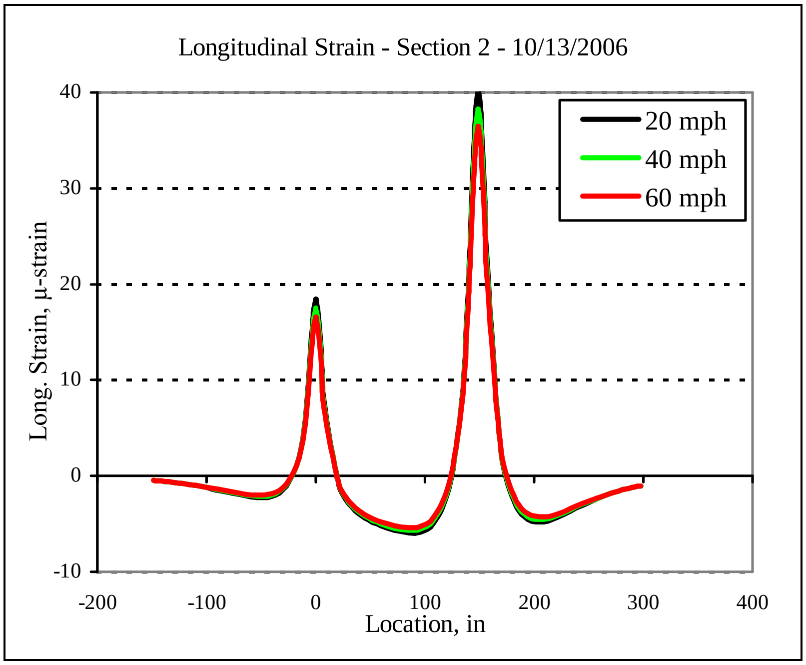


Figure C-11: Longitudinal Strain – Section 2 – 10/13/2006

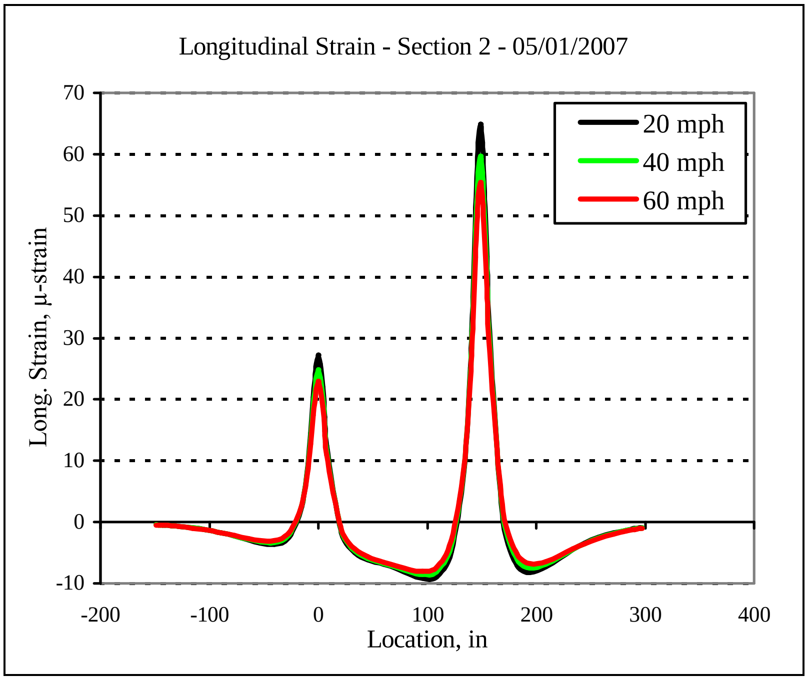


Figure C-12: Longitudinal Strain – Section 2 – 05/01/2007

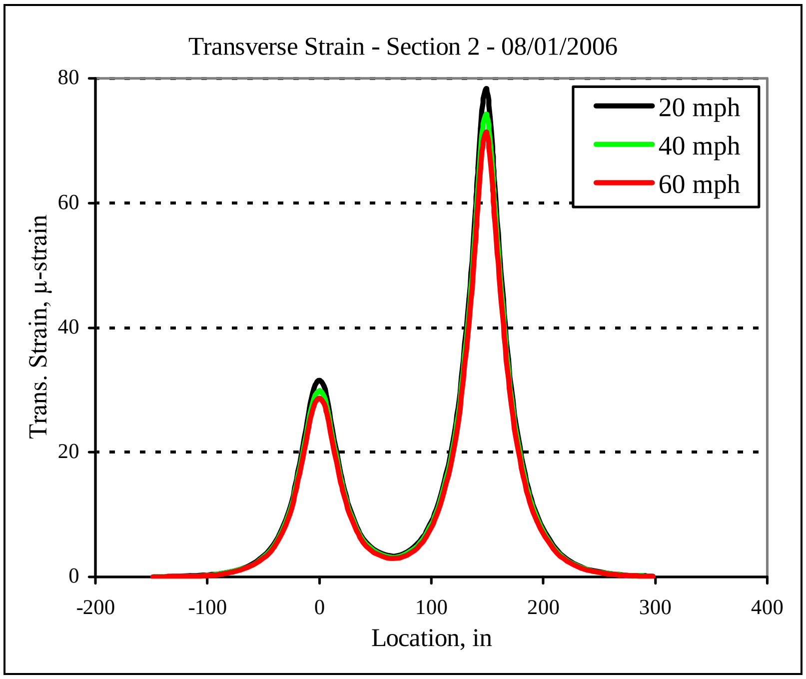


Figure C-13: Transverse Strain – Section 2 – 08/01/2006

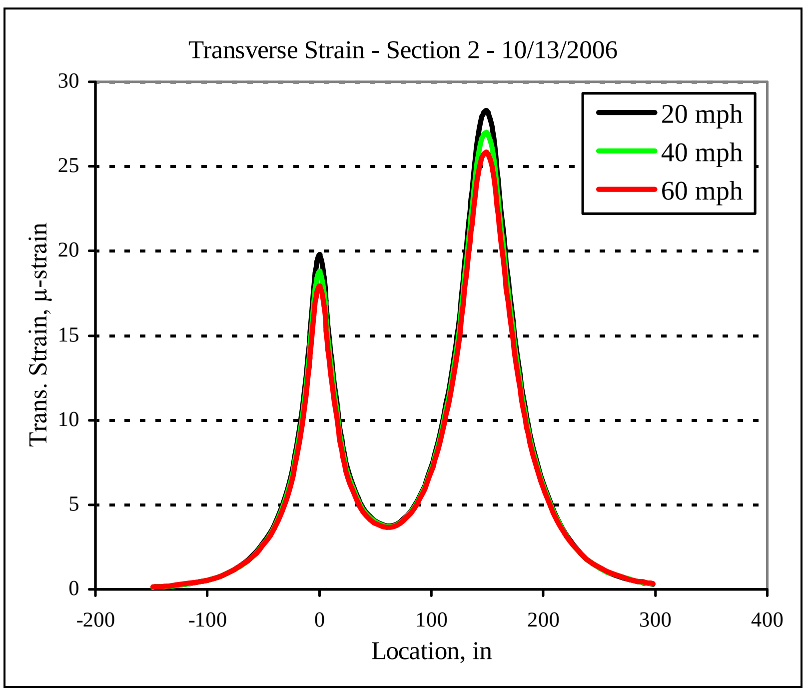


Figure C-14: Transverse Strain – Section 2 – 10/13/2006

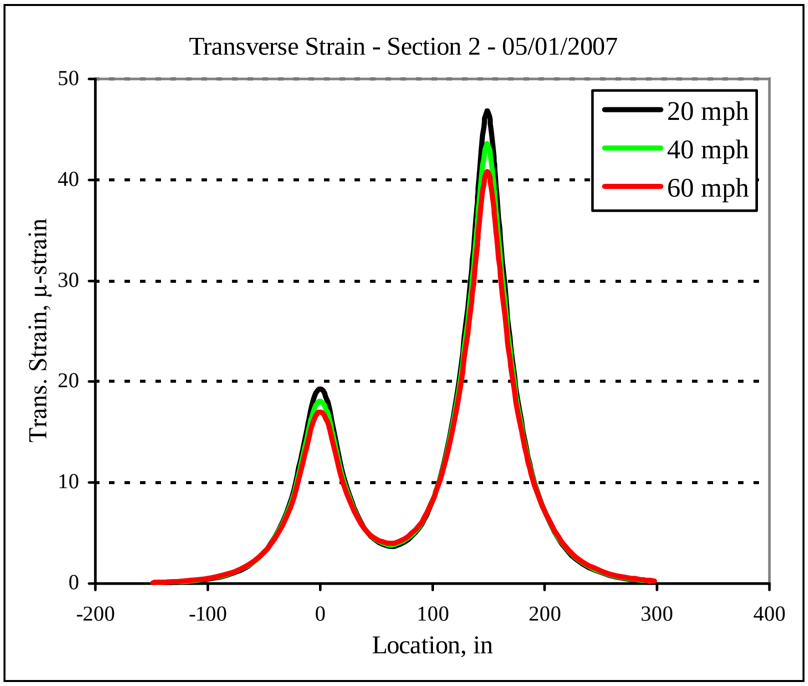


Figure C-15: Transverse Strain – Section 2 – 05/01/2007

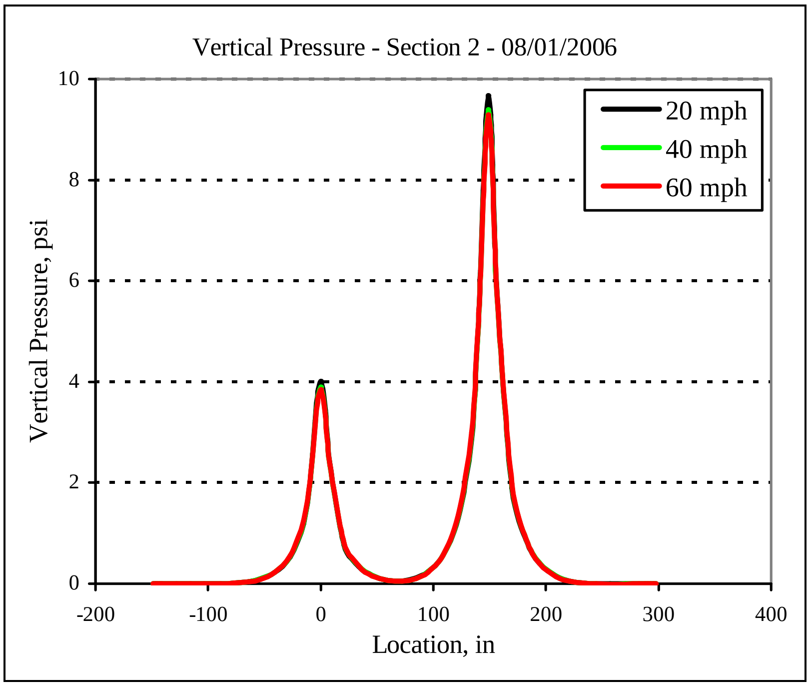


Figure C-16: Vertical Pressure – Section 2 – 08/01/2006

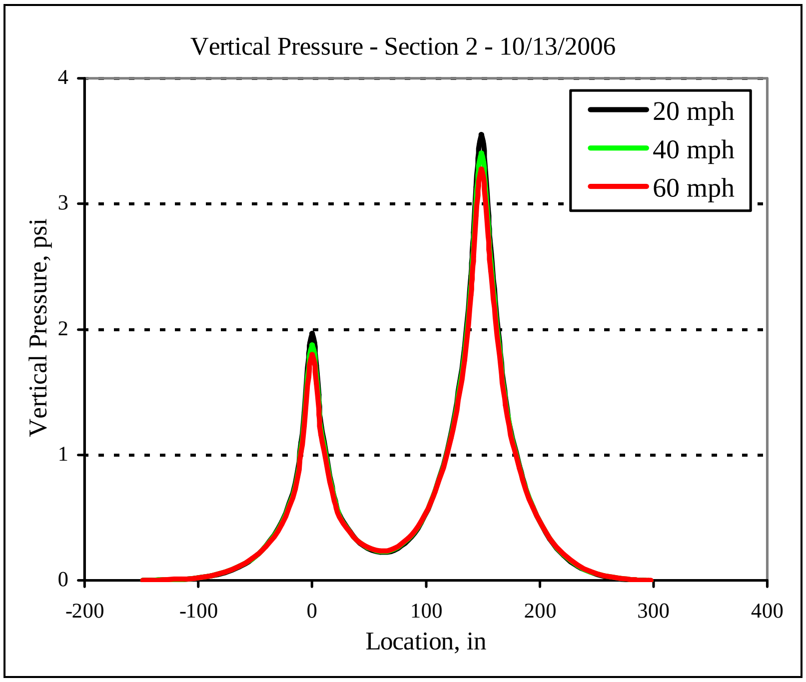


Figure C-17: Vertical Pressure – Section 2 – 10/13/2006

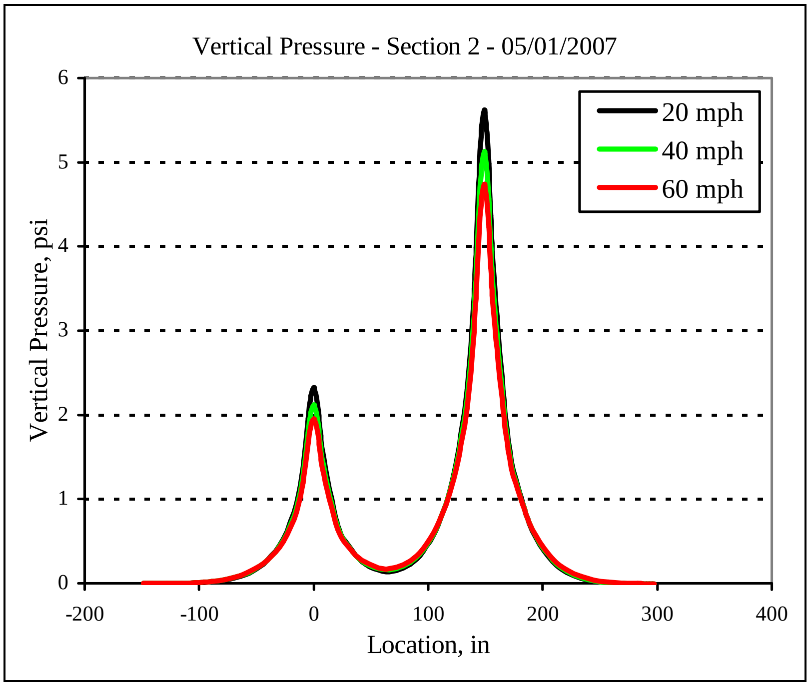


Figure C-18: Vertical Pressure – Section 2 – 05/01/2007

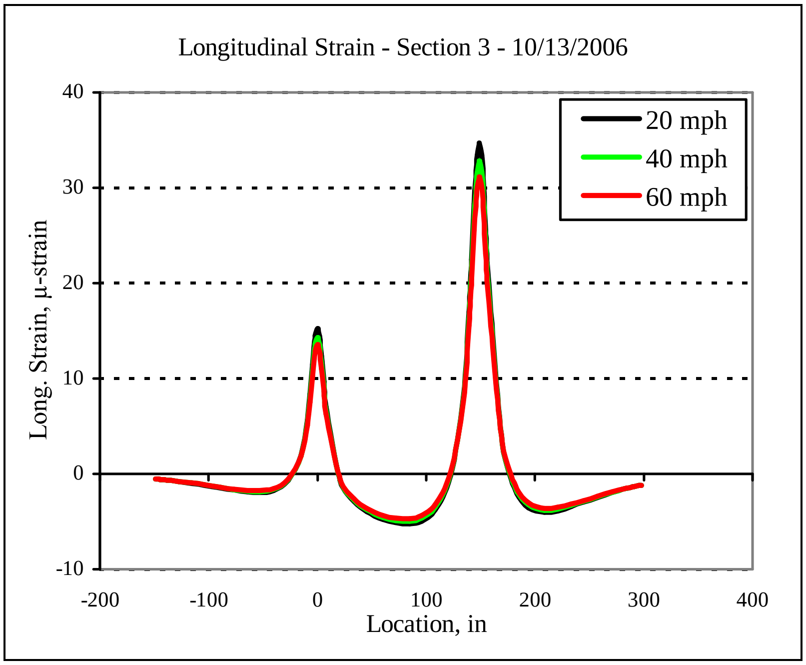


Figure C-19: Longitudinal Strain – Section 3 – 10/13/2006

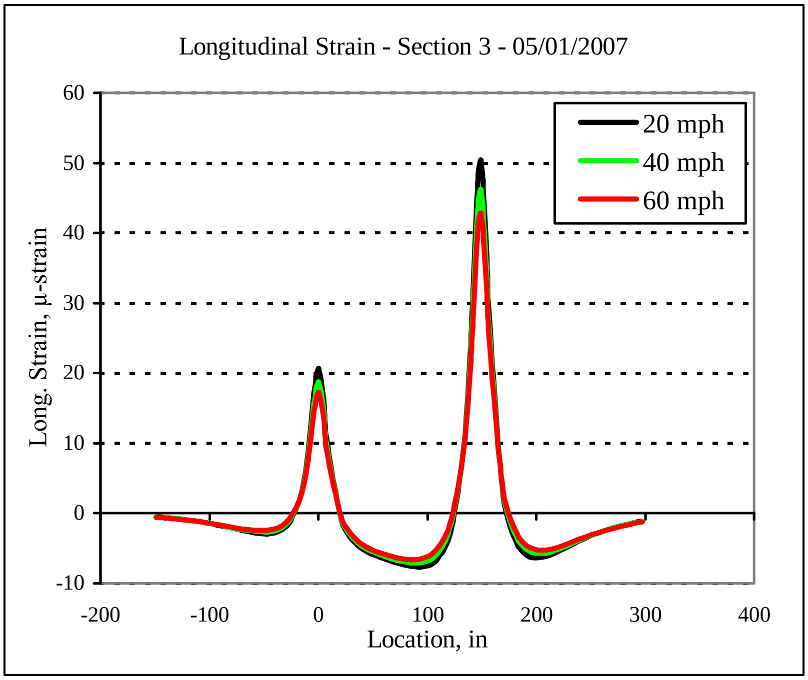


Figure C-20: Longitudinal Strain – Section 3 – 05/01/2007

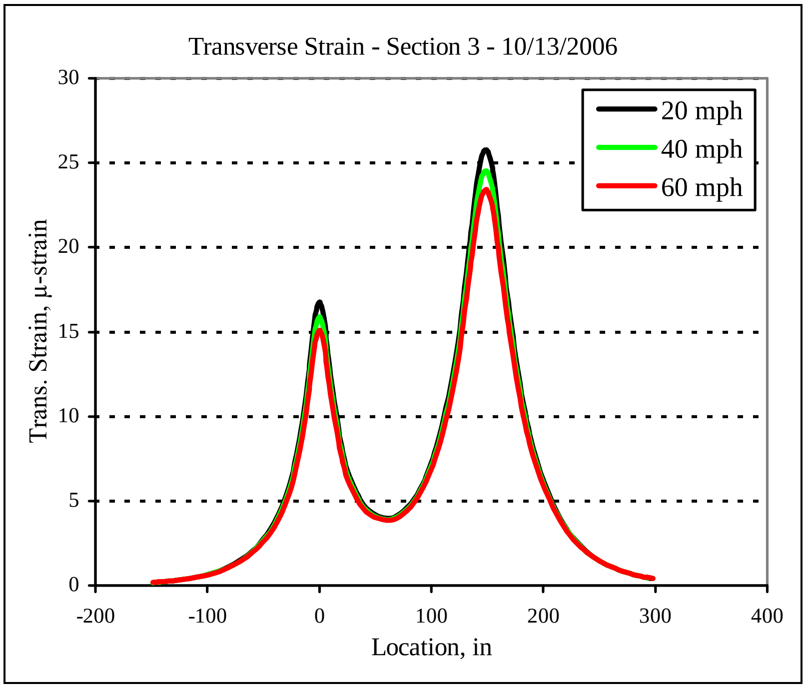


Figure C-21: Transverse Strain – Section 3 – 10/13/2006

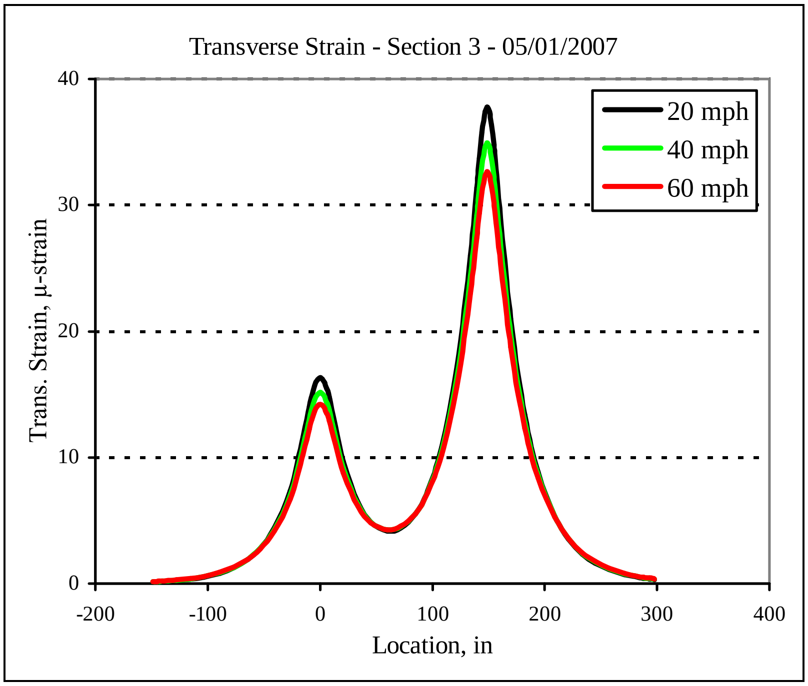


Figure C-22: Transverse Strain – Section 3 – 05/01/2007

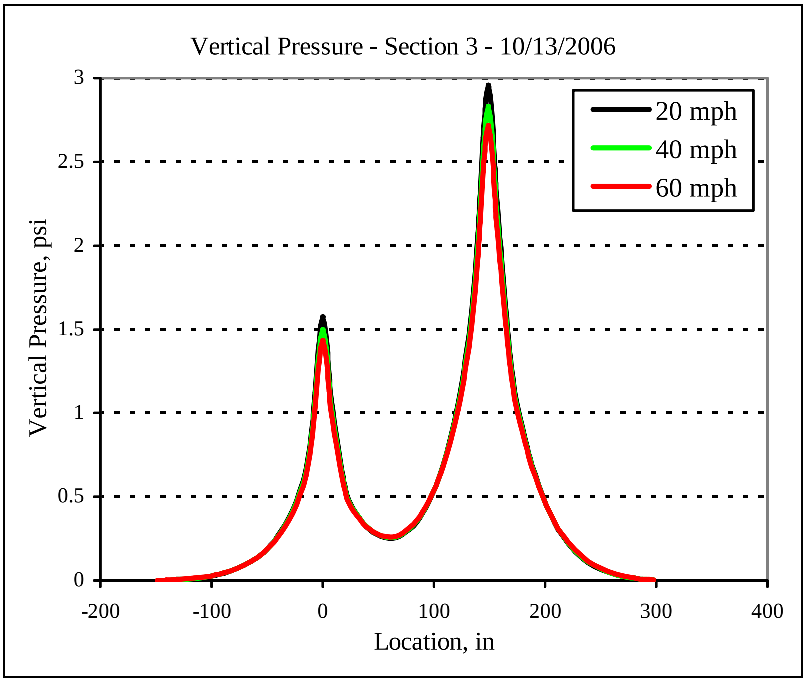


Figure C-23: Vertical Pressure – Section 3 – 10/13/2006

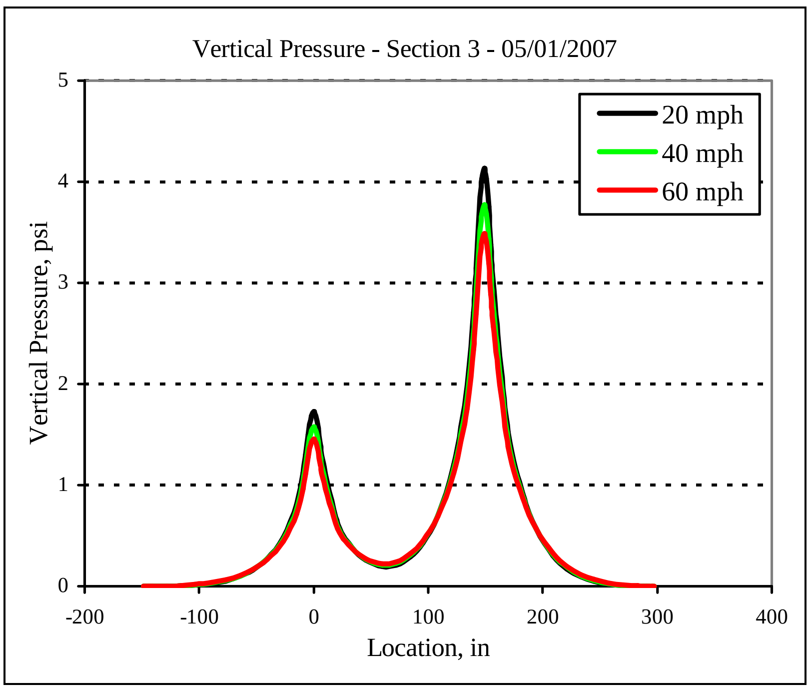


Figure C-24: Vertical Pressure – Section 3 – 05/01/2007

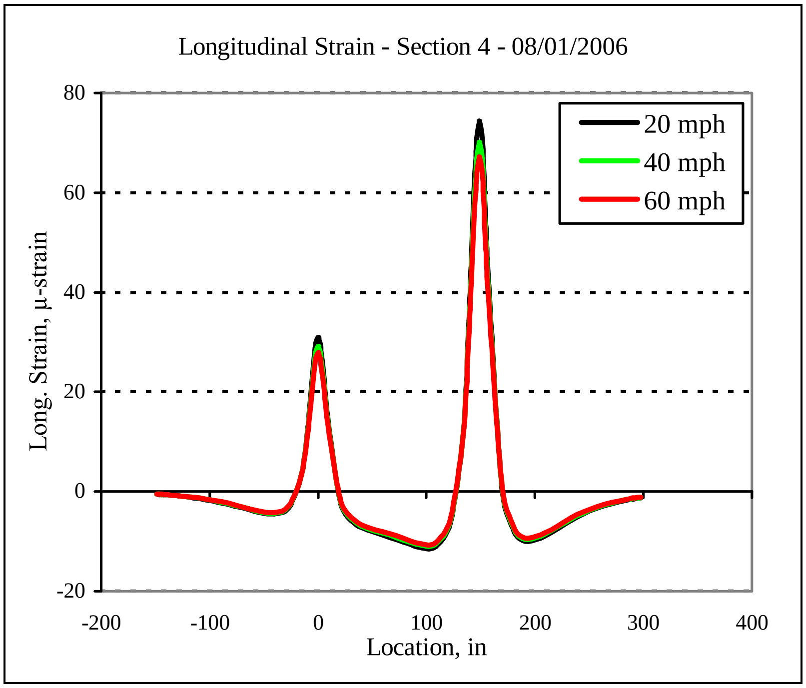


Figure C-25: Longitudinal Strain – Section 4 – 08/01/2006

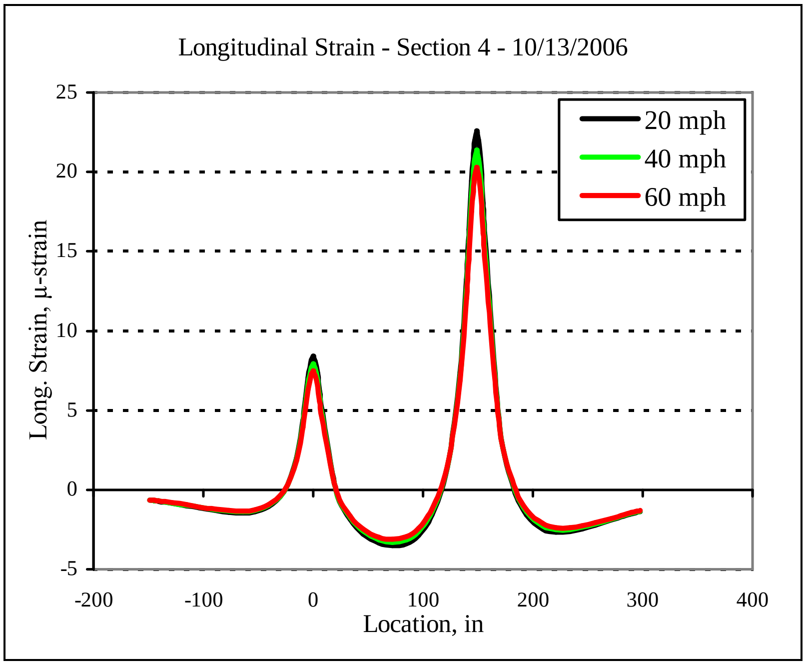


Figure C-26: Longitudinal Strain – Section 4 – 10/13/2006

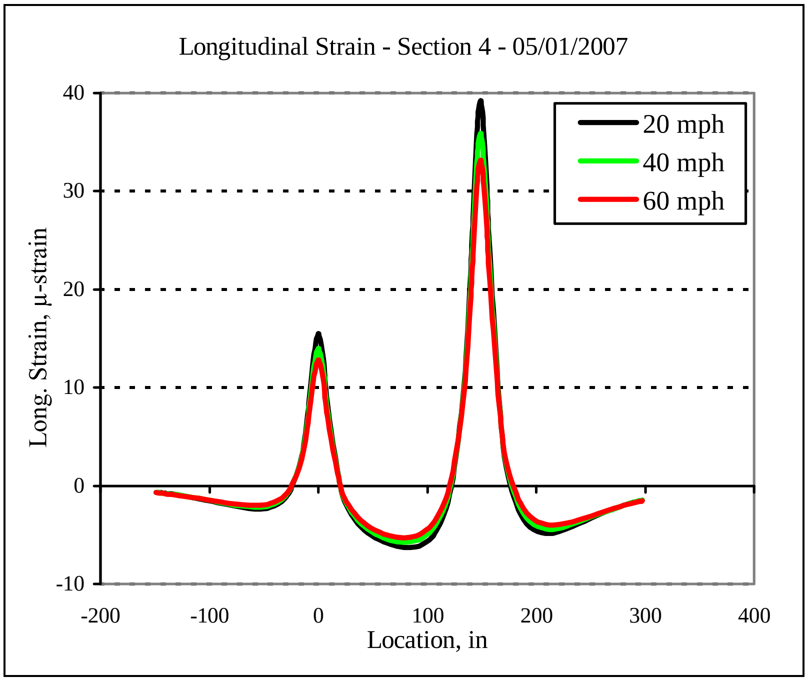


Figure C-27: Longitudinal Strain – Section 4 – 05/01/2007

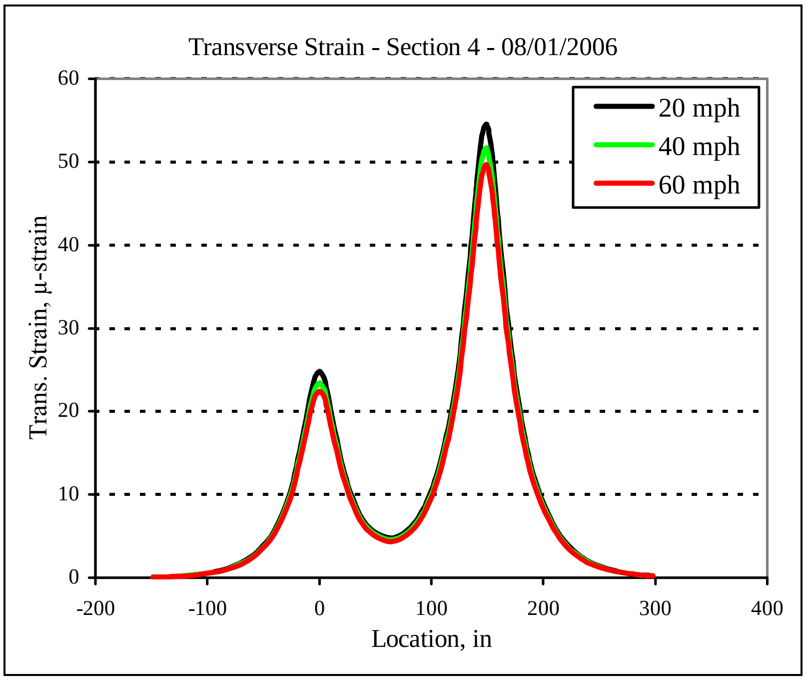


Figure C-28: Transverse Strain – Section 4 – 08/01/2006

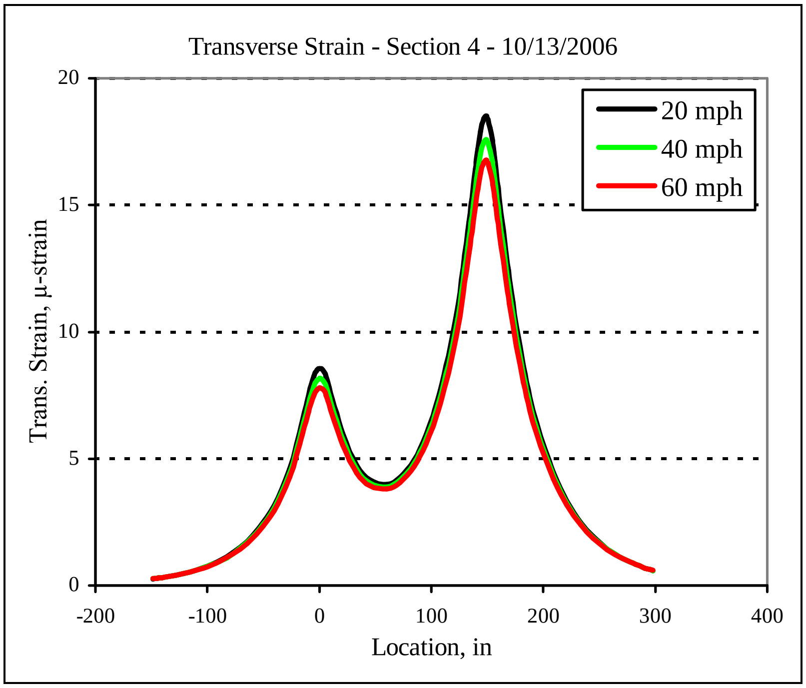


Figure C-29: Transverse Strain – Section 4 – 10/13/2006

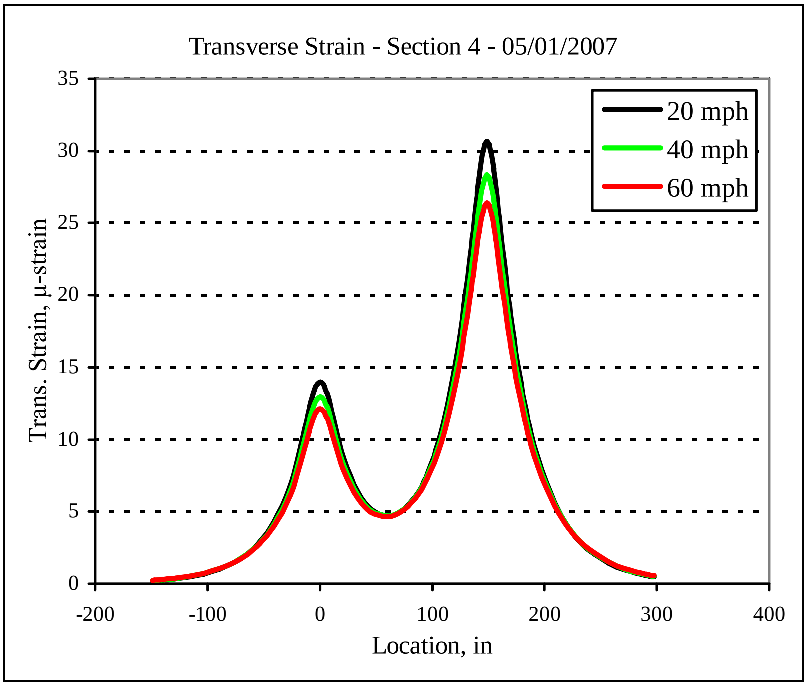


Figure C-30: Transverse Strain – Section 4 – 05/01/2007

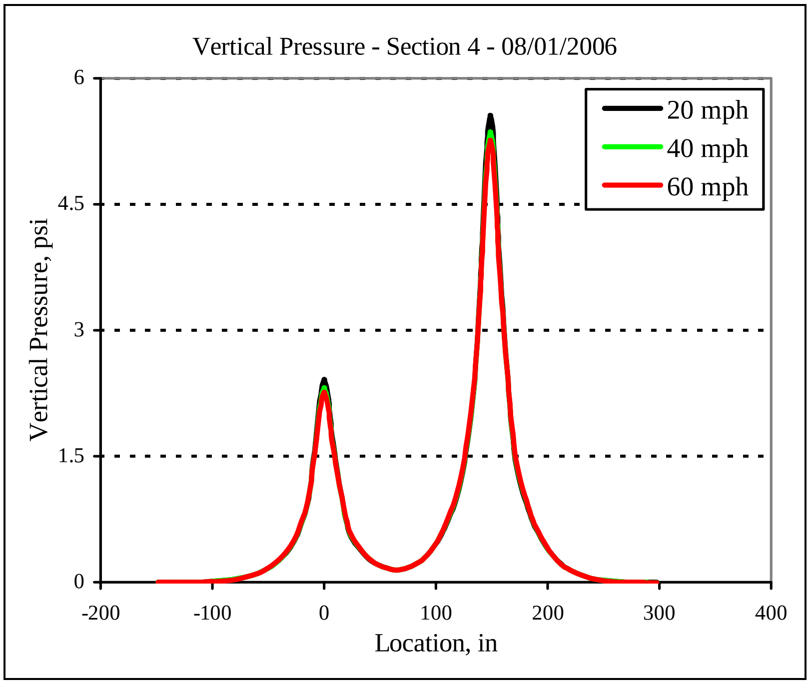


Figure C-31: Vertical Pressure – Section 4 – 08/01/2006

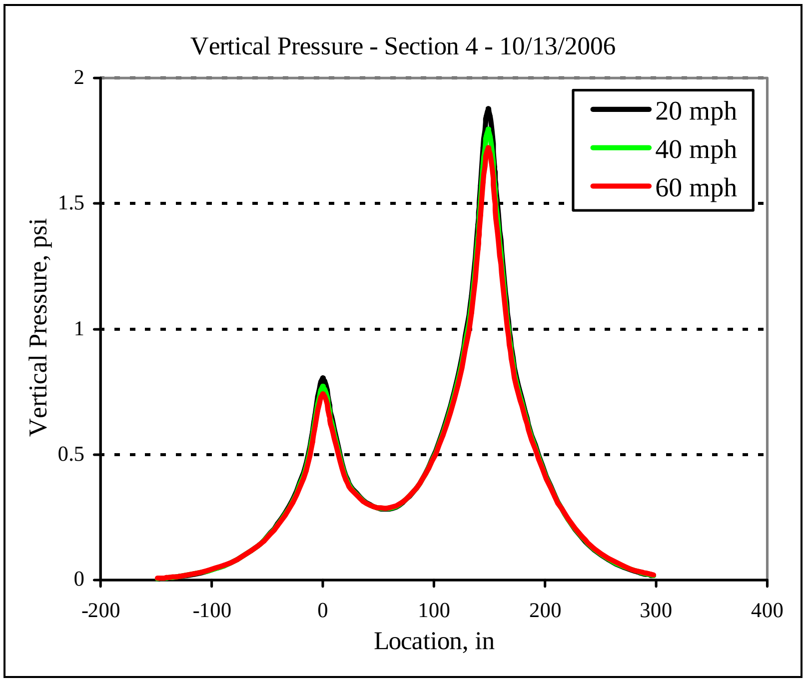


Figure C-32: Vertical Pressure – Section 4 – 10/13/2006

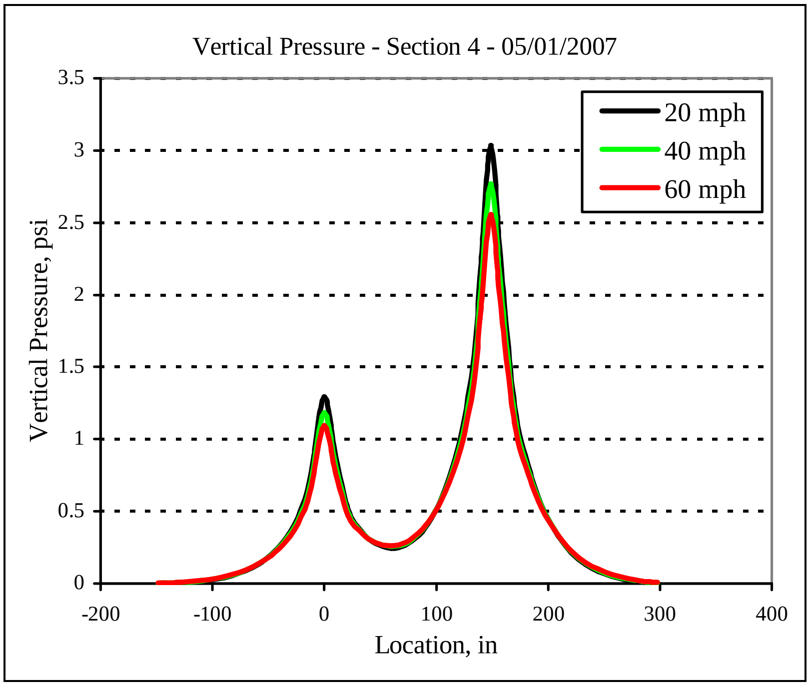


Figure C-33: Vertical Pressure – Section 4 – 05/01/2007

# APPENDIX D

# MEASURED VS PREDICTED DYNAMIC MODULUS CHARTS

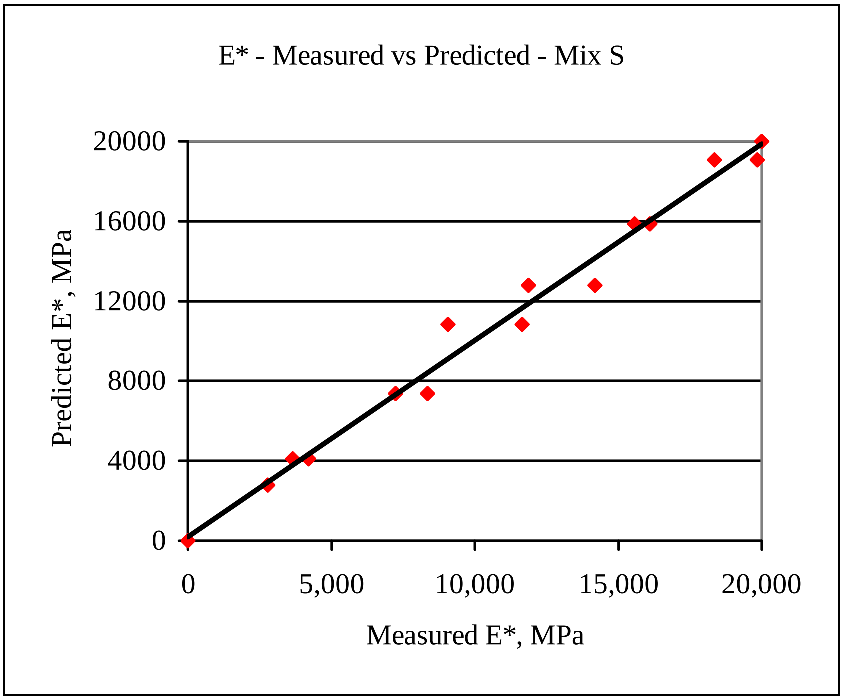


Figure D-1: E* - Measured vs Predicted – Mix S

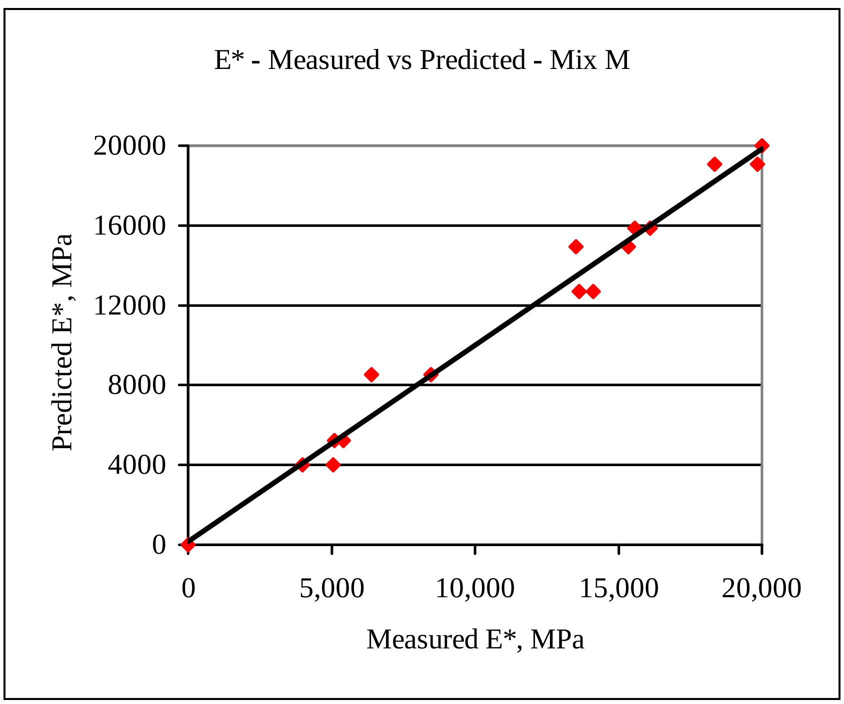


Figure D-2: E* - Measured vs Predicted – Mix M

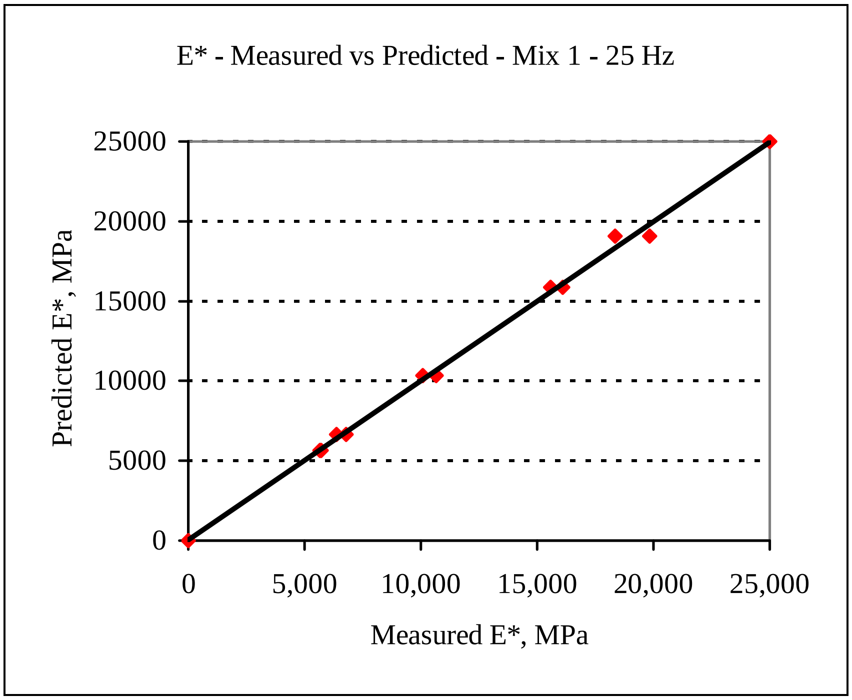


Figure D-3: E* - Measured vs Predicted – Mix 1

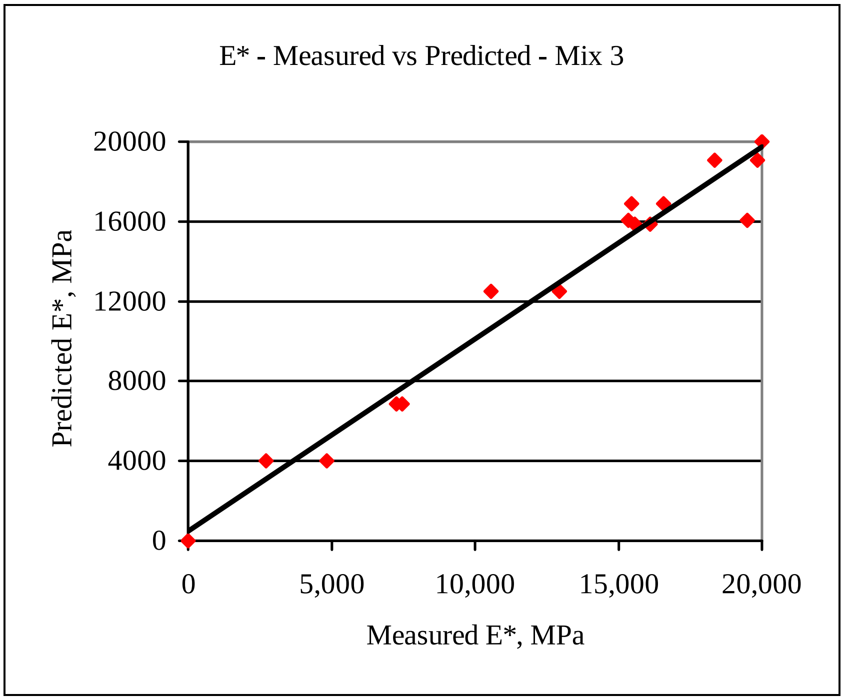


Figure D-4: E* - Measured vs Predicted – Mix 3

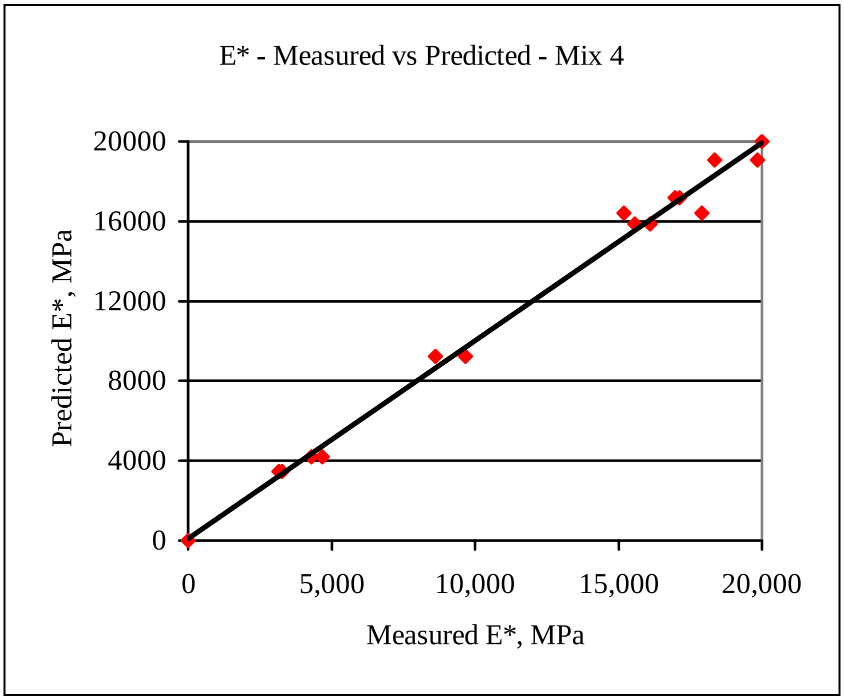


Figure D-5: E* - Measured vs Predicted – Mix 4

# APPENDIX E

# SHIFT FACTORS VS TEMPERATURE CHARTS

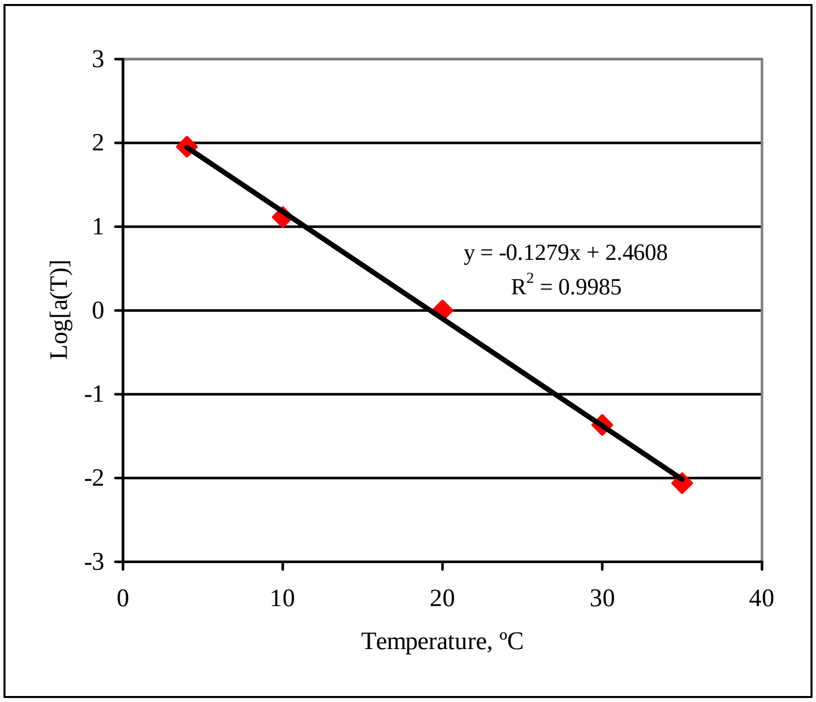


Figure E-1: Shift Factor vs Temperature Curve – Mix S

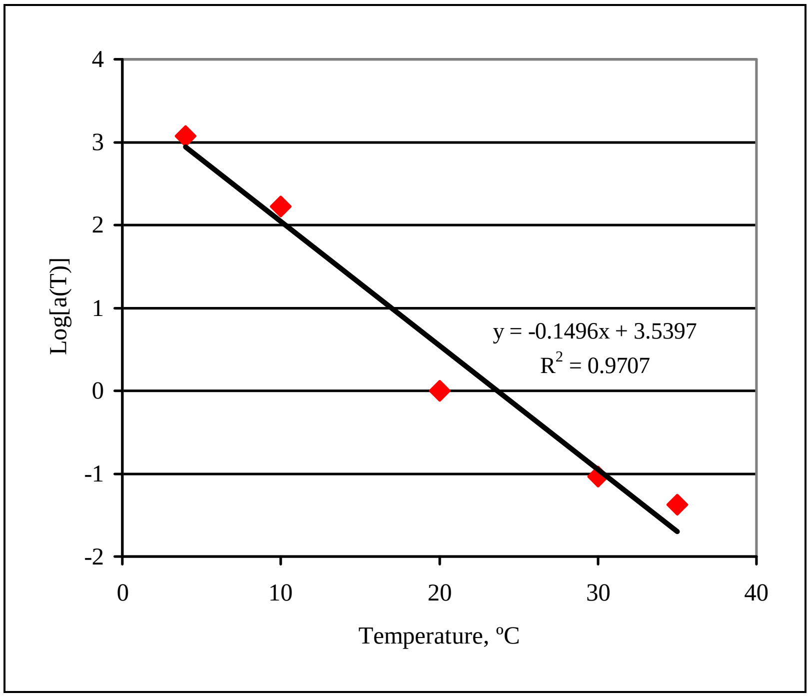


Figure E-2: Shift Factor vs Temperature Curve – Mix M

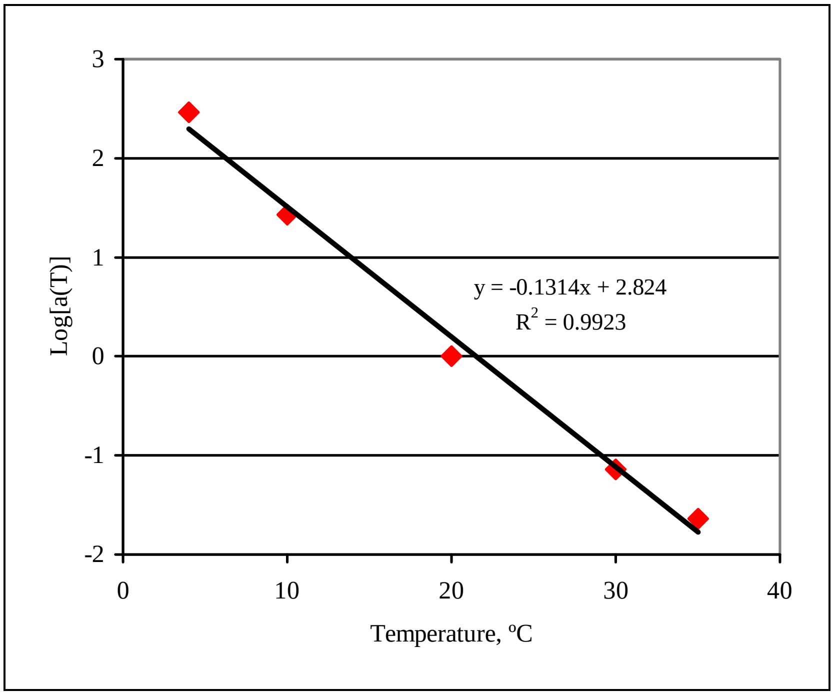


Figure E-3: Shift Factor vs Temperature Curve – Mix 1

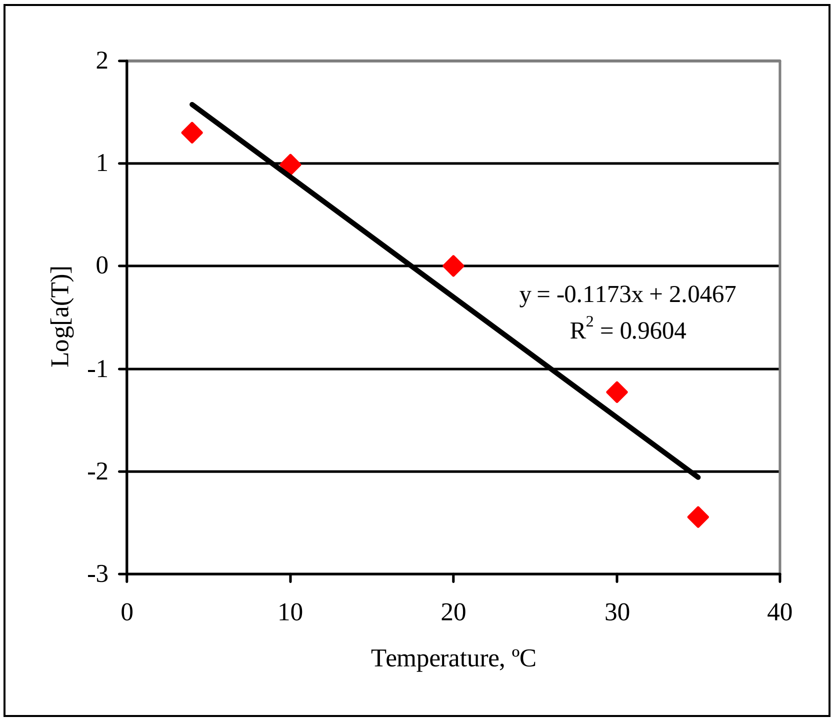


Figure E-4: Shift Factor vs Temperature Curve – Mix 3

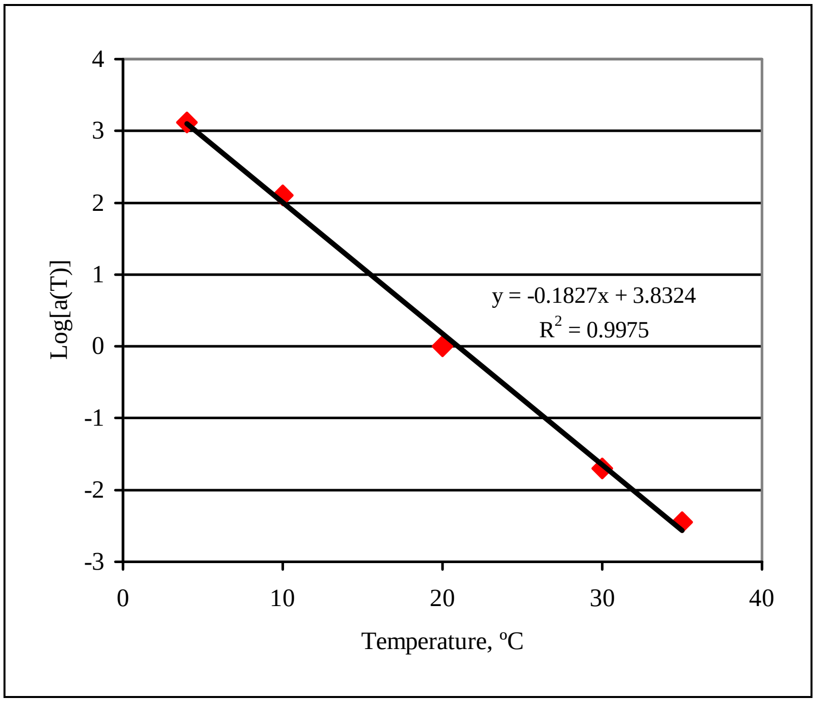


Figure E-5: Shift Factor vs Temperature Curve – Mix 4

# APPENDIX F

# DYNAMIC MODULUS MASTER CURVES

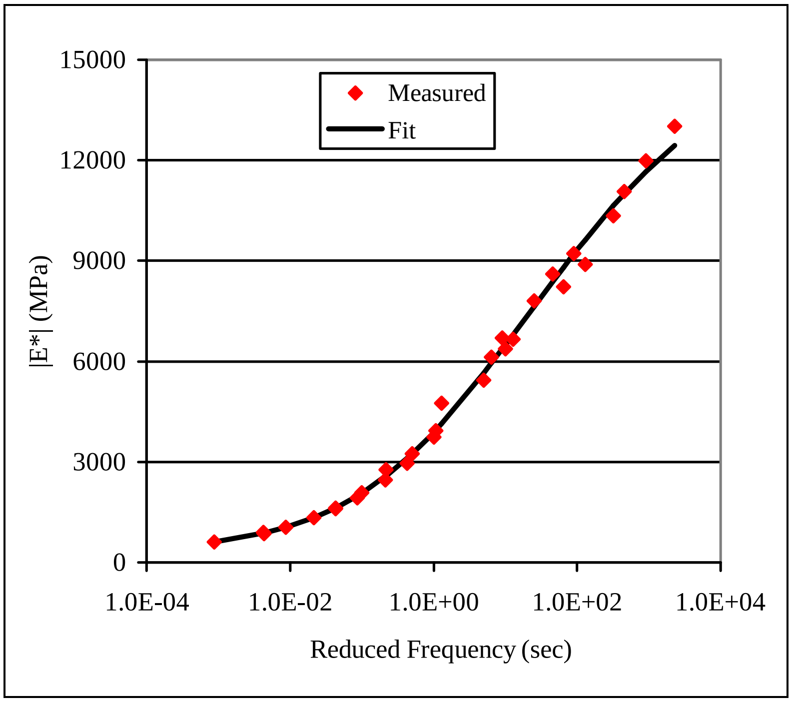


Figure F-1: Dynamic Modulus Master Curve – Mix S

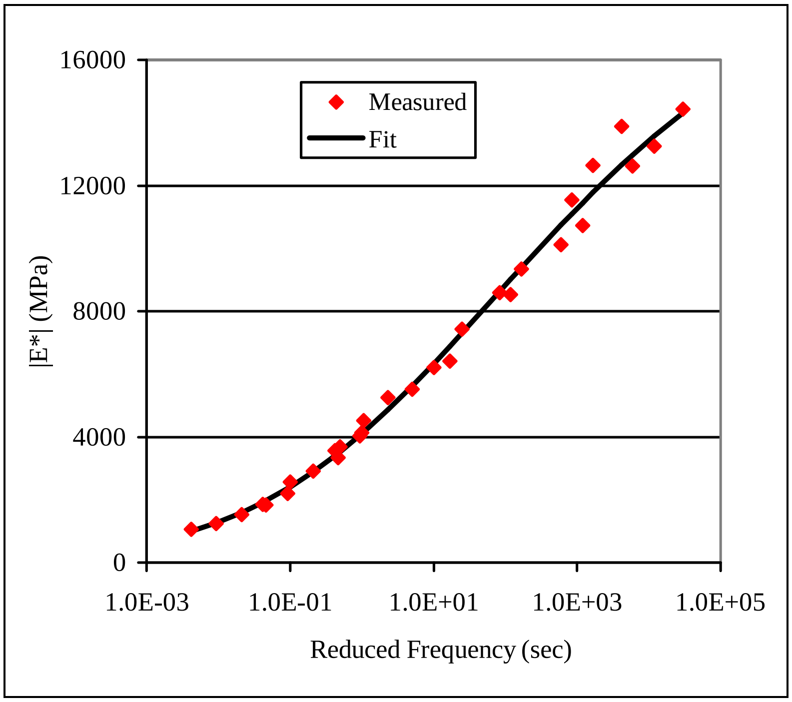


Figure F-2: Dynamic Modulus Master Curve – Mix M

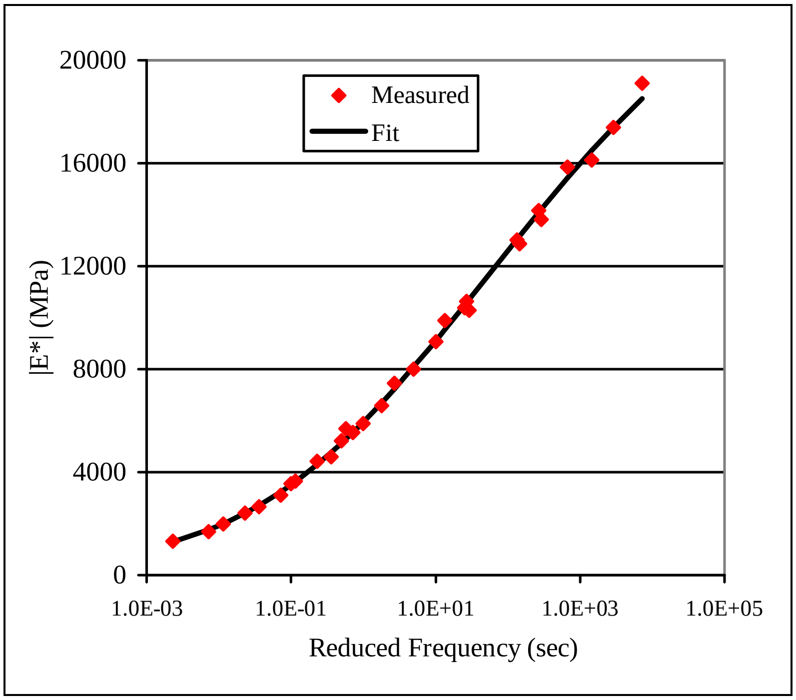


Figure F-3: Dynamic Modulus Master Curve – Mix 1

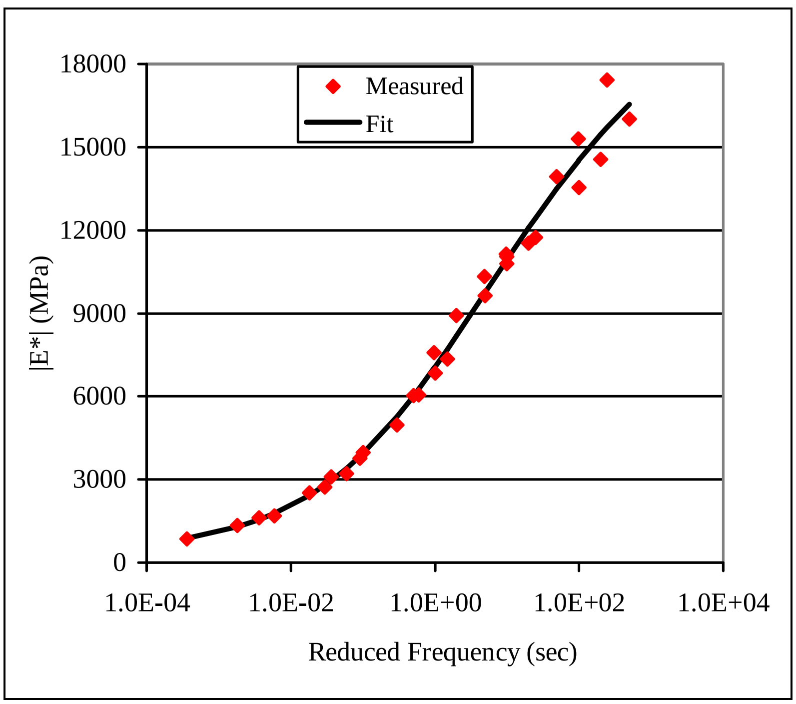


Figure F-4: Dynamic Modulus Master Curve – Mix 3

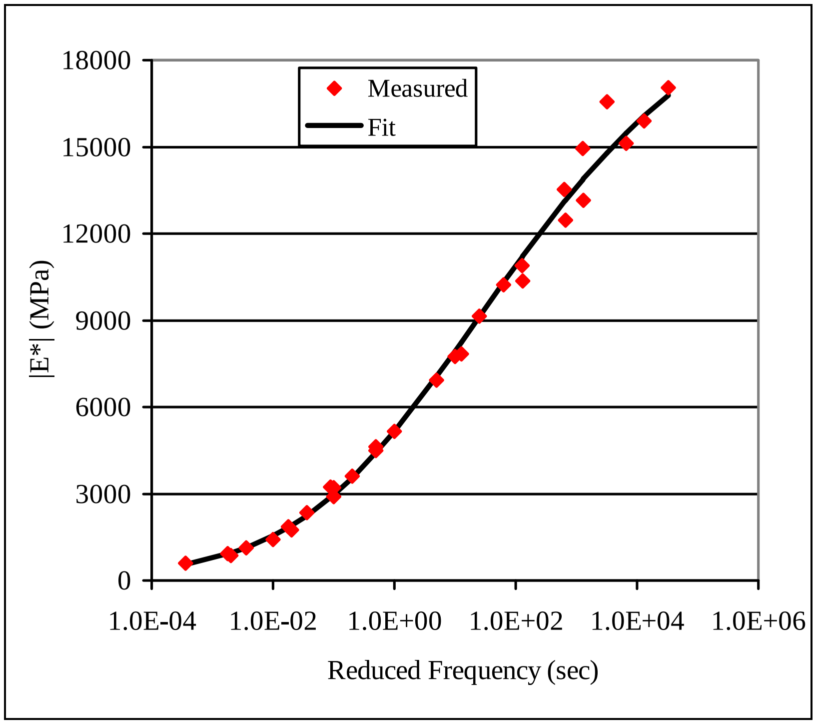


Figure F-5: Dynamic Modulus Master Curve – Mix 4

# APPENDIX G

# SHEAR RELAXATION MODULUS MASTER CURVES

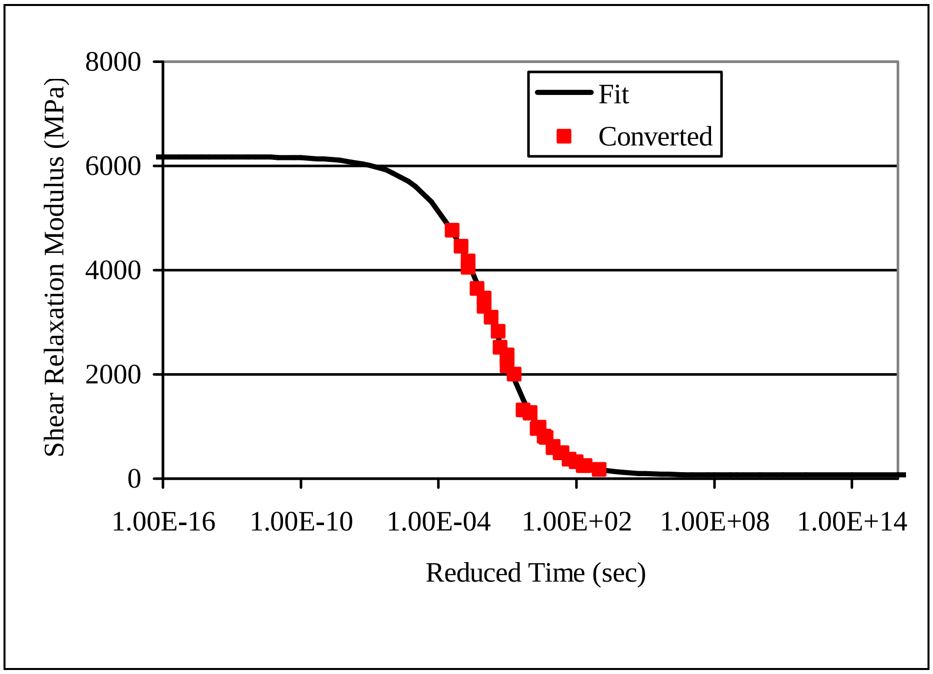


Figure G-1: Shear Relaxation Modulus Master Curve – Mix S

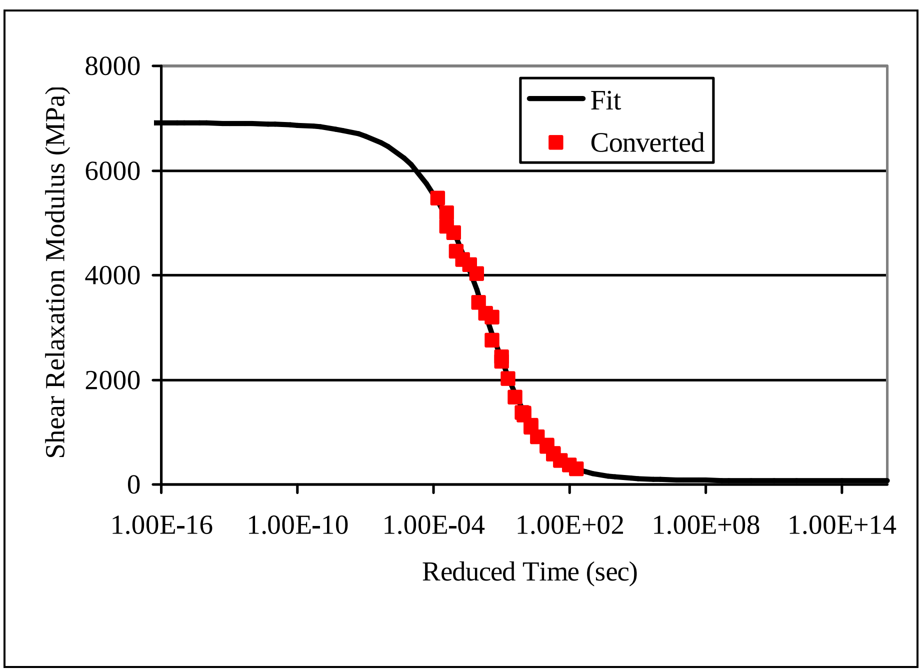


Figure G-2: Shear Relaxation Modulus Master Curve – Mix M

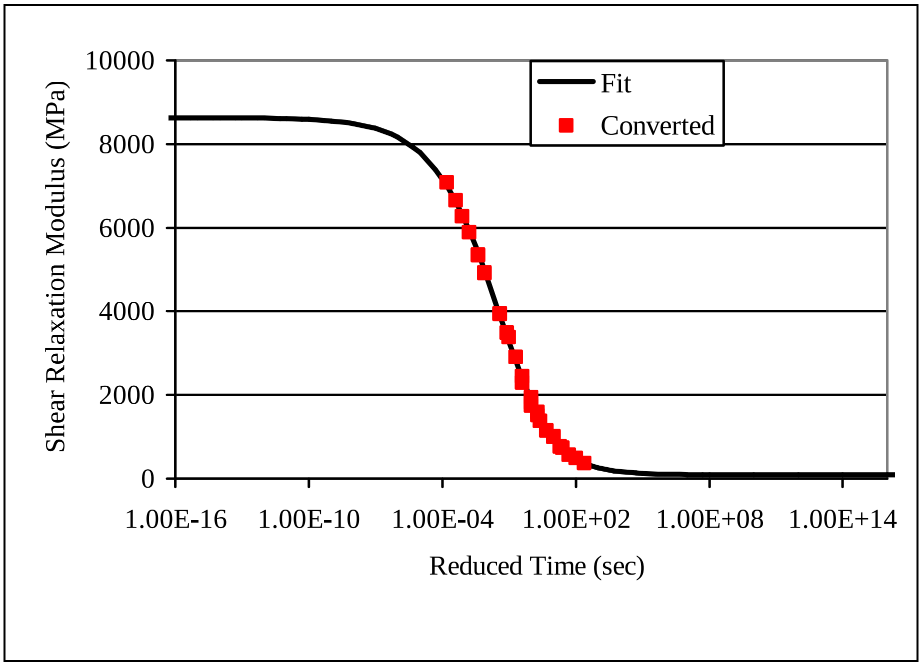


Figure G-3: Shear Relaxation Modulus Master Curve – Mix 1

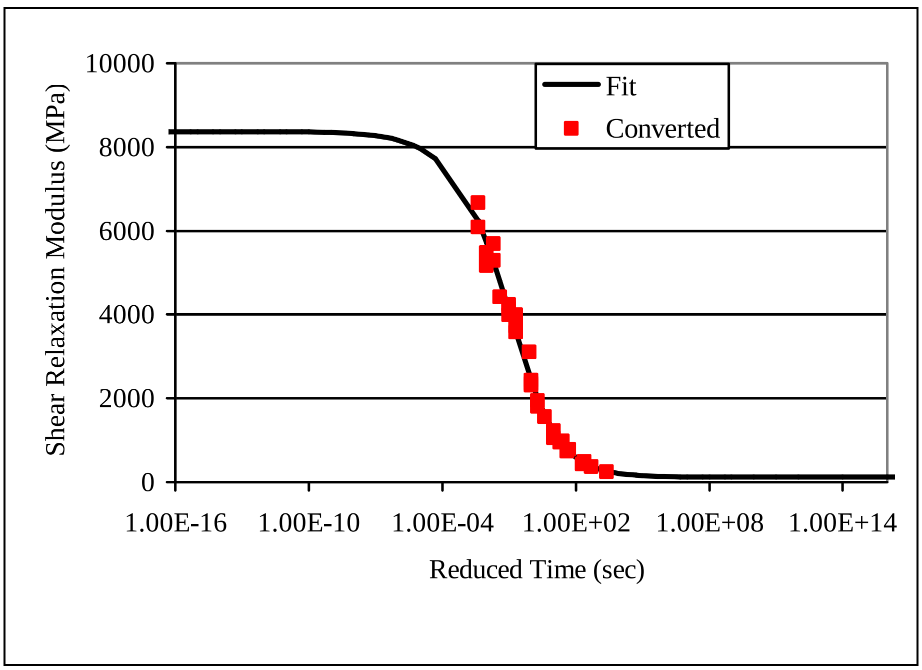


Figure G-4: Shear Relaxation Modulus Master Curve – Mix 3

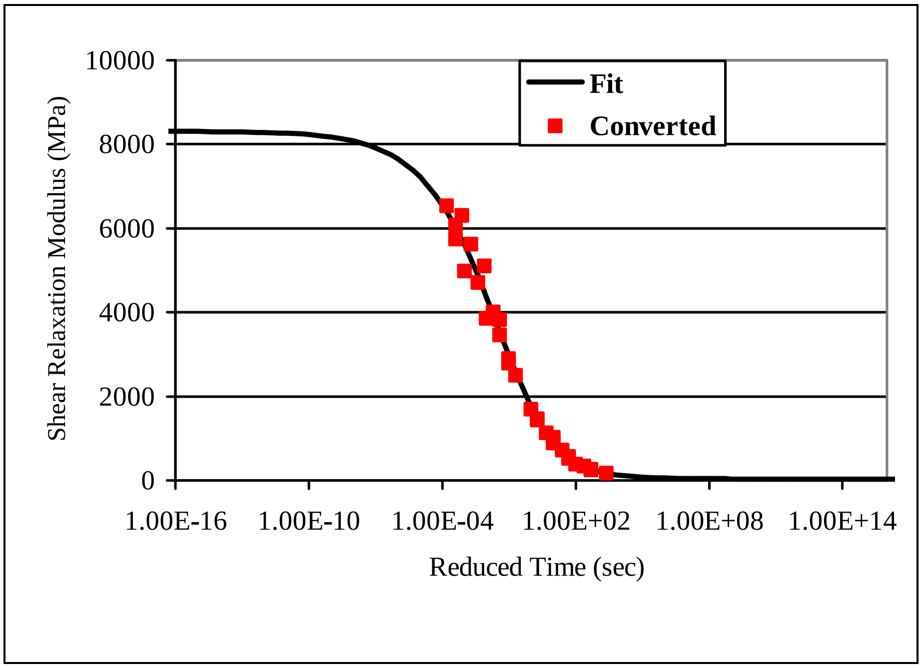


Figure G-5: Shear Relaxation Modulus Master Curve – Mix 4

# APPENDIX H

# BULK RELAXATION MODULUS MASTER CURVES

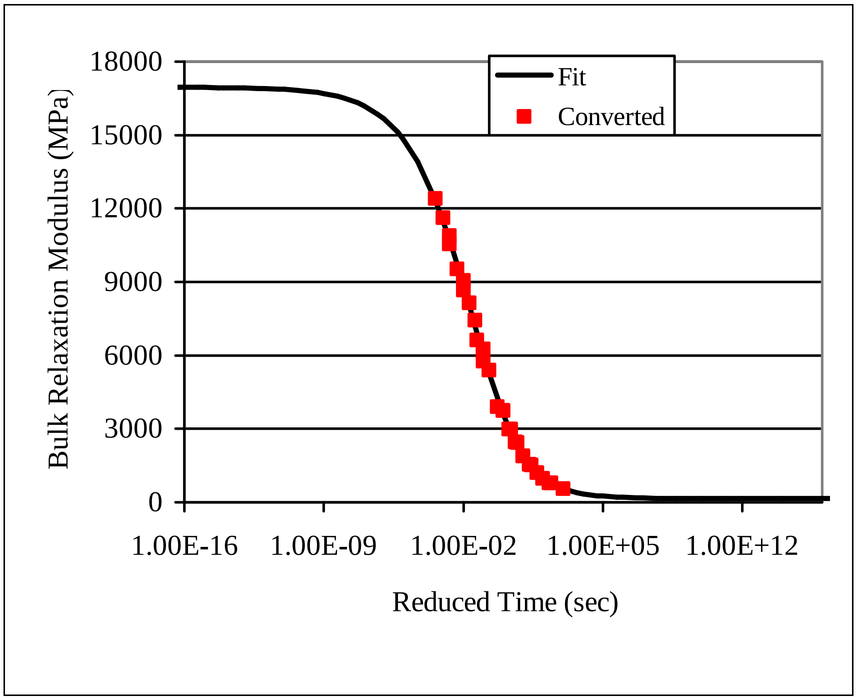


Figure H-1: Bulk Relaxation Modulus Master Curve – Mix S

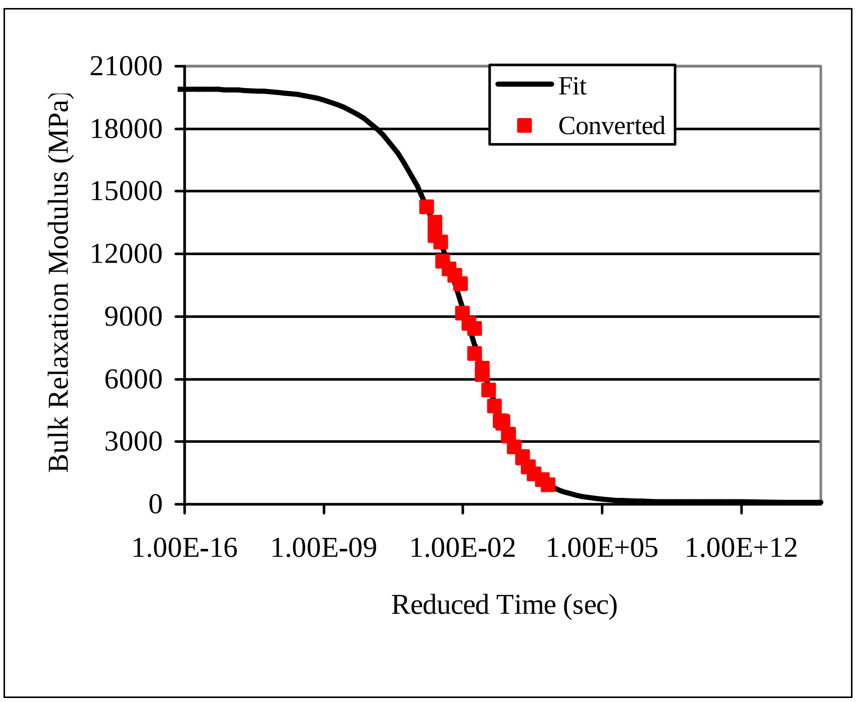


Figure H-2: Bulk Relaxation Modulus Master Curve – Mix M

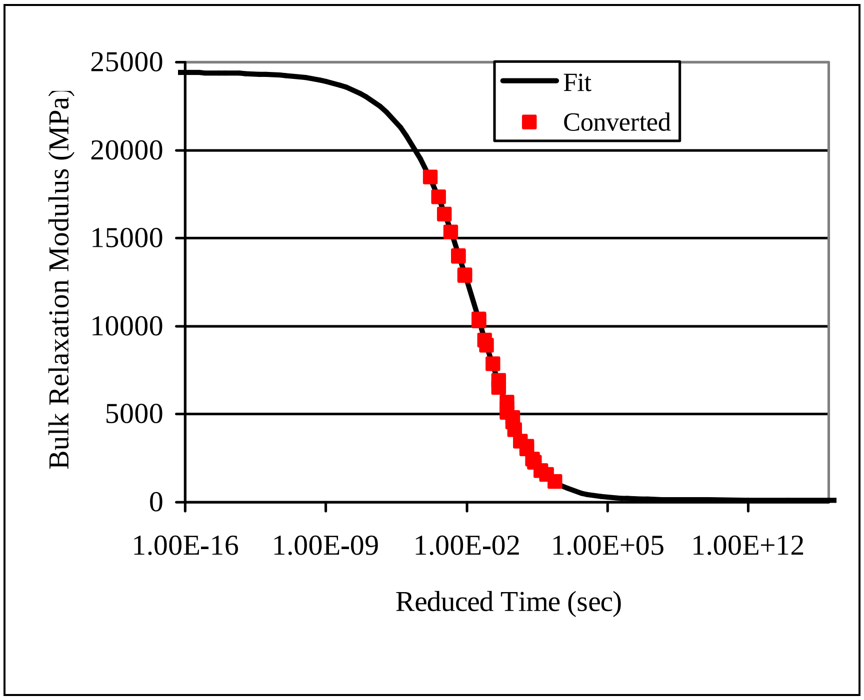


Figure H-3: Bulk Relaxation Modulus Master Curve – Mix 1

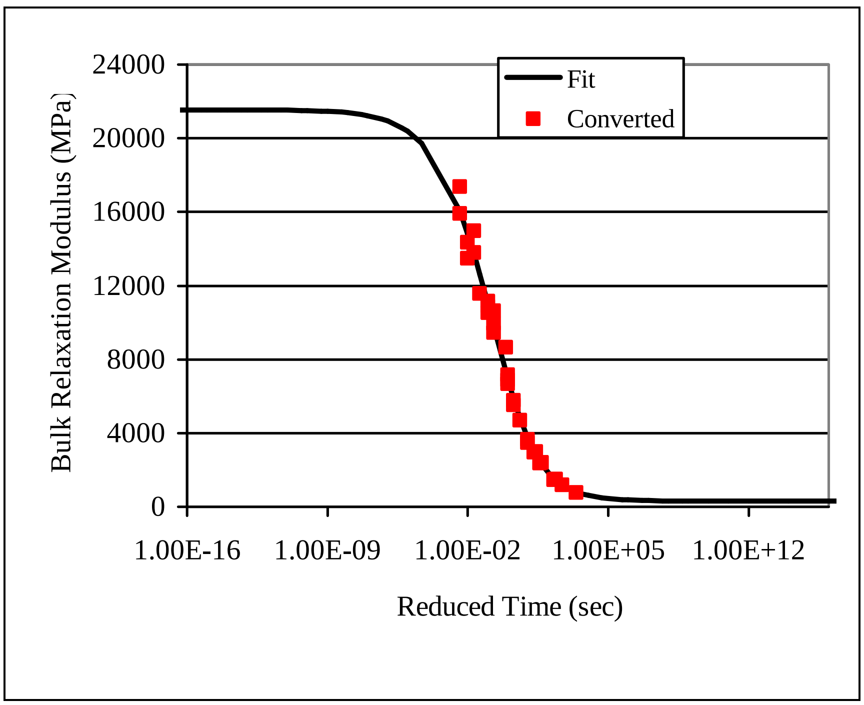


Figure H-4: Bulk Relaxation Modulus Master Curve – Mix 3

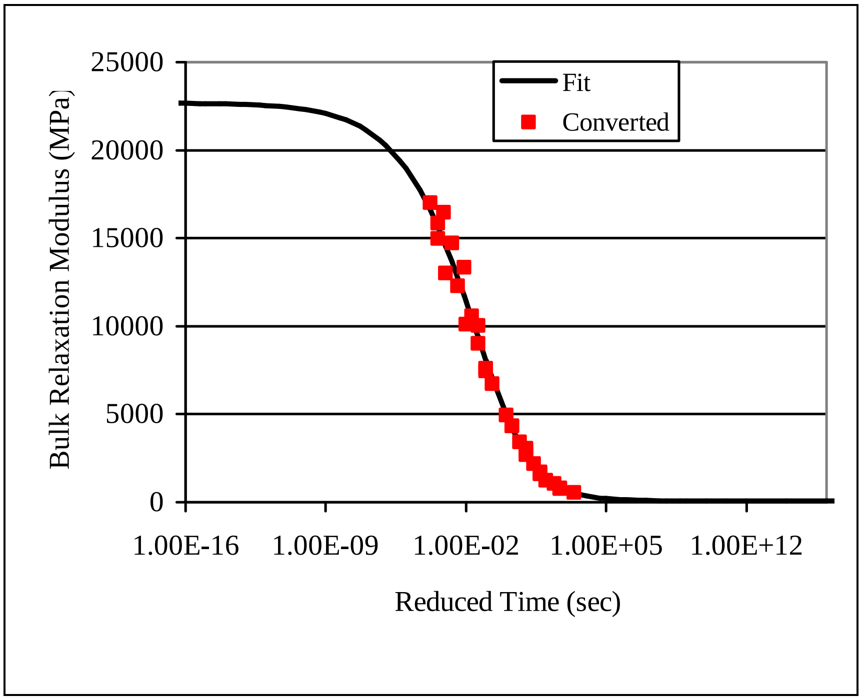


Figure H-5: Bulk Relaxation Modulus Master Curve – Mix 4

REFERENCES


ABAQUS/Standard User's Manual–Version 6.7. (2007). Finite Element Computer Program. Hibbitt, Karlsson and Sorenson, Inc., Pawtucket, RI, USA.

Chapra, S. C. and R. P. Canale, "Numerical Methods for Engineers", McGraw-Hill, New York, 1988.

Dumitru, C. (2006) "A Comparison of Measured and Computed Strains in Experimental Thin PCC Overlays." MS Thesis, Department of Civil Engineering, Kansas State University, Manhattan, KS.

Elseifi, M.A., Al-Qadi, I.L., and Yoo, P.J. (2006) Viscoelastic Modeling and Field Validation of Flexible Pavements. *Journal of Engineering Mechanics, Vol. 132, No. 2*.

ERES Consultants Division. (2004) *Guide for Mechanistic-Empirical Design of New and Rehabilitated Pavement Structures*. Final Report NCHRP 1-37A, Champaign, IL.

*EVERSERIES© USER'S GUIDE. Pavement Analysis Computer Software and Case Studies*, Washington State Department of Transportation, August 2005. Web document: http://www.wsdot.wa.gov/biz/mats/pavement/EVERSERS/EverseriesUserGuide.pdf)

Huang, Y. (1993). Pavement Analysis and Design. Prentice Hall, NJ.

Ioannides, A. M. "Analysis of Slabs-on-Grade for a Variety of Loading and Support Conditions", Ph.D. dissertation, University of Illinois, Illinois, 1984

Mahoney, J. P., Anderson, K., W., Pietz, M., D. and Pierce, L., M., "A Framework for WSDOT Research", Research Report, Educational Task Order T1242, Task 4, December, 2000.

Metcalf, J. B., "NCHRP Synthesis of Highway Practice 235: Application of Full-Scale Accelerated Pavement Testing", TRB, National Research Council, Washington, D.C., 1996.

Mikhail, M. (1996). “Three Dimensional Mechanistic Analysis of Vehicle-Pavement Interaction.” Ph.D. Dissertation, Arizona State University, Tempe, AZ.

Nassar, W. M. (2001). “Utilization of Instrument Response of SuperPave™ Mixes at the Virginia Smart Road to Calibrate Laboratory Developed Fatigue Equations.” Ph.D. Dissertation, Virginia Polytechnic Institute and State University, Blacksburg, VA.

Palacios, C.. (2007) “Performance Evaluation of Fiber-Reinforced Stress-Absorbing Membrane Interlayers for Low Volume Roads.” MS Thesis, Department of Civil Engineering, The Pennsylvania State University, University Park, PA.

Perpetual Bituminous Pavements. *Transportation Research Circular 503*, Transportation Research Board, National Research Council, December 2001.

Romanoschi, S. (1999). “Characterization of Pavement Layer Interfaces.” Ph.D. Dissertation, Louisiana State University, Baton Rouge, LA.

Schapery, R.A. and S.W. Park (1999). “Methods of interconversion between linear viscoelastic material functions. Part II- an approximate analytical method.” *International Journal of Solids and Structures*, Vol. 36, pp. 1677-1699.

Transportation of the United States. (2008). Retrieved October 26, 2008, from http://nationalatlas.gov/transportation.html

Thompson, M. R. and Carpenter, S. H. (2006). “Considering Hot-Mix-Asphalt Fatigue Endurance Limit in Full-Depth Mechanistic-Empirical Pavement Design.” University of Illinois at Urbana-Champaign, Urbana, IL.

Yin, H. (2007). “Integrating Instrumentation Data in Probabilistic Performance Prediction of Flexible Pavements.” Ph.D. Dissertation, The Pennsylvania State University, University Park, PA.

Yin, H., Solaimanian, M., Kumar, T., and Stoffels, S. (2007) “The Effects of Loading Time on Flexible Pavement Dynamic Response: A Finite Element Analysis.” *Mechanics of Time-Dependent Materials Vol. 11*, Issue 3-4, December 2007, 265-288.

Yoo, P. J., Al-Qadi, I. L., Elseifi, M., and Janajreh, I. (2005) "Flexible Pavement Responses to Different Loading Amplitudes Considering Layer Interface Condition and Lateral Shear Forces." *The International Journal of Pavement Engineering Vol.* 7, No. 1, March 2006, 73–86.

Yoo, P. J. (2007). “Flexible Pavement Dynamic Response Analysis and Validation for Various Tire Configurations.” Ph.D. Dissertation, University of Illinois at Urbana-Champaign, Champaign, IL.

## BIOGRAPHICAL INFORMATION

Miguel M. Portillo is originally from Asuncion, capital of Paraguay. He graduated with a Bachelors of Science in Civil Engineering from Kansas State University in December of 2006. In January of 2007 he started the Master of Science in civil engineering program at Kansas State University in the area of pavements. In August of 2008, he transferred to the University of Texas at Arlington to continue his M.S. in civil engineering, and graduated in December of 2008. His research interests are mainly in the pavement and geotechnical areas of the civil engineering field. The author has worked in a variety of projects under the guidance of Dr. Stefan Romanoschi involving the design, construction, and monitoring of experimental pavement sections in the field, as well as pavement sections for accelerated pavement testing. One example of such a project would be the US-75 project, which is presented in this work. The author’s future plans include returning to Paraguay and begin working and acquiring field experience, to later be able to establish his own civil engineering company.